

Some pages of this thesis may have been removed for copyright restrictions.

If you have discovered material in AURA which is unlawful e.g. breaches copyright, (either yours or that of a third party) or any other law, including but not limited to those relating to patent, trademark, confidentiality, data protection, obscenity, defamation, libel, then please read our [Takedown Policy](#) and [contact the service](#) immediately

**A BIOLOGICAL-INSPIRED SUPPORT FRAME FOR AN
ARTIFICIAL CORNEA**

**David William Green
Doctor of Philosophy**

THE UNIVERSITY OF ASTON

August 1999

This copy of the thesis has been supplied on condition that anyone who consults it is understood to recognise that its copyright rests with its author and that no quotation from the thesis and no information derived from it may be published without proper acknowledgement.

Thesis Summary

Bilateral corneal blindness represents a quarter of the total blind, world-wide. The artificial cornea in assorted forms, was developed to replace opaque non-functional corneas and to return sight in otherwise hopeless cases that were not amenable to corneal grafts; believed to be 2% of corneal blind. Despite technological advances in materials design and tissue engineering no artificial cornea has provided absolute, long-term success. Formidable problems exist, due to a combination of unpredictable wound healing and unmanageable pathology. To have a solid guarantee of reliable success an artificial cornea must possess three attributes:

- an optical window to replace the opaque cornea
- a strong, long term union to surrounding ocular tissue
- the ability to induce desired host responses

A unique artificial cornea possesses all three functional attributes- the Osteo-odonto-keratoprosthesis (OOKP). The OOKP has a high success rate and can survive for up to twenty years, but it is complicated both in structure and in surgical procedure; it is expensive and not universally available. The aim of this project was to develop a synthetic substitute for the OOKP, based upon key features of the tooth and bone structure. In doing so, surgical complexity and biological complications would be reduced. Analysis of the biological effectiveness of the OOKP showed that the structure of bone was the most crucial component for implant retention. An experimental semi-rigid hydroxyapatite framework was fabricated with a complex bone-like architecture which, could be fused to the optical window. The first method for making such a framework, was pressing and sintering of hydroxyapatite powders; however, it was not possible to fabricate a void architecture with the correct sizes and uniformity of pores. Ceramers were synthesised using alternative pore forming methods, providing for improved mechanical properties and stronger attachment to the plastic optical window. Naturally occurring skeletal structures closely match the structural features of all forms of natural bone. Synthetic casts were fabricated using the replamineform process, of desirable natural artifacts, such as coral and sponges. The final method of construction by-passed ceramic fabrication in favour of pre-formed coral derivatives and focused on methods for polymer infiltration, adhesion and fabrication. Prototypes were constructed and evaluated; a fully penetrative synthetic OOKP analogue was fabricated according to the dimensions of the OOKP. Fabrication of a cornea shaped OOKP synthetic analogue was also attempted.

keywords: Oste-odonto-keratoprosthesis, Hydroxyapatite, Coral, Ceramers, Replamineform Process

ACKNOWLEDGEMENTS

I afford immense thanks for the originator of this fascinating project, Christopher Liu from the Sussex Eye Hospital, who imparted a good deal of encouragement to me. My gratitude also goes to my supervisor, Professor Brian Tighe for his constructive criticisms of my research and his supreme patience.

My sincere, heartfelt thanks go to the following people for their genuine support, help and inspiration: Zoltan and Peter Fehervari (for philosophical discussions), Dr. Aisling Mann, Shilpa Moses, Babinder Samra and Steve Tonge (for their great moral support), Beverley Benning and Dr. Fiona Lydon (for their kind assistance and encouragement). Thank you to Dr. Valerie Franklin for her assistance, too. I also acknowledge the helpfulness of my project collaborators, Jesse Shirley Advanced Ceramics, the Birmingham Dental School, and Chris Parker of the Dental Technology Group at Matthew Boulton College. Lastly I would like to thank Dr. Surinder Kooner of DERA at Farnborough, for her great advice.

This CASE research Ph.D was funded by the EPSRC. The commercial sponsor was Vista Optics.

LIST OF CONTENTS	Page
No.	
Thesis Summary	2
Acknowledgements	3
List of Contents	4
List of Tables, Figures and Photographs by Chapter	10

LIST OF CONTENTS

Page No.

CHAPTER 1 Literature Review:

Keratoprostheses

1.1 Introduction	26
1.2 The Cornea in Health and Disease	27
1.2.1 Structure and Physiology	27
1.2.2 Corneal Blindness	30
1.2.3 Corneal Transplantation	31
1.3 The Need for an Artificial Cornea	32
1.4 Conclusions	34
1.5 The Keratoprosthesis	35
1.5.1 Introduction	35
1.5.2 Early History of the Artificial Cornea	36
1.5.3 Recent Developments in the Design of Artificial Corneas	41
1.5.4 Exceptional Artificial Corneas Support Frames	45
1.5.41 Expanded PTFE Meshwork Support Frame	45
1.5.42 pHEMA/HEMA Hydrogel Support Frame	46
1.5.43 Collagen Gel Support Frame	47
1.5.44 Tooth and Bone Plate Support Frame	48
1.6 Features of the Ideal Artificial Cornea	48
1.7 Conclusions	51

CHAPTER 2 Literature Review and Analysis:

The Osteo-Odontokeratoprosthesis and Beyond

2.1 Introduction	53
2.2 Osteo-Odontokeratoprosthesis (OOKP) Surgery	58
2.2.1 Brief Summary of the OOKP Operation	62
2.3 OOKP: Nature and Structure	64

2.4	Anatomy of Living Dental (Periodontal) Tissue	66
2.4.1	Dentine	66
2.4.2	Periodontal Ligament	66
2.4.3	Cementum	67
2.4.4	Alveolar Bone	67
2.4.5	Buccal Mucosa	69
2.5	Ocular Attachment and Integration	69
2.6	Mode of Attachment to the Eye	70
2.7	Discussion	71
2.8	<u>Towards a Synthetic OOKP: Scope and Objects of this Project</u>	75
 CHAPTER 3 MATERIALS and METHODS		
3.1	<u>Materials</u>	80
3.2	<u>Experimental Methods: Fabrication of Porous Ceramic Discs</u>	87
3.2.1	Histological Staining	87
3.2.2	Measurement of Biological Ceramic Grain Sizes	87
3.2.3	Die Pressing of Ceramic Particles	87
3.2.4	Calculation of Packing Densities and Packing Arrangements	88
3.2.5	Die Pressing of Assorted Particle Mixtures	92
3.2.6	Scanning Electron Microscope Analysis of Pressed Discs	94
3.2.7	Measurement of Porosity	94
3.3	<u>Experimental Methods: Fabrication of Ceramers</u>	95
3.3.1	Synthesis of Polymer Membranes	95
3.3.2	Ceramer Blends	97
3.3.3	Plasma Etching of the Polymer Phase	99
3.4	<u>Experimental Methods: Biomimetic Synthesis of Ceramic and Polymer Composites</u>	101
3.4.1	Deposition of a Bone-Like Apatite Layer onto Polymer	101
3.4.1.1	Calcification Solution	103

3.4.2	Langmuir Blodgettry	104
3.4.3	Calcium Carbonate Deposition on Polymer Membranes	104
3.4.4	Synthesis of Collagen Gels	105
3.4.5	Sol-Gel Deposits	105
3.4.6	Replamineform Processing	106
3.5	<u>Experimental Methods: Conglomeration of Polymer and Porous Biological Ceramics</u>	108
3.5.1	Incorporation of Polymer into Biological Ceramics	108
3.5.2	Measurment of Viscosity	111
3.6	<u>Experimental Methods: Materials Characterisation</u>	112
3.6.1	Goniophotometer Measurements of Surface Roughness	112
3.6.2	Fractal Analysis	112
3.6.3	XRD Analysis of Biocoral [®] and Bone-Like Coral	114
3.6.4	Physical Characterisation of Cellular Solids	114
3.7	<u>Biological Evaluation</u>	115
3.7.1	Cell Culture	115

CHAPTER 4 RESULTS:

Fabrication of a Porous Biological Ceramic Support Frame for an Artificial Cornea

4.1	Introduction	117
4.2	<u>Biomedical Ceramics</u>	117
4.2.1	Carbon	118
4.2.2	Oxide Ceramics	119
4.2.3	Bioactive Glasses and Glass Ceramics	119
4.2.4	Calcium Phosphate Ceramics	120
4.3	Cellular Responses to Hydroxyapatite Discs	121
4.4	Histological Observations of the Dental Lamina	125

4.5 Fabrication of Hydroxyapatite Ceramic Discs	126
4.6 <u>Fabrication of Porous Ceramics</u>	129
4.6.1 Powder Compacting and Packing Arrangements for Ceramic Particles and the Creation of an Ordered Uniform Porosity	129
4.6.2 Examination by Scanning Electron Microscope	137
4.6.3 Measurement of Porosity	137
4.7 Summary and Conclusion	138

CHAPTER 5 RESULTS:

Fabrication of a Ceramer Support Frame for an Artificial Cornea

5.1 Introduction	143
5.1.1 Ceramers for Biomedical Applications	143
5.2. Fabrication of Ceramers	144
5.2.1 Introduction to Experimental	144
5.2.2 Ceramers and Polymer / Ceramic Conglomerates	146
5.3 Plasma Etching of Polymer Phase	152
5.4 Sol-Gel Synthesis of Porous Ceramics	155
5.5 Deposition of a Bone-Like Apatite Layer onto Polymer Surfaces	157
5.6 Summary and Conclusion	157

CHAPTER 6 RESULTS:

Marine Derived Natural Artifacts as Potential Structures for an Artificial Cornea Support Frame

6.1 Introduction	164
6.2 Survey of Porous Structures in the Animal and Plant Kingdoms	165
6.3 Examination and Selection of Natural Artifacts as Potential Candidates for a Keratoprosthesis Support Frame	170
6.3.1 Introduction to Selection Scheme	170
6.3.2 Marine Derived Skeletal Frameworks of Particular Interest	172

6.3.21 Bryozoans	175
6.3.22 Sponge Skeletons	177
6.3.23 Sea Urchin Spines	183
6.3.24 Coral Skeletons	185
6.3.25 Selection Criteria for Coral Skeletons	186
6.3.4 Polymer Casting of Sponge and Coral Skeletons	193
6.3.5 Final Remarks about the Suitability of Marine Skeletons	197
6.4 Processed Coral Skeletons and Trabeculated Cow Bone Ceramics	198
6.4.1 Pro-Osteon®	199
6.4.2 Biocoral®	200
6.5 Summary and Conclusion	204

CHAPTER 7 RESULTS:

Fabrication of a Prototype Artificial Cornea from Coral and pMMA

7.1 Introduction	208
7.2 <u>Surface Characterisation</u>	209
7.2.1 Fractal Analysis	209
7.2.2 Goniophotometry	214
7.3 <u>Fabrication of Keratoprotheses</u>	218
7.3.1 Design Solutions for Common Causes of Implant Failure	218
7.3.2 <u>Stage 1: Polymer Bonding to Coral</u>	219
7.3.21 Incorporation of Polymer into Biological Ceramic	219
7.3.22 Thermal Cast Polymerisation	220
7.3.23 Ultraviolet Radiation Assisted Polymerisation	221
7.3.3 Measurement and Manipulation of Polymer Uptake into Coral	222
7.3.4 Measurement of Viscosity	229
7.4 <u>Stage 2: Construction of the Prototype Keratoprosthesis</u>	230
7.4.1 Introduction	230
7.4.2 Assembly of Component Polymer and Coral Skeleton	231

7.4.21 Biocoral® Shaping	235
7.4.3 Discussion: Likely Surgical Performance of Prototypes	243
7.4.4 Future Directions: Changes to the Optical Cylinder	247
7.4.5 Production of a Full Thickness Cornea Shaped Coral and Perspex Keratoprosthesis	248
7.5 Conclusions	251

CHAPTER 8 Recapitulation, Discussion and Conclusion

8.1 Recapitulation of Material Synthesis	255
8.2 General Discussion	264
8.3 Conclusion	277
8.1 Suggestions for Further Work	279

LIST OF REFERENCES	281
---------------------------	-----

APPENDICES

APPENDIX 1

A1.1 A Detailed Description of Attributes for an OOKP Analogue	296
A1.11 Porosity	296
A1.12 Mineral Properties	299
A1.13 Rate of Resorption	299
A1.14 A Periodontal Ligament Substitute	300

APPENDIX 2

A2.1 Methods for Making Ceramic Blocks	303
A2.11 Fabrication of Biological Ceramics with Uniform Porosity	304
A2.12 Dynamic Changes to the Porosity of Ceramics	305

APPENDIX 3

A3.1 A More Detailed Assessment of the Potential Usefulness of a Prosthesis by Tissue Culture	306
--	-----

LIST OF TABLES, FIGURES AND PHOTOGRAPHS BY CHAPTER **Page No.**

CHAPTER 1: LITERATURE REVIEW: Artificial Corneas

CHAPTER 1 Figures

Figure 1.1 <i>Diagrammatic Cross-Section of a Healthy Human Cornea</i>	28
Figure 1.11 <i>Structure of a Modern Artificial Cornea: The Popular Core and Skirt Model</i>	35
Figure 1.12 <i>The Major Causes of Implant Rejection</i>	36
Figure 1.13 <i>Schematic Cross-Section of the Glass Ceramic and Bone Keratoprosthesis</i>	40
Figure 1.14 <i>Microporous Fluorocarbon Meshwork Support Frame and polymethyl Methacrylate (pMMA) Core</i>	45
Figure 1.15 <i>A Two-Part Hydrogel Analogue of the Cornea</i>	46
Figure 1.16 <i>Dental Lamina Support Frame Attached to polymethyl Methacrylate (pMMA) Core</i>	48
Figure 1.17 <i>Nutrient and Metabolic Transfer in the Cornea.</i>	49
Figure 1.18 <i>Features of the Ideal Artificial Cornea</i>	50

CHAPTER 1: Tables

Table 1.1 <i>Autotissues Used for Artificial Corneas</i>	39
Table 1.11 <i>Key Steps in the Early Development of Artificial Corneas From 1789 to 1993</i>	41

CHAPTER 1: Graphs

Graph 1.1 <i>Global Corneal Blindness</i>	30
--	----

CHAPTER 2: The Osteo-odontokeratoprosthesis: Tooth and Bone Keratoprosthesis

CHAPTER 2: Figures

Figure 2.1 <i>The Strampelli Osteo-odontokeratoprosthesis: A Cross-Section Through an Implanted OOKP.(After Strampelli)</i>	53
Figure 2.11 <i>Biologically Induced Changes in the Tooth and Bone Support Frame</i>	56
Figure 2.12 <i>Major Reasons for Success of the OOKP</i>	57
Figure 2.13 <i>Shape and Size of Dental Fragment</i>	60
Figure 2.14 <i>Stereogram of Osteo-odontal Lamina</i>	65
Figure 2.15 <i>Cancellous Bone Surrounding an Incisor</i>	67
Figure 2.16 <i>Diagrammatic Representation of an Artificial OOKP (right) and an OOKP (left) for Comparison</i>	76
Figure 2.17 <i>Possible Ways of Making a Ceramic Support Frame for an OOKP Analogue</i>	78

CHAPTER 2: Tables

Table 2.1 <i>OOKP Solutions to Common Reasons for Keratoprosthesis Failure</i>	73
Table 2.11 <i>Pore Size Distribution Likely to Cause Tissue Interlock</i>	78
Table 2.12 <i>Potential Materials for a Periodontal Ligament Substitute</i>	78

CHAPTER 2:Photographs

Photograph 2.1 <i>Basal Surface of a Freshly Excavated Section of Tooth Root and Alveolar Bone with Optical Cylinder Inserted</i>	54
Photograph 2.11 <i>Ocular Pemphigoid</i>	58
Photograph 2.12 <i>Example of Cornea Opacity Caused by a Chemical Burn</i>	58
Photograph 2.13 <i>Fungal Keratitis</i>	59
Photograph 2.14 <i>Mucosa Wrapped around Dental Fragment</i>	62
Photograph 2.15 <i>Insertion of OOKP Encapsulation in Mucosa into Subcutaneous Pocket Just Below the Eye</i>	62
Photograph 2.16 <i>Insertion of ODAL onto Bulbar Surface</i>	63

Photograph 2.17 <i>Cross-Section Through the Periodontal Ligament</i>	66
Photograph 2.18 <i>Region of Compact Spongy Bone Adjoining the Periodontal Ligament</i>	68
Photograph 2.19 <i>Final Placement of OOKP into the Anterior Eye</i>	70
Photograph 2.2 <i>OOKP with Cosmetic Lens</i>	70

CHAPTER 3

MATERIALS and METHODS

CHAPTER 3: Figures

Figure 3.1 <i>Diagram of a KBr Press Experimental apparatus for Compacting of Ceramic Powders into Discs.</i>	88
Figure 3.11 <i>Packing Arrangements of Spheres</i>	89
Figure 3.12 <i>Measurements for Determining the Space-to-Circle Ratio</i>	90
Figure 3.13 <i>A Two-Dimensional Packing Distribution and Measurements for Determining dimension of Pore Spaces (i.e. pore diameter)</i>	91
Figure 3.14 <i>Particle Shape Profiles (500 to 36 μm)</i>	91
Figure 3.15 <i>A Coin Box for Measuring Packing Efficiency and Sizes of Voids Between Different Sizes of Spheres.</i>	92
Figure 3.16 <i>Construction of Polymer Membrane Mould</i>	96
Figure 3.17 <i>A Highly Diagrammatic Interpretation of Ceramer membranes; Cross-Sectional View</i>	98
Figure 3.18 <i>Two Fabrication Processing Routes of Combining Polymer with Ceramic</i>	99
Figure 3.19 <i>Diagrammatic View Showing Removal of Polymer by Plasma Etching</i>	100
Figure 3.2 <i>Apparatus For In-Solution Mineralisation of Polymer Membranes</i>	101
Figure 3.21 <i>Graphic Representation of a Langmuir Film</i>	103
Figure 3.22 <i>Porous Ceramics Fabricated by a Sol-Gel Process</i>	106
Figure 3.23 <i>Basic Apparatus for Acid Titration to Determine the Strength of Acid Capable of Dissolving the CAB Cast or Bio-inorganic Mould</i>	107
Figure 3.24 <i>The Replamineform Process</i>	107

Figure 3.25 <i>Vacuum Assisted Polymer Impregnation Into a Porous Ceramic Block</i>	108
Figure 3.26 <i>Diagram of Apparatus for Thermal Polymerisation of Keratoprosthesis Shapes to Coral</i>	109
Figure 3.27 <i>Diagram of Apparatus for Ultraviolet Assisted Polymerisation of Keratoprosthesis Shapes to Coral</i>	110
Figure 3.28 <i>Ostwalds Viscometer</i>	111
Figure 3.29 <i>Pattern of Reflectance From A Very Rough Surface</i>	112
Figure 3.3 <i>Diagram Showing How Fractal Surfaces were Measured</i>	113
Figure 3.31 <i>Edge and Face Connectivity</i>	114

CHAPTER 3: Tables

Tables 3.1-3.16 Chemical Reagents Used in this Study

Table 3.1 <i>Chemical Reagents Used for In-situ Mineralisation</i>	80
Table 3.11 <i>Chemical Reagents for Biomimetic Ceramers</i>	80
Table 3.12 <i>Chemical Reagents for Histological Staining</i>	81
Table 3.13 <i>Chemical Reagents for Polymer Membrane Synthesis</i>	81
Table 3.14 <i>Other Chemical Reagents Used</i>	81
Table 3.15 <i>Biological Ceramics Used in this Study</i>	81
Table 3.16 <i>Natural Artifacts Used in this Study: Corals and Sponges</i>	82
Table 3.17 <i>Natural Artifacts Used in this Study: Other Natural Artifacts</i>	83
Table 3.18 <i>Biological Ceramics Used in this Study</i>	83
Table 3.19 <i>Compacted Ceramic Powders</i>	85
Table 3.2 <i>Particle Size Dimensions (μm)</i>	90
Table 3.21 <i>Pore Dimensions that Provide Strong Tissue Interlocking According to Different authors</i>	91

CHAPTER 4 RESULTS:

Fabrication of a Porous Biological Ceramic Support Frame for an Artificial Cornea

CHAPTER 4: Figures

Figure 4.1 <i>Diagram of a ` Jesse Shirley ` Hydroxyapatite Ceramic `Washer`</i>	122
Figure 4.11 <i>Stylised Diagram of OOKP Dental Plate Support Frame Highlighting Alveolar Bone Pore Sizes</i>	126
Figure 4.12 <i>Effect of Mixing Different Grain Sizes on Resultant Pore Size</i>	140
Figure 4.13 <i>Cartoons of the Different Types of Powder Mixtures</i>	141

CHAPTER 4: Photographs

Photograph 4.1 <i>Part of a Hydroxyapatite Disc Composed of Compacted and Sintered Particles</i>	121
Photograph 4.11 <i>Jesse Shirley Hydroxyapatite `Polo` (Porous type)</i>	122
Photograph 4.12 <i>3T3 Fibroblasts Residing on a Jesse Shirley Hydroxyapatite Disc: Sample F (1.56μm average pore dimension)</i>	124
Photograph 4.13 <i>Cross-Section Through Dentine, Periodontal Ligament and Compact Spongy Bone</i>	125
Photograph 4.14 <i>Sample E</i>	127
Photograph 4.15 <i>Sample F</i>	128
Photograph 4.16 <i>Sample G</i>	128
Photograph 4.17 <i>Sample H</i>	129
Photograph 4.18 <i>Grains of Hydroxyapatite: Sample A</i>	130
Photograph 4.19 <i>Grains of Hydroxyapatite: Sample B</i>	130
Photograph 4.2 <i>Grains of Hydroxyapatite: Sample C</i>	131
Photograph 4.21 <i>Grains of Hydroxyapatite: Sample D</i>	131
Photograph 4.22 <i>SEM Image of Coalesced 100μm Powder Grains with the Resultant Porosity</i>	135
Photograph 4.23 <i>SEM Image of Coalesced 36μm Powder Grains with the Resultant Porosity</i>	135

Photograph 4.24 <i>SEM Image of Coalesced 500μm Powder Grains With the Resultant Porosity</i>	136
Photograph 4.25 <i>Surface View of a Compacted and Sintered Hydroxyapatite Disc Made from 36μm and 100μm Grains</i>	136
Photograph 4.26 <i>Surface View of a Compressed Disc Composed of 100μm and Particles a</i>	137

CHAPTER 4: Tables

Table 4.1 <i>Biomedical Ceramics Considered as a Material for the Support Frame</i>	120
Table 4.11 <i>Hydroxyapatite Discs Fabricated by Jesse Shirley Ceramics</i>	121
Table 4.12 <i>Biological Evaluation of Jesse Shirley Ceramic Discs: A Summary of Results</i>	124
Table 4.13 <i>Powder Mixtures Compacted into Discs (All 50:50 by weight)</i>	133
Table 4.14 <i>Pore Dimensions for a Two-Dimensional Packing Distribution (μm)</i>	133
Table 4.15 <i>Percentage Packing Efficiency of Grain Mixtures</i>	134
Table 4.16 <i>Space-to-Circle Ratio of Grain Mixtures</i>	134
Table 4.17 <i>Porosity of Selected Compacted Grain Mixtures</i>	138
Table 4.18 <i>Basic Requirements for a Synthetic Structure that Imitates the OOKP Support Plate</i>	139
Table 4.19 <i>Achievements and Problems of Making Hydroxyapatite Discs from Assorted Powders</i>	141

CHAPTER 4: Graphs

Graph 4.1 <i>X-Ray Elemental Analysis of Sample F</i>	123
--	-----

CHAPTER 5 RESULTS:

Fabrication of a Ceramer Support Frame for an Artificial Cornea

CHAPTER 5: Figures

Figure 5.1 <i>Two Methods for Combining Polymer and Ceramic</i>	147
Figure 5.11 <i>Potential Designs for a Support Frame Copying the Tooth and Bone Structure</i>	152
Figure 5.12 <i>Porous Ceramics Fabricated by a Sol-Gel process and Adsorped</i>	

<i>onto a Hydroxyapatite disc</i>	156
Figure 5.13 Schematic Cross-Sections Through 4 Types of Ceramer	160

CHAPTER 5: Tables

Table 5.1 Polymers used in Hydroxyapatite Ceramers Taken from Recent Scientific Literature	144
Table 5.11 Porous Resin and Hydroxyapatite Mixtures (Ceramers) Fabricated in this Study	145
Table 5.12 Biogenic Additives Mixed with Ceramers	146
Table 5.13 Results of Ceramer Argon Plasma Etch	153
Table 5.14 Surface Roughness Measurements of Ceramers and Compacted Ceramic Grain Mixtures Using a Goniophotometer	155
Table 5.15 Basic Requirements for a Synthetic Structure that Mimics the OOKP Support Frame	161
Table 5.16 Achievements and Problems Fabricating Hydroxyapatite and Polymer Composites	162

CHAPTER 5: Photographs

Photograph 5.1 Cross-Sectional View Through a Ceramer (A) Comprised of Hydroxyapatite Beads	148
Photograph 5.11 A Ceramer Membrane Comprising a pMMA Matrix Embedded with 100μm grains of Hydroxyapatite and Particles of (soluble) Sucrose (125μm)	149
Photograph 5.12 A Ceramer Membrane Comprising a pMMA Matrix Embedded with Whiskers and Hydroxyapatite Particles (375μm)	149
Photograph 5.13 Failed Attempt to Synthesise a Periodontal Ligament Analogue Surface	151
Photograph 5.14 The Surface of a Ceramer Etched with Plasma (MMA and small Hydroxyapatite particles) for 3 hours	153
Photograph 5.15 Transverse Section of Ceramer Containing Hydroxyapatite Whiskers and Poly-tetrahydro-fur-furylmethacrylate (pTHFFMA) Polymer	154

Photograph 5.16 <i>Transverse Section of Ceramer Composed of Hydroxyapatite Whiskers and poly-tetrafurfurylmethacrylate (pTHFFMA) Polymer after 3 Hours of Plasma Bombardment</i>	154
Photograph 5.17 <i>Thermal SEM Image of Silica Gel Attached to a Hydroxyapatite Disc</i>	156
Photograph 5.18 <i>Image of Small Well-Dispersed Nucleating Foci of Calcium Carbonate Adsorbed onto a Hydrophilic Hydrogel (HEMA)</i>	158
Photograph 5.19 <i>Small Well-Dispersed Nucleating Foci of Calcium Carbonate Adsorbed onto a Hydrophilic Hydrogel (HEMA)</i>	158
Photograph 5.2 <i>Small Well-Dispersed Nucleating Foci of Calcium Carbonate on the Surface of a Hydrophilic Hydrogel (HEMA)</i>	159

CHAPTER 6 RESULTS:

Marine Derived Natural Artifacts as Potential Structures for an Artificial Cornea Support Frame

Figure 6.1 <i>A Selection of Invertebrate Skeletal Structures</i>	170
Figure 6.11 <i>Diagrammatic Representation of a Zooid Structure</i>	175
Figure 6.12 <i>Pore Structures of Sponges after Brusca and Brusca</i>	178
Figure 6.13 <i>Basic Anatomy of Coral Skeleton</i>	186
Figure 6.14 <i>Global Distribution Map of Porites species.: Most Commonly used Coral for Bone Replacement</i>	192
Figure 6.15 <i>Replamineform Processing of Natural Artifacts</i>	194

CHAPTER 6:Tables

Table 6.1 <i>A List of Foam Structures In the Plant And Animal Kingdom: Angiosperms and Lower Invertebrates</i>	166
Table 6.11 <i>A List of Foam Structures In the Plant and Animal Kingdom: HigherInvertebrates and Vertebrates</i>	167
Table 6.12 <i>Observed Pore Architecture for Natural Marine Artefacts Selected in this Study</i>	171
Table 6.13 <i>Naturally Derived Frameworks Applied for Human Reconstructive Surgery</i>	173

Table 6.14 <i>Final List of Animal Groups (mainly Marine) Investigated as Candidates for an Artificial Cornea Support Frame</i>	174
Table 6.15 <i>Pore Sizes of Selected British Marine Bryozoans</i>	177
Table 6.16 <i>Pore Sizes (diameter in μm) for Selected Sponges</i>	179
Table 6.18 <i>Pore Sizes (diameter in μm) of Spines for Three Species of Sea Urchin</i>	183
Table 6.19 <i>Physical Characterisation of <u>Goniopora</u> and <u>Porites</u> Corals</i>	188
Table 6.2 <i>Pore Sizes (diameter in μm) of Common Trabecular Bone-like Corals</i>	191
Table 6.21 <i>Physical Characteristics of Biocoral[®]</i>	201
Table 6.22 <i>Selected Physical Properties for Commercially Available Bone Replacements</i>	203
Table 6.23 <i>Achievements and Problems with the Selection of Suitable Natural Porous Solids and with the Replamineform Process</i>	206
 <i>CHAPTER 6: Photographs</i>	
Photograph 6.1 <i>Cross-Section Through the Stem of Mature Bamboo (<u>Phyllostachys</u> sp)</i>	168
Photograph 6.11 <i>Cross-Section Through the Stem of Immature Bamboo (<u>Phyllostachys</u> sp)</i>	168
Photograph 6.12 <i>An SEM Image of the Cellular Structure of Cuttlebone</i>	172
Photograph 6.13 <i>Enlarged Exterior View of Bryozoan Zooids</i>	176
Photograph 6.14 <i>Contrast of Porosity Between Bryozoan (Natural History Museum) and Trabecular Bone (Birmingham Dental Hospital)</i>	177
Photograph 6.15 <i><u>Potamolepis schoutedeni</u>; (x10 magnification) A freshwater sponge from the Congo. One of the candidates selected for casting and cell culture because of the regular hexagonal pattern of voids.</i>	180
Photograph 6.16 <i><u>Grantia compressa</u>; (x4) A Selected Calcareous Sponge</i>	180
Photograph 6.17 <i><u>Crateromorpha meyeri</u>; (x10): Belonging to the group of bath sponges</i>	181
Photograph 6.18 <i><u>Ianthella flabelliformis</u> (x4) A Selected Verongid Sponge</i>	182

Photographs 6.19 <i>Light Microscope Images of the Internal Structure of an Echinoderm Spine (<u>Heterocentrotus trigonarius</u>) (x18)</i>	184
Photograph 6.2 <i>Contrast Between a Section Through an Echinoderm Spine and Trabecular Jaw Bone</i>	185
Photograph 6.21 <i>Thermal SEM Images Comparing two Open Cell Natural Foams of <u>Goniopora lobata</u> (left) and <u>Porites porites</u></i>	187
Photograph 6.22 <i><u>Goniopora coral</u></i>	189
Photograph 6.23 <i>Surface of <u>Porites astreoides</u> Coral Showing a Unique Porosity and Surface Texture.</i>	189
Photograph 6.24 <i>Internal Structure of <u>Seriatopora octoptera</u> Featuring Two Grades of Pore Size</i>	190
Photograph 6.25 <i>An SEM Image of <u>Seriatopora sp.</u> Coral</i>	190
Photograph 6.26 <i>Contrast Between a Large Open Cell Coral (marked A) and Compacted Trabecular Jaw Bone.</i>	193
Photograph 6.27 <i>A pMMA Negative Cast (U.V polymerisation) of <u>Stylophora</u> Bifurcated Macropore Channels. (B. in Figure 6.82)</i>	195
Photograph 6.28 <i>A pMMA Negative Cast (U.V polymerisation) of a small Section of <u>Goniopora lobata</u>.</i>	195
Photograph 6.29 <i>A pMMA Positive Cast of <u>Stylophora</u> Showing the Distinctive Micropores and Macropores</i>	196
Photograph 6.3 <i>A pMMA Negative Cast (B) (U.V polymerisation) of a <u>Spongia(Keratosa)</u> Sponge with Broken Struts Caused by Repeated Acid Washing</i>	197
Photograph 6.31 <i>Positive pMMA cast (C) of a <u>Keratosa</u> Species</i>	197
Photograph 6.32 <i>Thin Transverse Section Through a Piece of <u>Biocoral</u>[®], Showing an Interconnected Void Structure</i>	200
Photograph 6.33 <i>SEM Thermal Image of a Fragment of <u>Biocoral</u>[®] Showing the Large Struts between Channels</i>	201

CHAPTER 7 RESULTS:

Fabrication of a Prototype Artificial Cornea from Coral and pMMA

CHAPTER 7: Figures

Figure 7.1 <i>Diagrams Illustrating the Reasons for Maximising Polymer Coverage into Pore System</i>	210
Figure 7.11 <i>Fractal Concepts Discussed in this Section</i>	210
Figure 7.12 <i>Typical Distribution of Polymer In a Small Block of Coral</i>	219
Figure 7.13 <i>A PTFE Mould Assembly for Cast Polymerisation</i>	220
Figure 7.14 <i>Two Mould Assemblies Fabricated in this Study (a) With Coral periphery (b) Without Coral</i>	221
Figure 7.15 <i>Criteria to Measure the Degree of Polymer Integration and Adhesion to Coral</i>	225
Figure 7.16 <i>STAGE A of Construction of a Prototype</i>	232
Figure 7.17 <i>STAGE B of Construction of a Prototype</i>	233
Figure 7.18 <i>STAGE C of Construction of a Prototype</i>	233
Figure 7.19 <i>Available Biocoral[®] Shapes</i>	235
Figure 7.2 <i>STAGE D of Construction of a Prototype</i>	236
Figure 7.21 <i>Figure 7.36</i> STAGE E	237
Figure 7.22 and 7.23 <i>STAGE F (Option 1 and Option 2)</i>	237
Figure 7.24 <i>Demonstrating the Two Alternate Positions for the Support Frame and Cornea</i>	240
Figure 7.25 <i>The Coralline Hydroxyapatite Artificial Cornea Devised by Leon</i>	241
Figure 7.26 <i>A Marine Inspired Coral and pMMA Keratoprosthesis.</i>	242
Figure 7.27 <i>Specific Dimensions of Marine-Inspired Artificial Cornea</i>	243
Figure 7.28 <i>Ideal Support Frame Shape</i>	244
Figure 7.29 <i>Two Shapes of Artificial Cornea Commonly Used</i>	245
Figure 7.31 <i>Attached Nylon Mesh for Insertion of Sutures</i>	246
Figure 7.32 <i>Likely Evolution of a Keratoprosthesis Optic by Artificial Selection</i>	247
Figures 7.33 to 7.35 <i>Illustrating the Stages of Assembly for a Natural Cornea Shaped and Coral Ringed Artificial Cornea</i>	249
Figure 7.33 <i>Stage 1: Shaping of the Coral Support Frame</i>	249

Figure 7.34 (a)-Stage 2:Method of Attachment Between Coral and Optical Cylinder	250
Figure 7.35 (b) Final Shape and Dimensions	250
Figure 7.36 The Best Attempt to Fabricate a Natural Cornea Shaped Coral and Perspex Artificial Cornea	251
CHAPTER 7:Photographs	
Photograph 7.1 Sintered Particles of Hydroxyapatite (Large particles mixed with whiskers)	211
Photograph 7.11 Thermal SEM Image of Sintered Particles of Hydroxyapatite (a mixture of 100 and 36μm particles)	212
Photograph 7.12 Thermal SEM Image of Biocoral[®] Crystals	212
Photograph 7.13 Embossed (to depth of 15μm) Surface View of Ceramic Disc Made from Spherical Particles (500μm)	217
Photograph 7.14 Embossed (to depth of 5μm) Surface View of Ceramic Disc Made from Hydroxyapatite Particles (100μm and a)	217
Photograph 7.15 Embossed (to depth of 5μm) Surface View of Ceramic Disc Made from Hydroxyapatite Whiskers	218
Photograph 7.16 <u>Porites</u> Coral Coated with pMMA in a Vacuum	227
Photograph 7.17 Fully Impregnated Region of <u>Porites</u> Coral in a Vacuum	227
Photograph 7.18 Contact Region Between pMMA Polymer and Base of <u>Goniopora</u> Coral Showing Contrasting Areas of Pore In-filling	228
Photograph 7.19 Prototype I: A Simple Optical Rod of pMMA Glued to a Biocompatible (Jesse Shirley) Hydroxyapatite `Washer`	231
Photograph 7.2 Close View of the pMMA Rod with Repeated Machining Grooves	232
Photograph 7.21 Region of Biocoral[®] Completely Infilled with Acrylic Glue. (From prototype III) Two pores are highlighted.	234
Photograph 7.22 Layer of Acrylic Glue Bonding Biocoral[®] to Optical Cylinder	234
Photograph 7.23 A Biocoral[®] Trepine Plug with a 5mm Hole for the Insertion of an Optical Cylinder	236
Photograph 7.24 Biocoral[®] Shapes and the First Prototype Prosthesis	238

Photograph 7.25 <i>The Second Prototype with a Larger Support Frame Diameter and Smaller Base</i>	238
Photograph 7.26 <i>Layer of Acrylic Glue Bonding Biocoral[®] to Optical Cylinder</i>	239

CHAPTER 7: Tables

Table 7.1 <i>Surface Roughness Measurements of Ceramers, Corals and Compacted Ceramic Grain Mixtures Using a Goniophotometer</i>	209
Table 7.11 <i>Assessment Criteria for the Completeness of Bonding Between <u>Porites</u> and pMMA</i>	212
Table 7.12 <i>Distances from Base, that MMA Monomer is Carried to by Capillary Action after 5 minutes of Immersion</i>	213
Table 7.13 <i>Distances from Base, that MMA Monomer is Carried to by Capillary Action after 90 minutes of Immersion</i>	214
Table 7.14 <i>Percentage Coverage and Integration of Polymer into 'Open Celled Coral Skeletons</i>	215
Table 7.15 <i>Relationship Between Irradiation Time and Viscosity Caused by Increased Cross-Linking Density</i>	219
Table 7.16 <i>Achievements and Problems Associated with the Design and Fabrication of Prototype Coral and Perspex Artificial Corneas</i>	252

CHAPTER 7: Graphs

Graph 7.1 <i>A Richardson Plot Comparing Three Kinds of Biological Ceramic Considered as a Tissue Bonding Support Frame</i>	213
Graph 7.2 <i>Goniophotometer Measurements: Trace of Light Intensity for <u>Porites</u> Coral</i>	214
Graph 7.3 <i>Goniophotometer Measurements: Trace of Light Intensity for Collagen Gel</i>	215
Graph 7.4 <i>Goniophotometer Measurements: Trace of Light Intensity for Hydroxyapatite Beads</i>	215
Graph 7.5 <i>Extent of Polymer Infiltration into Open Celled Corals and Cow bone (with standard error bars)</i>	226

Graph 7.6 <i>Graphical Representation of the Extent of Polymer Infiltration into Pores (with standard error bars)</i>	228
--	-----

CHAPTER 8:

RECAPITULATION, DISCUSSION and CONCLUSION

CHAPTER 8: Tables

Table 8.1 <i>Key Requirements for a Synthetic Structure that Imitates the OOKP Support Frame</i>	256
Table 8.11 <i>Achievements and Challenges of Making Hydroxyapatite Discs from Assorted Powders</i>	260
Table 8.12 <i>Cross-sectional Cartoon Through Ceramics Fabricated in this Thesis</i>	261
Table 8.13 <i>Achievements and Challenges of Selecting Suitable Natural Porous Solids and Employing the Replamineform Process</i>	262
Table 8.14 <i>The Major Causes of Artificial Cornea Failure (a)</i>	268
Table 8.15 <i>The Major Causes of Artificial Cornea Failure (b)</i>	269
Table 8.16 <i>A Cost Comparison Between the OOKP and a Future Synthetic OOKP</i>	271
Table 8.17 <i>Positive Attributes of Hydroxyapatite as a Biological Material for Human Implantation</i>	272

CHAPTER 8: Figures

Figure 8.1 <i>Cartoons of Assorted Powder Mixtures Before Compacting that were Employed in this Thesis</i>	257
Figure 8.11 <i>Schematic Representation of Methods Used for Making a Ceramic Support Frame for a Synthetic OOKP</i>	258
Figure 8.12 <i>A Flow Chart Summarising the Types of Experimental Work Carried Out in this Thesis</i>	259
Figure 8.13 <i>Stylised Cross-sectional Cartoon Through Ceramics Fabricated in this Thesis</i>	260
Figure 8.14 <i>Stages of Fabrication of a Coral and pMMA Artificial Cornea</i>	264

Figure 8.15 <i>A Schematic Drawing of a Standard Design of Artificial Cornea</i>	266
Figure 8.16 <i>Hypothetical Synthetic Periodontal Ligament Analogue Between pMMA and Porous Coral</i>	274
Figure 8.17 <i>Fabrication Strategies for a Biomimetic OOKP</i>	275
Figure 8.18 <i>Essential Features of the Coral and pMMA Artificial Cornea</i>	276
Figure 8.19 <i>Cross-sectional View Through the Anterior Eye to Show an Implanted Coral and pMMA Artificial Cornea</i>	277
Figure 8.2 <i>Suggested Additional Features of Design for a Coral and pMMA Artificial Cornea</i>	279
Figure 8.21 <i>Summary of Suggested Further Work</i>	280

CHAPTER 1
LITERATURE REVIEW: Artificial Corneas

CHAPTER 1

LITERATURE REVIEW: Artificial Corneas

"We are a bundle of genetic flaws. The body is a fragile, jury rigged device. Our job as physicians is to fix nature's oversight"

Nesse and Williams

1.1 Introduction

The artificial cornea is a device that replaces severely diseased, damaged and opaque corneas. Corneal transplantation is the preferred therapy for returning sight to the corneal blind, but where it does not work artificial corneas are used instead. There are two types of design currently in use—the core and skirt model and the one-piece model. Both models possess two distinctive parts. The optical window allows light to pass across the damaged corneal remnants onto the retina, while the surrounding flange or support frame bonds to ocular tissue and keeps the optical cylinder in one place. Many of the best and most recent implant designs employ a standard optical window supported by a novel support frame, made from an assortment of materials. Despite innovations in material type, implant shape and size many complications arise. Many of the most common complications arise from ulceration, necrosis and inflammation owing to biological causes, such as an accumulation and the upregulation of leukocytes and proteolytic enzymes rather than as a result of material toxicity. In fact it is material type (surface chemistry and charge) that provokes these responses and eventually leads to implant expulsion.¹

The material scientist has much to do in balancing the operation of two major functions: optical clarity and image stability, which is well worked out; biological incorporation, which is poorly enacted and lifetime interaction, a distant hope. Finally the matching of mechanical properties with the cornea maybe equally important for which the advent of semi-interpenetrating network hydrogels is an emerging possibility.² Research into keratoprosthesis has been, recently revitalised by refinements in the synthesis of composite materials and improvements in biological performance.³ Significant progress has been achieved along with the emergence and application of microsurgery, new drugs and rational design of materials.⁴ Many are

striving to overcome the effects of biological antagonism toward these novel materials, with the use of intricately structured materials and structural biological materials such as collagen.⁵

All but one kind of the batch of present artificial corneas have a proven record of long-term success. The Osteo-odontokeratoprosthesis (OOKP) is made from biological graft tissue and this enables the formation of a firm long term union to the optical window. There are other recent designs which, have emerged with the likelihood of matching the good success rates of the OOKP. Highly promising designs are those of Chirila⁶ and Legeais⁷ which have demonstrated excellent results from implantation. Further details are presented later on in this chapter. Before an investigation is made into the efficacy of the OOKP, this Chapter describes the biology of the cornea in health and disease, surgical interventions for returning sight and an overview of notable past and current keratoprosthesis designs.

1.2 The Cornea in Health and Disease

1.2.1 The Cornea: Structure and Physiology

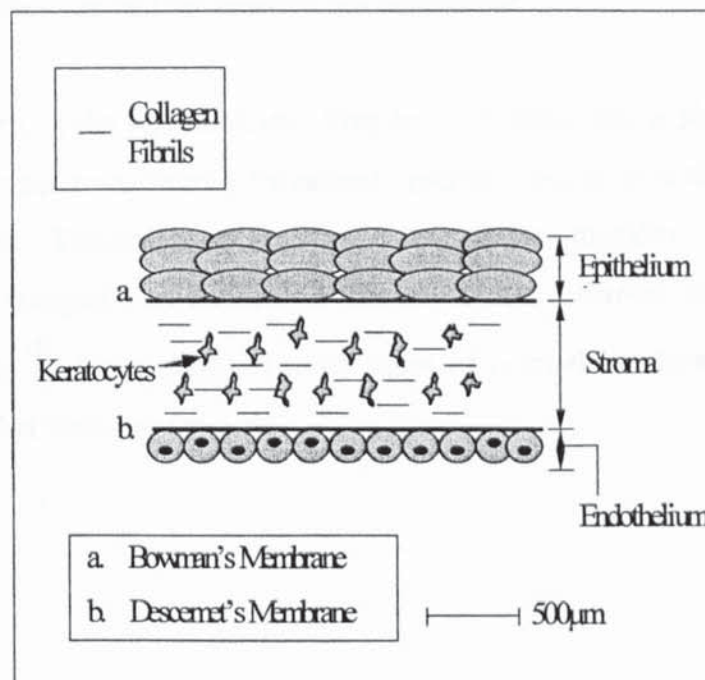
The eye is a gelatinous orb that collects, guides and filters light before transforming it into a series of electrical impulses which are marshalled and interpreted into a clear image by the perceptive centres of the brain. The cornea is the transparent window and although seemingly without substance carries out these specialised tasks, except for light perception and imaging.

The cornea is a thin multiple-layered transparent piece of tissue situated at the anterior of the eyeball. It is very tough, it does not have blood capillaries; which would otherwise reduce transparency and is highly innervated to ensure rapid detection of damage and instigation of repair.⁸ The cornea is the point of entry for light into the eyeball. It transmits and bends incoming light onto the lens, but also serves as a barrier to the entry of pathogens and to fluid loss. Its surface is protected and lubricated by a multi-functional layer of watery fluid called the tear film. Tears are made from a complex mixture of lipid oils, mucus, carbohydrates and cells involved in immunity.⁹ Without a tear film the ocular surface dries out, warps or thins and leads to blindness.

At the outermost layer of the cornea epithelial cells are regularly shed and renewed and therefore moderate physical damage has no disruptive effect. This process also ensures that bacteria and viruses attempting to penetrate the eyeball are removed from the surface of the cornea. When the tear film is poorly formed or lacking the passage of pathogens is made easier. Also, healing is slower and less well defined.

Three distinct layers of tissue make up the cornea; outermost is the epithelium composed of five to seven layers of cells resting on a basement membrane in contact with a connective tissue stroma. Below the stroma is the endothelium. The cells of the epithelium are very active. The epithelial surface is covered with sugar residues which are immersed in the mucous layer of the tear film and serve as points of attachment for antibodies (IgG).¹⁰ The middle region, the stroma forms the bulk of the cornea (90%) and is composed of a highly ordered meshwork of collagen fibrils interspersed with keratocytes.¹⁰

Figure 1.1 Diagrammatic Cross-Section of a Healthy Human Cornea



The exact orientation of fibrils in addition to the radius of curvature of the cornea are

crucial to giving the cornea its transparency. Collagen fibrils are arranged in a manner in which, the wave pattern of light passing straight through the cornea and the wave pattern of light scattered by the solid elements making up the cornea become perfectly aligned in what is called constructive interference. It is more likely that light scatter is removed by the scaling of the refractile elements to just below the wavelength of visible light.¹¹

Diseases and disorders which affect nutrition of the cornea and the flow of water across the cornea do so by changing the thickness and amount of bound water. Water pressure in corneal tissue, structures the fibrillar matrix and acts as a reservoir for gaseous exchange. The amount of water is regulated by a complex series of intercellular pumps and the structuring and arrangement of cell junctions. When the mechanism of hydration breaks down severe visual impairment and blindness result.¹²

Very severe diseases of the cornea alter collagen fibril arrangement and while the epithelium is able to properly regenerate the stroma cannot do the same. The initiators of collagen fibril arrangement are the keratocytes. They are highly specialised cells and once damaged they can neither function nor regenerate.

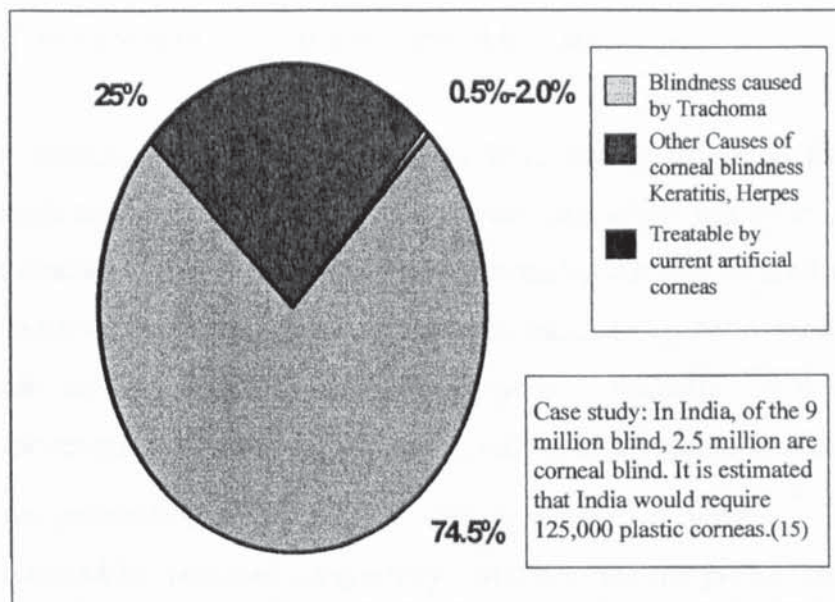
Lying posteriorly is the endothelium. This layer of tissue has a physiological role in maintaining corneal transparency by actively pumping water from the stroma into the anterior chamber. This maintains the stroma at a constant turgidity. If too much or too little water is pumped posteriorly the fibrils become distorted and clump together causing opacity.¹² Surprisingly in most cases of corneal blindness the endothelium remains intact but does not function.

1.2.2 Corneal Blindness

There are approximately 42 million blind people world wide (Research to Prevent Blindness Incorporated).¹³ A quarter of this total reside in developing countries (21.4 million in Asia; 7.1 million in Africa). The tragic irony of this staggering figure comes with the underlying statistic in which, 75% of adult blindness is curable or preventable with current medical interventions.¹³

An important percentage of incurably blind suffer due to non-transparent corneas- globally 11 million are reported to be corneal blind (a large proportion have light perception) mainly as a result of trachoma¹⁴ (Graph 1.1). A large proportion of these people cannot obtain or morally accept use of donor corneas used in less severe forms of corneal defects and dysfunction, e.g Herpes and keratoconus. In developed countries the vast majority of corneal blindness can be corrected by insertion of a donor cornea, but not always. Thus, the potential for artificial corneas is vast and is likely to expand.¹⁵

Graph 1.1 *Global Corneal Blindness Divided into its Major Causes*



It is estimated that six to nine million are blinded by a preventable infectious disease, trachoma, caused by *chlamydia* in water supplies. Since trachoma affects the most economically poor with the highest population growth this figure will double to twenty million in the next ten years.¹⁶

1.2.3 Corneal Transplantation

Corneal transplantation is preferred treatment for correcting abnormalities of the cornea with a 90% success rate. Successful retention of a corneal graft depends upon three factors peculiar to each patient, these being: the degree of vascularisation, age of the recipient and the size of the corneal button.²³ Unfortunately donors are difficult to obtain and once received donor material has to be used within weeks or sometimes days from the time of death of the donor. As with all awaiting recipients, there is not always a donor available.

A corneal transplant may also be contaminated with diseases like syphilis, leukaemia and Acquired Immune Deficiency Syndrome (AIDS) even after careful screening. Consequently, there is still need for a worthy artificial replacement which in addition to treating severe cases of corneal blindness would offer an alternative therapy for patients intolerant of transplants or where donor material is in short supply.

New developments in cornea reconstruction have mostly arisen in the science of corneal transplantation where much of the money and effort has been concentrated. There are a number of existing approaches to enhancing the role of graft tissues of the cornea in replacing opacified corneas, such as vaccines, genetic modification and biodegradable scaffold sustained cultured biopsies. Recently Thoft developed a procedure for severe ocular surface disorders, only ever corrected by keratoprosthesis where normal penetrating keratoplasty carries unsatisfactory results.¹⁸ However, its efficacy is blighted by increased antigenicity. Methods for the prevention of rejection will significantly reduce the remaining ten percent of corneal transplants that fail.

Many techniques in genetic manipulation have been developed to reduce the incidence of graft-host rejection which, is still quite apparent. These techniques include more accurate human leukocyte antigen (HLA) typing and the possibility of Xeno-transplantation. Xeno-transplantation is becoming increasingly more likely with the ability to introduce human genes into other animals safely with greater levels of expression. Corneal xeno-transplants are likely to be removed from pigs because pig corneas are very similar to the human cornea. Though it must be realised that they too will be subject to the same problems that afflict human graft corneas without the hindrance of poor availability.

Influenced by this preference for biological replacements rather than synthetic materials, research at one stage focused upon the creation of corneal replicas made from natural materials that clearly possess the attributes of graft tissues for melding with host tissues. Examples are retention plates made from bone,¹⁹ nail and claw,²⁰ tooth (Further details in Chapter 2), cartilage²¹ and more recently reconstituted collagen patterned by design.²²

1.3 The Need for an Artificial Cornea

Much like any other externalised region of the body, the cornea is susceptible to wounding from a variety of causes from scratching, warping, etching and thinning through to scarring of the ocular surface. The cornea is subjected to disruption and impairment through the deleterious effects of infectious agents, (e.g. herpes simplex virus), degenerative diseases (e.g., dystrophy) and physiological abnormalities, (e.g. glaucoma) Unlike other ectodermal tissues, however its ability for functional self-repair is impoverished in all the most severe forms of corneal blindness where progenitor cells are all but destroyed and the intricate nerve apparatus is disfigured. Skin is often damaged and quickly repairs itself because its primary function is defence. Natural selection has enabled tissues to regenerate according to frequency of damage and capabilities that optimise fitness (adaptation to survive in the current environment)

The cornea, which is prone to damage, is swathed in protective mechanisms that act

quickly to prevent damage to delicate regions of the anterior eye. Once these are made dysfunctional repair manifests itself in a chaotic manner to seal the wound as rapidly as possible, yet as a consequence the original function is lost. Usually complex organs are so far differentiated that reconstruction by redifferentiation of remaining and recruited cells is insufficient. Furthermore, there are implications for surgical intervention such, that when the cornea is either in the initial open and inflamed state or healed into a soft vascularised fibrous scar tissue it becomes much more intolerant to corrective surgery.

At present, seriously harmed cornea can be surgically replaced with donor grafts, or resurfaced with host limbus. In such transformed corneas, outlying regenerative 'stem' cells divide and migrate, eventually weaving together with their surroundings into one coherent, healed and reformed cornea.²³ In cases with good prognoses success occurs in nine out of every ten patients. As a result of injury and the effects of host responses, the stroma (the element that gives the cornea its structure) is replaced by a protective fibrous scar tissue and a layer of epithelium or conjunctiva. If this protective barrier is altogether removed and replaced with a transplanted cornea it may return and finally overrun the inserted corneal graft and cause opacification, so grafts are not entirely without problems. Severe damage to the corneal stroma, i.e those caused by caustic burns cannot be adequately treated and corrected.

Although dramatic advances have been made in corneal transplantation, and as a successful cure for mild forms of corneal blindness there remains a set of restrictions to it being universally available and widespread among all forms of corneal blindness. These vary from lack of available donors to strong religious objections, particularly in the developing world.²⁴ In contrast, a truly successful artificial cornea, once a number of formidable challenges (e.g. gradual ulceration) are dealt with, would have the potential to become widespread, because it would be simple to manufacture into a simple shape and form and so, therefore simple to implant, cheaper to obtain and it would be freely customised to suit the features of a patients eye.⁴ Advantages of this kind are difficult to make real because it requires fabricating tailor made materials with the propensity to manipulate a complex interconnected network of biological subtleties.

Due to the overwhelming lack of success, i.e. frequent rejection, most current types of artificial cornea are temporary 'stop gap' measures, whose primary function is to seal the anterior chamber of the eye from infection at least until a suitable graft replacement can be found. In a number of severe conditions where the stroma is badly damaged and disfigured (for example, chemical burns) keratoprosthesis offer the only hope of returning sight to a patient.²⁵ Visual acuity and light perception are oftentimes vastly improved in the short run. (visual acuity varies from 1/20 to 6/12 after implantation. Visual acuity is the fraction that expresses the ratio of two distances equivalent to the ratio of the patients visual acuity to a normal person²⁵).

Implant exclusion and rejection of the device is the most serious, and unfortunately the most common, post-operative complication notwithstanding administration of drugs to suppress excessive host reactions and inflammation. Approximately, 80% of keratoprostheses will fail the patient within the first 2 years. That is well above the level for donor corneas.²⁵ For years the poor comparison with donor corneas has it seems been attributed to an absence of good design and a misconceived idea of how material attributes are meant to behave in the human body.

1.4 Conclusions

The cornea is an amazingly complex organ which performs many functions. It is highly resilient and resistant to damage. However, like every structure evolved through a process of optimisation, there are limits to its vitality and ability to correct damage while retaining perfect vision. Incidents involving severe damage such as, chemical burns and auto-immunity cannot be satisfactorily repaired and corrected without human intervention and even then, sight is impaired. So long as other parts of the eye are in good functioning order, surgery can introduce graft replacements or in exceptional circumstances synthetic replacements. Corneal blindness is particularly prevalent in the third world. A safe and reliable alternative to grafting and the option to return sight in the most severe cases of blindness, would be of great value and help in improving the quality of life for a substantial number of people, as illustrated in Graph 1.1.

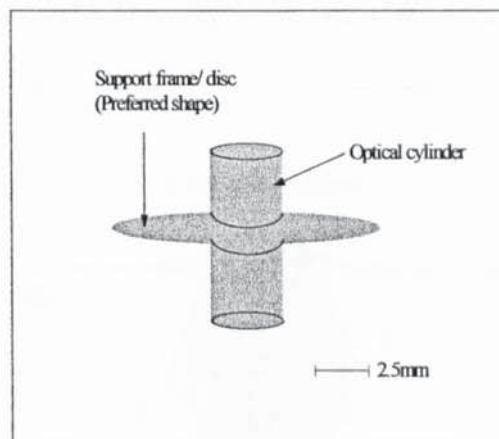
1.5 Keratoprosthesis

1.5.1 Introduction

The keratoprosthesis is a synthetic implant, designed to permanently deputise the functions of a normal transparent cornea in eyes with severe opacities and leucomas. The modern artificial cornea consists of two structural elements, the optic transmits and refracts light onto the retina, while a peripheral retaining plate functions to fuse with surrounding inward growing tissue from the periphery of the globe and so,

- (a) supports the entire implant and
- (b) reinforces the cornea.

Figure 1.11 *Structure of a Modern Artificial Cornea: The Popular Core and Skirt Model.*^{14,24,27} (Other types of model include monoblock and Tissue Graft)



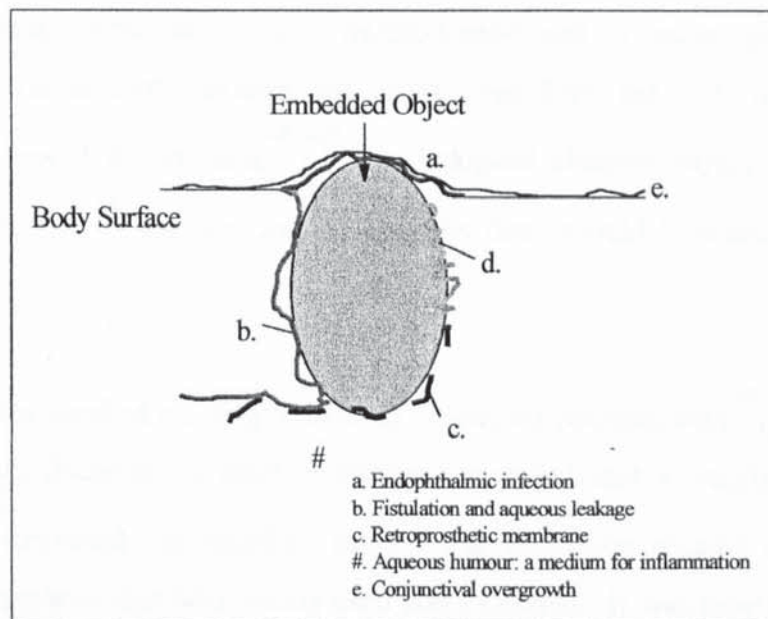
A vast majority are implanted into the cornea, complemented by autotissue reinforcement such as the sclera and conjunctiva, although a few types of artificial cornea are placed on top of the cornea and secured by more substantial quantities of graft tissue.²⁶

Presently there is a move toward better use of well designed high performance materials-made to stringent guidelines-especially polymer felts. The term superstructure has been 'coined' to structural designs incorporating a number of levels of fibre organisation.²⁷ Felts, webs (looser versions of felts with greater vacuities) and planned, ordered networks have been implanted into eyes with moderate colonisation

by ocular cells.²⁸ Modern polymers have been very useful because, they can be easily moulded into any desired shape and are resilient to a range of chemical solvents and physical conditions.

A synthetic replacement for any severely damaged cornea is unfortunately a far from universal solution, but not far enough to favour surgical redundancy. Every design has been subject to numerous complications and however many design modifications are made, these problems are not removed (See Figure 1.12). Material type and structure are elements of design that need to be dramatically improved to stop necrosis, ulceration and fibrous tissue build-up. Infection, conjunctival overgrowth, epithelial downward growth, dystrophy and vitreous coagulation are only to be solved by meticulous surgery and tissue engineering strategies.²⁸

Figure 1.12 *The Major Causes of Implant Rejection*



1.5.2 Early History of the Artificial Cornea

The extraordinary idea for a replacement cornea came into life in 1789. Guillaume Pellier de Quengsy wrote a comprehensive treatise on the insertion of a silicate-lime glass plate into the human eye to cure corneal blindness.²⁹ Medics in Germany took up the concept of implanting glass plates and discs into the corneal stroma, with a little more success. In 1852 Nussbaum implanted a plate into the rabbit cornea that lasted

for three years, by adding extra-corneal fittings.³⁰ In humans Weber reported a retention time of six months and von Hippel reported one case out of seven surviving for one year.³¹ Modifications were made of the Nussbaum model; Dimmer³² for instance, incorporated celluloid and Salzer³³ ingeniously combined egg membranes for tissue attachment, but all were extruded. Surgery at that time compounded the brave efforts to fabricate an artificial cornea. Aqueous humour infiltrate caused infection and tissue destruction. There were many complications which lead to extrusion. Retroprosthetic membranes would readily encapsulate the optic and the implant surfaces caused tissue melting.

Work began once more in the late 1940's with acrylic variations on the Nussbaum, 'stud model'.³⁰ By 1950 new models appeared that were distinctly different from previous designs, combining extra-corneal and intra-corneal retention plates.³⁴ Intra-corneal plates were punctured with holes to allow corneal tissue to grow through and secure the implant. Perforations were deemed important to maintaining a healthy balance and distribution of nutrients and electrolytes from the underlying aqueous humour and so avoid dehydration.^{35,36,37} Pathological changes would not manifest themselves so severely.³⁵ Thinner, smaller diameter discs should have reduced corneal degeneration.

Stone and Herbert worked on design features in varying permutations³⁵ (perforations, thickness of disc, diameter of disc) Cardona concluded that a deeply penetrating retention plate increased the retention time.³ Cardona soon created a mushroom shaped keratoprosthesis that was widely used and emulated. It was proposed that the anterior *contact lens* was a barrier to excessive evaporation and tissue wasting.³⁸ Later silicon and metals were tested in animals, as they were with joint prosthesis, but had little affect on membrane formation and corneal thinning, hinting at further structural improvements.³⁹ Fyodorov recorded an extrusion (or ejection) rate of 20%- quite low in comparison with previous types- suggesting the additional influence of surgical technique to the success of an artificial cornea. A principal tendency during the early

1970's was to make the retaining plate as thin as possible to do the following:-

- reduce separation of lamellae of the cornea
- allow diffusion across the material.

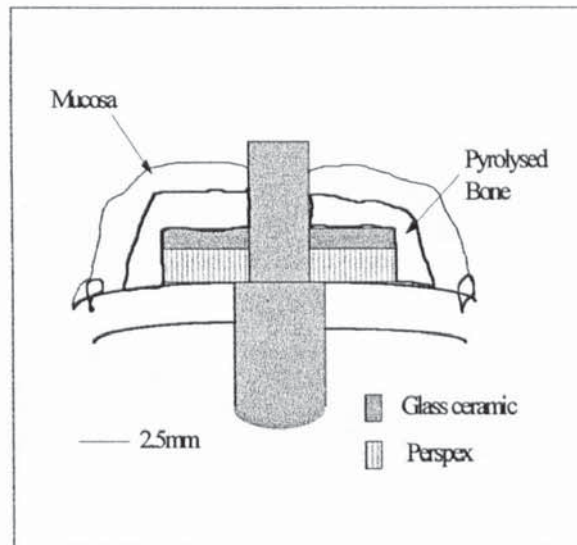
Stone and Choyce believed that a removable optical cylinder was beneficial, because it reduced 'operational injury' and allowed for post-operative care, but in hindsight this was a retrograde step since the model was cumbersome and impermeable.³⁹ One of the most influential and useful techniques of re-inforcing the cornea for implantation of an artificial cornea was enlistment of live tissue from elsewhere in the body. Krasnov employed conchal cartilage, while Cardona and his team used rabbit claw, due to the embryological and histological similarities and uniformity of protein production expressed by both biological materials.⁴⁰ The use of autotissues (same tissues from the same individual) and homotissues (same tissues from related individuals) such as bone and knee cartilage limits contact of live cornea to the implant and therefore, limits unwanted tissue responses (up-regulation of proteolytic enzymes)(See Table 1.1).

Table 1.1 *Autotissues Used for Artificial Corneas: Autologous tissues provide components with multiple action, provide stable physical and biological interactions with the wound, provide an adaptive response and have the capacity to regenerate.*^{19,20,21,40,41,42,44,45}

Homo-and Autotissue for Securing Implant	Supporting Plate
Mucous membrane overlying periosteum	Rabbit claw
Conjunctiva	Knee joint cartilage
Tendon	Silica gel
Periosteum	Bone
Mucous membrane	Ceramic glass
Claw particles	oxide ceramic
Conchal cartilage	Periosteum
Sclera	Ear cartilage
Lip mucosa	Conjunctiva
femoral fascia	Dried cornea
Dura mater	
Egg membrane	

With the advent of the OOKP (Explained in Chapter 2) there followed ceramic glass and aluminium oxide ceramic analogues.

Figure 1.14 *Schematic Cross-Section of the Glass Ceramic and Bone Keratoprosthesis.*



The first synthetic Osteo-odonto-keratoprosthesis analogue was developed in 1978 by Blencke et al. and Hoffman et al.^{45,46} Ceravital[®] glass ceramic is the replacement for dentine. From 1967 synthetic fibres were extensively tested and applied, PTFE and Dacron[™] were remarkable improvements because they would shape well and form webs and felts with a macroporous structure.⁴⁷ They are the favoured materials of current artificial corneas.

Table 1.11 *Key Steps in the Early Development of Artificial Corneas From 1789 to 1993*

Innovation	Advantages
Single plate substitute (30)	
Two-plate substitute (stud type)(31)	Greater stability
Surgical techniques to improve fixation to outer eye	e.g. Sutures: tied to stronger support tissue away from cornea
Intra-corneal and extracorneal securing devices	Prevent expulsion by formation of membranes
Nut and bolt type (with removable optical cylinder) (3)	Allows for surgical intervention after insertion and change of optics
Openings in the plate	Free flow of nutrients and water across prosthesis
Radial processes (25)	Stronger fixation
Increased diameter of supporting plate	Better mechanical support
Experimentation with different sized plates, shapes, numbers of holes and arrangement of holes in the plate (3,5)	Best compromise between mechanical fixation, biointegration and fluid flow
Increased size of the perforated plate	Improve integration with stroma
Use of autologous tissues (20,21,40,42)	Highly compatible and long lasting. Perfect shape
Perfect shape of plate and further expand perforate area (35)	Reduce stress field around device & increase cell integration
Sophisticated technique in polymer synthesis (6)	Remove core-skirt interface
Hydrogel plate substitutes (6)	Mimic tissue structure and enable ingrowth of cells

#

1.5.3 Recent Developments in Keratoprosthesis Design.

In the past few years significant improvements have been made to the artificial cornea to eliminate delamination and dis-adhesion.^{28,48,49} Recent innovations in the design of keratoprotheses has increased optimism that in the future a device will be retained

#Very significant advances for retention are in **bold**

comfortably and permanently in the most severely damaged of corneas.

A powerful device for resolving implant centred complications has been void structure. The shape and dimensions of voids affects tissue structure inside the pores. Suprisingly, it was found that only recently that porous skirt materials encourage a more coherent union with the wound edges and this substantially reduced the rate of expulsion.^{49,50} This is because, cells and matrix proteins can infiltrate much deeper into the material. With a sufficiently strong adhesion between tissue and material surface, leakage of aqueous humour to the surface and the potential for infection are minimised.

Pores and channels must be large enough and arranged in a specific configuration to acquire a tight interpenetration. Webs and meshes create accessible spaces which maximise the area of cell contact while at the same time optimise mechanical strength and flexibility.²¹ Webs and meshes are thought to be the most useful structures for incorporation into the remaining elements of the cornea. A web or mesh consists of many interwoven filaments. An individual filament restricts space to its own volume, unlike a porous system. which, restricts space to the surrounding area and volume. As a result, possible cell contacts are more restricted. A highly ordered interconnected porosity would, however allow contact in three dimensions. All cells sense their environment in three dimensions.

Meshworks can possess a measure of toughness and modulus closer to the normal cornea, than say a porous solid, but the porosity has less permanency under the deforming force of the eyelids during blinking and the pressure of intra-ocular fluids which are usually increased after the anterior segment is reconstructed.²⁷ To a great extent the infiltrated tissue should resist the bulk of such destructive forces. However, they are often not tough enough to prevent sutures from tearing through the material after insertion.

Polymers intended for artificial corneas have originated from contact lenses and corneal inlays because, transparency and permeability are generally similar to that required for residency in the stroma.⁵¹

Polymers must be fully polymerised to prevent elution of residuals of monomer and they must also be processed avoiding noxious solvents. Villain points out that long term success will result from more rigorous polymer selection and quality control.⁵²

It was Kain who first attached a highly porous rim to an artificial cornea made from silicone rubber. Incidentally silicone was later to feature quite strongly in later keratoprosthesis by virtue of its combination of high oxygen permeability, rigidity and optical clarity.⁵³ The periphery of the Kain model was composed of a mesh of carbon fibres arranged into a network of filiform shaped voids.⁵³ Capecchi et al. fabricated a mass of melt drawn fibres having a similar pore network made from polyolefins, polyvinylalcohol (PVA) and polyvinylpyrrolidone (PVP).⁵⁴

White et al. employed a silicone ceramic and complexed it with chemically modified human tissue.⁴⁵ Kain was one of the first to incorporate a highly porous rim in an artificial cornea made from a silicone rubber.⁵³ Other researchers tested the validity of the principle for inserting hydrogel sponges with some success.

Trinkaus Randall paralleled the design features of Kain, with a fibrous structure composed of a blend of two polyolefins, glued to a vinyl containing polymer core.^{12,55} Stromal fibroblasts were able to invade the fibrous periphery but problems arose because there was an inadequate union between core and periphery. Legeais et al. has made a careful and important contribution with a retention plate designed to improve tissue tolerance and adhesion. Micropores and macropores enable the formation of highly organised collagen fibrils. Other researchers tested the validity of inserting hydrogel sponges with some success.

Hydrogels are polymers with a high water content provided by swelling between macro-molecular chains. Water is a good solvent and permits consistent, relatively unhindered transport of gases and solutes across the hydrogel membrane. The surface chemistry can be quite accurately tailored to suit compatibility with the tear fluid by

adding functional groups to the polymer backbone. Much is known about the chemistry of synthesis and combination of different monomers. Materials can be carefully designed to possess varying physical structures and unique chemical properties. This is exceptionally important to the design and fabrication of important materials which, require a carefully balanced set of properties for a specific situation.

Chirila and his team of researchers have employed simple hydrogel chemistry to manufacture a keratoprosthesis that can biologically integrate⁵⁶ (See Section 1.5.41). They have been able to overcome the problem of combining a solid transparent element or (the optical core) with a spongy, opaque periphery, using interpenetrating polymer network forming (IPN) technology to form a graduated fully interpenetrative bond between the two elements. The spongy periphery encourages rapid fibrovascular inward growth into the pore spaces. The rate of inward growth is crucial to the formation of a strong attachment and to prevent infection from taking hold. As it develops, and builds in all directions the tissue interlocks firmly with the struts and cell vertices. Chirila has recorded retention in eight out of ten of patients, with very few complications.^{56,57}

Wu's group compared the biological interaction of corneal stroma between varying polymer types and the activity of extracellular matrix.⁵⁵ All were modified with argon plasma bombardment. In a twelve week study the following processes were identified and measured: extent of fibroplasia (relates to amount of tissue integration), distribution of matrix proteins (ability to support and shape regenerated tissue) and the quantity of growth factors (Beta Fibroblast growth factor (β -FGF) and tissue growth factor (TGF- β) for improved collagen binding) (the signals which direct tissue re-growth in time and space).

With plasma bombardment of synthetic surfaces both corneal oedema and neo-vascularisation were significantly reduced.⁵⁵ Quantities of collagen were not material dependent and is most probably related to architecture, but the expression and distribution of growth factors was dependent on material type

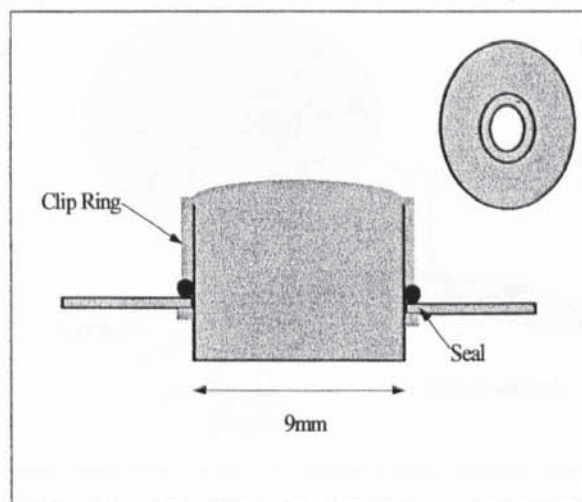
1.5.4 Exceptional Artificial Corneas

In the past decade there has been growing activity in the design and development of novel keratoprosthesis and a number of these have shown considerable promise in experimental trials. Exceptional is defined by: the average number of complications that occur after implantation, the efficacy of biological attachment (i.e. average retention time) and the accuracy of solutions to material problems.

First mentioned in this section is Legeais et al., who have fabricated an artificial cornea comprising polymer meshworks inserted into the corneal stroma.⁴⁹ Healthy tissue invades the structure and maintains its structure and function. The rate of expulsion is very low and inflammation is uncommon. The device engineered by Chirila has sought to tackle the supreme problem of combining two differently structured materials, where one must function as an optic and the other as a tissue bonding element.⁵⁴ Kornmehl invested a plastic optic with reconstituted collagen, the main structural ingredient of the cornea. Use of collagen is noteworthy for it is an attempt at recreating a more natural replacement using naturally occurring building materials.⁵⁸

1.5.4.1 The Artificial Cornea of Legeais et al.

Figure 1.14 *Microporous Fluorocarbon Meshwork Support Frame and polymethyl methacrylate (pMMA) Core*⁴⁹



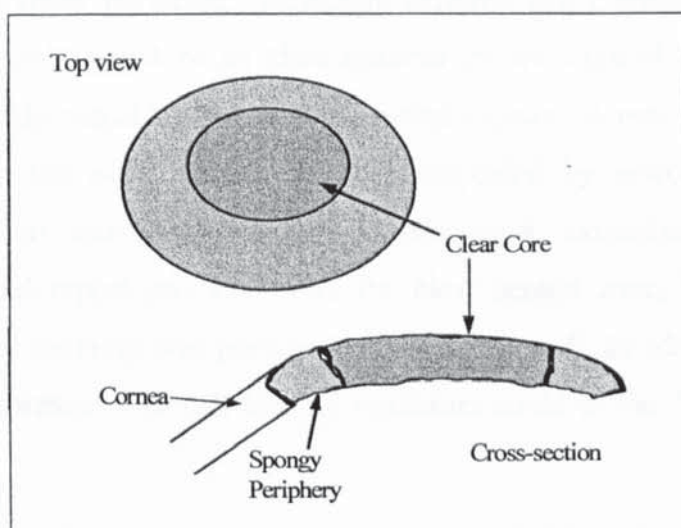
Porous polytetrafluoroethylene has been used extensively in many of the most recent

keratoprotheses, with minor modifications.⁴⁹ There are three basic types of polytetrafluoroethylene (PTFE) patented and designed for vascular prosthesis and waterproof clothing materials. ProplastTM consists of PTFE melded with carbon fibres to give added strength. Goretex[®], a more familiar, everyday material is a meshwork of PTFE with pore sizes between 15-90 μ m. Impira is a variation of Goretex[®] with an altered fibre orientation to give greater anisotropic rigidity and homoelasticity. Average porosity varies between 100-500 μ m.

White and Gona were the first research group to incorporate porous PTFE and created a porosity of between 80-400 μ m.⁵⁹ Caldwell and LaBarre⁶⁰ created a smaller porosity of 15-90 μ m, but the most successful PTFE keratoprosthesis made by Legeais possessed a porosity between 18-22 μ m. Legeais et al. employed an expanded PTFE with pore dimensions which they assessed by experimentation as giving high tissue adhesion, high permeability, least encapsulation, optimal collagen synthesis, organisation and infiltration. With a follow-up time of 16 months there is a success rate of 7 out of 10, and a visual acuity, at best of 20/100.

1.5.42 The Artificial Cornea of Chirila et al.

Figure 1.15 *A Two-Part Hydrogel Analogue of the Cornea*⁴⁹



Chirila et al have been very active in the area of hydrogel keratoprosthesis and improvements in tissue interpenetration into those same hydrogel materials. They have conducted detailed studies on the effects of pHEMA sponge structure on the quality of

tissue invasion and published many papers on their highly original two-phased hydrogel keratoprosthesis.^{50,57}

Hydrogel sponges with differing geometrical characteristics both *in vivo* and *in vitro* lead to contrasting biological responses. Sponges with pore sizes between 5-10 μ m were encased in thin fibrous membrane containing only a sparse scattering of cells and therefore, no invasion or penetration occurred. This was at complete variance to sponges possessing pore sizes between 15-30 μ m which, were invaded by a richly neo-vascularised tissue populated by large numbers of cells and filled with mature collagen fibres. The best performing polymer sponges contained interconnected channels which at the surface formed pores 10 to 30 μ m in diameter.

In conclusion, Chirila's group deduced that the size of pores, not void volume decided the actual depth of cellular penetration and strength of attachment.

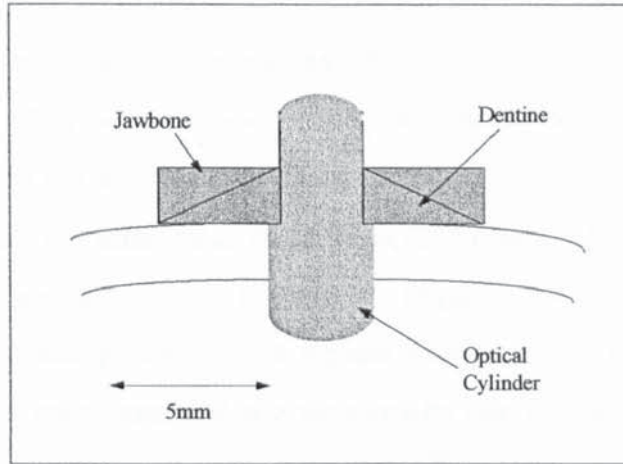
1.5.43 The Artificial Cornea of Kornmehl et al.

*Rabbit Derived Collagen Autograft*⁵⁸

The continued search for a truly biologically compatible material has explored the use of collagen. Collagen is the primary structural protein of the cornea and could, therefore present fewer problems. Kornmehl believed that corneal derived collagen allografts from rabbits could be an ideal material for an artificial cornea. Collagen allografts are readily available, disease free, optically clear. A neo-vascularised tissue developed within the outer fibrous zone accompanied by re-epithelialisation and fibroblast migration and development. Consequently extrusion did not occur. However, they did report problems over the clear central zone, because it lacked porosity, epithelial coverage was poor and necrosis occurred. In addition they seemed confident that treatment with cell binding mediators could in the future prevent this from occurring.

1.5.44 The Artificial Cornea of Falcinelli et al.

Figure 1.16 Dental Lamina Support Frame Attached to polymethyl Methacrylate (pMMA) Core



A detailed description of the tooth and bone keratoprosthesis is dealt with in Chapter two.

1.5.45 Features of the Ideal Artificial Cornea

Each one of the exceptional artificial corneas described, in the previous section is flawed, because they do not possess all the desirable features of an *ideal* artificial cornea.

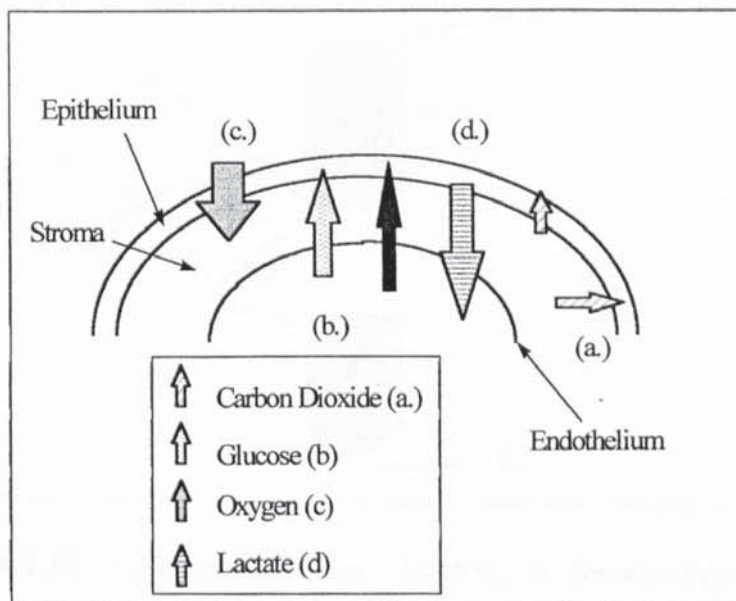
The ideal artificial cornea would have the natural shape of the cornea, a wettable exterior surface to support an epithelium, an inner core with moderate refractive power fully integrated with a porous rim for tissue penetration and adhesion.⁶¹ Discs of this nature are difficult to make and difficult to anchor in the eye. Rather by using the classic “core and skirt” model, (Figure 1.11) the ideal features necessary for good retention and few complications are much less difficult to fabricate. Proper anchorage would require the use of tissue re-inforcement.

The optical cylinder should be just longer than the full thickness of the normal cornea to reduce tissue overgrowth. At the anterior there would need to be a circular flange under which flaps of conjunctiva could be buried, but allowing for host corneal

epithelium to cover the anterior surface of the optical cylinder. The optical cylinder should be cylindrical and smooth to discourage the attachment of scar tissue and bacteria. In composition the optic would be both a non-toxic and non-hydrolysable rigid or semi-rigid polymer. Such rigidity prevents astigmatism and optical aberrations.

Polymers can be shaped and made to have excellent transparency and a refractive index equal to the cornea. The posterior end of the optic should be smooth and non-sticky and much thicker than the anterior end. Fused centrally there should be a flexible oval shaped disc preferably the same material as the optic to reduce fracturing possessing a graded centripetal porosity. Such porosity is required for transport of nutrients, regulatory molecules and penetration of topical medication to the posterior cornea. The issue of nutrient mass transport is a very crucial one because a stable epithelium must be allowed to develop over the artificial cornea⁶¹ (See Figure 1.18).

Figure 1.18 *Nutrient and Metabolic Transfer in the Cornea*⁶²



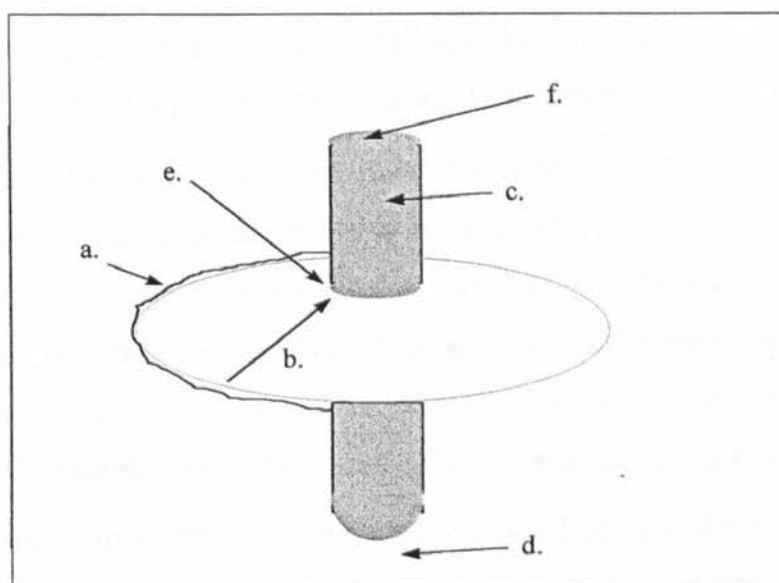
Ideally the prosthesis must not interfere with corneal physiology, particularly the supply of glucose (main source of energy) and removal of lactate from the regenerating epithelium. The support frame, in particular should possess a permeability to all nutrients and regulatory agents that ensure a return to near normal tissue architecture.

At the periphery there should be porosity sufficient to allow inward growth and the

attachment of keratocytes and matrix proteins to create a water tight junction between the graft and host tissues. Also situated at the periphery, there should be pre- attached cardinal sutures. In conclusion, the size and shape of the device should be specifiable to suit the dimensions of the eye and aid repeated examinations.⁶¹

Future artificial corneas must, therefore possess properties which retard the growth and development of fibrous encapsulating membranes and inhibit the progression of complement activation (to beyond the C₃ stage). A carefully managed arrangement of biologically active molecules involved in cell signalling, cell recognition, and attachment at a material surface would ameliorate excessive cellular proliferation and suppress the possible damaging effects of host responses. They must also be permeable to nutrients and regulatory agents to sustain epithelium and stroma.

Figure 1.19 *Features of the Ideal Artificial Cornea (core and skirt model)*



Key for Figure 1.19: a Heparin/ Collagen Coating; b. Graded Porosity; c. Smooth Surfaced and Semi-Rigid Optical Cylinder; d. Smooth and Non-Sticky Base; e. Flexible Water Tight Junction; f. Aspheric Wetable Top Surface

In summary, an ideal artificial cornea should possess the following attributes:

- a specifiable optic zone diameter
- a structure to allow diffusion of topical medication
- a surface which reduces protein deposition to reduce giant papillary conjunctiva
- a structure with non-allergenic properties and so resist destruction by white blood cells
- a structure that resists hydrostatic pressure
- a number of pre-attached cardinal sutures
- a periphery able to incorporate keratocytes and matrix proteins
- a highly polished surfaces
- a permeable periphery to (i) maintain proper nutrition of anterior. cornea and, (ii)
- allow diffusion of topical medications

1.6 Conclusions

A truly successful artificial cornea would have the potential to become widespread because it would be cheaper to obtain and would be universal since a synthetic cornea can be custom designed to suit the particular patient.⁶¹ As demonstrated in the literature review it has been exceedingly difficult to achieve this, because it requires the manipulation of a complex interconnected network of biological subtleties, such as wound healing and angiogenesis. Thus, there are very good reasons for the inclusion of a self-similar biological factor in the fabrication of an artificial cornea, whether it be patient biopsies (keratocytes or fibroblast cells), growth factors; spatial cues instigating repair (TGF-Beta) or tissues mined from other areas of the body (bone, cartilage).⁶³

Tooth and bone is the most favourable structure for strong, long lasting attachment of an artificial cornea, to the ocular surface as demonstrated by a couple of recent studies, and is the inspiration of research to design and fabricate a novel synthetic cornea as described in this thesis.

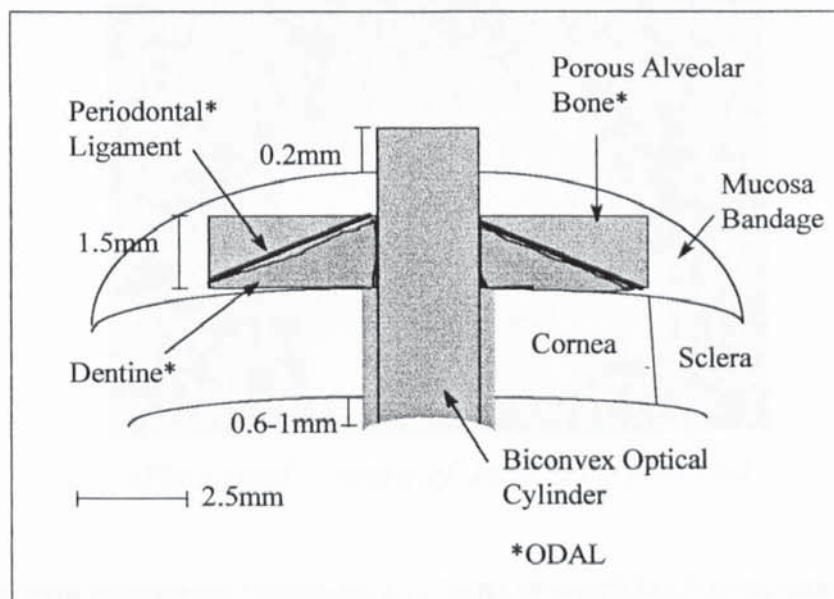
**CHAPTER 2: Literature and Analysis: The
Osteo-odonto-keratoprosthesis: Tooth and Bone
Artificial Cornea**

CHAPTER 2: Literature and Analysis: The Osteo-odonto-keratoprosthesis: Tooth and Bone Artificial Cornea

2.1 Introduction

The Osteo-odonto-keratoprosthesis, abbreviated to OOKP, is an ingenious solution to many of the biological complications that afflict corneal implants. It came to prominence in 1963, but after a flurry of world-wide interest it fell into obscurity as the rates of failure were, on average no better than its competitors.⁶⁴ Extrusion occurred between two months and a few years after surgery, primarily as a result of gradual degradation of the tooth and bone. (Figure 2.1). After numerous modifications the procedure has proved clinically successful in a large number of cases.²⁶

Figure 2.1 *The Strampelli Osteo-odontokeratoprosthesis: A Cross-Sectional View Through an Implanted OOKP (After Strampelli).*⁶⁴

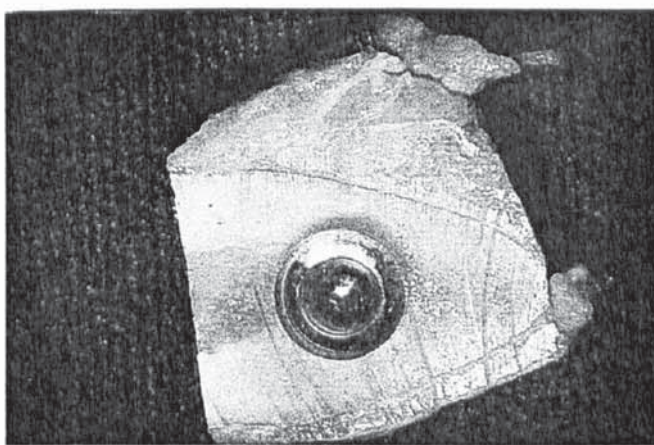


Implantation of the Osteo-odontokeratoprosthesis (OOKP) is a highly satisfactory treatment for ungraftable corneal blindness.⁶⁴ There was reported a success rate of 75% with visual acuity of 6/12 or better, after, on average five years. Follow-up time ranged from two months to up to 20 years. However, the complexities of preparation

and implantation have severely hindered its widespread use. The aim of this chapter is to detail recent results of a modified version of the 1963 original and provide explanations for the attributed successes.

The chapter begins with an evaluation of the unique attributes of the tooth and bone prosthesis, as shown in photograph 2.1. It will be emphasised throughout that the unique quality of the OOKP, to bond biological matter securely with solid plastic is a fundamental advance. Few other artificial corneas have been able to contrive, what is termed a *true* biological union. This will be defined more clearly later. After describing the lengthy surgery, and recent improvements there is an explanation of the function of the living graft component and the mode of attachment that keeps the implant firmly in place (**Table 2.1**).

Photograph 2.1 *Basal Surface of a Freshly Excavated Section of Tooth Root and Alveolar Bone with Optical Cylinder Inserted; Prior to re-attachment of periosteum and insertion into a subcutaneous pocket (After Falcinelli).*



(Photograph courtesy of Mr. Christopher Liu)

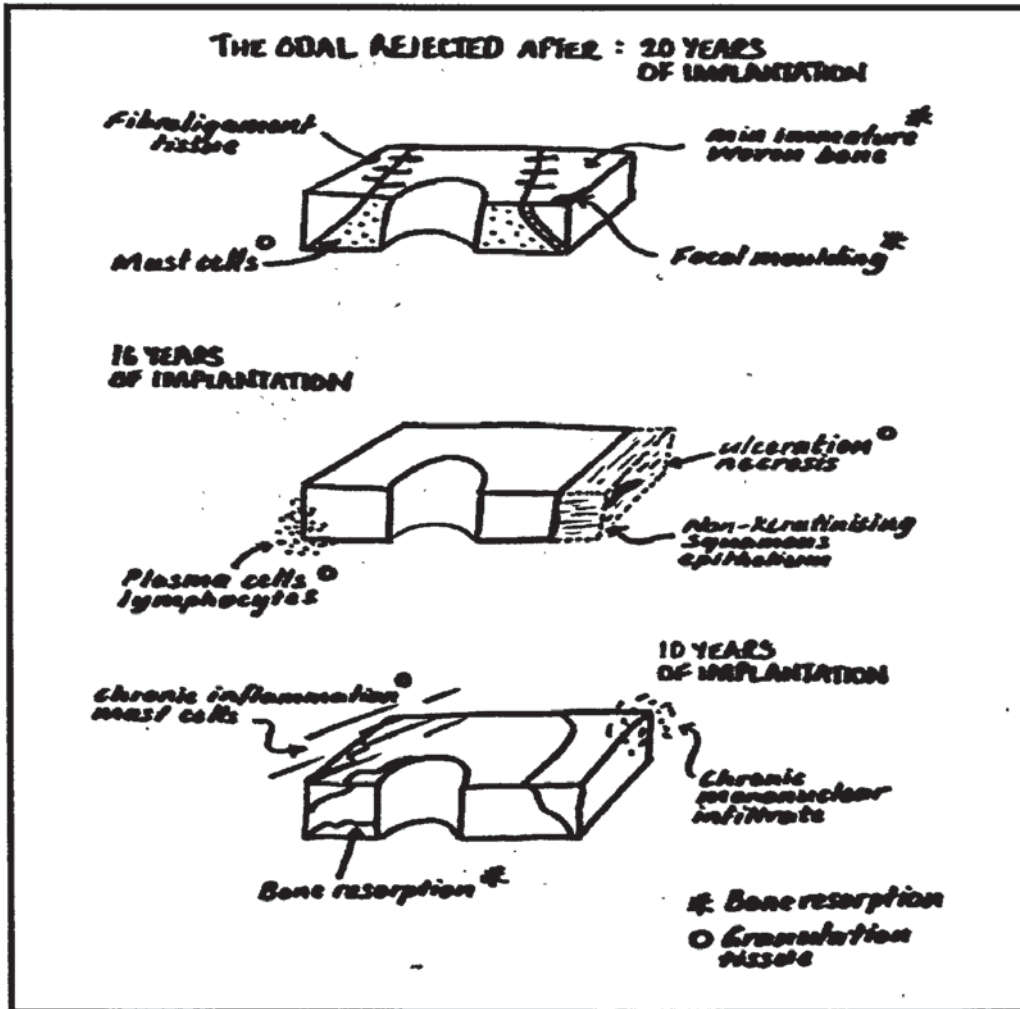
Good long term integration (attachment of bone to overlying buccal mucosal bandage) attachment is difficult to achieve, but details of the OOKP mode of attachment reveals some useful clues for the keratoprosthesis engineer. For example, the apparent success of spongy bone to provide an interlock with host tissue.

Conventional keratoprostheses are held in place mainly by mechanical fixation. For example when a lamellar pocket is made to incorporate the implant flange, before it is

secured with sutures (Figure 2.1). Biological attachment of host tissue to an implant is exceptionally difficult to formulate and prepare, since synthetic surfaces are in biological terms, unresponsive. Without a mutual response adhesion may be poor. Instead many have employed graft tissue from other areas of the body.

Benedetto Strampelli was a pioneer of the biological artificial cornea, when he employed tooth and bone as a securing device⁶⁴ After implantation of the implant, a firm and un-complicated healing developed between the support frame and surrounding tissue, partly attributed to the fact that healthy host tissue was used and all elements of the implant were separated from pathogenic corneal tissue. Others reported on and experimented with the OOKP but it fell into disfavour, as mentioned before in the introduction.^{64,65,66} Giancarlo Falcinelli developed an enhanced version of this graft-synthetic hybrid.²⁶ An independent analysis of the work of Falcinelli was made by Liu et al.⁶⁷ and the success rate was confirmed to be very high. (See in Table 2.1) For example, 77.4% of eyes could see 6/12 or better and not one was extruded from the body. The reason for these results is attributed to the function of the cementum in preventing epithelial downward growth and hence, expulsion. Leukocytes accumulate when elements of the dental fragment degenerate and give rise to complications as shown in the figure below.

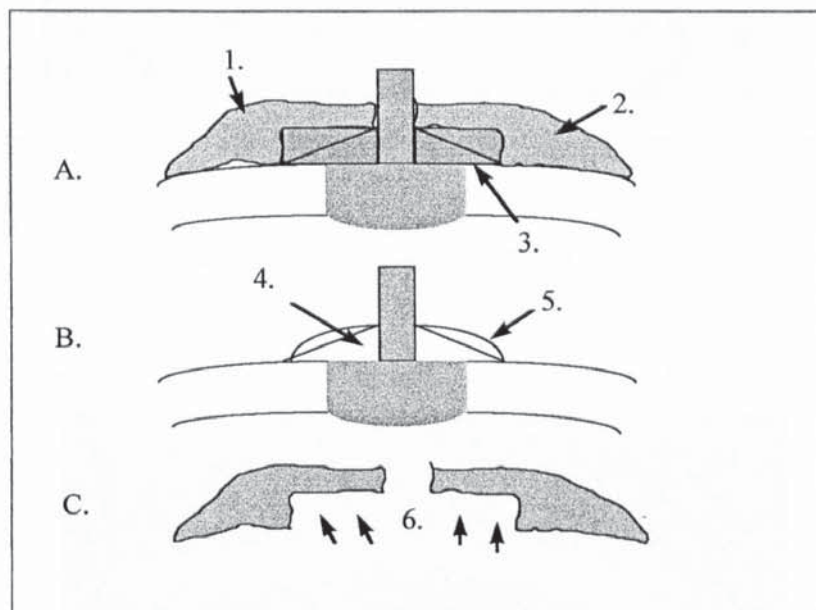
Figure 2.11 *Biologically Induced Changes in the Tooth and Bone Supporting Frame (or the Osteo-odontal acrylic lamina) During 20, 15 and 12 Years of Residency on the Bulbar Surface of the Eye.*⁷³



Failure of the Osteo-odonto-keratoprosthesis (OOKP) occurs as a result of degradation or resorption of bone in the ODAL and chronic inflammation over the surface, but is uncommon.⁶⁸ Degradation of the ODAL is described in greater detail in Figure 2.11. From the sparse evidence available, there are three causes of failure: an excessive quantity of mast cell infiltrate, chronic inflammation and bone fragmentation.⁷³ It is important to note that there is additional fibrous epithelial tissue tied to the periodontal ligament. This could be a remnant of an uncompleted encapsulation of the implant stopped by contact with the ligament.⁶⁹

Wherein contact with alloplastics, the corneal epithelium poses particularly threats to the continued stability of the implant. In the OOKP system epithelium is integrated with the skirt material and safely impeded from migrating further, on contact with cementum. A firm epithelial seal of this nature greatly reduces the number and severity of complications, e.g. anterior optical surface coverage and fistula formation. The opposition to epithelium and adequate thickness and vascularisation of the mucosal coverage are key properties of the Strampelli-inspired Osteo-odonto-acrylic lamina (ODAL) for they allow the polymer to remain for lengthy periods when the ligament, cementum and bone remain alive. The main reasons for the success of the OOKP are listed in Figure 2.12. There are no existing non-living alternatives or analogues exhibiting features of the OOKP, although, attempts have been made by Blencke⁴⁴ and Hoffman.⁴⁵

Figure 2.12 *Main Reasons for Success of the OOKP*



Key to Figure 2.12:

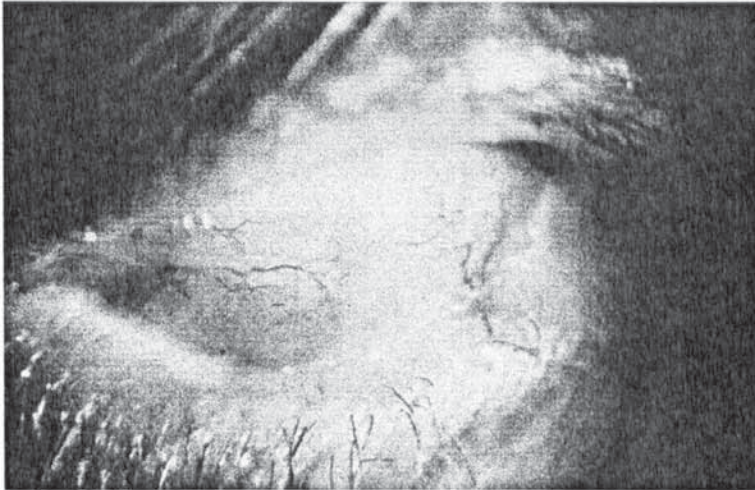
1. *Buccal mucosa: free skin flaps*
2. *High vitality: repair proliferation and immunity*
3. *Firm contact of buccal mucosa with ODAL bone*
4. *Strongly mineralised element*
5. *Tolerates the presence of embedded foreign objects*
6. *Absence of centripetal growth of new conjunctiva around the artificial cornea*

2.2 Osteo-Odonto-keratoprosthesis Surgery

The OOKP is a successful treatment for bilateral corneal blindness resulting from:

- severe dry eye syndrome (ulceration, bullous eruptions and epithelial defects)
- ocular pemphigoid (bullous eruptions of mucous membranes surrounding eyeball)

Photograph 2.11 Ocular Pemphigoid



- trachoma (*Chlamydia* induced swelling, lesions and pustule formation, causes scarring)
- chemical burns (ulceration and death to all cells in contact area of chemicals)

Photograph 2.12 *Example of Corneal Opacity Caused by a Chemical Burn*

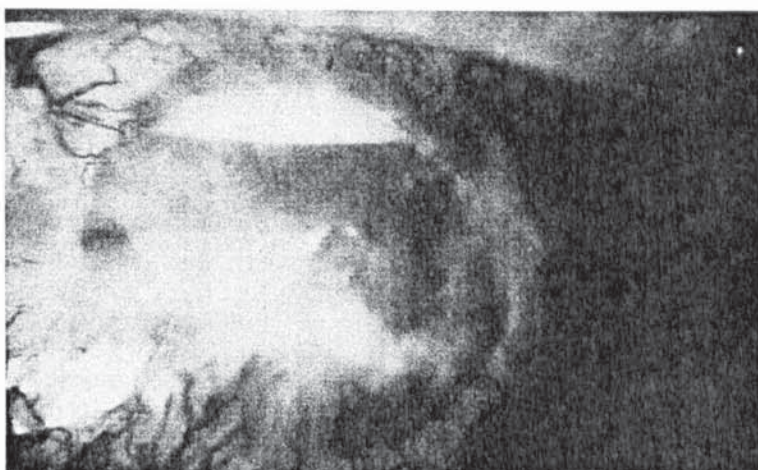


(Photographs courtesy of Mr. Christopher Liu)

- keratitis (chronic inflammation of the cornea caused by fungal or bacterial

infection)

Photograph 2.13 Fungal Keratitis



- multiple graft rejection (over-sensitive immune reaction)

Therefore, the Osteo-odonto-keratoprosthesis (OOKP) is implanted only as a last resort when either corneal graft is repeatedly rejected or is unlikely to work. It is a complicated but effective procedure despite criticism and suspicions about its true worth among some members of the surgical community.

The OOKP uses an osteo-odontal lamina for the support frame. The lamina is a section of the afflicted patient's canine tooth (including dentine, cementum, periodontal ligament) and a region of surrounding jawbone in which the tooth is supported. The method of attachment to the bulbar surface of the eye is somewhat analogous to odontoiatrics. Naturally, in the soft tissue lining the mouth, the outer protective layer of the gum (gingival epithelium) is interrupted by the dental crown and so becomes fixed to the cementum. (mortar between dentine and bone). Similarly in the OOKP, buccal mucosa becomes fixed to the periodontal ligament and is embedded into the cementum below. Thus, there is separation of the two elements, tooth fragment and buccal mucosa. If they were to separate, the space would form a trough collecting tissue fluid and aqueous humour. This pool of fluid can act as a source for chronic infection.

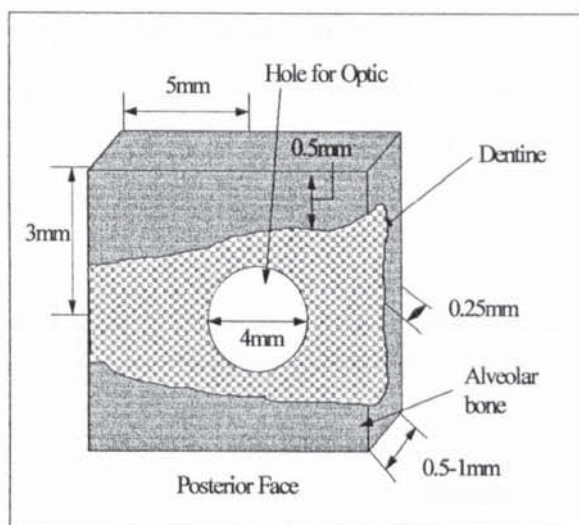
By using tooth root rejection and tissue loss are analogous to the processes by which a tooth detaches from the gum. Parodontosis is a causal factor in tooth detachment and

similarly in the tooth and bone system. Tooth decay leads to detachment from the covering mucosa. Both rejection and tissue loss are identical to the process by which a tooth detaches from the gum. Thus, it is important that during an OOKP operation the dental tissue must remain alive, so that it becomes a true graft rather than a simple inclusion in which the mode of attachment is mechanical not biological.⁶³

The dental plate is complex and many layered. During OOKP surgery the fragment of tooth and bone is cut longitudinally to create maximum continuity for each shell of tissue bandaging. Tissue that covers the dental fragment must be well vascularised with normal epithelium. Once a healthy epithelial covering is established the implant is incorporated and proper healing will occur around the implant. Buccal mucosa is the vascularised tissue used to cover the bone fragment because it closely resembles gingival mucosa cushioning and moistening the rigid fragment.

Despite the best efforts of surgeons to apply a strict sterile technique there are problems with the health of the dental lamina. They include granulomata (consisting of macrophages, neutrophils and connective tissue) and inflammation of periodontal tissue. The maximum size possible for the dental lamina is determined by the amount of surrounding tissue able to provide support and is, ten by ten by three millimetres.⁶⁶

Figure 2.3 *Shape and Size of a Reasonably Healthy ODAL (The size of the ODAL can vary with the degree of tissue damage, caused by oral infections).*



In comparison with other keratoprostheses this is unusually large though the sclera does not deeply embed into the periphery. The size of the frame is necessary to gain enough purchase onto the mucosa to support the heavier and denser optical cylinder. It is important that any root surface not covered by the alveolar dental ligament should be removed. Otherwise it is liable to decay possibly threatening the good health of accompanying tissue.

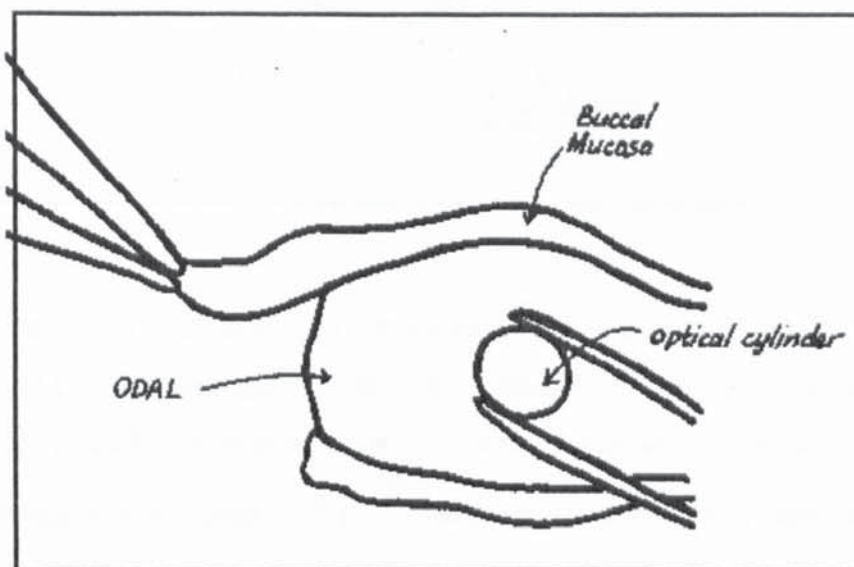
The fragment and optic are joined together with dental acrylic glue and placed in a sub-muscular pocket under the lower eyelid for at least two months before insertion into the anterior eye. The fragment becomes encapsulated in a layer of protective soft tissue. In a successful ODAL insertion, buccal mucosal tissue does not attach to the dentine surface, but only to bone.⁶⁸

2.2.1 Brief Summary of OOKP Surgery⁶⁹

There are three stages to OOKP surgery:

- Stage 1 Covering of eyeball with buccal mucosa
- Stage 2 Preparation of the osteo-odental acrylic lamina; This includes cutting and drilling of the ODAL, gluing of the optical cylinder into the ODAL and covering of buccal mucosa over the ODAL (**Photograph 2.14**).

Photograph 2.14 *Mucosa Wrapped Around Dental Fragment*



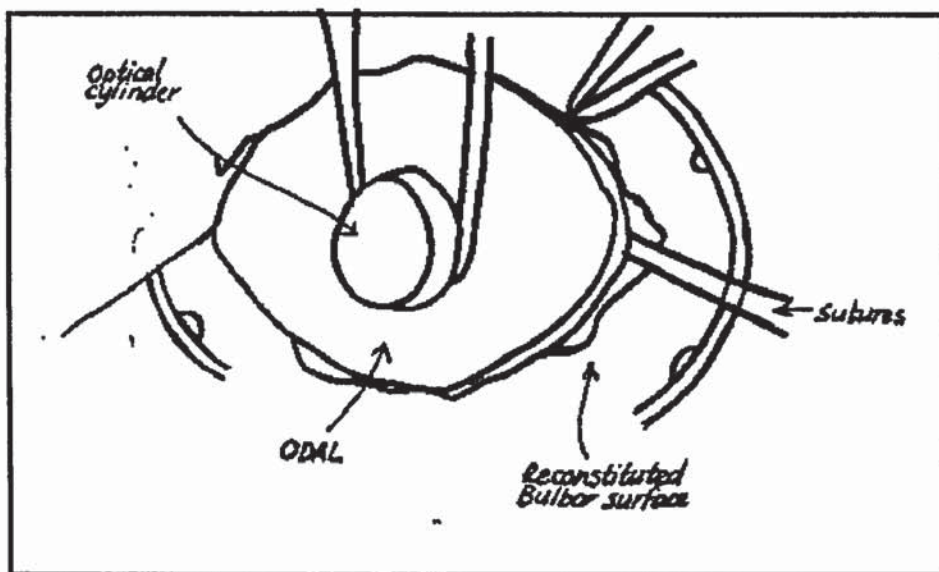
- Stage 3 Implantation of the ODAL (**Photograph 2.15**).

Photograph 2.15 *Insertion of the OOKP (Encapsulated in Periosteum along the edges and Mucosa) into a Muscular Pocket Just Below the Eye*



(a) *Withdrawal of ODAL from subcutaneous pocket*

(b) Insertion of ODAL onto bulbar surface (Photograph 2.16, below)



The fundamentals of this technique were much later improved upon by Falcinelli, to overcome the excessively high numbers of complications. Post-operatively infection, glaucoma and retinal detachment featured highly. A fundamental concern highlighted by the investigations of Caiazza et al.⁷⁰ was bone resorption and bacterial residence. Bacteria are highly opportunistic and exploit traumatised tissue and open or poorly healed wounds, even within a sterilised operating theatre. Despite this, the vast majority of problems are never very serious to warrant removal or total reconstruction.

Falcinelli made 14 modifications to the original Strampelli technique and in doing so significantly improved the results. Falcinelli not only improved the effectiveness and success, his efforts increased the number of potentially treatable patients by cyclosporin application and use of blood relations teeth, carefully typed for HLA matching.¹² Problematic posterior segment complications were considerably reduced by removing the lens and iris and removing the vitreous while anterior segment complications were reduced by increasing the diameter of optic and reduction of the optic axis and application of biometry techniques. Such physical changes in design, however are unlikely to eliminate all these complications.²⁶

Falcinelli et al.²⁶ and are listed in brief, below:-

- temporary coverage after the operation with conjunctival flap to prevent necrosis
- collagenase reducing agents to prevent tissue melting
- steroids to suppress uveitis and retroprosthetic membranes
- glaucoma shunts to relieve excessive intra-ocular pressure (IOP)²⁶

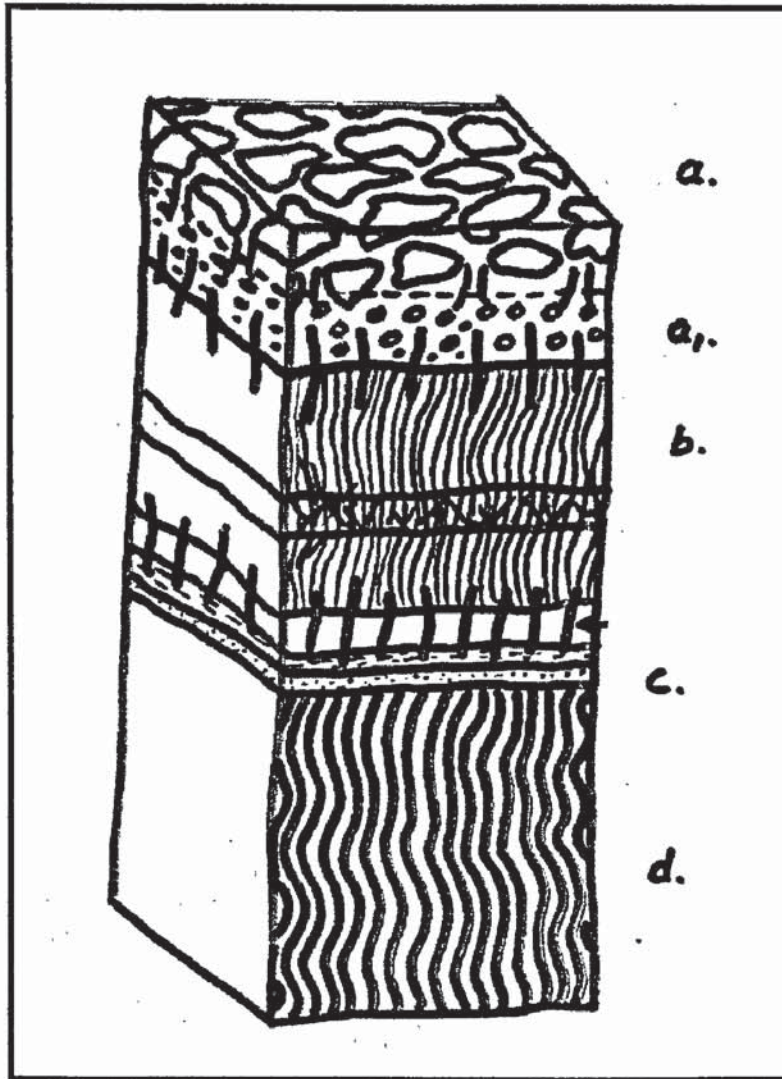
2.3 Osteo-Odontokeratoprotheses:

Nature and Structure

The crucial element of the success of the OOKP appears to centre on the use of many different types of grafted tissue (75% are retained with minor complications achieving a visual acuity of 6/12-the second line of an eye chart). At one end of the structure there is a mineral element which can be firmly attached to plastic, and at the opposite end there is a rigid porous framework for tissue inter-digitation and inter-locking. In addition, living graft tissue can repair itself and proliferate in a controlled manner. It also has an inherent immunity.

The multi-layered structure of tooth and bone is a complex mixture of dentine, periodontal ligament, cementum, trabecular bone, periosteum, endosteum and buccal mucosa. The individual function of each of these layers appears to be important and in need of discussion (**Figure 2.14**).

Figure 2.14 *Stereogram of Osteo-odontal Lamina: (a) spongy alveolar bone, (a1) cribiform plate (0.1-0.5mm) containing numerous vascular canals, (b) periodontal ligament of soft specialised connective tissue that provides support and resistance, (c) cementum, a hardened non-vascularised connective tissue with a thin soft, permeable cellular region abutting onto the dentine (d).*⁷¹



2.4 Anatomy of Living Dental (Periodontal) Tissues

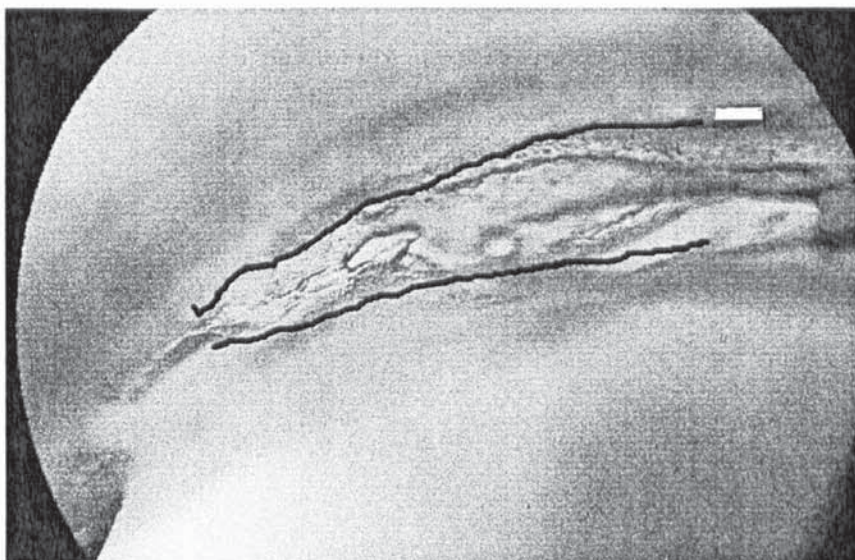
2.4.1 Dentine

This is a very stiff mineralised tissue. It is living and is not metabolised by the body even when it is surgically removed from the oral cavity, and implanted in the eye. The role of dentine in the Strampelli OOKP was to provide a solid, stable surface onto which the optical cylinder was securely glued. It also serves to shield the perspex surface from living tissue and the immune system.⁶⁹

2.4.2 Periodontal ligament

This is a special type of connective tissue which it possesses some characteristics of foetal tissue.⁷¹ It is highly responsive to mechanical stimulation and is packed with cells which are involved in the repair of adjoining dental tissues. The periodontal ligament consists of densely packed collagen fibres, supporting a mass of fibroblast cells and structural proteins, forming a matrix. The fibres are involved in mechanical stabilisation of the tooth in the jawbone while the cells are present to repair damaged tissue. The ligament is a kind of shock absorber for the tooth absorbing displacement forces generated during mastication.

Photograph 2.17 *Cross-section Through the Periodontal Ligament. The periodontal ligament is a meshwork of dense collagen fibres that stabilises the tooth in the jawbone during its displacement by mastication etc. In the OOKP it functions as a barrier to epithelial downward growth (Scale Bar = 200 μ m).*



When it is part of the Strampelli (and Falcinelli version too) prosthesis it may serve to buffer the dentine and optical cylinder from compressive forces generated during blinking and movement of the eyeball and so preventing them from being dislodged (**Photograph 2.17**).

2.4.3 Cementum

Cementum is a thin layer of calcified tissue which is contiguous with the periodontal ligament. Its main function is to give attachment to collagen fibres from the periodontal ligament.⁷¹ In physical and chemical properties it is similar to bone except that it is avascular. Investing membranes which, come into contact with the cementum stop proliferating, in the same way they do on contact with the periodontal ligament.⁶⁸ The reason for this contact inhibition of epithelium and conjunctiva tissues which often find and exploit gaps and vacuities between different tissue types and inert surfaces is unknown. It is thought to be primarily a surface phenomenon involving biological markers.

2.4.4 Alveolar Bone

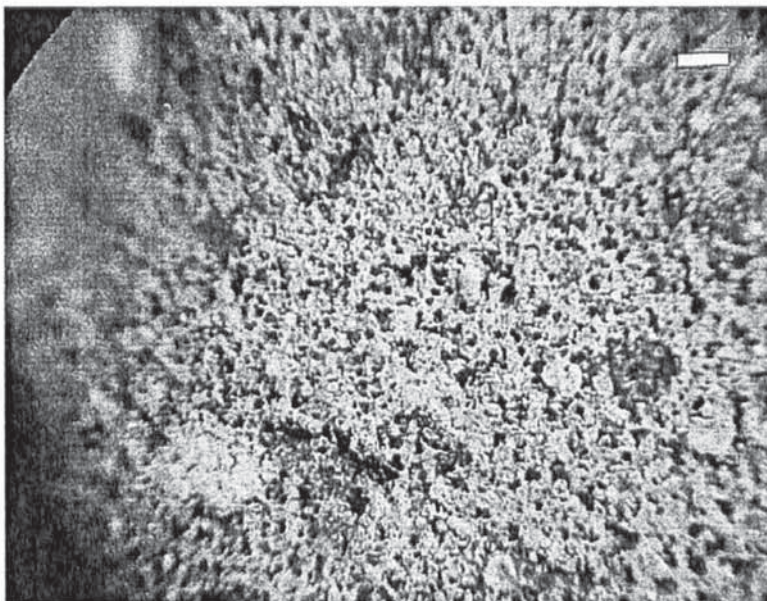
Alveolar bone is a highly porous structure which provides anchorage for the tooth and gingival lining of the oral cavity. It is the crucial intermediary structure in the OOKP in that it fuses with the soft mucosa which, itself is fused to the eye; and the dentine which is securely bonded to the plastic optic (**Figure 2.15**).

Figure 2.15 *Cancellous Bone Surrounding an Incisor*



Looking at the above image there are two regions of bony architecture. The cribriform plate is dense and punctured with interconnected spaces (small dots in trace below). It gives way to a more open, less dense region of cancellous bone.⁷¹ A small triangular region of this open foam, with interconnecting pores (0.5mm-2.8mm) is present in the ODAL when it is implanted.

Photograph 2.18 *Region of Compact Spongy Bone Adjoining the Periodontal Ligament (x18 magnification; Scale Bar = 200 μ m).*



2.4.5 Buccal Mucosa

This is the skin tissue lining the inside of the mouth. The fact that it is highly elastic and tough make it ideal as a material to stretch over the eyeball and to suture in the whole device in place. It is composed of three distinct layers: a moistened outer epidermal layer, a supporting dense connective tissue, the lamina propria and thirdly, below this layer looser submucosal connective tissue, containing fat deposits and glands which secrete mucous onto the epidermis.⁷¹ Buccal mucosa is quite thick and highly vascularised since the maintenance of a good blood supply is important for the survival of the bone and underlying dental tissues.

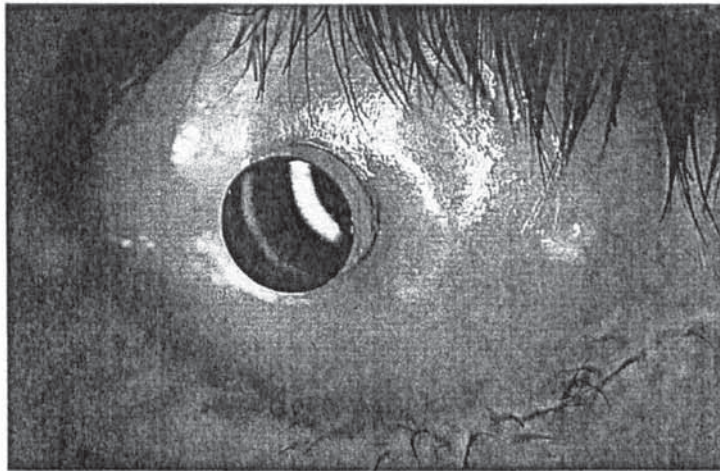
Mucosal layering forms a barrier to infection, abrasion and prevents dehydration of implanted tissue because the submucosa is in contact with the alveolar bone and periosteum, cells and structural proteins from this tissue infiltrate the pores of bone and re-organise to form a well structured tissue which is adherent to the surface of bone.²⁶

2.5 Ocular Attachment and Integration

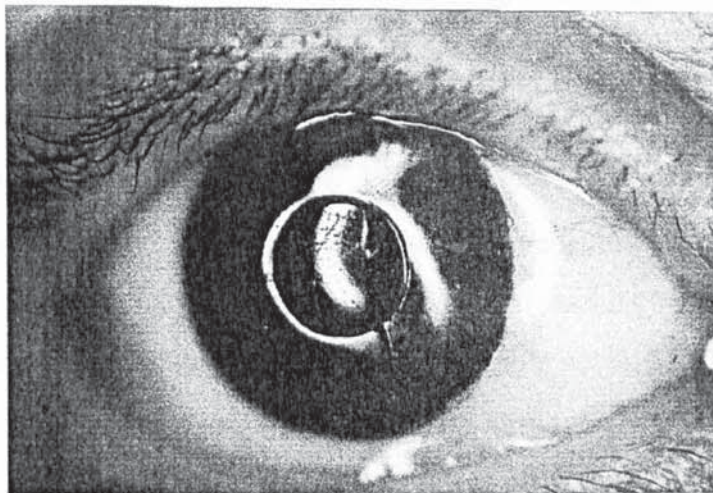
The tooth and bone prosthesis is retained only when a true biological connection between the buccal mucosa and bone is established. The connection could be purely biochemical, or it could be as a result of structure? It is apparent that the surface chemistry of cementum and periodontal ligament inhibits colonisation, on contact, of *unwanted* sheets of epithelial cells and basement membrane which, form retroprosthetic membranes and scar tissue.^{66,69} Cementum and ligament also act as tissue fasteners and restraints. Interfacial bonding between collagen fibres of connective tissue (buccal mucosa) stabilises the artificial cornea and hinders migration and excessive fibrous tissue deposition.

In addition, the structure of spongy bone ensures a strong mechanical interlocking with buccal mucosa. The interconnected pores provide a framework onto which tissue can be organised and strongly attached to, thus the geometry is important. Other keratoprosthesis with synthetic support frames rely purely on mechanical contact, but even then the internal pore geometry is haphazard.

Photograph 2.19 *Final Placement of OOKP into the Anterior Eye: The plastic optic is surrounded by soft and moist buccal mucosa bandage removed from the inner cheek of the afflicted patient.*



Photograph 2.2 *OOKP with Cosmetic Iris*



(Photographs provided by Mr. Christopher Liu)

2.6 Mode of Attachment to the Eye

The key elements of attachment are the bonding of mucosa to bone and the structural properties of the periodontal ligament, for dissipating shear forces, and cementum, as a glue for attachment of collagen fibres.⁷¹ Cell adhesion, cell confluency and the arrest of cellular proliferation and epithelial migration beyond the shelf material (proliferation can lead to ulceration and rejection of the device) are phenomena controlled by an equal mix of ligand-receptor mediated biological chemistry of surfaces and matrices, and spatial cues.

The outermost layer, the mucosa adheres strongly to the bone and cementum much as it would do naturally in the mouth where it fastens the tooth in the gum.⁶⁴ To improve attachment of dental prosthesis, the mechanism of gingival sealing around mineralised structures has been closely investigated.^{66,69} With an effective biological seal there is no inflammation and epithelial migration.²⁶ Some of this histological information is useful to understanding the mode of connection between mineral and live tissue.

There are two points of attachment for mucosa to mineral, one is to the alveolar bone and the second is to the cementum. Mucosa is made from a dense network of collagen fibrils and has a well defined polarity, non-keratinised junctional epithelium makes contact with the enamel surface and embeds itself in cementum, while the opposing surface apposes interdigitated bone creating a frictional interlocking.⁷¹

The porous structure of bone and the biology of self-adjustment and self-renewal are key properties that ensure and maintain stability. Not nearly so important is the chemical composition of the bone surface.⁷² The arrangement of spaces facilitates rapid inward growth of tissue and creates an interdigitated locking with soft connective tissue. It also provides a framework for the assembly of a network of blood vessels.

2.7 Discussion

So far this chapter has appraised the osteo-odonto-keratoprosthesis, based upon a relatively small number of published papers and anatomical literature.^{64,68,69,70}

Unfortunately, owing to the complexity of surgery required to insert an OOKP the technique is unpopular. Some have even doubted its true efficacy. Indeed early trials were rather unsuccessful and this must explain the established distrust in the procedure. Recent modifications though, have removed all the glaring difficulties manifest in the original.²⁶ Furthermore, one independent statistical study of the newer version provides clear proof of sound attachment and good, stable vision.²⁰

The histology of tissue attachment at the junction between covering mucosa and dental

lamina evidences a firm attachment.⁷³ Mucosa is continuous with internal surfaces of bone and with the cementum. Thus, there are no gaps available for bacterial colonisation. In addition, there are consistent signs of health and vitality represented by dense vascularisation and an absence of inflammation.⁷³ Although, an underlying explanation of the actual mechanisms for attachment does not receive as much credence. This is due to the paucity of tissue biopsies that have been carried out⁷³. In the first instance, such knowledge is important for understanding why and how the ODAL works. It also would be important if the design were to be intelligently copied.

After analysis of the literature two major elements to explain the stable, long term retention of the OOKP emerged, they were:

- structure and
- biochemistry and physiology.

The structure is crucially important for it determines the way in which forces are dealt with, safely or not.⁷⁵ Structure also allows for the incorporation and re-assembly of tissue into the body of the prosthesis, with the added effect of preventing membrane proliferation and expulsion.

Biochemistry and physiology play a part in controlling inflammation, repairing damage and normalising the immune system. In the OOKP system periodontal ligament tends to inhibit migration of investing membranes deeper inside the support plate. As yet the mechanism for such contact inhibition is unclear, because there have been no experimental studies, only observation and description.

Table 2.1 *OOKP Solutions to Common Reasons for Artificial Cornea Failure*

Artificial Corneas: Common Reasons for Failure	OOKP: Reasons for Success
Lack of Vascularisation	Porous bone encourages vascularisation
Degradation of tissue by enzymes	Antiproteases brought in by blood
Infiltration of leucocytes Proliferation of conjunctiva	Hindered by protrusion of optical cylinder and tight mucosal seal at edges
Unsupported Cornea	Cornea held in place by buccal mucosa and contact with base of artificial cornea
Proliferation of epithelium	Inhibited by tight epithelial seal and contact with periodontal ligament and cementum
Shear forces on supporting frame Lack of flexibility	The oral mucosa cushions against compressive shear forces

The tooth and bone keratoprosthesis (OOKP) is a great source of ideas for deciding what structures and systems would be useful for successful tissue integration uncomplicated by necrosis, ulceration and fistulation. This unique device demonstrates how an inert plastic window (the true artificial cornea) can be combined with living tissues to create a true biological connection with the eye. The extensive use of living graft tissue is an undoubted reason for success but cannot be a conclusive explanation. It may be argued that structure and to a lesser extent, the surface chemistry of bone and cementum (mineral composition) play the leading roles in manipulating uncomplicated wound healing.

All available evidence and speculation favours the role of structural attributes in ensuring OOKP attachment. The structure of bone is crucial to a rapid tissue interpenetration and development of a tight tissue interlock. These two facts have further important consequences in that the likelihood of infection is reduced and fluid leakage of intraocular fluid loss from the eye is similarly reduced. Structure, in itself can optimise cellular responses to mechanical loads, so preventing tissue damage.

Structure also patterns the morphology and state of penetrated tissue. A good framework encourages the formation of healthy and stable tissue.

The structure of a framework can optimise tissue responses to mechanical loads, and so prevent damage to them. Structure also imprints a particular morphology on impregnated tissue. It determines the degree of quality of impregnated tissue. A good framework encourages the formation of healthy tissue. Natural frameworks are able to adapt to changes in the surroundings and this improves their resilience and longevity. How can we modify the OOKP to increase its availability and reduce the surgical complexities?

2.8 Towards a Synthetic OOKP: Scope and Objects of this Project

Development of a successful implant requires the use of structural materials that are compatible with, but not necessarily identical to, host tissues. Materials must form strong bonds with tissue and be patterned in such a way, as to lead to orderly tissue reconstruction. This would ensure long-lasting anchorage to the body. Over four decades of study into the design of a successful artificial cornea few examples possess this level of biological compatibility*. The Osteo-odontokeratoprosthesis is one such example. It is exceptional in that it creates a 'true' biological union between the plastic optical cylinder and surrounding tissue.

Despite the good clinical successes of the OOKP there are a number of problems which, limit its use and give rise to expulsion in the long term. Tooth extraction is an unpleasant activity for patient due to the extra pain, lengthy surgery and the disfigurement caused. Surgeons may have difficulty finding a completely healthy tooth (incisor) so there is sometimes a limited quantity of available tissue. Even the use of blood relations teeth does not overcome this difficulty because they may also be poor in quality, and the recipient will need to be immunosuppressed with toxic drugs.

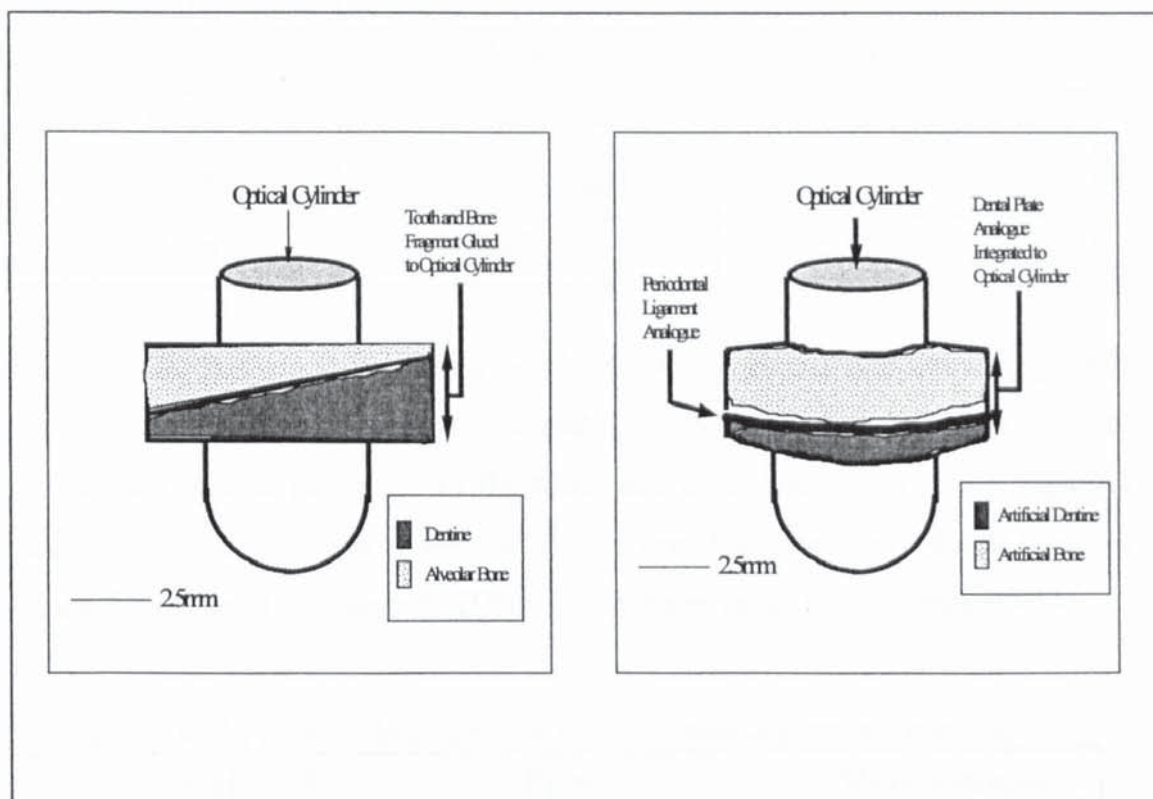
The physical dimensions of dental tissue available is limited and this reduces the functional performance. For example, a larger region of bone should allow for stronger attachment and shaping to suit the dimensions of the patients eye. Clearly if the OOKP technique could be simplified by drastic reduction in the amount of tissue removed; using instead a structural material that is not biologically degraded, more of them (the new variant OOKP) would be implanted and the long term success rate may be improved. There is, therefore very substantial justification for making a synthetic version. It would reduce surgical complexity (by nearly half), time spent on selecting and removing a piece of tooth and bone and so, it would be more popular to ophthalmologists. The comparative cheapness of a synthetic version of the OOKP should ensure greater use.

*Concept of biological tolerance can be summarised as "*the exploitation by materials of the proteins and cells of the body to meet a specific performance goal*"**

A synthetic OOKP is a distinct advantage to the standard OOKP with graft tissues, for many important reasons. With a synthetic OOKP, the first stage of OOKP surgery is reduced by 1/2, since extraction of tooth and bone is unnecessary. An oral surgeon is required to do this. The oral surgeon needs only to cut-away and remove a piece of buccal mucosa from the mouth. There may not need to be an oral surgeon at all, if the ophthalmic surgeon is properly trained in the techniques of removing buccal mucosa. As a result patients, and patients relatives suffer less from trauma, but more importantly it frees-up time to enable removal of cataracts, that are common in an increasingly ageing population. A synthetic OOKP would be considerably safer for patients who do not have teeth. Normally, such patients would have to have cyclosporin and immune suppressive drugs to accept homografts. These drugs are bad for the kidney and so, require expertise from an internal physician with all the additional costs involved. Another key advantage of a synthetic OOKP are that future advances in optical design can be implanted into patients to replace previous designs without the prohibitive cost and surgery involved. Any problems that arise post-operatively and threaten extrusion, can also be managed in this way. It would be possible to just make a new relatively inexpensive artificial cornea and replace the troubled old one.

The first objective was to determine how the tooth and bone functions in providing long term success; What mechanisms were involved? In chapter two the reasons were discussed and it was found that porous bone and periodontal ligament are the key features of long term stable attachment. The second objective was to adapt the tooth and bone to make a single unified structure, artificially, as displayed in Figure 2.15.

Figure 2.16 Diagrammatic Representation of an Synthetic OOKP (right) and an OOKP (left) for Comparison



To achieve this, it was necessary to synthesise biological ceramics with properties likely to encourage long term fixation in and on the eye (in the stroma or sclera or on the bulbar surface attached to extraneous supporting tissues) such as, an open interconnected porous structure with pore dimensions between those listed in Table 2.11. These are reliable limits to work toward but their arrangement is open to experiment to accomplish the optimum fixation scaffold. Long term fixation maybe stronger and more stable with a Vronoi foam structure or periodic minimal surface structure.

Table 2.11 *Pore Sizes Likely to Create a Tight Tissue Interlock by Providing a Suitable Framework for the Infiltration of Cells, Vessels and Biopolymer Matrix.*

Minimum pore size	Maximum pore size	Reference
15-40 μm	18-20 μm	Hulbert (75)
50 μm	200 μm	Bobyn (76)
190 μm	230 μm	Liu (77)
70 μm	150 μm	Piddock (78)

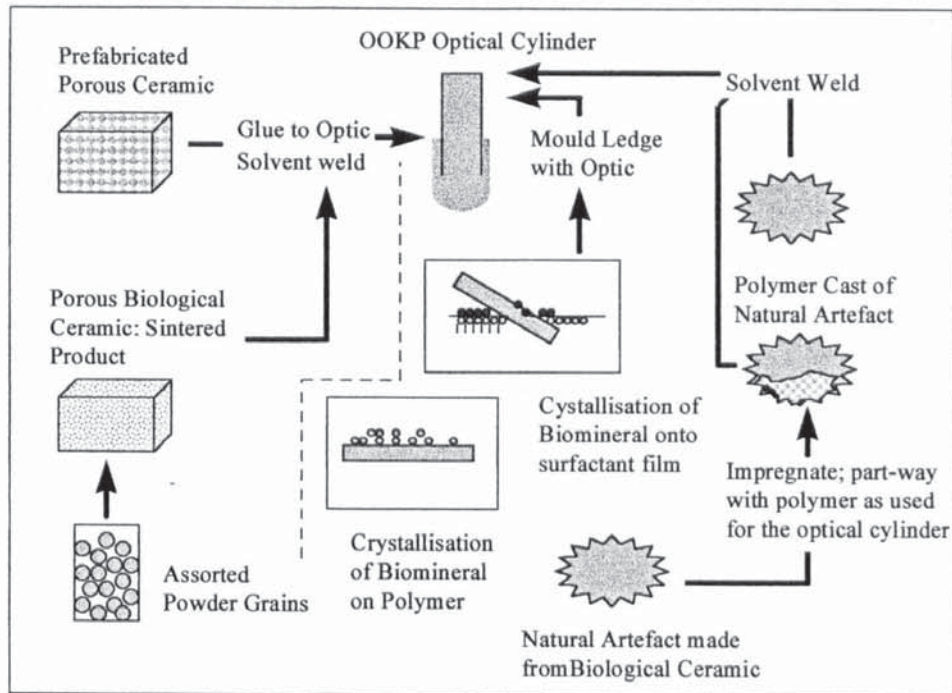
A structure with these attributes would provide a framework to guide and arrange cells and order the deposition of extracellular matrix scaffolding. Secondly, the material should possess mineral properties of the tooth and bone (metastable hydroxyapatite) that additionally minimises resorption, and lastly there should be a periodontal ligament substitute for epithelial containment. (Discussed in more detail in **Appendix A1.14**)

Table 2.12 *Potential Materials for a Periodontal Ligament Substitute*

Material	Type	Reference no.
Dacron	PTFE fibrous mesh	Caiazza (123)
Reconstituted collagen	Glutaraldehyde cross-linked or formalin	Nimni (130)

A final objective was to employ elements of biomimetics; the practice of artificial copying of biological structures and processes. Biomimetics could provide a number of novel approaches to making a tooth and bone (OOKP) analogue. These approaches are illustrated on the right-hand side of the following diagram. They include crystallisation of biological ceramic by a precipitation reaction onto a synthetic polymer optical cylinder, crystallisation of biological ceramic onto surfactant films or micelles adsorbed onto a synthetic polymer optical cylinder and casting of replicates bonded to a synthetic polymer optical cylinder.

Figure 2.17 Possible Ways of Making a Ceramic Support Frame for an OOKP Analogue



If a synthetic approach to biomimesis does not prove feasible, there is the potential to exploit natural artefacts, since many natural artefacts (particularly marine invertebrates) possess the mineral composition and the pore structure of alveolar bone.

1

CHAPTER 3

MATERIALS and METHODS

CHAPTER 3

MATERIALS and METHODS

3.1 Materials: Tables 3.1-3.16 Chemical Reagents Used in this Study

Table 3.1 *Chemical Reagents used for In-solution Mineralisation Experiments*

Chemical Reagent	Supplier
Calcium Phosphate (Dibasic)	Sigma-Aldrich Chemicals, St.Louis, USA
Calcium Carbonate 99.5%	Sigma-Aldrich Chemicals, St.Louis, USA
Sodium Chloride	Sigma-Aldrich Chemicals, St.Louis, USA
Sodium Sulphate (Anhydrous ACS Reagent)	Sigma -Aldrich Chemicals, St.Louis, USA
Potassium Carbonate	Sigma -Aldrich Chemicals, St.Louis, USA
Calcium Chloride dihydrate	Sigma -Aldrich Chemicals, St.Louis, USA
Calcium Chloride (Desiccant ACS Reagent)	Sigma -Aldrich Chemicals, St.Louis, USA
Trishydroxyethylaminomethane (buffer)	Sigma -Aldrich Chemicals, St.Louis, USA
Sodium hydrogencarbonate	Sigma -Aldrich Chemicals, St.Louis, USA
Calcium hydrogencarbonate	Sigma -Aldrich Chemicals, St.Louis, USA
Sodium hydroxide	Sigma -Aldrich Chemicals, St.Louis, USA
Potassium Chloride (ACS Reagent)	Sigma -Aldrich Chemicals, St.Louis, USA

Table 3.11 *Chemical Reagents used for Fabrication of Biomimetic Ceramers*

Reagent	Supplier
Citric acid (binder)	Sigma-Aldrich Chemicals, St.Louis, USA
Alginic Acid (binder)	Sigma-Aldrich Chemicals, St.Louis, USA
Stearic Acid 95% (solvent)	Sigma-Aldrich Chemicals, St.Louis, USA
Polyacrylic Acid (deflocculant)	Sigma-Aldrich Chemicals, St.Louis, USA
Batesons Monomer Solution (MEMA/ EEMA/ MMA)	Polysciences Inc., USA
Methylmethacrylate (MMA)	Vista Optics, Stockport,UK
Araldite Rapid (resin)	Ceiba Geigy Plastics,USA
Polyethylene Glycol 8000 (Carbowax)	BDH Chemicals, Poole,UK
Tetraethoxysilane (TEOS) (silica gel)	Sigma-Aldrich Chemicals, St.Louis, USA
Hydrochloric acid	BDH Chemicals, Poole,UK
Cellulose Acetate Butyrate (CAB)	BDH Chemicals, Poole,UK
Dextrin Particles 36 microns (porosigen)	BDH Chemicals, Poole,UK
Dextrin Particles 100 microns (porosigen)	BDH Chemicals, Poole,UK
Dextrin Particles 250 microns (porosigen)	BDH Chemicals, Poole,UK
Sucrose Particles 36 microns (porosigen)	BDH Chemicals, Poole,UK
Sucrose Particles 100 microns (porosigen)	BDH Chemicals, Poole,UK

Table 3.12 *Chemical Reagents for Histological Staining*

Histological Stains	Supplier
Alcian Blue	PS Park Science
Congo Red	PS Park Science
Haemotoxylin	Aldrich Chemical Company
Bromopyrogallol Red	Aldrich Chemical Company

Table 3.13 *Chemical Reagents for the Synthesis of Polymer Membranes*

Reagent	Supplier
AZBN (Thermal Initiator)	BDH Chemicals, Poole, UK
EDMA (cross-linker)	BDH Chemicals, Poole, UK
Tetrahydrofuran (THF) (Solvent)	BDH Chemicals, Poole, UK
THFMMA (Stiff Hydrogel monomer)	Vista Optics, Stockport, UK
Hydroxyethylmethacrylate (HEMA)	Vista Optics, Stockport, UK
Uronyl nitrate (UV crosslinker)	BDH Chemicals, Poole, UK
Irgacure 184 (UV crosslinker)	First Water Ltd., Coventry, UK
Methoxyethylmethacrylate (MEMA) (hydrophobic monomer)	Ubichem Ltd., Eastleigh, UK
EEMA (hydrophobic monomer)	Ubichem Ltd., Eastleigh, UK
Bateson`s monomer mixture (EEMA/ MEMA/ MMA)	Polysciences Inc., USA
Polyurethane (PU) (toughening agent)	BDH Chemicals, Poole, UK
Methylmethacrylate (MMA) (hydrophobic monomer)	Vista Optics, Stockport, UK

Table 3.14 *Other Chemical Reagents Used*

Reagent	Supplier
N-Octane (porosity estimation)	Sigma-Aldrich Chemicals, St.Louis, USA
Paraffin wax pellets (Pore Infiller and bonding substance)	Polysciences Inc, USA
Mineral Oil: Light White Oil (solvent)	Sigma-Aldrich Chemicals, St.Louis, USA
Collagen: Acid Soluble From Kangaroo Tail (collagen gel)	Sigma-Aldrich Chemicals, St.Louis, USA
Sodium Hypochlorite (removal of organics)	Sigma-Aldrich Chemicals, St.Louis, USA

Table 3.15 *Commercially Produced Biological Ceramics Used in this Study*

Biological Ceramic	Supplier	Origin
Biocoral (R)	New Splint plc, 9 Murrell Green Business Park, London Road, Hook, Hampshire, RG27 9GR	Derived from reef coral in French West Indies and New Caledonia, South Pacific
Pro-Osteon (R)	Interpore, 181, Technology Drive, California, USA	Derived from reef coral in West Indies and Belize
Endobon (R)	Merck Biomaterials Darmstadt, Germany	Derived from cow bone

Table 3.16 and 3.17 Natural Artifacts Used in this Study.

Table 3.16 Corals and Sponges

Natural Artefacts	Supplier	Origin
<i>Seriatopora octoptera</i> (Lamarck 1816)	Sheila Halsey, Coral Section, The Natural History Museum, London	Red Sea, Saudi Arabia
<i>Seriatopora hystrix</i> (Dana 1846)	Sheila Halsey, Coral Section, The Natural History Museum, London	Sabah, Eastern Malaysia
<i>Stylophora pistillata</i> (Schweigger 1819)	Sheila Halsey, Coral Section, The Natural History Museum, London	Malaysia
<i>Goniopora fruticosa</i> (de Blainville 1830)	Sheila Halsey, Coral Section, The Natural History Museum, London	Pulau Babi, Hujung, East Coast Peninsular, Malaysia
<i>Goniopora lobata</i> (de Blainville 1830)	Sheila Halsey, Coral Section, The Natural History Museum, London	Pulau Seri Buat, East Coast Peninsular, Malaysia
<i>Montastrea annularis</i>	Sheila Halsey, Coral Section, The Natural History Museum, London	East Malaysia
<i>Polyphyllia talpina</i> (Lamarck 1801)	Sheila Halsey, Coral Section, The Natural History Museum, London	East Malaysia
<i>Porites porites</i> (Link 1807)	David Barnes, Australian Institute of Marine Sciences, Townsville, Queensland	Great Barrier Reef, Central Section, Townsville
<i>Porites astreoides</i> (Link 1807)	Sheila Halsey, Coral Section, The Natural History Museum,	Grand Cayman, Bahamas
<i>Porites digitata</i> (Link 1807)	Sheila Halsey, Coral Section, The Natural History Museum,	Indian Ocean, Aldabra
<i>Ianthella basta</i> (Gray)	David Barnes, Australian Institute of Marine Sciences, Townsville, Queensland	Great Barrier Reef, Northern Section, Townsville
<i>Keratosa sp.</i>	Esponjas NKS, S.L., San Jose, Pinto	West Indies
<i>Heterocentrotus trigonarius</i>	David Barnes, Australian Institute of Marine Sciences, Townsville, Queensland	Great Barrier Reef, Northern Section, Townsville

Table 3.17 *Other Natural Artifacts*

Natural Artefact	Supplier	Origin
<i>Sea Urchin Testa (Echinus esculentus)</i>	The National Sea Life Centre, The Waters Edge, Brindleyplace, Birmingham, B1 2HL	English Channel
<i>Dogfish eggcase (Scyliorhinus caniculus)</i>	Not applicable	Aldwick Beach, West Sussex
<i>Bamboo (Phyllostachus sp.)</i>	Not applicable	Back Garden, Bognor Regis, West Sussex
<i>Bryozoan (Turbicellepora avicularis (Hincks))</i>	The Natural History Museum, Cromwell Road, South Kensington, London, SW7 5BD	English Channel
<i>Cuttlefish Bone (Cephalopoda nitidins)</i>	Not applicable	Aldwick Beach, West Sussex

Table 3.18 *Biological Ceramics Used in this Study*

Name of Biological Ceramic	Supplier	Origin
Hydroxyapatite Powders (A,B,C,D,500,250, 100,36*)	Jesse Shirley, Advanced Ceramics, Etruscan Street, Etruria, Stoke-on-Trent, ST1 5PQ, Staffordshire	Cow Bone
Hydroxyapatite Discs (E,F,G,H)	Jesse Shirley, Advanced Ceramics, Etruscan Street, Etruria, Stoke-on-Trent, ST1 5PQ, Staffordshire	Cow Bone
Hydroxyapatite Whiskers	Jesse Shirley, Advanced Ceramics, Etruscan Street, Etruria, Stoke-on-Trent, ST1 5PQ, Staffordshire	Cow Bone

3.2 Experimental Methods

3.2.1 Histological Staining

Pieces of canine tooth and adjoining bone were obtained from the Birmingham Dental School and cut into thin sections to thicknesses of 0.5mm and 1mm, using a Leica diamond edge cutting saw. Cut samples were immersed in Alcian blue dye for one hour followed by a Congo red dye to stain mineralised and non-mineralised tissue respectively. (1.5g dye in 3.5g water) (*Results Section 4.4, Chapter 4*) The same dyes were used to pigment the polymer 'syrup' impregnated into porous ceramics, to highlight the distribution patterns and coating phenomena.

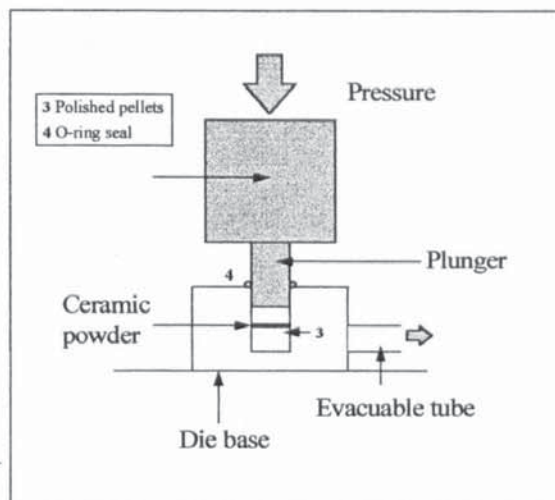
3.2.2 Measurement of Biological Ceramic Grain Sizes

A number of different grain sizes and powders were obtained from a commercial supplier of bone replacement ceramic, Jesse Shirley Advanced Ceramics, of Stoke-on-Trent. The shape and size of individual grains and the average dimensions of grains in a powder were measured to calculate the gap size between grains after compaction. Grain diameters were accurately measured under a powerful light microscope (Dialux 20) with a slide graticule (*See Results Section 4.6.1, Chapter 4*).

3.2.3 Die Pressing of Ceramic Particles

Powders were compacted using a die press into thin discs (0.2-0.5 mm thick and 5mm diameter) at pressures varying between 1-5 tons/ per inch² (50-100kN). Attempts were made to fabricate discs with a porosity above 50%, with pore sizes above 50 µm, and that did not crumble under their own weight. Binding agents, such as starch solution (Schottlander and Davis, Letchworth, U.K) widely used for solidifying dental ceramics and de-ionised water enhanced bonding of powder particles into a coherent mass.

Figure 3.1 Diagram of a KBr Press (Graseby Specac). Experimental Apparatus for Compacting Ceramic Powders into Discs.



Porosity and average pore sizes were measured for the following compacted materials entered in **Table 3.18**.

Table 3.18 Compacted Ceramic Powders (Grain Diameters in μm)

Grain diameters
36
100
250
500
36 mixed with 100
36 mixed with 500
100 mixed with 500
Spheres 500

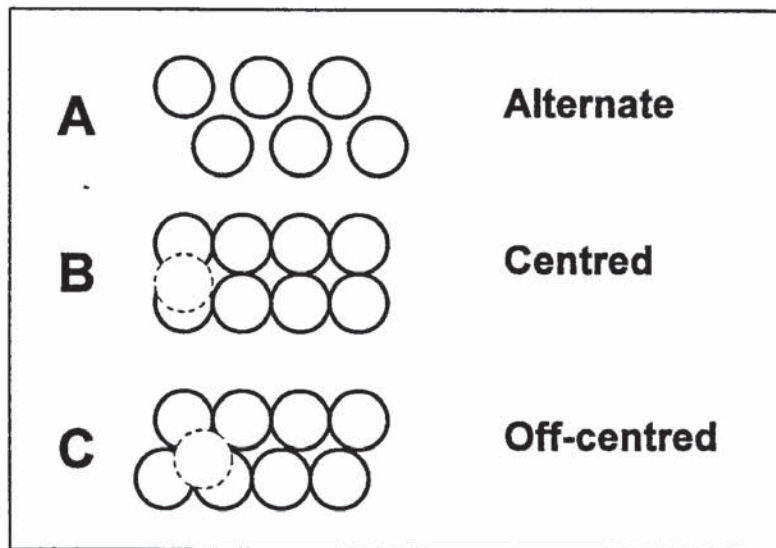
Results are in Section 4.6.1

3.2.4 Calculation of Packing Densities and Packing Arrangements

There is a simple relationship between the way in which particles are packed together and the spaces that are left between each spherical particle. The analytical theory for calculating packing arrangements of specified particle dimensions in unit space was taken from the analysis of the structure of metals. Metals adopt a close packed

structure when solid and in their lowest, preferred energetic state they adopt the most efficient use of space available. Similarly natural porous artefacts optimise their modes of building structures to do the same and maximise space filling with minimal inputs of resources. In two dimensions there are three sorts of packing arrangements as drawn in Figure 3.11.

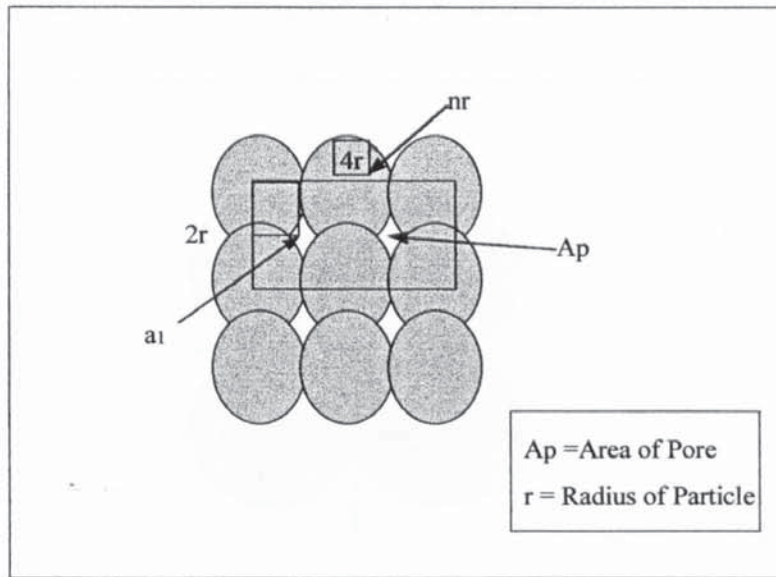
Figure 3.11 *Packing Arrangements of Spheres*



the following calculations were made:-

(i) The space-to-circle ratio compares the quantity of solid and spaces. A least efficient packing organisation possesses a larger amount of void than solid, i.e. a value greater than 1.

Figure 3.12 Measurements for Determining the Space-to-Circle Ratio



(ii) The area (in two dimensions) and volume (in three dimensions) of space between roughly spherical particles.⁷⁴

Starting with (ii) area of square (representative of solid) occupied by pore spaces:-

Equation (3.1) $A_2 = a^2 (1 - \pi/4)$

or,

Equation (3.11) $A_2 \times 4 = A_p$

(where A_1 = Area of frame covered by solid particles)

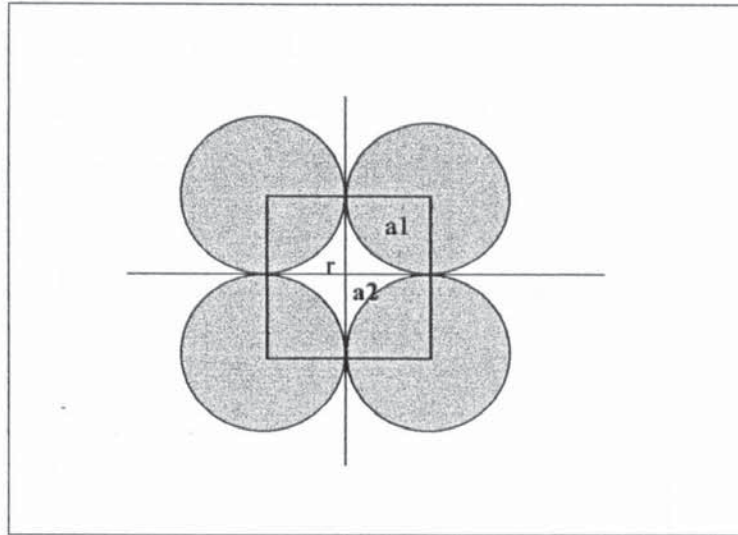
(i) While the fraction of the area of the square occupied by the circles, f , is given by:-

Equation (3.12) $f = (nr)\pi r^2 / (nr^2)r^2$

The space-to-circle ratio is thus,

Equation (3.13) $f \times 100$

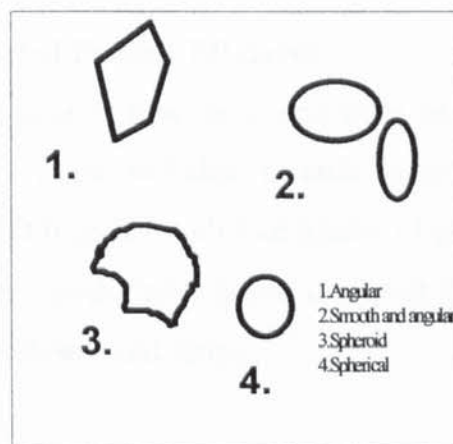
Figure 3.13 A Two-Dimensional Packing Distribution and Measurements for Determining dimension of Pore Spaces (i.e. pore diameter).



r =radius; np =number of particles ; A =Area

Particle shape also had a bearing on particle packing arrangements and thus, pore dimensions. They were characterised using the following key. The equations laid out on the preceding page, are more accurate for spherical particles (4)

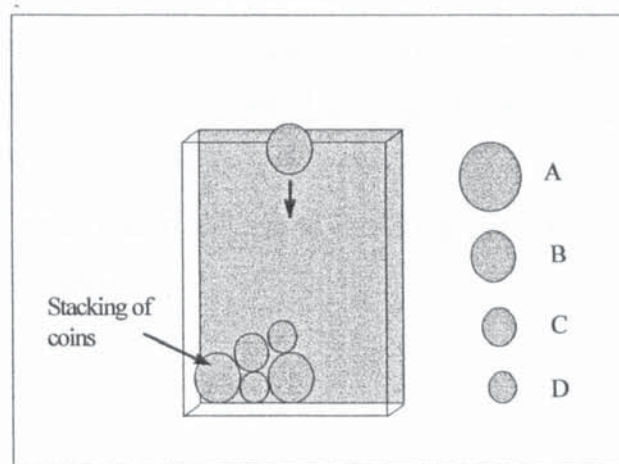
Figure 3.14 Particle Shape Profiles (500 to 36 μm)



A packing sequency of ceramic grains with the lowest percentage packing efficiency (<74%) creates large pores. Ceramic materials were fabricated with the aim of creating discs with large pores. Calculations from equations 3.1 to 3.14 were used to determine which combinations of particles might be best for manufacturing a desired

void pattern (**Results Table 4.5**). Equations 3.1 to 3.4 were used to calculate void dimensions in stochastic mixtures of grains settling under the force of gravity and with only moderate to slight compaction. To make measurements easier, coins represented the differing sizes of ceramic grains (A,B,C,D) as illustrated below. A glass box was made to hold and contain the inserted coins. After insertion the front glass plate was removed and a pencil rubbing of the coins was made on plain paper for the purpose of measurement. (*Results in Section 4.6.1, Chapter 4*)

Figure 3.15 *A Coin Box for Measuring Packing Efficiency and Sizes of Voids Between Different Sizes of Spheres.*



3.2.5 Die Pressing of Assorted Particle Mixtures

A series of differing sized apatite powder grains were obtained from Jesse Shirley Ceramics (Stoke-on-Trent) these included ceramic grade hydroxyapatite powder samples designated: A,B,C,D together with four grades of powder varying between 36 μm and 500 μm in diameter. In the table below are listed the grain types used in this study. The grains vary in both size and shape.

Table 3.2 Particle Size and Shape (μm)

Particle radius	Particle shape#
500	Angular*
250-500	*
100	Spherical*
36	Spherical*
A(250)	Smooth/Angular
B(50)	Smooth/Angular
C(25)	Spherical
D(18)	Spheroid+spherical

*Finely sieved

A table of all possible powder combinations was drawn-up to assist developing a strategy for making hydroxyapatite tablets with a bone-like porosity. A selected number of powder mixtures were pressed into tablets under a small range of pressures (between 50-100kN) and hydrated states (dry, moist (5-10%) or soaked (80-90%). The size of pore spaces that result from particular particle mixtures were calculated from the following equations:-

Equation (3.14) $a \times 0.25 = a^1$

Equation (3.15) $a^1 - b = c$

Equation (3.16) $c + (b \times 0.25) = d$

applicable when $a = b \times 4$, otherwise $a^1 + b \times 0.25 = d$

Where a = large grain diameter; a^1 = pore size of grouped a particles; b = small grain diameter; c = pore size of grouped a particles - diameter of b grain. d=average pore size; (Results Section 4.5.1)

3.2.6. Scanning Electron Microscope Analysis of Pressed Discs

All pressed discs were first cleaned in Tween solution to remove dust and dirt, and dried in an oven heated to 60° C before gold coating. The surface of pressed discs were viewed under a scanning electron microscope (S90B), to identify materials with surface sculpture fit for tissue interlocking and cellular integration, according to the attributes in Table 3.19. Observations of surface features were recorded together with measurements of pore dimensions in view.

Table 3.21 *Pore Size Distributions Likely to Create a Tight Tissue Interlock*

Minimum Pore Size	Maximum Pore Size	Reference
15-40 µm	18-120 µm	Hulbert (75)
50 µm	200 µm	Bobyn (76)
190 µm	230 µm	Liu (77)
70 µm	150 µm	Piddock (78)

(Please Refer to Section 4.5.2, Chapter 4)

3.2.7. Measurement of Porosity

Porosity (expressed as the percentage of space enclosed by a unit of solid) of coral and fabricated hydroxyapatite solids was measured in one of two ways. The first method required total immersion into a highly polar solvent or hydrocarbon liquid which would completely wet the surface of hydroxyapatite and fill its pore system. Simply the ratio of weights before and after immersion were taken and multiplied by 100 (See Equation 3.17).

(Equation 3.17) *Immersion into Octane to measure % porosity (total pore volume) =*
$$\text{Weight of solid} / (\text{Weight of solid after immersion} \times \text{density of liquid}) \times 100$$

(Refer to Results Section 4.6.3, Chapter 4)

3.3 Fabrication of Ceramers

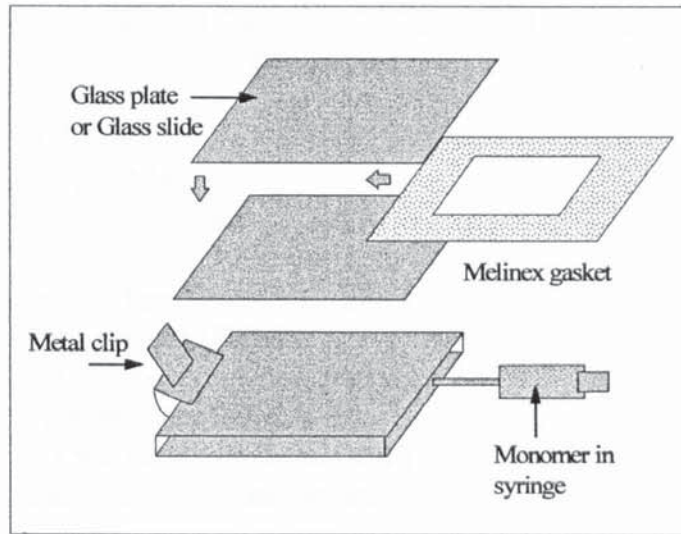
3.3.1 Synthesis of Polymer Membranes

Polymers were made into small membranous sheets by free radical polymerisation of a methylmethacrylate (MMA) monomer solution (0.5% (w/w) initiator AZBN (BDH Chemicals), 1%(w/w) cross-linker, EGDMA (BDH Chemicals) 94% MMA), in glass moulds. Each of the two pieces of glass were covered with Melinex[®] which were glued with spray mount (3M[®] spray mount). This prevented the polymer from bonding to the glass. The two glass plates were pressed together onto three polyethylene gaskets with a section removed for containing monomer. More gaskets were added dependent on the viscosity of monomer solution to be added. Highly viscous monomers required fewer gaskets because they were less likely to run and leak away.

Polymers were synthesised of MMA and co-polymers of Ethoxymethylmethacrylate (EMA) and Methoxymethylmethacrylate (MEMA) cross-linked with EGDMA and a thermal initiator. Later polymers were synthesised with a fast acting ultraviolet radiation initiator (absorption band = 365nm): Irgacure 180 (Ceba-Geigy). Monomers were weighed out into a small sample bottle on a microbalance. The bottle was shaken to create a homogenous mixture. Nitrogen gas was bubbled through all monomer solutions for ten minutes, to exclude reactive oxygen present in solution.

The entire assembly was compressed together with sprung bulldog clips. Monomer was injected into the assembly using a syringe, the needle piercing between the polyethylene gaskets and glass plates.⁷⁹ The mould was placed in a sixty degree oven for three days to enable complete cross-linkage, followed by a three hour post cure in a ninety degree oven. The polymer membrane was hydrated for one week, changing the water daily to remove any unreacted monomers.

Figure 3.16 Construction of Polymer Membrane Moulds, after Lydon ⁷⁹.



The following polymer membrane compositions were prepared for ceramer synthesis, and in solution apatite mineralisation experiments (Introduced in Section 3.). Polymers were toughened with added polyurethane for the same purposes. Although, pMMA was mostly used, and exclusively so during implant fabrication.

Composition of Polymer Membranes (Option (a) Hydrophobic monomers; Option (b) Hydrophilic monomers)⁷⁹

Standardised Quantities of Ingredients for Synthesising Polymer Membranes:	
0.025g	AZBN Azo-iso-butyronitrile
0.050g	Cross-linker EDMA
5.000g	Monomer:
<i>Option (a) monomers:</i>	
	Methyl methacrylate MMA*
	Ethoxyethyl methacrylate EEMA*
	Methoxyethyl methacrylate MEMA*
	Polyurethane(interpenetrant)
<i>Option (b) monomers:</i>	
	Acryloyl morpholine ACMO
	N-vinyl pyrrolidone NVP
	Hydroxyethylmethacrylate HEMA*

* Selected for use in this study

Compositions of Toughened Methylmethacrylate Polymer Membranes (MMA)⁷⁹

Standardised Quantities for Toughened Polymer Membranes:

0.5% Azo-iso-butyronitrile (AZBN)
1% (EDMA)
5.000g Monomer

(a) 5% Tetrahydrofuran (THF) + MMA +
Polyurethane (PU) 5%

(b) Tetrahydrofuryl methacrylate + THF +
Polyurethane (PU) 5%

(c) 5% Tetrahydrofuran (THF) +
Methylmethacrylate (MMA) +
Cellulose acetate butyrate (CAB) 5%

THFMMA-A stiffening monomer with a 5% water content

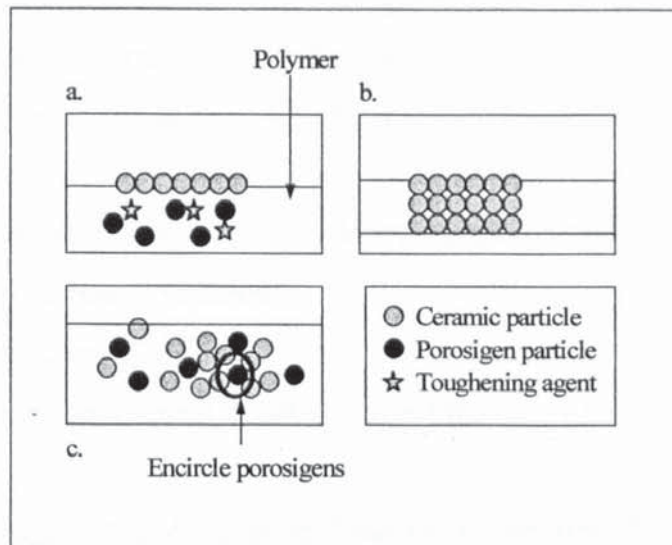
THF-A solvent for dissolving polyurethane (toughening interpenetrant)

Origins of all chemical reagents listed are to be found in Table 3.13 in the Materials section.

3.3.2 Ceramer Blends

The following blends of polymer and ceramic particles and composites of polymer and ceramic foams were made in the laboratory by blending, tape casting and vacuum impregnation.

Figure 3.17 *A Highly Diagrammatic Interpretation of Ceramer membranes; Cross-Sectional View*



The above diagram illustrates the three distinct types of ceramer, a, b and c, that were fabricated in this study. All ceramers were made by a tape casting method. Ceramer types, b and c were subject to plasma bombardment (As described in Section 3.3.3) to remove the polymer layer and expose ceramic. Type a) ceramer membranes, consisted of a thin surface layer of ceramic particles, embedded in polymer and mixed with soluble porosigens. Type b) polymer membranes were included with a moderate to high volume (75% \pm 10%) of ceramic powder mixed in a disordered fashion. Type c) ceramers were fabricated with large closely packed grains glued together with a small quantity (20% volume) of polymer. The following ceramer materials were fabricated in proportions varying from 50% to 75% volume ceramic and 50% to 25% of monomer.

Methyl methacrylate monomer was mixed with the following hydroxyapatite particles:-

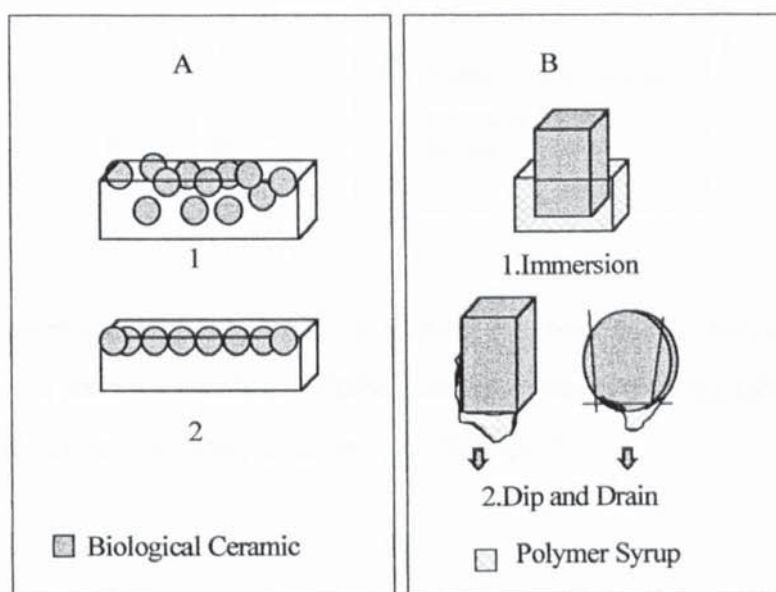
- whiskers (50 μ m \pm 25 μ m)
- spheres (500 μ m)
- particles (36 μ m; 100 μ m; 250-500 μ m)

In figure 3.18 are displayed the two ceramer fabrication techniques (combination of

polymer and ceramic) used in this study. Methods under A involve particulate ceramics forming a surface layer on the pre-polymer 'syrup'. Methods under B, use a whole block of porous ceramic that is either immersed or briefly dipped into monomer solution. Experiments were devised to impregnate monomer part-way into the pore system of pre-formed ceramic foams. The types of pre-formed ceramic foams (all natural artefacts) selected for polymer impregnation are listed below:-

- Biocoral[®] (Bone replacement material derived from coral skeletons)
- *Goniopora lobata* (Coral skeleton)
- *Porites porites* (Coral skeleton)
- Endobon[®] (Bone replacement material derived from cow bone)

Figure 3.18 Two Fabrication Processing Routes of Combining Polymer with Ceramic



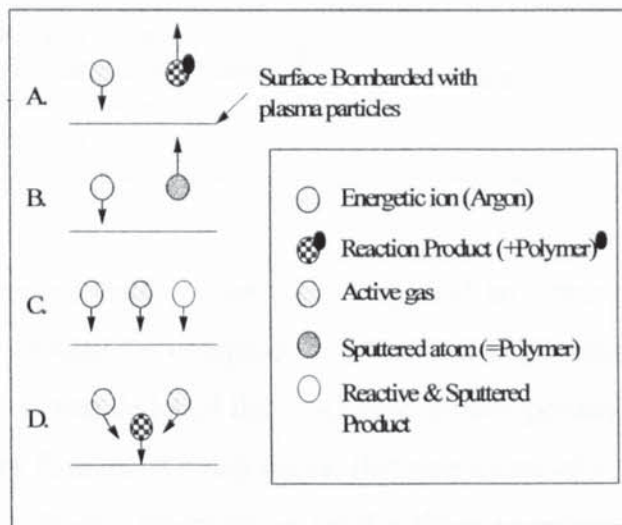
Results of methods A are detailed in Chapter 4. Results of methods B are detailed in Chapter 6.

3.3.3 Plasma Etching of the Polymer Phase

The plasma etching system employed was originally developed to strip away minute layers of protein and lipid from contact lens polymers.⁸⁰ A number of ceramics were etched with argon plasma to remove the polymer phase only, and expose the ceramic fraction.

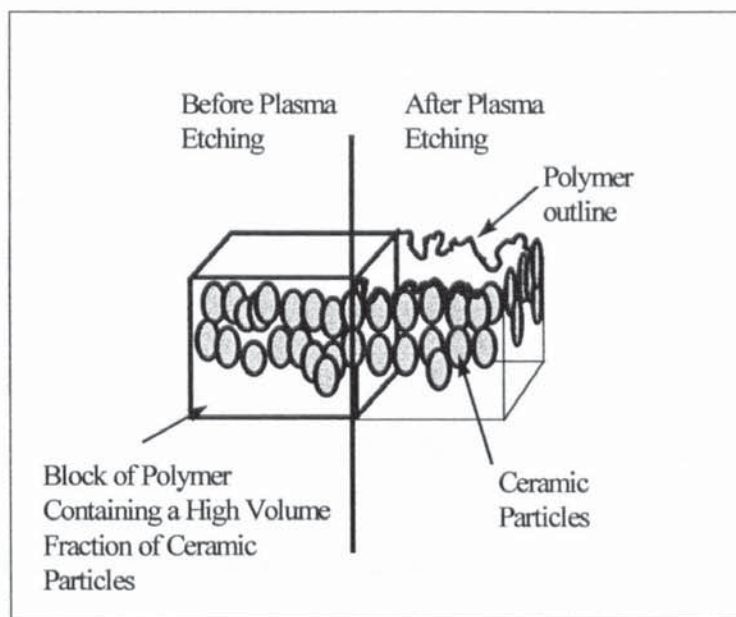
Argon plasma bombardment removed thin slices of pMMA to reveal hydroxyapatite particles below. Each sample of ceramer was photographed before they were bombarded with plasma for 3 hours. Etching time was restricted to 3 hours to reduce deposition of reactive species generated by surface bombardment (c and d reaction mechanisms illustrated in **Figure 3.19**).

Figure 3.19 Reaction Mechanisms Thought to Operate During Plasma Etching (adapted from Singh-Gill)



Immediately after etching, a graph was plotted to show the quantity (by weight) of material removed from the surface. Etched ceramers were photographed under a light microscope for comparison (See Section 5.3, Chapter 5).

Figure 3.2 Diagrammatic View Showing Removal of Polymer by Plasma Etching



Each sample was viewed under a light microscope and an assessment was made of the additional porosity created by comparison with microscope images generated before etching took place. It was deduced that a suitable surface porosity or frictional surface could be created, for fixation of living tissue, that may eventually support the weight of an optical cylinder. Plasma treatment lasted for three hours for each material, and a graph was plotted of weight of material lost over time.

3.4 Biomimetic Synthesis of Ceramic and Polymer Composites

3.4.1 Deposition of a Bone-Like Carbonate Layer onto Polymer

Uniform layers of carbonate containing apatite mineral can be deposited onto polymer surfaces in carefully prepared solutions saturated with mineral ions at body temperature. The mineral is chemically coupled to the polymer surface and grows into a continuous layer. Surface modifications can alter the character of mineral development and so construct a rough surface topography upon which, a layer of hydrated silica forms and develops. Silica and calcium ions are exchanged into the solution from a layer of calcium oxide silicate glass ceramic granules. These calcium ions serve increase the activity product for apatite ions in solution while the adsorbed silica act as nucleation points for crystal growth on the surface of polymer. Deposition and chemical adsorption can occur onto polyvinylalcohol (PVA), polyethyleneterephthalate

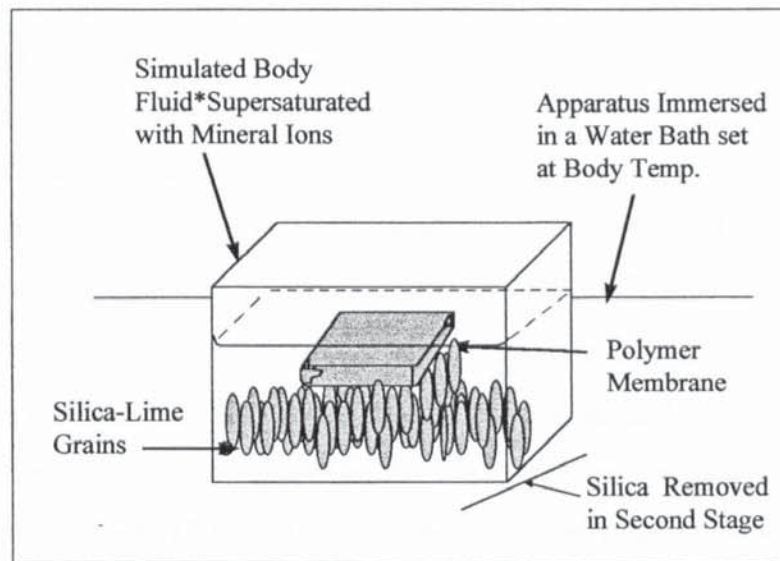
(PET), polymethylmethacrylate (PMMA) and polyethersulfone (PESF).⁸¹

Interestingly the period of mineral layer formation is 24 hours irrespective of polymer type. It is the degree of affinity of the silica ion for the polymer substrate and the diffusion coefficient which control the rate or speed at which nucleation occurs. The concentration of polar groups, whether molecular chains separate easily from the bulk of material and surface roughness positively influence the strength of adhesion of the apatite layer to the polymer surface.⁸¹ Accordingly the following three polymers were synthesised in this study and were selected for the following reasons:-

- pMMA was the preferred polymer for an artificial cornea because of its long term, widespread use.
- pHEMA is water binding polymer with abundant polar groups for mineral nucleation
- pTHFMMA is a stiff polymer, as pMMA, with higher water content

Similar attempts were made to initiate the deposition of a carbonate layer onto pMMA membranes. Membranes were immersed in a simulated body fluid, placed on a bed of silica grains. The solution was heated to a temperature of 36.7°C for 24 hours. The membrane samples were then placed in SBF without silica grains present, and left for a week. Some membranes were abraded with strong hydrochloric acid (5 Molar) to expose chemical side groups for nucleation and also encourage hydroxylation (*See Results Section 5.5, Chapter 5*).

Figure 3.21 Apparatus For In-Solution Mineralisation of Polymer Membranes



* SBF-Simulated Body Fluid, Ingredients are listed below (In Section 3.4.11).

3.4.11 Calcification solutions

A simulated body fluid was produced following the method of Kokubo-saturated with carbonate mineral ions.⁸¹ All were mixed in de-ionised water at body temperature, 36.7 °C.

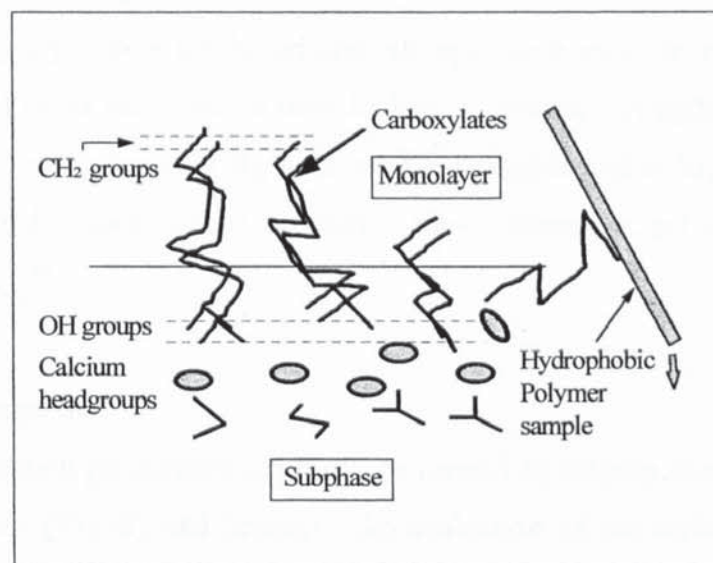
Ingredients for a Simulated Body Fluid Supersaturated Calcium Carbonate Solution:	
<u>Substance</u>	<u>Volume: mmol/dm³</u>
Sodium salt Na ⁺	142
Potassium salt K ⁺	5
Calcium salt Ca ⁺⁺	2.5
Magnesium salt Mg ⁺⁺	1.5
Chlorine salt Cl ⁻	150
Hydrogen carbonate HCO ₃ ⁻	4.2
Hydrogenphosphate HPO ₄ ²⁻	1
Sulphate SO ₄ ²⁻	0.5
Trishydroxyethylaminomethane	50

Calculations were made to determine the quantity of compounds containing mixtures of the above listed reagents

3.4.2 Langmuir Blodgett

Monolayer films of stearic acid and hexane solvent were deposited on supersaturated calcium bicarbonate solutions in a Langmuir mini-trough (JL Automation). Calcium carbonate solutions consisted of 0.1 mmol dm^{-3} / 8 mmol dm^{-3} Calcium dihydrate. The pH was set at between (5.8-6.0) above the pKa of stearic acid. The surfactant layer was compressed and left for 48 hours for mineralisation to take place. Polymer membranes (pMMA and pHEMA) were dipped into the mineral monolayer and subphase to allow attachment by adsorption to the membrane surface (*Please Refer to Section 5.5, Chapter 5*).⁸²

Figure 3.22 *Graphic Representation of a Langmuir Film: Template for Mineral Layer Deposition*



**Polymer sample gently dipped in solvent and solution*

3.4.3 Calcium Carbonate Deposition on Polymer Samples

A solution of supersaturated calcium hydrogencarbonate was prepared using a metastable method. 8 mmol dm^{-3} sodium hydrogen carbonate and 8 mmol dm^{-3} calcium

chloride di-hydrate were dissolved in a solvent containing 0.1 mol dm^{-3} of Sodium hydroxide. The solution was stirred for 15 minutes and placed in a water bath at 25°C while the materials were prepared.

Membrane samples were mounted on glass cover slips and placed at the bottom of a glass dish containing supersaturated calcium hydrogen carbonate solutions and left at 37°C for 48 hours. The reaction can be summarised, thus:



Carbon dioxide and water are unwanted by-products.⁸³

(Refer to Results Section 5.5, Chapter 5)

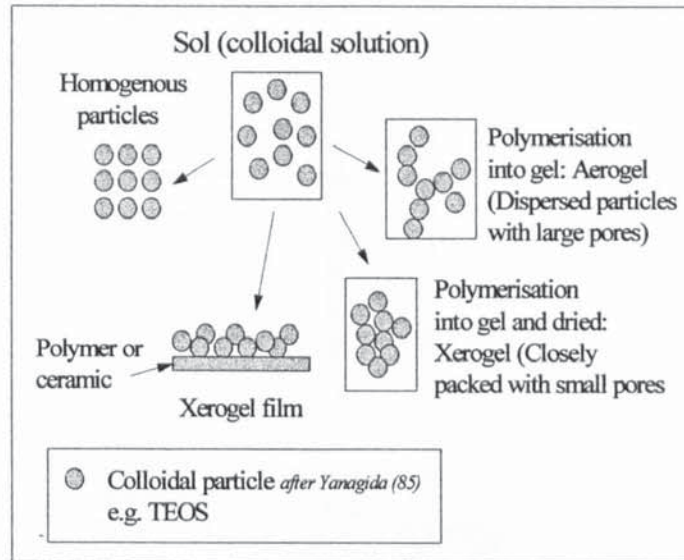
3.4.4 Synthesis of Collagen Gels

Sheets of collagen gel were fabricated and attempts were made to generate a fibrous organisation and to fix the collagen onto biological ceramic. A hydrated collagen gel was formed by mixing together 3g acid soluble kangaroo tail collagen (type I) with 0.5ml sodium hydrogencarbonate solution.. Observations of gel morphology were made under SEM.⁸⁴

3.4.5.Sol-Gel Deposits

Thin films of solution gel derived solids can be formed by dipping them in a solution of tetraethoxysilane (TEOS) and heating. An evaluation of the surface structure was made by light microscopy and scanning electron microscopy (*Results Chapter 5, Section 5.4*).⁸⁵

Figure 3.22 Porous Ceramics Fabricated by a Sol-Gel Process

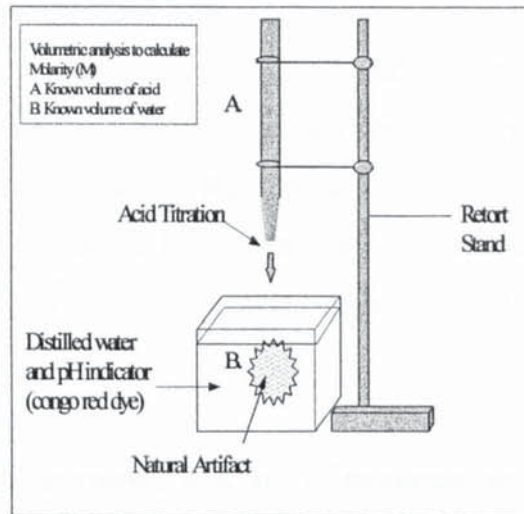


3.4.6 Replamineform Processing

The Replamineform processing is a technology for copying the physical structure of natural foams by a linear series of casting and moulding activities (**Figure 3.23**). An attempt was made to fabricate casts made from a mixture of polymer and ceramic; something which has not been attempted before.

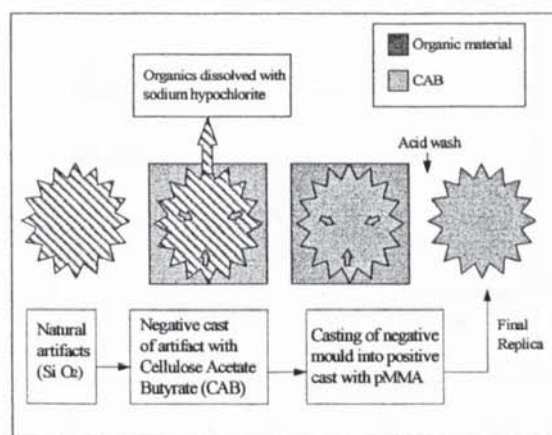
Two natural foams (Keratosa bath sponge and Scleractinian coral) were fully coated in cellulose acetate butyrate giving rise to a negative cast of the pre-formed structure. The next step involved complete dissolution of the remaining organic construct. This was achieved by immersion in heated hydrochloric acid (3 Molar). A solution of methyl methacrylate (MMA) was immersed into the cellulose acetate butyrate mould to form a positive cast. Cellulose acetate butyrate (CAB) was dissolved in dilute hydrochloric acid (0.5-1M) which, was then heated to 50°C. Extreme difficulties arose in both steps dissolving away one material from another. A carefully controlled titration experiment was carried out to record the acidity at which, each material dissolved separately in the presence of the other.⁸⁶

Figure 3.23 *Basic Apparatus for Acid Titration to Determine the Strength of Acid Capable of Dissolving the Cellulose Acetate Butyrate (CAB) Cast or Biological Inorganic Mould.*



Since acrylate polymers have a dissimilar chemical structure to CAB (CAB degrades much faster with acid hydrolysis) we would expect dissolution to occur at a different temperature and pH regime. The difficulty was to capture the optimum conditions for casting and re-casting (*See Chapter 5, Section 5.4.27*).

Figure 3.24 *The Replamineform Process. A technique of fabricating exact copies of porous structures and involves intricate steps of casting and moulding.*



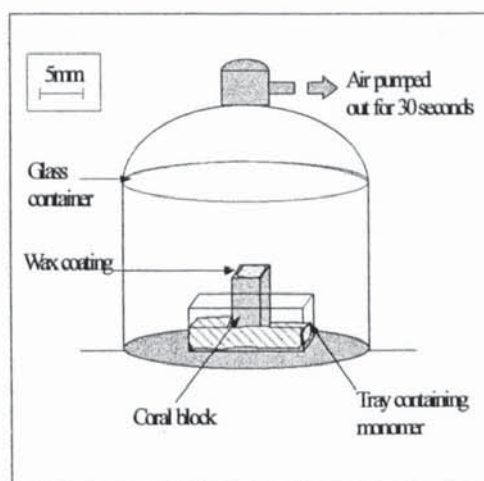
3.5 Conglomeration of Polymer and Porous Biological Ceramics

3.5.1 Incorporation of Polymer into Biological Ceramic

To achieve a tight physical union between the optical cylinder and ring of biological ceramic it was necessary to find a method of integrating the two structures, both rapidly and effectively. The effectiveness of bonding was guaranteed by the large difference in surface energy between methacrylate monomer and ceramics. Thus, experiments were devised to assist the uptake of monomer solutions and partially polymerised monomer/polymer solutions into porous ceramics by placing them in a vacuum. The apparatus for vacuum assisted polymer uptake into a porous ceramic is illustrated below.

A coral block was partly immersed in a tray of monomer and placed in a vacuum jar. The wax coating impeded the spread of monomer to prevent complete coverage of the block. Air was pumped out of the jar for 30 seconds to create a vacuum. The considerable reduction in pressure caused greater capillary flow into the pore system. The apparatus was then placed either under an ultraviolet lamp or in a water bath, to polymerise monomer in and around the porous ceramic block.

Figure 3.25 *Vacuum Assisted Polymer Impregnation into a Porous Ceramic Block*



On other occasions, samples were placed in an ultrasound bath to temporarily fluidise the polymer, causing the monomer/ pre-polymer to penetrate deeper into the pore system.

On other occasions porous ceramic blocks and ceramic discs (supplied by Jesse Shirley Advanced Ceramics) were immersed briefly, for one minute in a methacrylate monomer solution (together with 5% ultraviolet light induced initiator and 1% crosslinker; EGDMA). The blocks or discs were suspended by a paperclip to dry-out and allow excess monomer to drain away. Polymerisation took place over a high power ultraviolet lamp, as displayed in Figure 3.27.

Figure 3.26 *Diagram of Apparatus for Thermal Polymerisation of Keratoprosthesis Shapes and Coral: Thermal polymerisation was carried out in a water bath at constant temperature (60°C for 3 days).*

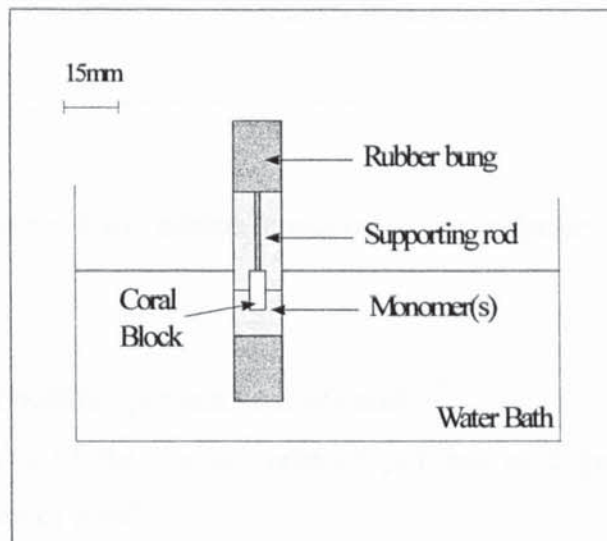
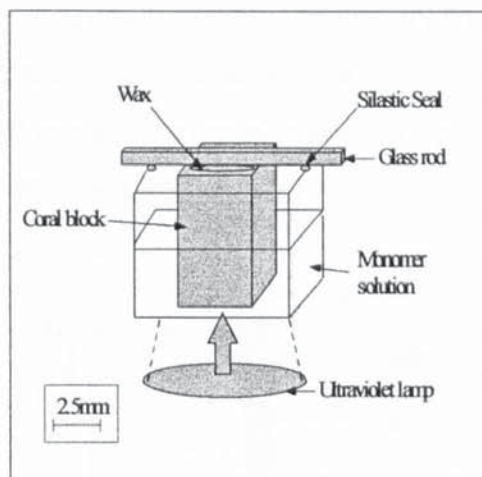


Figure 3.27 *Diagram of Apparatus for Ultraviolet Polymerisation of Keratoprosthesis Shapes and Coral Blocks: Ultraviolet (U.V.) polymerisation was carried out over a high power output ultraviolet lamp (220-240W) for approximately, 35 to 45 minutes.*



A set of criteria assessed the completeness of fit for polymer 'syrops' into the pore system.

- contact area of polymer per unit area of coral.

This gave a measure of the contact area of polymer as a percentage of the total available surface area of coral.

- the percentage infiltration of pore spaces.

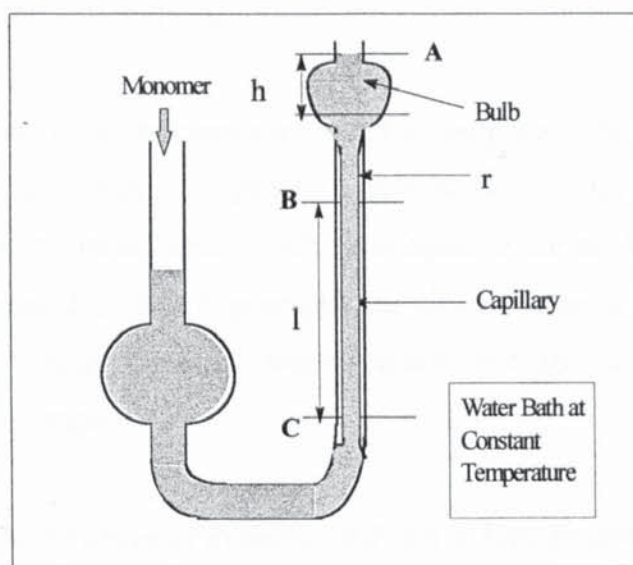
To determine the quantity of polymer as a percentage of the total volume of available pore space. It was necessary to have the line of polymer in contact with the coral surfaces as opposed to between them, so as to minimise the area of possible contact with inward growing tissue.

On every occasion an assessment using the above criteria was made from photographs taken through a light microscope (*See Results Chapter 7, Section 7.3.3*).

3.5.2 Measurement of Viscosity

Four sample vials of 50cm³ monomer, with initiator and cross-linker were measured out in a glass measuring cylinder. The first monomer solution was irradiated with ultraviolet light for 5 minutes and its viscosity was measured in an Ostwald viscometer by measuring the time for the solution to move through a certain length of capillary. A second sample was irradiated with ultraviolet light for 10 minutes, the third for 15 minutes and so on, up to 30 minutes-a guaranteed period for polymerisation.

Figure 3.28 Ostwalds Viscometer



Viscosity was measured by the following equation, with reference to Figure 3.29:

Equation (3.18) $\eta_1 / \eta_2 = \rho_1 t_1 / \rho_2 t_2$

Where ρ_1 = density of monomer(s)

ρ_2 = density of reference liquid, water

t_1 = time for the upper level of monomer to fall between marks A and B

t_2 = time for the upper level of water to fall between marks A and B

η_2 = viscosity of reference liquid

η_1 = viscosity of monomer

(See Results Chapter 7, Section 7.3.4)

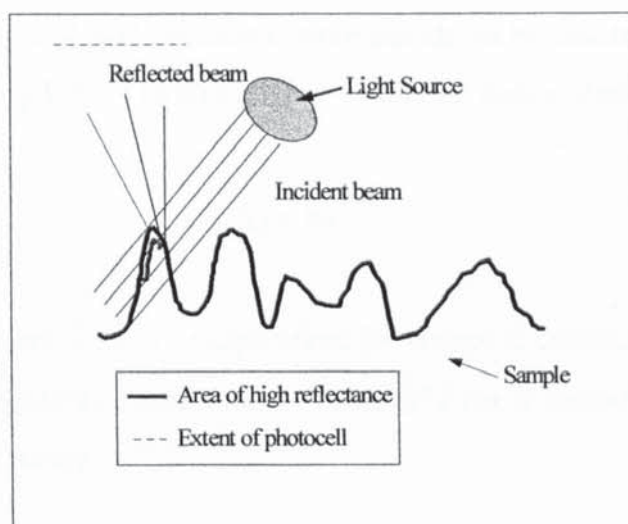
3.6 Materials Characterisation

3.6.1 Goniophotometer Measurements of Surface Roughness

The Goniophotometer is a very precise and useful method of quantifying the texture of a surface⁸⁷. A beam of light of known intensity is projected onto the surface of a material and the extent of deterioration in the intensity (quality) of light is detected by a photo-detector cell. Such a change in light intensity is due mainly to the scattering of light reflected when it strikes a bumpy surface, some of course will be transmitted and reflected. The more rugose the surface the more scattering of light results and hence the more diffuse is the reflected beam.

To make sense of this value the change in quality is compared with a value calibrated to a very smooth surface, such as a polished glass slide. A plot is made comparing intensity with the angle of reflectance (which is equal to the angle of incidence). All materials that possessed surface topography, as viewed under a light microscope or SEM (roughness, pitting, porosity) were characterised by Goniophotometry (See *Results Chapter 7, Section 7.2.2*).

Figure 3.29 *Pattern of Reflectance From A Very Rough Surface*⁸⁷

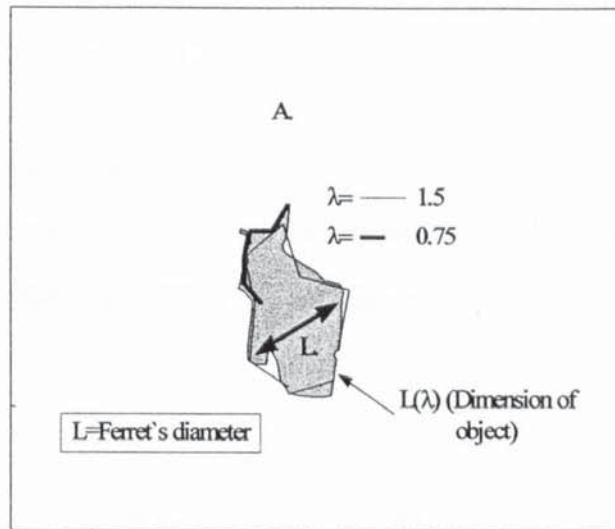


3.6.2 Fractal analysis

The degree of irregularity along a rugose surface can be measured and quantified using mathematical models. Goniophotometry measures rugosity through the behaviour of scattered light and the identification of each segment of roughness is limited in scale by

the thickness of the beam of light and the sensitivity of the photo-detector.

Figure 3.3 Diagram Showing How Fractal Surfaces were Measured



A fractal quantity can be assigned to roughness of a surface by measuring the perimeter with dividers (l) a number of times at serially decreasing length scale and relating this to the maximum width of the object.⁸⁸ As the size of the measuring stick approaches zero the length or area approaches infinity. Fractal dimensions occur when the yardstick is raised to a certain power for the measure of the object to be finite. Fractal dimensions of the surfaces of crystal agglomerations were calculated by constructing a Richardson plot of $\log L$ and $\log L(l)$. The straight line so formed is described by the function:

Equation (3.9.1)
$$L(\lambda) = \beta \lambda^{1-\alpha}$$

L = max width of object; λ = divider separation; β = empirical constant for the real object; α = measure of irregularity (α becomes a value of 1 for a smooth curve, and greater than 1 for a rough curve).

(See Results Chapter 6, Section 6.2)

3.6.3 XRD Analysis of Biocoral[®] and Bone-Like Corals

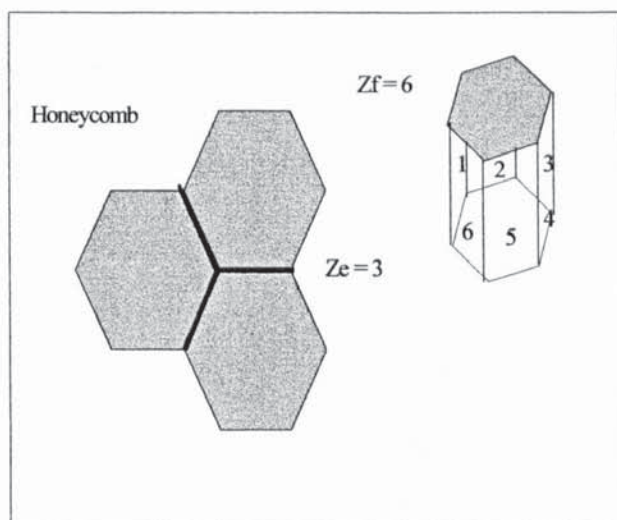
An elemental analysis was carried out on Biocoral[®], Endobon[®] to confirm their chemical composition and for comparison also with an untreated natural cellular solid (See Results Chapter 4, Section 4.3).

3.6.4. Physical Characterisation

Numerical measures were derived of physical and structural properties for comparison of natural artifacts collected⁸⁹. They are as follows:-

- Density (ρ)
- Contact between pores (3-Dimensional or 2-Dimensional) either interconnected on every face or not.
- Edge (Z_e) and face connectivity (Z_f) Edge connectivity is the number of edges that meet at a vertex. Face connectivity is the number of faces that meet at the vertex. Natural foams exhibit great variation in connectivity. Z_e and Z_f are easily counted from good SEM images.

Figure 3.32 Edge and Face Connectivity



- Cell shape is the determinant of packing configurations, and mechanical properties. Shape is a major influence on whether the foam is anisotropic or isotropic. Eulers law relates C,F,E,V. (C=cells; V=number of vertices; F=number of faces; E=number of edges)
- Shape anisotropy ratios (L_1/L_2); Ratio of cell length to cell breadth

(Results are displayed in Section 7.3.25, Chapter 7)

3.7. Biological evaluation

3.7.1 Cell culture

Three kinds of test were carried out in sterile cell culture to gauge the degree of material biological tolerance or biological compatibility. Biological compatibility testing of sample materials served to, (a) identify the average population number of viable cells to determine the level of cytotoxicity and (b) determine the average number of cells firmly adhered to the sample. Cytotoxicity, adhesion and viability assays were carried out on Jesse Shirley samples according to protocols as described by Graham.⁹⁰

CHAPTER 4 RESULTS:
Fabrication of a Porous Biological Ceramic
Support Frame for an Artificial Cornea

CHAPTER 4 RESULTS:

Fabrication of a Porous Biological Ceramic Support Frame for an Artificial Cornea

“The requirements for a synthetic substitute appear deceptively simple..to produce an interconnected porosity, which promotes rapid bone ingrowth, but possesses sufficient strength to prevent crushing under physiological loads.”

William Bonfield

4.1 Introduction

Porous bone is the key feature of the OOKP that should be included in a successful synthetic OOKP replicate and is the first element to be fabricated. As stated in chapter two, the chemical composition of bone causes few biological complications, along with structure (which was regarded as the most important) This chapter begins with the possibilities for employing a biological ceramic rather than conventional polymers, as the principal material for a keratoprosthesis support frame. Hydroxyapatite is the safest inorganic material to implant in the human body because it is virtually identical to hydroxyapatite in bone and other hard tissues (with low rate of infectivity, non-toxicity and does not illicit any immunological response). Hydroxyapatite is highly biologically tolerant, because it induces the body to readily form biological linkages at its surface. Biological ceramics are, thus an obvious choice for the manufacture of a tooth and bone analogue. The bulk of the chapter presents results of experiments to re-create a bone-like morphology from hydroxyapatite grains and powders. Complex void architecture was demonstrated in this study by varying forming conditions, particle sizes and grain mixture contents. Intrinsic problems of brittleness and formation of complex shapes are highlighted and how they might be overcome.

4.2 Biomedical Ceramics

Ceramics are non-metallic polycrystalline inorganic solid materials created by thermal treatment at high temperatures. They comprise chemical elements residing in the second and third rows of the periodic table which include metallic oxyanions, phosphates and borates. These elements are held together by strong and short covalent

bonds conferring strength and durability.⁹¹ Ceramics are highly resistant to shearing which means they are non-ductile and hard (Mohs hardness:5) but are very weak in tension. Consequently, ceramics required to operate in environments with high strain must be combined with a polymeric matrix, which has great implications for those intended for human implantation. Polymer augmentation is commented upon later in the chapter.

There are three classes of ceramic that can be implanted into the human body, carbons, bioactive glasses and calcium phosphates. Each material has been used to construct all or one part of a keratoprosthesis. For example, carbon was used to toughen and enhance polymer meshworks while Bioactive glasses and calcium phosphates were used in the construction of analogues to the Osteo-odontokeratoprosthesis (OOKP) dental lamina (plate of dentine, cementum, fibrous ligament and spongy bone). Details of artificial corneas made with ceramics and their clinical outcomes are outlined in chapter one.

What follows is a brief summary of the physico-chemical and biological characteristics of each ceramic type and the suitability both for implantation into the human body together with a few sentences summarising its use as a keratoprosthesis support frame.

4.2.1 Carbon

Carbon is a very common element in the universe. It is quite un-reactive and very readily forms chemical liaisons with many other elements. For these reasons, carbon is the primary element of organic compounds and makes the subtly intricate property of life possible.⁹² Carbon is an element to be found at the top right of the periodic table close to nitrogen and oxygen, allies in the assembly of living organisms. Carbon implanted into the body elicits a token host response because of the similarity to the basic chemistry of every working component in the body. Carbon exists in many different physical forms; turbostratic carbon is the form implanted into the human body. In structure it is close to graphite, composed of a many layered hexagonal array, but with many more pores in the latticework, which provides greater resistance to shearing stress and fracturing without reducing stiffness. Carbon has been used to fabricate a

number of artificial cornea support frames with moderate results.

4.2.2 Oxide ceramics

Oxide ceramics are closely packed crystalline minerals with significant quantities of oxygen ions in the latticework. These ions serve to stabilise the structure from chemical degradation. There are two oxide ceramics of great interest to medicine; aluminium oxide and zirconia. The main oxide ceramic used in restorative surgery is aluminium oxide, which is very stable and non-reactive when placed in the body.⁹³ Zirconia possesses good compatibility and gives rise to similar tissue responses as aluminium oxide, and because they are both fully oxidised, there are no leachables liable to cause inflammation. Aluminium oxide has been employed in the fabrication of a single artificial cornea by Polack and Heimke with reasonable tissue bonding and a lack of inflammatory reactions. The reason for this good success is that aluminium oxide is extremely wettable and adsorbs a biologically active layer.

4.2.3 Bioactive Glasses and Glass Ceramics

Biologically active glasses arose from the need to optimise interactions between implant and interfacial tissue. The term “biologically active” pertains to an associative encouragement of normal tissue formation and function. Up until the invention of bioactive glasses, novel biological materials were designed to be refractory to biological attack and dissolution.

There are five distinct types of glass-like ceramic, determined by the nature of biological reactivity. Reactions are almost entirely limited to the surface (50-300 μm depth of penetration) so that the bulk of the material remains unaffected. Type IV materials develop a silica film but are open to dissolution. Type V materials, after time, dissolve almost completely.⁹⁴

A particularly interesting result from the viewpoint of copying the OOKP method of insertion, was the ability of bioglasses to develop strong bonds with mucosal soft tissue, such as gingiva-soft gum tissue enclosing each tooth. Bonds form because the attachment of collagen fibres, derived from the mucosa, is preceded by the deposition

of a bioactive acellular layer rich in calcium phosphate, glycoproteins and mucopolysaccharides. However, attachment is only stable enough when mechanical stresses are small.⁹⁵ Biologically active ceramics were strong candidates for the peripheral support due to the high level of biological activity.

4.2.4 Calcium Phosphate Ceramics

Calcium phosphate ceramics have a long record of use as a material for prostheses and bone restoration. The major form is hydroxyapatite, the mineral of bones and teeth. Calcium phosphates have the general formula $M_{10} (X)_6 Z_2$. (where M=calcium, X=phosphate, Z=hydroxyl) The ratio of calcium salts to phosphate is indicative of chemical and physical properties. Hydroxyapatite lies in the range of ratios between 1.5 and 1.67 and this represents the most stable or metastable form in which calcium and phosphate can exist together in a crystalline form.⁹⁵

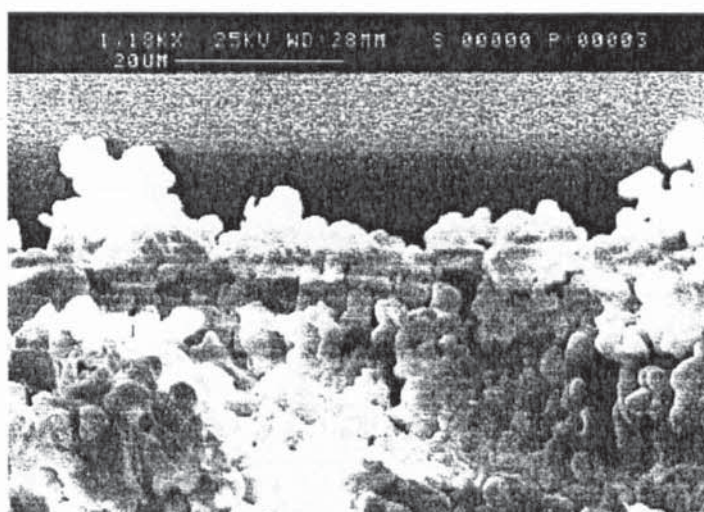
Medical grade hydroxyapatite (HA) is easy to obtain, experiment with, in many different ways and machine into intricate shapes. Hydroxyapatite has a long and successful history of use in bone surgery and consequently a number of bone void fillers were considered as candidates for a keratoprosthesis support frame. However, initial material fabrication work dealt with assorted hydroxyapatite powders.

Table 4.1 *Biomedical Ceramics Considered as a Material for the Support Frame*

Generic Group	Specific Name
Carbon	Turbostratic Carbon
Oxide Ceramic	Aluminium oxide and Zirconia
Bioglass	Type I-to-Type IV
Calcium Phosphate "Biological ceramic"	Hydroxyapatite and Calcium Carbonate

A simple cell culture study confirmed the affinity cells have for hydroxyapatite powders and sintered blocks (**Photograph 4.1**)

Photograph 4.1 *Part of a Hydroxyapatite Disc Composed of Compacted and Sintered Particles*



It also confirmed the absence of cellular degradation on contact with hydroxyapatite. This is described more fully in the next section.

4.3 Cellular Responses of Cells to Hydroxyapatite Discs

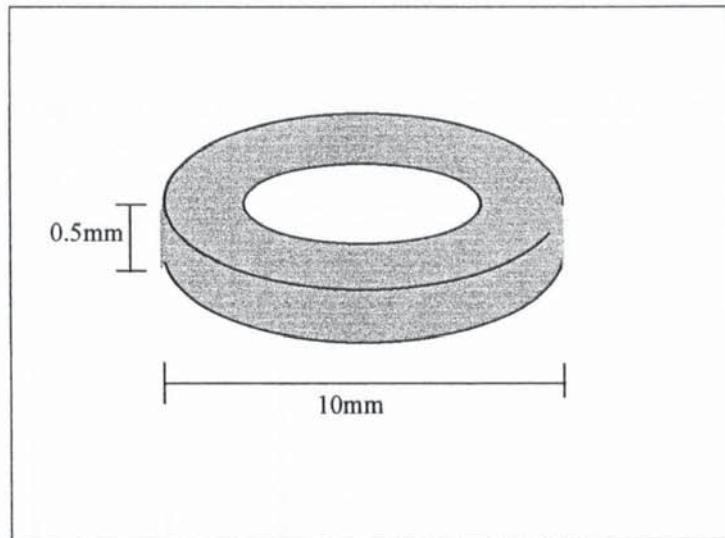
Two tests were performed to gauge the response of mammal fibroblasts (mouse 3T3 fibroblast primary cell line) to hydroxyapatite with differing pore sizes (0.9 to 6 μ m) and pore shapes (spherical, kidney shaped and oblate).

Table 4.11 *Hydroxyapatite Discs Fabricated by Jesse Shirley Ceramics*

Sample designation	Pore sizes in microns
Sample E	6
Sample F	1.6
Sample G	1.1
Sample H	15

These tests quantified the degree of cytotoxicity and adhesion. Further qualification of cell health was made by SEM images. Assorted powders and compacted discs (listed in **Table 4.11**), shaped like washers, 10 mm in diameter and 0.5mm thick (**Figure 4.1**) were provided by a manufacturer of orthopaedic ceramics (Jesse Shirley of Stoke-on-Trent).

Figure 4.1 *Diagram of a `Jesse Shirley` Hydroxyapatite Ceramic `Washer`*



Photograph 4.11 is a surface view of a porous “polo” shaped disc, manufactured for this project, by Jesse Shirley Ceramics. One can barely see the pores ‘fossilised’ within medical grade hydroxyapatite. This was the greatest concentration of porosity that could be produced within a powder-pressed disc, sintered to a thickness of 0.5cm (i.e suitable for insertion into the cornea and anterior segment).

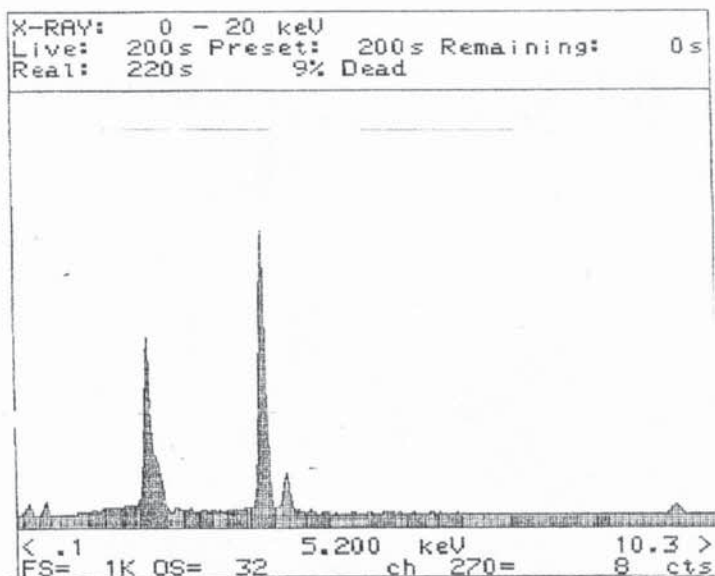
Photograph 4.11 *Jesse Shirley Hydroxyapatite `Polo` (Porous type)*



Under X-ray, the discs were shown to possess a preponderance of calcium (88%), oxygen (8%), phosphorus (2%), and carbon (0.5%), (See **Graph 4.1**) with additional trace heavy metals as by-products of machining. Thus, the calculated ratio of calcium to phosphate which, is an indication of biological stability was a staggering 4:1, clearly

non-stoichiometric and twice as large as the stable ratio of 1.67 (human bone=1.48-1.62).(See Graph 4.1)

Graph 4.1 X-Ray Elemental Analysis of Sample F `polo`

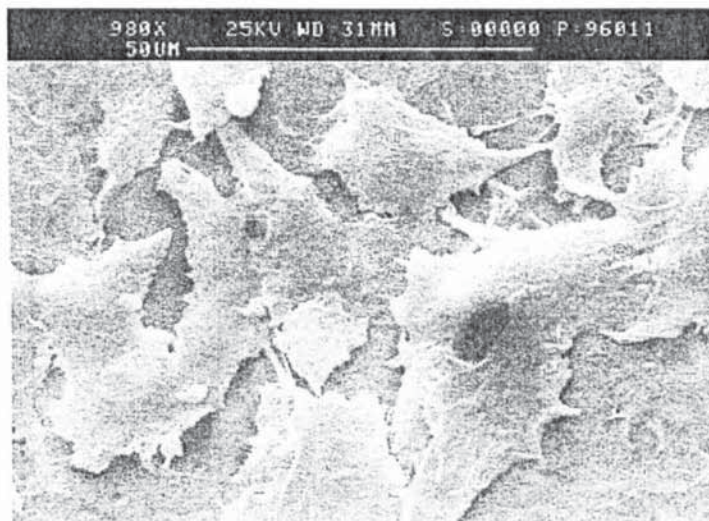


The testing procedures for fibroblast cell seeding and culture are described in detail in chapter three. In general, and excluding outliers, fibroblasts remained healthy and viable (mean of 93% survival after 18 hours; 20 days to confluence/ 8 days for control) but proliferated rather slowly. Their growth characteristics were as fibroblasts suspended in liquid culture medium, except for a less pronounced exponential growth phase.⁸⁴ The average density of fibroblast cells attached to the surface of hydroxyapatite was determined by washing with trypsin, concentrated to remove poorly attached and unattached cells from the surface of the material.

The extent of cell adhesion to the surface was small and this view was re-inforced by direct observations of SEM images (See **Photographs 4.14- 4.16**). A calculation of actual number of cells stripped from the surface by trypsin was correspondingly small. As determined by the trypan method, there was a high percentage of viable cells indicating that hydroxyapatite samples were sufficiently inert and did not release any cytotoxic factors. However, the trypan method is a nebulous guide to actual cell viability. Both surface roughness and cell culture were the most appropriate yardsticks

for the characterisation of cellular activities because of their simplicity, but were by no means the most exact.

Photograph 4.12 *3T3 Fibroblasts Residing on a Jesse Shirley Hydroxyapatite Disc: Sample F (1.56µm average pore dimension)*



Considering the cells were in an exponential growth phase, the increase in mean cell numbers was not exceptional. Additionally, there was an anomaly in the speed of cell confluency, as compared with fibroblasts grown on tissue culture plastic, but cell shape and habit clearly corresponded to fibroblasts growing in liquid culture.⁸⁴

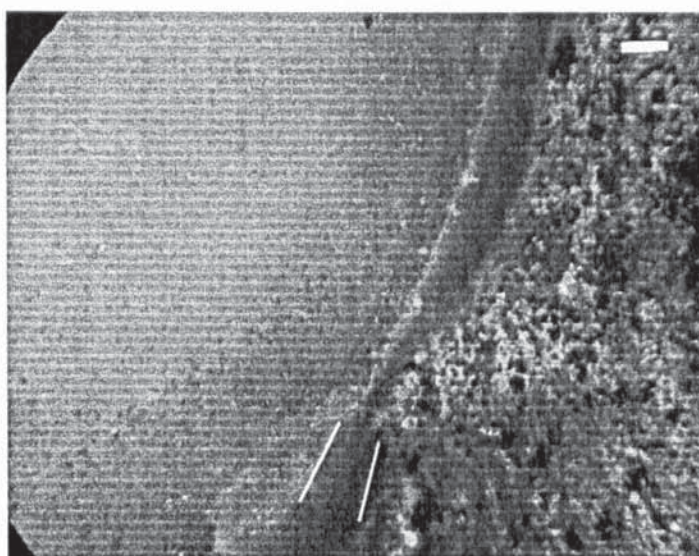
Table 4.12 *Biological Evaluation of Jesse Shirley Ceramic Discs: A Summary of Results*

Test	Method	Samples with Best Result
Mean number attached to substrate	Trypsin treatment	F and H (largest mean numbers)
Cytotoxicity	Trypan blue	F and H (smallest number to turn blue)
Viability (in long and short term)	Time to confluency	E and F (highest value)

4.4 Histological Observations of the Dental Lamina

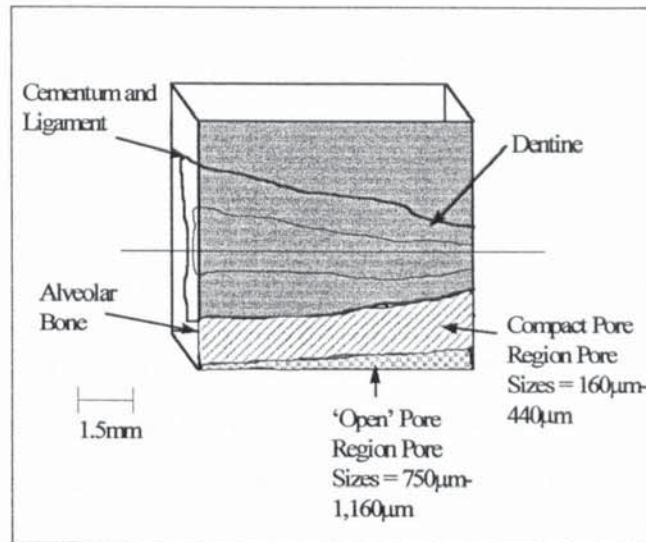
Microscopical observations were carried out on fresh specimens of the osteo-odontal ligament to record details of structure. Unfortunately, there was no way of obtaining and analysing biopsies of the OOKP dental plate, because of ethical objections. Although there is some evidence provided by other investigators of the OOKP, as described in Chapter 2.

Photograph 4.13 *Cross-Section Through Dentine(left), Periodontal Ligament and Compact Spongy Bone(right); (Scale Bar = 400 μ m).*



Grafted tooth and bone is a strongly mineralised structure with a graded blend of differing structures. Compact trabecular bone forms the outer shell of the dental plate and extends from the periodontal ligament for 1,500 μ m at one end before it narrows to 160 μ m at the other end (See **Figure 4.1**). Pores situated between 160 μ m and 500 μ m from the interface with dentine have a diameter of 300 μ m (+/-140 μ m). Beyond a distance of 1,500 μ m pore sizes can approach 1,160 μ m. (**Photograph 4.13**) and represented diagrammatically in **Figure 4.11** on the next page)

Figure 4.11 *Stylised Diagram of OOKP Dental Plate Support Frame Highlighting Alveolar Bone Pore Sizes*



The periodontal ligament consists of a mixture of collagen fibre bundles ($0.38\mu\text{m}-5\mu\text{m}$) and partially mineralised collagen fibres-Sharpey's Fibres ($4\mu\text{m}$)-which are embedded in the dentine. Dentine is heavily mineralised collagen with long isolated channels $4\mu\text{m}$ in diameter at a density of $3\mu\text{m}$.⁷³ Unlike the ligament and bone, dentine plays no biological role, rather it functions to anchor the shelf structure. Thus, between each end there is a gradation in void spaces from $1500\mu\text{m}$ to $4\mu\text{m}$, unconnected and separated by cementum and ligament.

4.5 Fabrication of Hydroxyapatite Ceramic Discs

Work began by formulating methods for constructing a biological ceramic (hydroxyapatite or calcium carbonate) with a graded void space, and perhaps crucially, ignoring the role of the ligament.

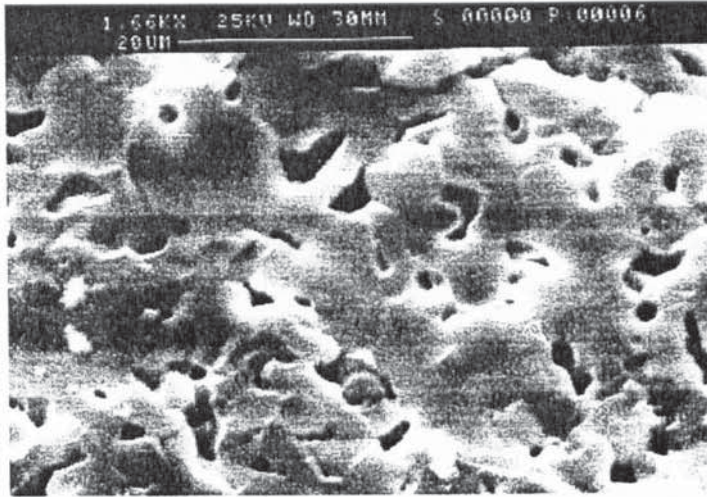
Attempts were made to form porous hydroxyapatite discs by varying compacting pressures ($50-100\text{kN}^2$), length of time for compacting (immediate, 3,4 and 5 minute spells). A fine mist of water was added (approximately 8-9% deionised water) to the powders before compacting took place. Discs were also made from powders with differing combinations, in equal volume, of discrete particle sizes (Chapter 3). After sintering at 1250°C for 1 hour, the ceramics possessed a uniform interconnected pattern

of micropores: 5-10 μm in diameter. The pores were more evenly distributed in the discs made from powders with the smallest particle dimension. Unfortunately macropores (20-200 μm) were absent in every sample. Scanning Electron Microscopy (SEM) images were generated of the consolidated discs to study the surface structure. The structural results of discs made by Jesse Shirley Ceramics, using the same method described previously are summarised below.

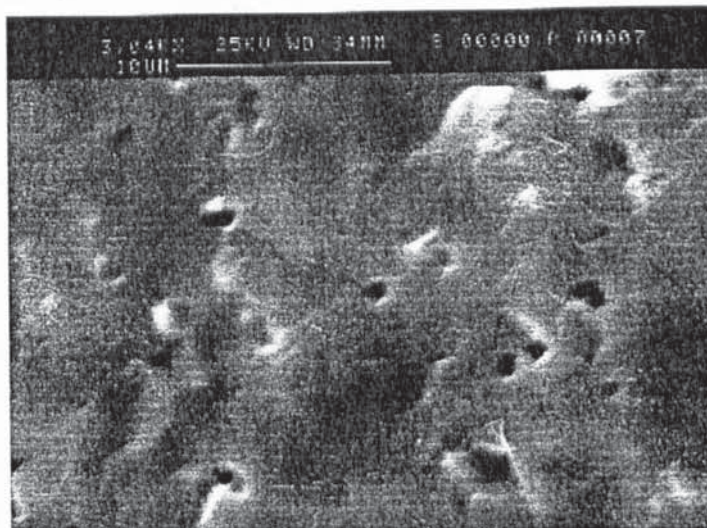
Photograph 4.14 Sample E (0.75 μm +/-0.51): *Sample E possesses a smooth but undulating surface. There is a very low density and great variation in pore size and shape. We could assume that there is a multiple orientation to the pores. The pore density is highly insufficient for comprehensive cell growth and integration.*



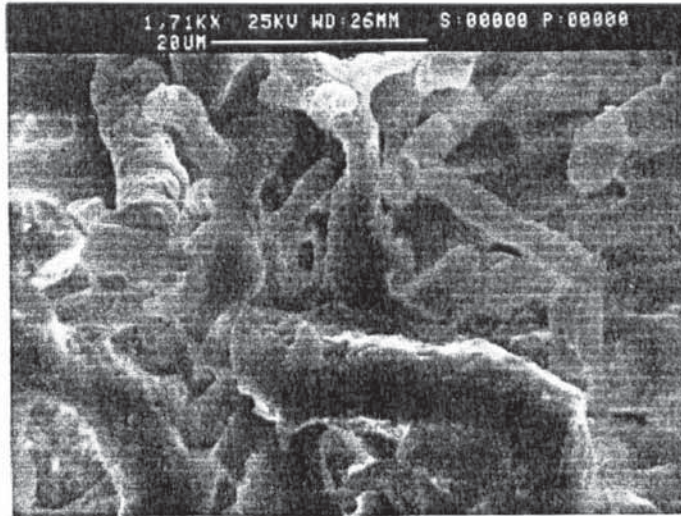
Photograph 4.15 Sample F ($1.56 \mu\text{m} \pm 0.84$): Possesses extensive smooth faces stepped in one plane. Also pitted areas are mainly around the irregularly shaped pores. All pores are apparently unconnected with other pores nearby.



Photograph 4.16 Sample G ($0.875 \mu\text{m} \pm 0.625$): Surface is very smooth (smoother than E) with regular fine stepping. There is a very low density of pores and no signs of interconnections between pores.



Photograph 4.17 Sample H (7.8 μm +/-2.1): *Consists of a meshwork of tubular processes with large elongated cavities producing a very open porosity.*



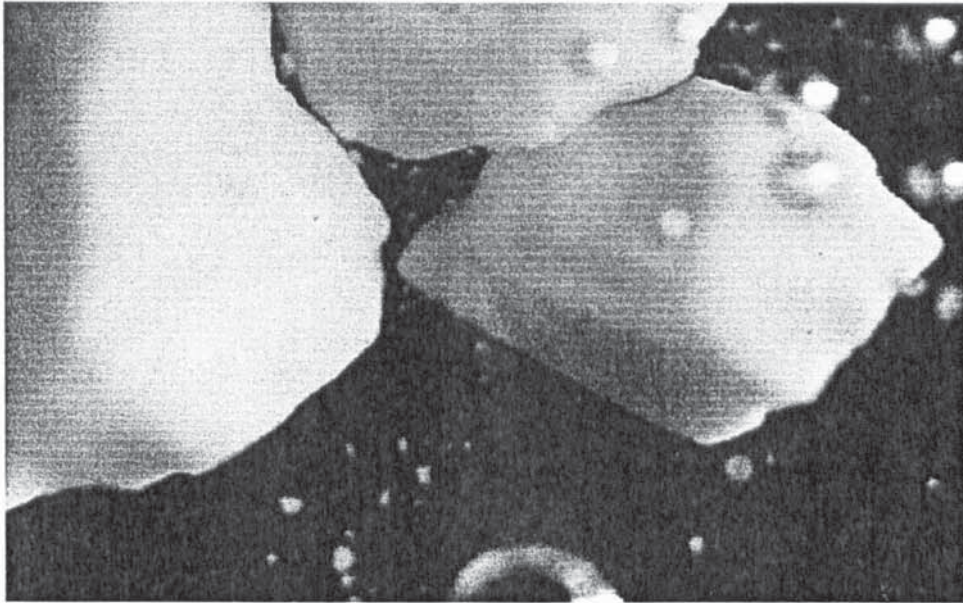
Assimilating the SEM observations of surface roughness and the results of biological compatibility tests it was found that sample F and sample H with the highest pore sizes sustained larger numbers of cells. Interconnected cavities (present in sample H only) did not, as expected improve cell viability above all others. Confluency without clear explanation, was more rapid in sample F and in sample E. In conclusion, biological compatibility tests were confusing and the emphasised differences between samples were only just significant.

4.6 Fabrication of Porous Ceramics

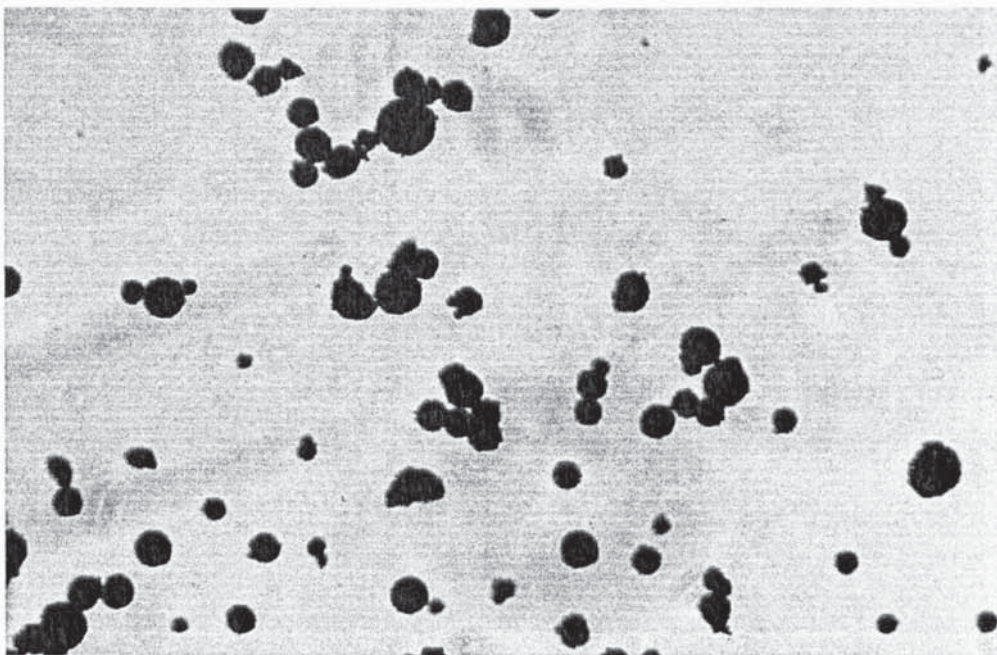
4.6.1 Compacting and Packing Arrangements of Ceramic Powders and the Creation of Ordered Uniform Porosity

The first strategy for the fabrication of a porous ceramic began with selection of ceramic powders for cold isostatic pressing into a porous disc shaped 'green body'. At disposal were hydroxyapatite powder grains of dimensions varying from 18 μm -500 μm in diameter. If grains with a single diameter were allowed to collect into a small container under the force of gravity, they would pack themselves in a relatively ordered arrangement.

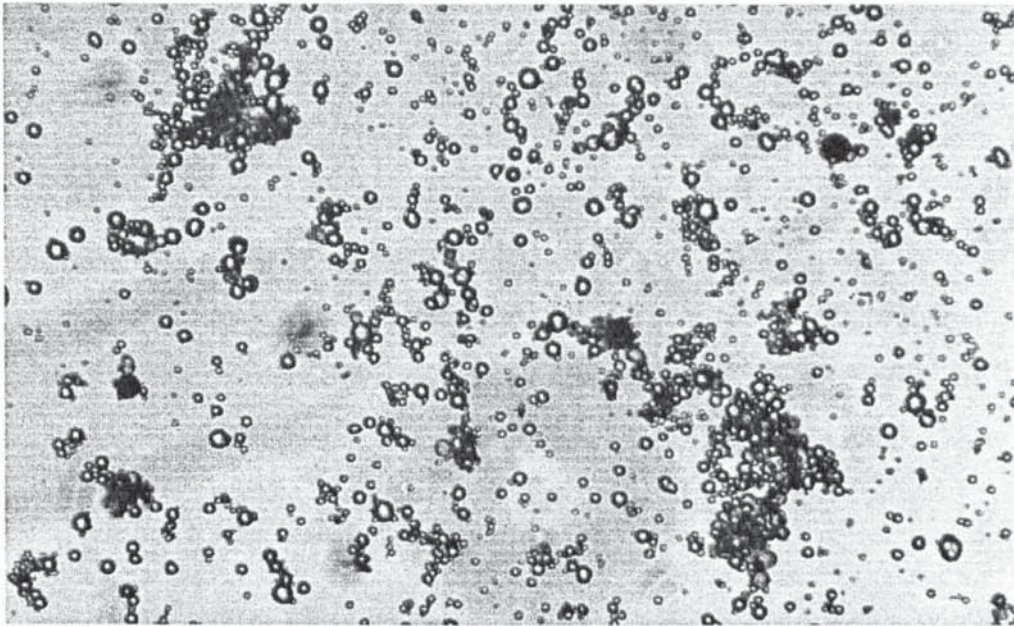
Photograph 4.18 *Grains of Hydroxyapatite. Sample A; There is a large range of grain sizes in this sample. The large particles are straight edged and angular in form. (30 μm -146 μm)(x10 magnification)*



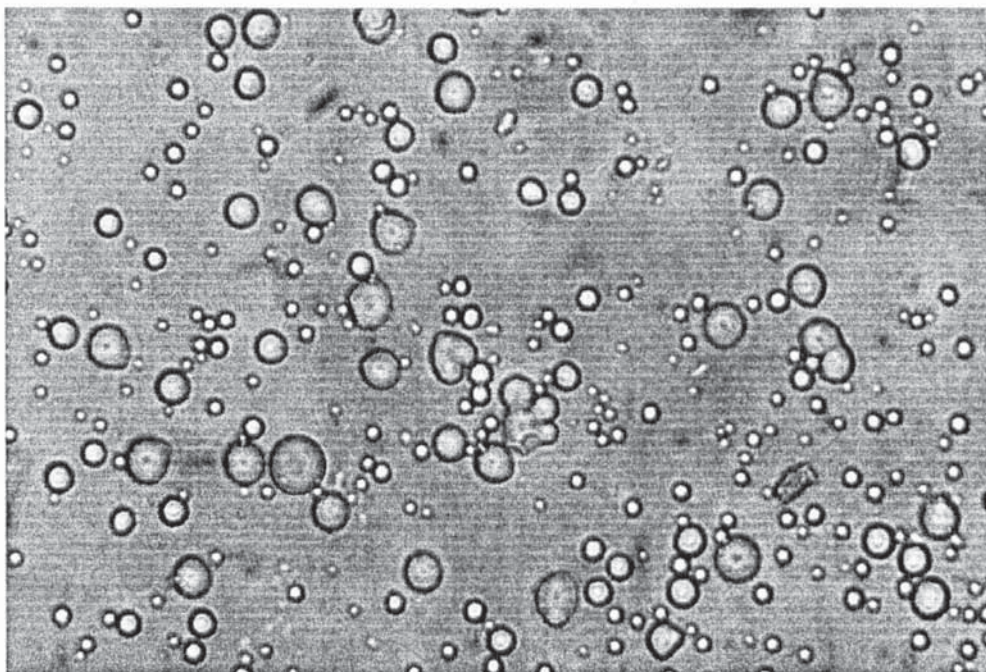
Photograph 4.19 *Grains of Hydroxyapatite. Sample B; Much as grain sample A there is a large range of grain sizes except that the edges are more rounded (20-97 μm)(x25 magnification)*



Photograph 4.2 *Grains of Hydroxyapatite. Sample C; The grains in this sample are much more uniform in both shape and size. (4-20 μm)(x10 magnification)*



Photograph 4.21 *Grains of Hydroxyapatite. Sample D; Grains in this sample are very uniform and are nearly perfect spheres in outline. (2.5-4 μm)(x10 magnification)*



The size of gap between particles can then be calculated, assuming they are spherical or quasi-spherical using simple geometry.

It was found that powder grains with diameter of 500 μm gave a consistently larger interparticle space than other different sized grains. This would hold true even if we were to apply pressure and compact grains because, the particles will up to a point, pack more efficiently. Increasing pressure, however eventually leads to inhomogeneities in packing and an overall reduction in void volume. The same also occurs during sintering as the pointed ends of the space, become rounded and smaller in area due to melting. Matters are further complicated if the grains have irregular shapes. Compacting in these experiments was set at 1 ton/inch² (50kN) to make 50 μm thick tablets with some porosity.

The challenge therefore, was to pack grains in a manner that would maximise void volume after compacting and sintering, but also engender an ordered uniform porosity. Mass for mass mixing of two differently sized and shaped grains reduced packing efficiency and so increased porosity. To produce a conspicuously large porosity it was necessary to have mixtures with a small difference in grain size and shape. This was reflected in the powder mixtures selected for compacting into discs (Table 4.13). Shape differences disturb efficient packing arrangements for example, a 500 μm /125 μm mix in a 50:50 ratio yielded a pore size average of 156 μm while a 50:50 mix of 500 μm /36 μm grains where the difference between largest and smallest grains is 464 μm gave rise to a pore size of 98 μm . This was reflected in the powder mixtures selected for compacting into discs. Table 4.13 shows all the permutations of powder mixtures possible and those that were actually fabricated. The tendency, although not clear in the table, was to select powder mixtures according to the above criteria.

Table 4.13 Powder Mixtures Compacted into Discs (All 50:50 by weight)

	A(500)	B(50)	D(15)	100	500/ 200	36	36/100	Wh. (50x3)	Sph. (500)
A(500)	###	###	###	###	###	###	###	###	###
B(50)	###	###	###	###	###	###	###	###	###
D(15)	###	###	###	###	###	###	###	###	###
100	###	###	###	###	###	###	###	###	###
500/ 200	###	###	###	###	###	###	###	###	###
36	###	###	###	###	###	###	###	###	###
36/100	###	###	###	###	###	###	###	###	###
Wh.(50x3)	###	###	###	###	###	###	###	###	###
Sph.(500)	###	###	###	###	###	###	###	###	###

(μm) Average Pore Sizes are in Brackets

Wh. = Hydroxyapatite Whiskers (500 μm length by 3 μm)

Sph. = Hydroxyapatite Spheres (500 μm)

Table 4.14 Pore Dimensions for a Two-Dimensional Packing Distribution (μm)

Particle Size	Pore Volume +	Pore Space
36	285	7.2
100	2200	20
375	30937	75
500		100

Packing densities and packing arrangements

+ μm^2

Packing arrangements are affected by shape and size of grains and each one yields a characteristic porosity and pore distribution. The results of an experiment to simulate the packing of real ceramic grains are summarised below. The figures relate to the amount of space between grains of differing sizes. The arrangements of assorted grain sizes were visualised using a makeshift viewer to assist with the interpretation of results.

Table 4.15 Percentage Packing Efficiency of Grain Mixtures

	A(500)	B(50)	C(25)	D(15)
A(500)	81%	87%	72%	59%
B(50)		70%	79%	55%
C(25)			72%	65%
D(15)				89%

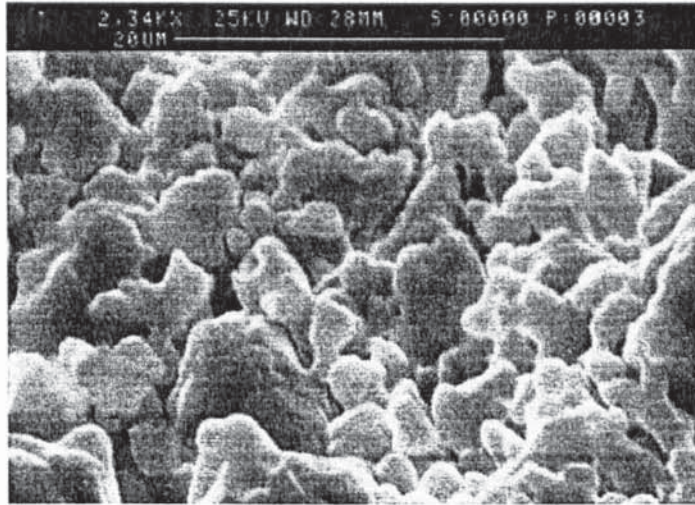
Grain types A to D with diameters in brackets

Table 4.16 Space-to-Circle Ratio of Grain Mixtures

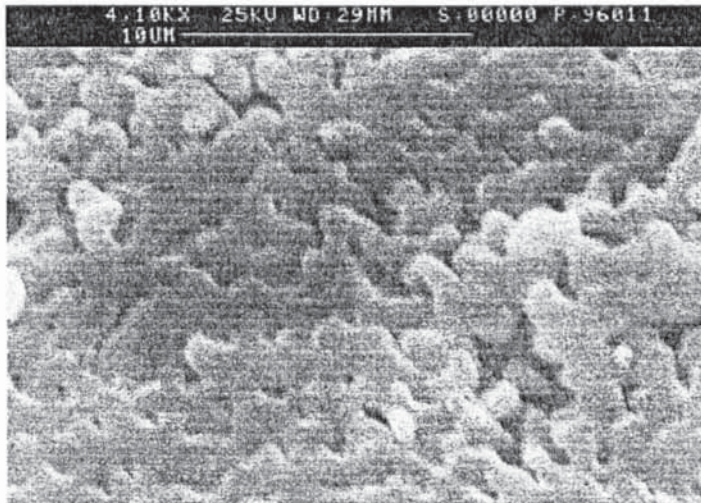
	A(500)	B(50)	C(25)	D(15)
A(500)	1	0.6	1	1
B(50)		1	1	1
C(25)			0.75	0.83
D(15)				0.8

With *discs* D there is the least packing efficiency when combined with A,B, and C (Table 4.15). This result tells us that the smallest grains disrupt the arrangement by settling in between normal contacts. D on its own gives the highest total. This is exactly to be expected due to the uniformity of grain profile and being the smallest grain there should be the least amount of space. This is supported by the ratio of space-to-circle calculation (Table 4.16). With C, there is a uniformly high packing efficiency (74.3%) in combination with every other grain size (A and B) B shows slightly better packing than C mixed with large *discs*, A. Mixtures incorporating D are always least efficiently packed. With sample C least packing efficiency is found when mixed with either *discs* A or D. *Discs* A, unmixed, as B,C and D creates high packing densities and low void space. A mixed with D creates the least packing efficiency along with B. These results contradict the assumption that the larger the difference in grain sizes the less would be the void space due to infilling. Mixtures comprising either *discs* A or B with *discs* D gave the largest porosity. However, no account of shape effects have been made. Unsymmetrical shapes though, only occur in *discs* A and B.

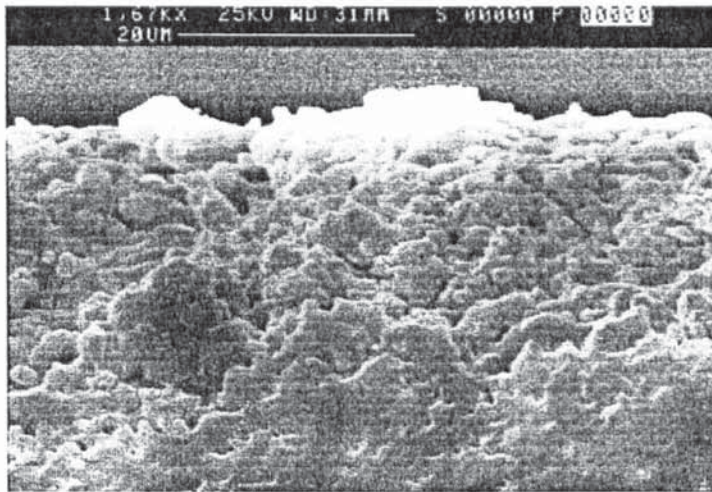
Photograph 4.22 SEM Thermal Image of Coalesced 100 μm Powder Grains with the Resultant Porosity (Surface View; 1.5-2 μm pore sizes)



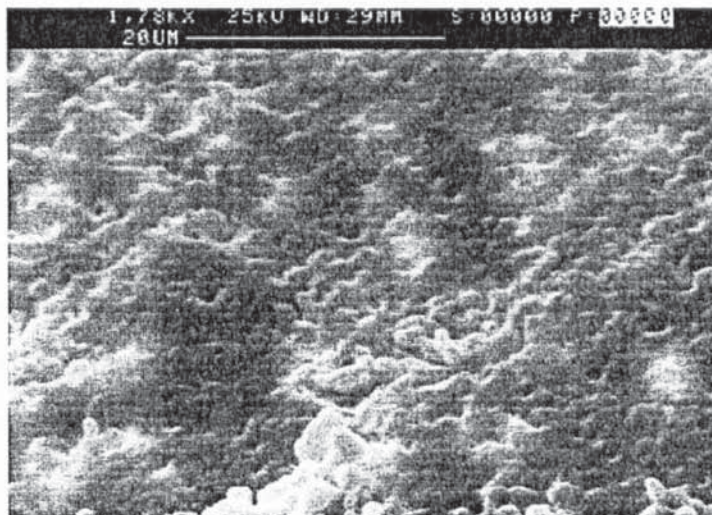
Photograph 4.23 SEM Thermal Image of Coalesced 36 μm Powder Grains with the Resultant Porosity (Surface View; 0.5-0.25 μm)



Photograph 4.24 SEM Thermal Image of Coalesced 500 μm Powder Grains with the Resultant Porosity (Surface View; 0.75-1 μm)



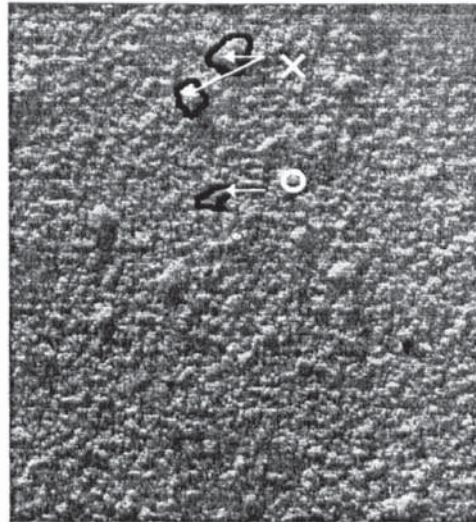
Photograph 4.25 Surface View of a Compacted and Sintered Hydroxyapatite Disc made from 36 μm and 100 μm Grains (1.25-0.5 μm pore sizes)



Unfortunately there was no satisfactory method of simulating the effects of sintering on estimations of porosity. It is known that sintering removes pore space as particles melt in order to minimise their surface free energy and fuse together, but it also creates more micropores and these are usually products of grain boundaries. Grain boundaries arise due to discontinuities in atomic orientation and electronic potential. The development of microporosity is complicated and occurs as a result of the liberation of excess surface free energy by a diffusion mechanism. Measured porosity drops rapidly during the first 10 hours of sintering until it reaches an equilibrium. At the onset of sintering, particles fuse and the area of contact increases gradually; this is neck growth

and particles shrink by 4-5%. At an intermediate stage, particles increase in size and shrinkage reaches 20%.⁸⁵

Photograph 4.26 *Surface View of a Compressed Disc Composed of 100 μ m and particles a (x18). Raised areas are marked x; pitted areas are marked with an oval.*



4.6.2 Examination by Scanning Electron Microscopy

Under SEM, the surfaces of the ceramic tablets were analogous to planetary surfaces created by volcanic phenomena. There was chaotic disorder in the arrangement and size of pores and coalesced particles. Common throughout were coalescences moulded into plates. Crystal plates could be seen in the coral skeletons. Unfortunately, porosity was not measured because the discs were friable and dis-integrated when immersed in solution. Instead measurements of surface topography (rugosity) using a goniophotometer were made on a small selection of discs (**Section 6.3**).

4.6.3 Measurement of Porosity

Porosity was measured for a range of natural (**Table 4.17**) and un-natural (synthetic) porous solids. Referring to table 4.17 the percentage pore volume is exceedingly low, from a slither of human tooth and bone at 2.5%, whisker particle combinations between 1.4-3.5%. Materials that approached pore volumes of natural foams (bath sponges at the top with 82%) were ceramers containing 100 μ m particles with whiskers (47%) and the large angular grains of sample B (33%). The building and aggregation of these must have allowed for monomer drainage during their formation. Surprisingly adding

soluble porosigens did not greatly increase pore volume.(15%), but the most confounding was 8.6% for *Porites* (Table 4.17). Sample F compared well to the low end of pore volume for natural corals which was also the level reached by adding sucrose particles to hydroxyapatite spheres. The spheres enhanced the distribution of sucrose particles and allowed for some connectivity between the pores.

Table 4.17 Porosity of Selected Compacted Grain Mixtures

Porous Ceramers	Void Volume	Comments
Sample A(116) and whiskers (50)	3.50%	Large grains augmented with fibres
Sample D(3.25) and whiskers (50)	1.36%	Small grains augmented with fibres
Sample A(116)	82%	Large grains
Sample B(38.5)	33%	Medium grains
HA spheres (500) and sucrose 100	15%	With a soluble porosigen
HA 100 and whiskers (50)	47%	
Sample F "polo"	13%	Large pore J.S.disc

J.S.=Jesse Shirley Ceramics

HA=Hydroxyapatite

()=In brackets: grain diameter in μm

4.7 Summary and Conclusion

Biological ceramics were the favoured material for a porous support frame. Three characteristic types of high performance ceramic (all previously employed in a keratoprosthesis) were identified and very briefly commented upon. They were: carbon, oxide ceramics (aluminium oxide), bioglasses (ceravital) and calcium phosphates (hydroxyapatite). Calcium phosphates were chosen as the substance for a porous support frame because, of a superior tissue response (the most biological like inorganic material available) and because of their widespread use in bone replacement

therapies, at many, varied body sites.

Table 4.18 *Basic Requirements for a Synthetic Structure that Mimics the OOKP Support Frame*

Property	Basic Requirements
Porosity (Tissue integration)	Highly interconnected in three dimensions Microporosity: 15-40 micrometers Macroporosity: 50-150 micrometers Graded Porosity
Mineral constituency (Biological tolerance, Bioadsorption)	High crystallinity *Ca/P ratio of 1.5-1.67 *Moderate ionicity *Calcium phosphate+ carbonates
Low rate of resorption in biological fluids (Stability & permanency)	*Non-stoichiometric hydroxyapatite *High fluorine-to-carbonate ratio
Periodontal Ligament/ cementum substitute (Stop membrane downgrowth)	Flexible, crosslinked network Cell adhesive but inhibits proliferation

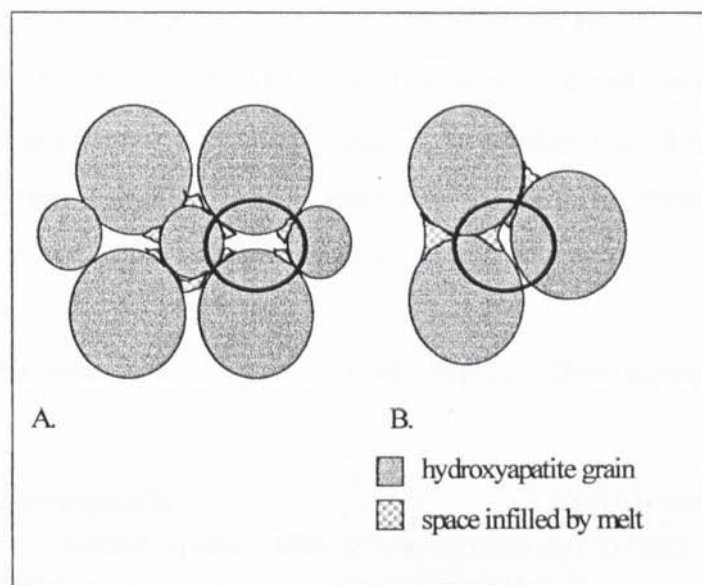
* denotes requirements satisfied by structures made; as described in this chapter; () denotes function

The aim of experiments presented in this chapter was to fabricate discs with pore diameters between 90-150 μ m and void volumes above 60%-70%. The discs were required to possess dimensions as those of the OOKP support frame, i.e. 0.5mm thick and 10mm in diameter. The pores in the ceramic discs made by Jesse Shirley were excessively small but were strong, tough and well made. Pressed discs were fabricated using an assortment of powders of different shapes and sizes.

The aim was to mix grains that provided the worst or most disordered packing arrangements; and therefore, give rise to the largest pores and pore volumes in each tablet after compacting under moderate pressures between 50-100kN.

After calculating space-to-circle ratios of various packing arrangements the largest pores arose from powder mixtures comprising the largest, irregular grains with fine powders (at the upper range of diameters). It was found that pore size of discs was approximately one quarter the diameter of the original grain diameters. For example, pore sizes between 90-150 μm can be fabricated with powder grains 280-600 μm in diameter. That rule roughly held true; even with moderate compacting (50kN) and sintering (1 hour), but it was not true when additives were mixed and compacting pressure was increased, or as a result of sedimentation.

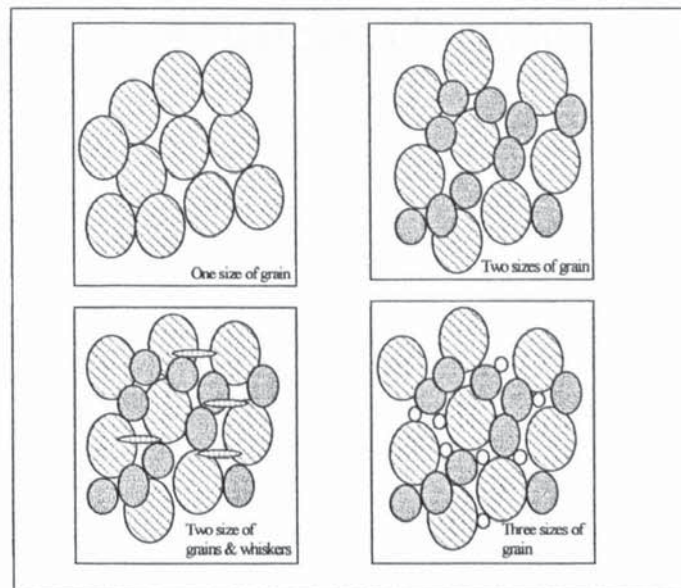
Figure 4.12 *Effect of Mixing Different Grain Sizes on Resultant Pore Size*



Pores were not connected in three dimensions. Powder grains melded together into plates closely packed together with regular co-ordination. Pore sizes were small (7.2-75 μm). The discs that were made from assorted grain and powder mixtures fractured readily in the hand. It must be added that discs mixed with fibres were less friable as they formed cross-bridges. Even if a binder such as carbowax (PEG 800) was employed, for example the pore system was inadequate for the proposed function of a

keratoprosthesis support frame.

Figure 4.13 Cartoons of the Different Types of Powder Mixtures



Assorted ceramic grains were fabricated into discs by die pressing to manufacture a bone-like porosity. By manipulating the mix of different size and shape of grains it was only possible to manufacture discs with small, sporadically spaced pores. And even after high temperature sintering the discs were very friable. The problem of mechanical stabilisation lead to synthesis of polymer and ceramic composites.

Table 4.19 Achievements and Problems of Making Hydroxyapatite Discs from Assorted Powders

Achievements	Problems
Ceramers (pMMA & hydroxyapatite) with pores, to limited extent	Phase separation of ceramic particles and polymer matrix
Etched surfaces generated rugosity to depth of 300 micrometers	Correct viscosity for dispersion of particles
Fabricated Xerogel and bonded it to hydroxyapatite disc	Growing crystals with complex structure
	Creation of a highly specific porosity

CHAPTER 5 RESULTS:
Fabrication of a Ceramer Support Frame for an
Artificial Cornea

CHAPTER 5 RESULTS:

Fabrication of a Ceramer Support Frame for an Artificial Cornea

“With what do you mix your colours? I mix them with my brains, sir”

John Opie

5.1. Introduction

The last chapter began with a brief look at inorganic materials as possible candidates for the support frame and then proceeded to experiment with various methods of fabricating a porous inorganic support frame, using hydroxyapatite powders. Compacting and sintering of assorted particles enabled the formation of brittle structures with small ($0.25\mu\text{m}$ - $1\mu\text{m}$) and restricted pore spaces (connected in 1 and 2 planes sporadically). The ideal pore sizes should be between 90 and $150\mu\text{m}$, preferably graded in size from one surface to the other and highly interconnected in 3-dimensions. A careful refinement in the forming conditions and greater use of selected additives should increase the pore sizes and the number of connections between pores. However, a more important concern was enhancing fracture toughness and strength of the sintered materials. Natural bone employs a biopolymer matrix to stop fracturing of the mineral. Therefore it was clear that polymer reinforcement was necessary to overcome the problem of toughness; and the problem of attachment to the optical cylinder (the artificial cornea).

The remainder of this chapter explores a group of composite materials: ceramers, and assesses their usefulness for the manufacture of tissue attachment structures in the same manner as tooth and bone. In short, such a structure must be composed of a material or composite of materials that are inexpensive, easy to obtain and simple to make.

5.1.1 Ceramers for Biomedical Applications

Ceramers are a combination of ceramic and polymer, involving a purposeful molecular contact involving charge or hydrogen bonding. Ceramers were not intentionally designed for biomedical applications, rather they were developed for aerospace and microlithography. More recently however, a number of materials have been fabricated for use as bone cements and as bone void fillers (Table 5.1). pMMA is a very typical

polymer filler for hard tissue replacements in orthopaedics and dentistry. Bonfield, in particular has advanced the application of ceramer to clinical trials with encouraging results.⁹⁶ The simple bone analogue he devised was a composite of monolithic hydroxyapatite re-inforced with polyethylene (HAPEXTM) and is closely modelled on the structure of cortical bone.⁹⁶

Table 5.1 *Polymers used in Hydroxyapatite Ceramers Taken from Recent Scientific Literature*

Polymer Types	Ref. No.
Poly (L-lactide)	Verheyen (97)
PolyL-Lactic acid (PLLA) and p(MMA)	Rodriguez-Lorenz (98)
Chitin (animal structural protein)	Yokogawa (99)

5.2 Fabrication of Ceramers

5.2.1 Introduction to Experimental

There are two fundamental approaches toward the fabrication of a ceramer-a ceramer is defined as a 'chimera' of polymer and ceramic). The first is to incorporate a reinforcing organic polymer into a glassy inorganic matrix ensuring that the two are chemically bonded together. A preferable alternative would be to do the reverse and incorporate inorganic fibres into a viscous organic polymer matrix and react the two simultaneously. Ideally there would be the corresponding ability to manufacture a surface rugosity or moderate porosity through precise control of the combination of ceramic and polymer.

Trial ceramers began with the use of an araldite resin mixed with hydroxyapatite (100µm, 36µm and whiskers (average length=50+/-25µm; 3-1.5µm thick)) and later with soluble porosigens. The flow characteristics (rheology) of polymer containing hydroxyapatite slurries, and the interfacial bond between particles and surrounding polymer matrix strongly influence mechanical properties.

A methacrylate monomer mix was later used as a replacement for araldite resin, because methyl methacrylate (MMA) was the natural choice of polymer for the base plate in the final design, since it was compatible with the optical cylinder. However, in all cases a labyrinthine void structure was not manufactured, because of the inability to manipulate the chemistry with any degree of dexterity. Rather, the surface was very rough and consisted of a spread of isolated pores. In one example, the original percentage porosity was 0.7% but after soaking in water it climbed to 12%. Nevertheless, this value of porosity was not large enough to approach the level of porosity found in open cell (spongy) varieties of bone.

Table 5.11 *Porous Resin and Hydroxyapatite Mixtures (Ceramers) Fabricated in this Study*

	Ceramic Powder	Polymer Matrix	Porosigen
1	Hydroxyapatite 100	Batson`s MMA mixture	
2	Hydroxyapatite 100	Batson`s MMA mixture	Dextrin 125
3	Hydroxyapatite 100	Batson`s MMA mixture	Sucrose 125
4	Hydroxyapatite 100	Batson`s MMA mixture	Sucrose 38-60
5	Hydroxyapatite 36	Batson`s MMA mixture	Sucrose 38-60
6	Hydroxyapatite Whiskers (50)	Batson`s MMA mixture	Dextrin 125
7	Hydroxyapatite Whiskers (50)	Batson`s MMA mixture	

* *Batson`s MMA mixture, section 3.1 Materials, Chapter 3*

Figures in Table are in μm

Experiments carried out to coat pMMA with a uniform layer of biological ceramic included the use of biogenic dispersants and gelling agents. Biogenic additives are a crucial ingredient in the successful outcome of clay-based processes. They underpin the superb shape forming abilities of clay and water pastes. After heating at low temperatures a soft pale white gel was produced. However, the hydroxyapatite particles dropped to the bottom of the beaker despite repeated (but not continuous) stirring. Thus, there was a surprisingly small volume fraction of ceramic dispersed within the gel. Behaviour of this kind was also observed in mixtures without MMA. Phase separation occurred due to the high viscosity of polymer. A dispersant was,

therefore required. The following biogenic additives were mixed into ceramers.

Table 5.12 *Biogenic Additives Mixed in with Ceramers*

	Polymer	Biological Ceramic	Dispersants (Biogenic Additives)
1	MMA	Hydroxyapatite	Alginic acid*
2	MMA	Hydroxyapatite	Polyacrylic acid#

**Biogenic additives are acidic bio-polymers which, enhanced colloidal dispersal of ceramic particles and improved quality of plasticity. Low molecular weight polyelectrolytes such as polyacrylic acid (PA) and an acidic biological polymer precursor, citric acid are recognised chemical dispersants.*¹⁰⁰

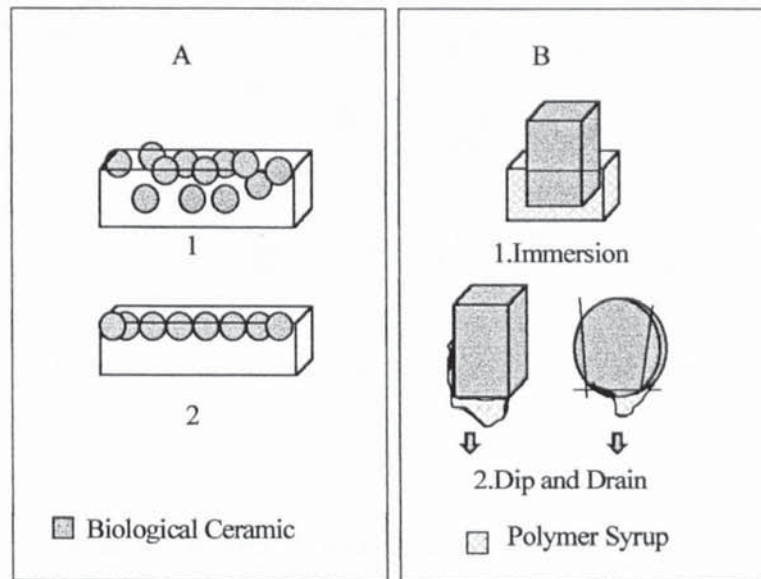
1. *A solution of the gelling agent, alginic acid enables dense packing of hydroxyapatite particles.(HA) pMMA solution is highly viscous and immiscible with alginic and so forms surface layer. Both were thermally polymerised.*

2. *A material was prepared with an acidic polyelectrolyte to reduce viscosity and minimise inter-particle interactions.*

5.2.2 Ceramers and Polymer / Ceramic Conglomerates

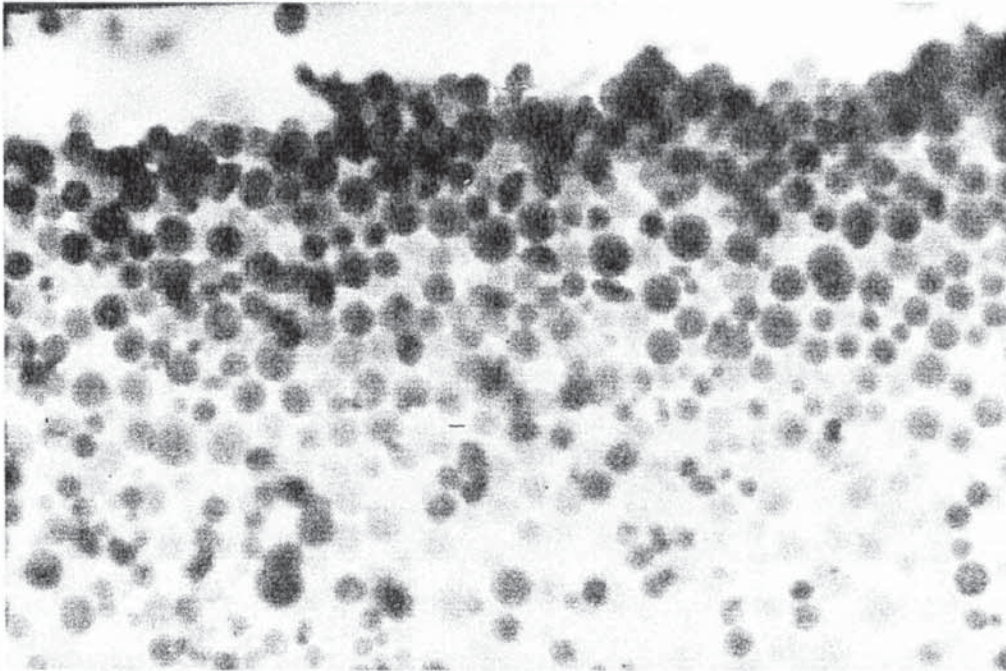
Two methods were developed for the fabrication of ceramer conglomerates (**Figure 5.12**). One group of experiments fabricated polymer, re-inforced with biological ceramics, (A₁ and A₂ Ceramers) and the other involved fabrication of biological ceramics re-inforced with polymer (B₁ and B₂ conglomerates).

Figure 5.1 *Two Methods for Combining Polymer and Ceramic: Methods under A involve particulate ceramics forming a surface layer on the monomer/polymer. Methods under B use a whole block of porous ceramic that is either immersed or briefly dipped into monomer solution. In addition, one Jesse Shirley disc was immersed in collagen solution and air dried to form a gel. (Photograph 5.13)*



Firstly, referring to B₂: Dip and drain experiments failed to coat enough monomer into the voids. The low rate of ultraviolet assisted polymerisation meant that 90% of the monomer drained away before the exponential phase of cross-linking had begun. The ultraviolet light (with a high power output) emitted from a large ultraviolet bench lamp was too diffuse to ensure polymerisation at a rapid rate and acceptable pore depth (at least 0.5mm to equal the thickness of dentine in the dental plate). Results of immersion experiments (B₁) are described in Chapter 7 (**Section 7.3.2**).

Photograph 5.1 *Cross-Sectional View Through a Ceramer (A) Composed of Hydroxyapatite Beads (x10)*

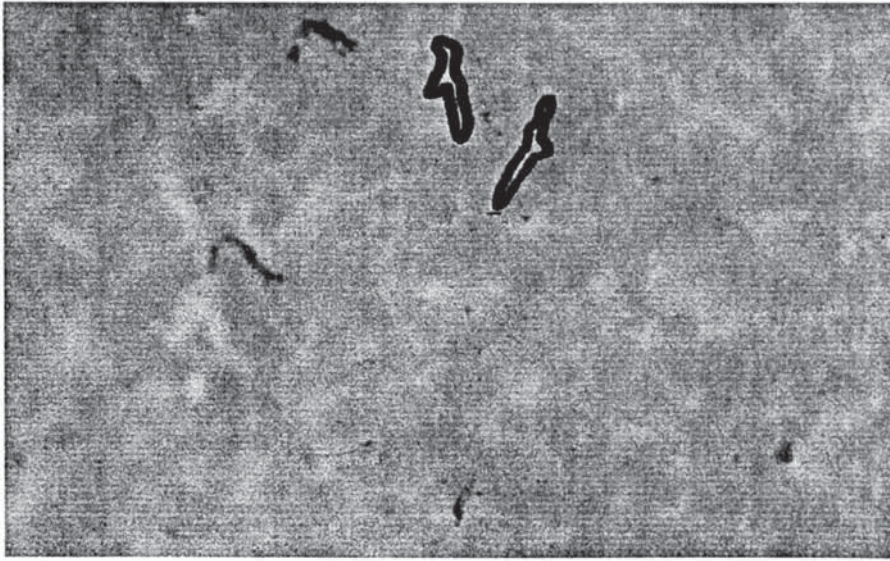


A further series of experiments fabricated ceramers re-inforced with whiskers. The three methods were as follows:-

- thermal polymerisation of pMMA with ceramic whiskers*
- immersion of particles or whiskers* in photopolymerisable monomer solutions.
- immersion of hydroxyapatite particles or whiskers* in semi-cured monomers

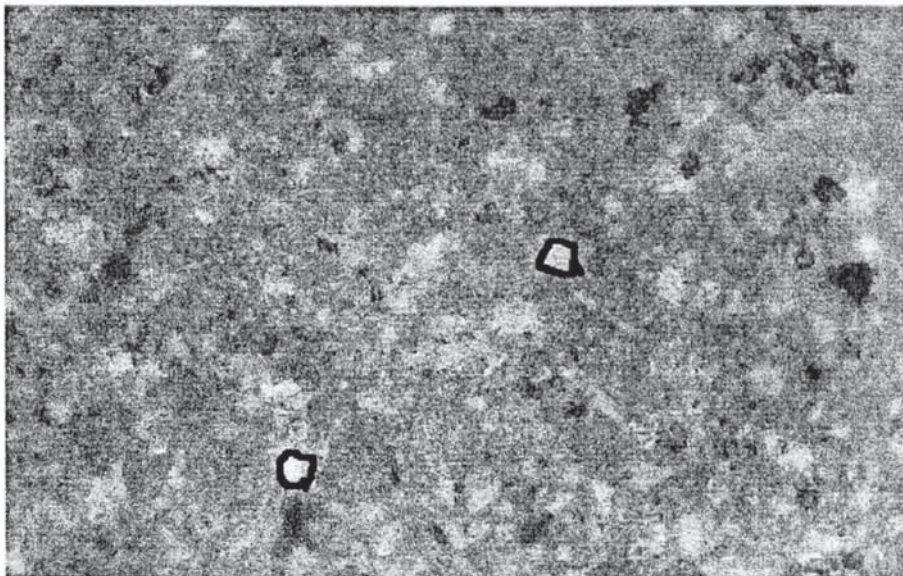
**whiskers engender greater toughness in the composite.*

Photograph 5.11 *A Ceramer Membrane Comprising a pMMA Matrix Embedded with 100 μm Grains of Hydroxyapatite and Particles of (soluble) Sucrose (125 μm).*



The grains of hydroxyapatite are evenly distributed in this ceramer. The gaps (pseudopores) between particles are thin, interconnected and ribbon shaped (perimeter marked in black).

Photograph 5.12 *A Ceramer Membrane Comprising of a pMMA Matrix Embedded with Whiskers and Hydroxyapatite Particles (375 μm).*



The hydroxyapatite particles are packed together in a disordered arrangement. This was typical of most fabricated ceramers. In the example above, the gaps are rounded and pore-like (perimeter marked in black).

A common problem with ceramers fabricated in this study, was phase separation. Phase separation and the presence of phase discontinuities are caused by the lack of bonding between the matrix phase and the reinforcing phase. Ensuring the even spread of the re-inforcing phase substantially improves the mechanical properties of a ceramer, but this requires precise control of reactants. Mechanical toughness is also much improved by making the particles as small as possible. Neither factor was satisfactorily resolved.

Composite materials consisting of a polymer matrix (Tetra Hydroxyfurfurylmethacrylate (THFFMA) and polymethylmethacrylate (pMMA); 96% monomer, 5% cross-linker and 1% initiator) were loaded with a moderate volume fraction of ceramic powder (60-70%). The materials were highly inconsistent. The powder grains would not disperse uniformly and shrinkage of polymer further degraded the grains. Furthermore, ceramic grains (500 μ m to 250 μ m size range) or powders (250 μ m to 75 μ m size range) immersed in polymer were easier to handle (mix, pour etc.) and cast than a mixture with a ceramic matrix.

Since surface porosity was generally undesirable, with few pores and no discernable connections between them, plasma bombardment was used to increase the surface rugosity (depth of pitting) of these materials (Section 5.3).

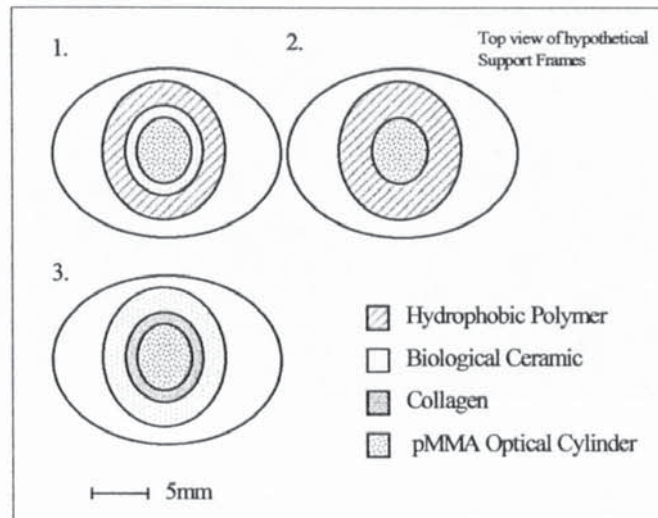
An attempt was made to combine collagen and hydroxyapatite as a step toward the construction of a tri-phasic structure, speculated upon in Figure 5.11, including a periodontal ligament analogue-collagen. Theoretical difficulties arose in (a) establishing a method of synthesising fibrous collagen and (b) finding methods to embed collagen into a porous ceramic.

Photograph 5.13 *Failed Attempt to Synthesise a Periodontal Ligament Analogue. The rope-like structure is made from type I kangaroo collagen and has been physically adsorbed onto a Jesse Shirley ceramic disc.*



A series of designs were formulated to include a periodontal ligament analogue as displayed in Figure 5.11. Owing to the complexity of constructing structures with three different component layers, none of the structures were manufactured (**Figure 5.11**). Thus, effort was concentrated upon producing two-phase composites, consisting of a stiff polymer and biological ceramic.

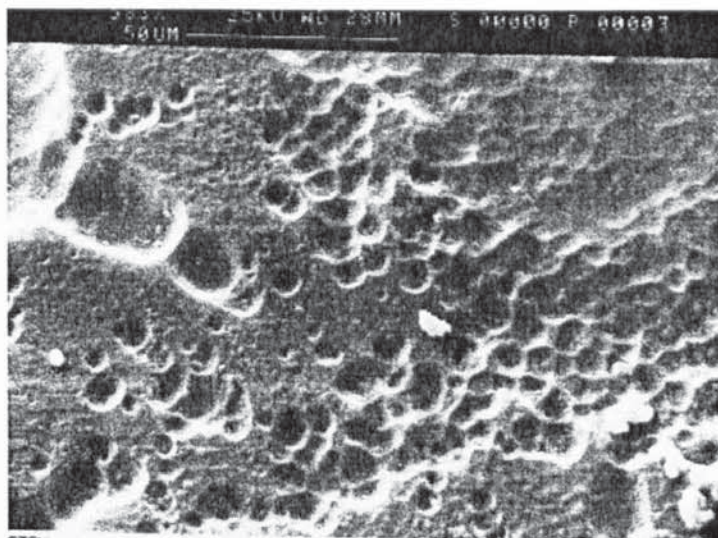
Figure 5.11 *Potential Designs for a Support Frame Copying the Tooth and Bone Structure. The favoured design (not shown in this Figure) was to fuse a ceramic ring on top of a polymer rim (Section 7.4.1) as opposed to the complex, but more accurate copies of the OOKP dental plate as shown below.*



5.3 Plasma Etching of Polymer Phase

The system for etching materials with plasma was specifically designed to serially slice thin segments of protein pre-adsorbed onto contact lenses. It therefore possessed little capacity for effectively removing semi-rigid polymer from the hydroxyapatite deposits to at least a depth of 5mm, the width of porous bone in the dental plate. Four different ceramer surfaces were each etched for 60 minutes and during that time there was virtually no loss of polymer from the surface.

Photograph 5.14 *The Surface of a Ceramer Etched with Plasma (MMA and small Hydroxyapatite particles) for 3 hours (x18 magnification)*



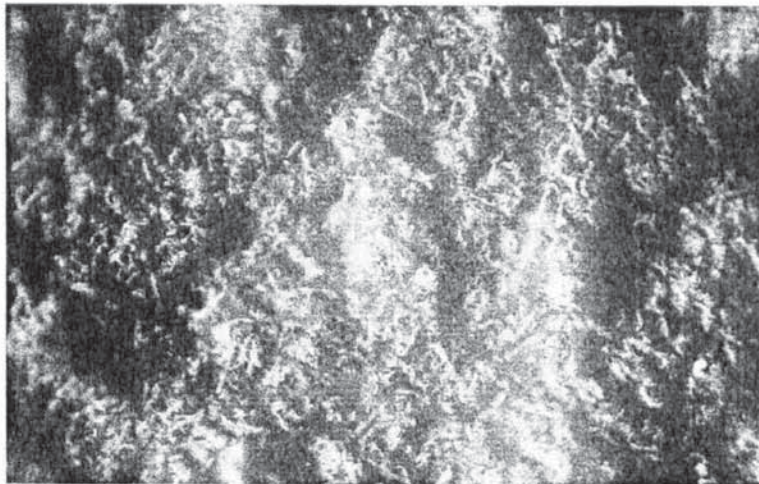
Each one of the measured gradients (in $\mu\text{g}/\text{sec}$) were imperceptibly small and therefore, insignificant. While there were small changes to the weight of ceramers containing spheres and ceramers containing whiskers the gradient of weight loss for the powder composites was flat. (pMMA and grains of sample B ($50\mu\text{m}$), pMMA and grains of sample A($116\mu\text{m}$))

Table 5.13 *Results of Ceramer Argon Plasma Etch*

Polymer	Hydroxyapatite	Gradient $\mu\text{g}/\text{sec}$
pMMA	spheres	0.13
pMMA	whiskers	1.16
pMMA	B grains	0
pMMA	A grains	0

Surface roughness was measured with a Goniophotometer and the results are tabulated below (Refer to **Section 7.11, Chapter 7**). There is a visible difference in etching of thinly coated hydroxyapatite compacted frameworks (**Photograph 5.15 and 5.16**).

Photograph 5.15 *Transverse Section of Ceramer Containing Hydroxyapatite Whiskers and polytetrahydrofurfurylmethacrylate (pTHFMMA) Polymer. The vacuities are clearly visible and open-out at the surface.*



Photograph 5.16 *Transverse Section of Ceramer Composed of Hydroxyapatite Whiskers and polytetrahydrofurfurylmethacrylate (pTHFFMA) Polymer After 3 hours of Plasma Bombardment. The vacuities are much more extensive and deeper in ribbons arranged down the image.*

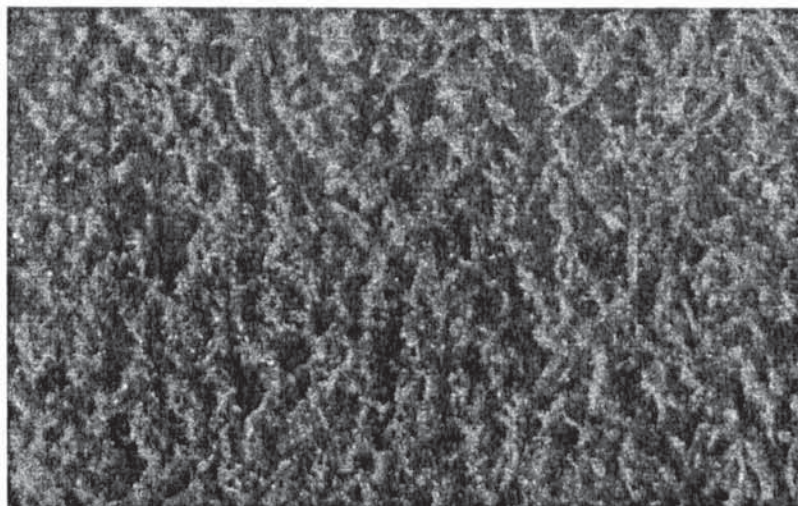


Table 5.14 *Surface Roughness Measurements of Ceramers and Compacted Ceramic Grain Mixtures Using a Goniophotometer*

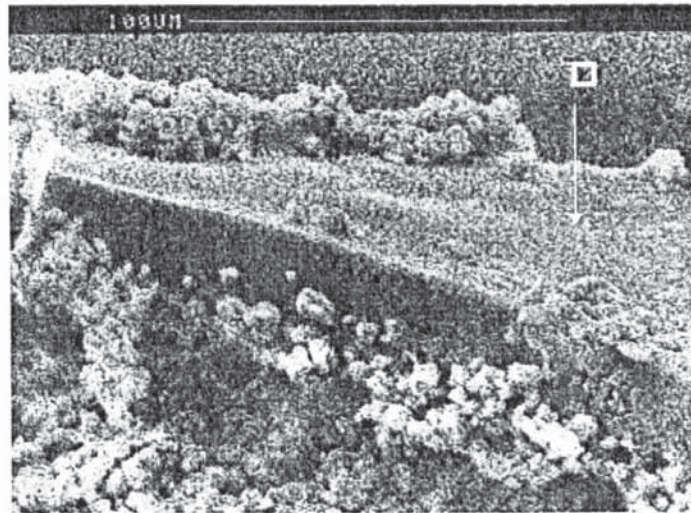
Biological Ceramic	Polymer	Description of Trace
Hydroxyapatite 36	pMMA	Small number of well dispersed peaks separated by an undulating plain
Hydroxyapatite 100	pMMA	Small number of well dispersed peaks separated by an undulating plain
Hydroxyapatite Spheres (500)	pMMA	Very regular series of peaks and deep troughs
Hydroxyapatite C	pMMA	Repeated series of jagged peaks
Hydroxyapatite A (500)	pMMA	Regular series of jagged peaks and troughs

5.4 Solution-Gel Synthesis of Porous Ceramics

The sol-gel process is a common liquid phase reaction for the polymerisation of molecules of oxide ceramics and glasses in solution. It involves rapid hydrolysis of a colloidal solution (evaporation of the solvent) giving rise to a solid polycondensate. By manipulating the forming conditions, a variety of forms can be made

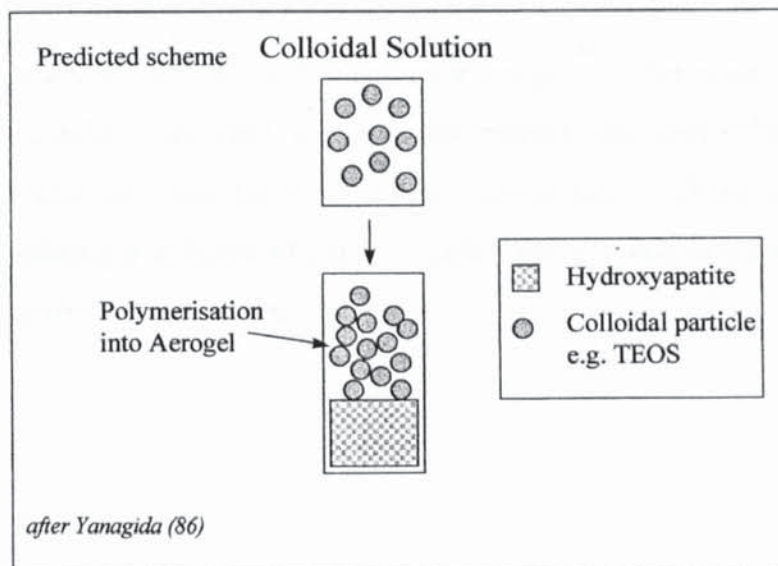
Experiments were carried out to synthesise and deposit a thin silicate gel to a non-porous hydroxyapatite disc, previously etched with weak acid. A uniform gel of tetraethoxysilane (TEOS) adhered to smooth discs of hydroxyapatite after drying in an oven and afterward remained relatively intact.

Photograph 5.17 *Thermal SEM Image of Silica Gel Attached to a Hydroxyapatite Disc (marked with square)*



Peeling of the TEOS layer was observed after 24 hours, at room temperature because of dehydration. Either too few hydroxyl groups were exposed by acid etching or the polymer and silanol were chemically incompatible.

Figure 5.12 *Porous Ceramics Fabricated by a Sol-Gel process and Adsorbed onto a Hydroxyapatite Disc*



The sol-gel process was an attractive technique because a porosity is developed during material formation. They enable the formation of structures with a hierarchy of composite building blocks (as bone), from a precise arrangement of interfacial bonds to

a precise arrangement of polymer chains and ceramic grains. This results in enhanced microstructural arrangements and mechanical properties.

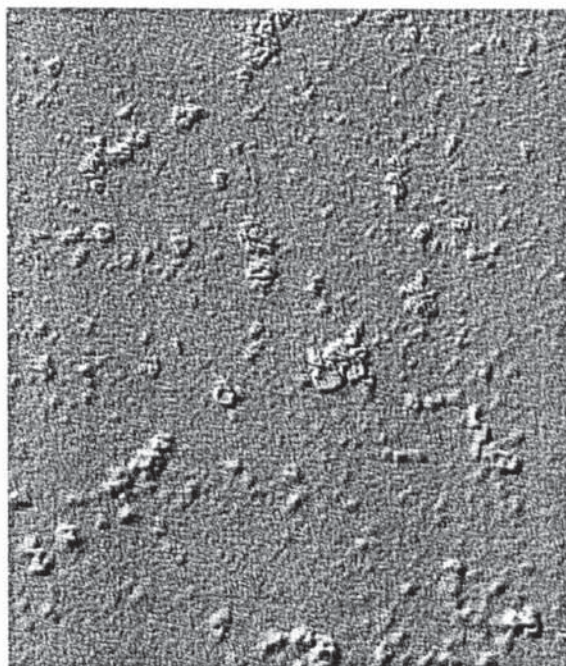
In conclusion, sol-gel processing was found to be the most valid technique available, since the forming conditions could be accurately tuned to create varying gel architectures. There was a facility to control morphology, the quantity of structural defects and pores. However, the chemistry of formulation required the strong presence of silica and heavy metals and delamination of the final structure was a particular problem.

5.5 Deposition of a Bone-Like Apatite Layer Onto Polymer

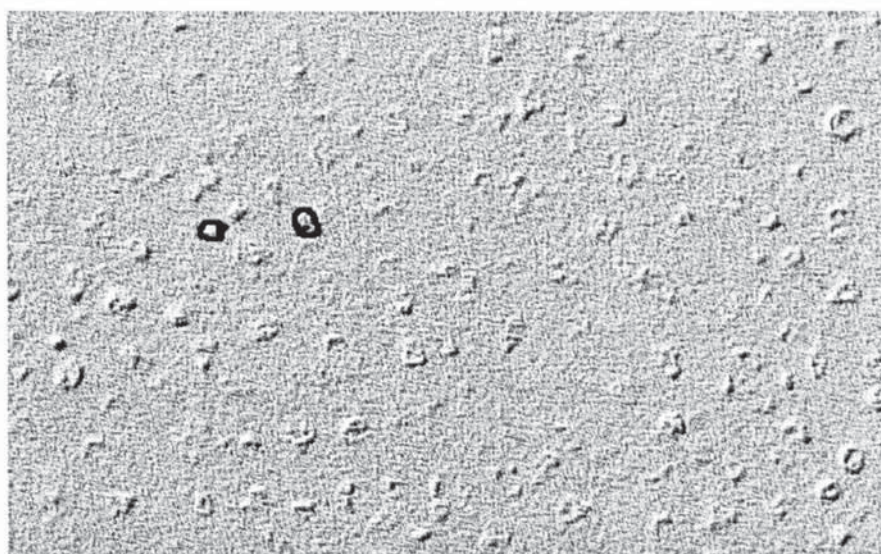
Calcification of polymer surfaces, even after prolonged acid etching or ultraviolet light irradiation, failed to occur as expected. This was primarily due to the poor formation of an adsorbed layer of hydrated silica on the polymer surface. There were, however, evenly distributed nucleating regions, but the strength of attachment to the polymer was weak, such that when a piece of sticky tape was attached to the surface and removed the density of crystals attached to the surface was reduced by a 25%.

Attempts were made to induce the formation of a monolayer template for carbonate mineral nucleation and crystallisation in a langmuir trough.⁸² After many experiments a coherent film of calcium carbonate was not precipitated out from solution onto the langmuir film, during the mandatory 48 hours waiting time. There was particular difficulty in formulating a solution of calcium carbonate at a concentration that freely precipitated out at room temperature.

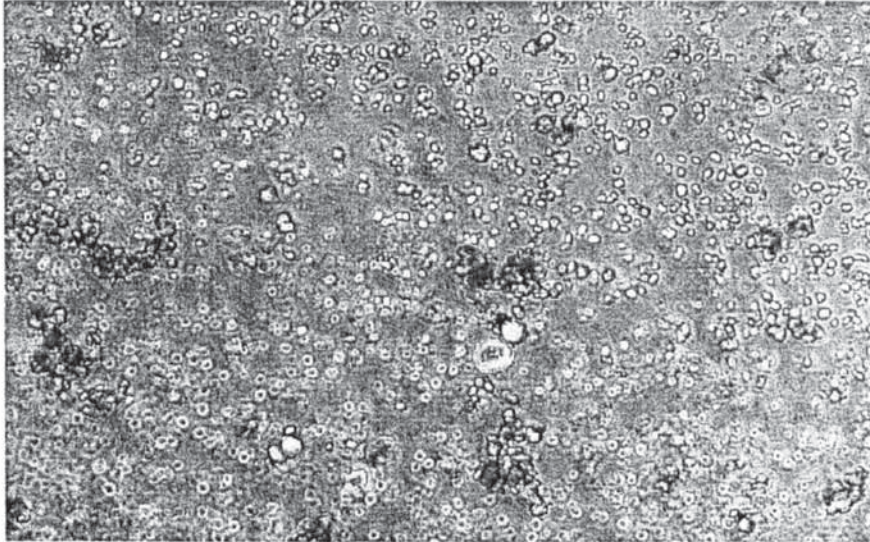
Photograph 5.18 *Image of Small well-Dispersed Nucleating Foci of Calcium Carbonate Adsorbed onto a Hydrophilic Hydrogel (HEMA). This image was embossed using Image-in-Color (Hi-Image SA) software to highlight the clumps of mineral.*



Photograph 5.19 *Small Well-Dispersed Nucleating Foci of Calcium Carbonate on the Surface of a Hydrophilic Hydrogel (HEMA). A large number of mineral grains are loosely attached to the polymer. The Image was embossed using Image-in-Color (Hi-Image SA) software to highlight mineral clumps.*



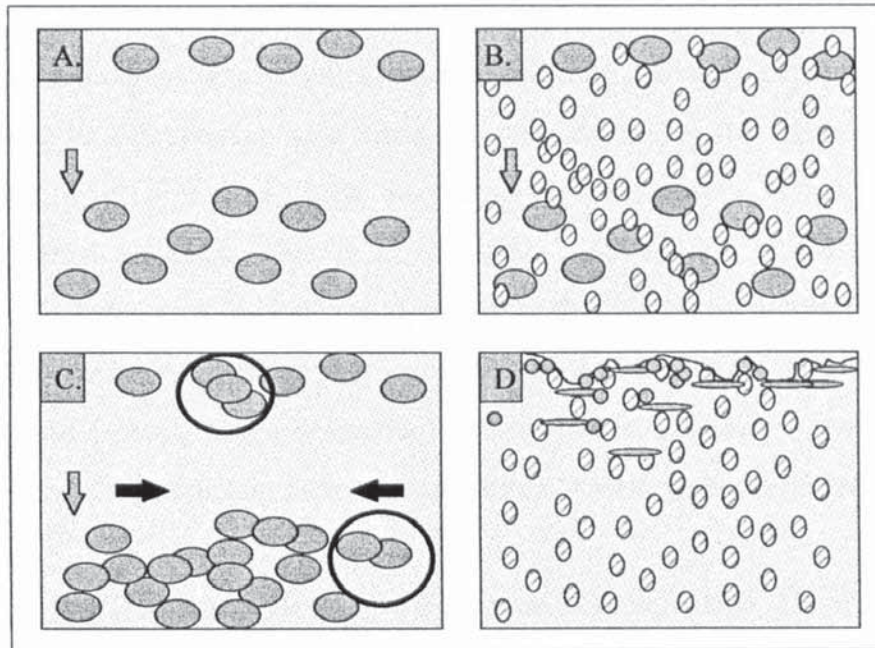
Photograph 5.2 *Small Well-Dispersed Nucleating Foci of Calcium Carbonate Adsorbed onto a Methyl/ Ethyl Methacrylate Co-polymer. Once again the crystals have not expanded from their nucleation foci.*



5.6 Summary and Conclusion

This chapter explored the idea of using ceramers as the material for the support frame and developed a number of materials with assorted structural (e.g. varying pore sizes or rugosity) and compositional attributes (e.g. varying volume fractions of hydroxyapatite powders). In experiments carried out in this study, mixing of particulates and blending with monomer mixtures proved a simple and efficient method for fabricating membranes and fabricating slurries for casting natural and synthetic sponges (developed in *Chapter 6; Section 6.3.4*). Unfortunately the membranes were not porous enough, due to sedimentation or phase separation, despite the employment of dispersants. As an alternative some membranes were etched to create a surface topology, perhaps as equally capable of tissue interlock and attachment as the porous solids. However, the distribution of ceramic was highly inconsistent. A resume of the structural results from mixing and blending of biological ceramic powders, porosigens and monomer are summarised below. It highlights the effects of phase separation and inconsistent packing formations.

Figure 5.13 Schematic Cross-Sections Through 4 Types of Ceramer



Referring to the schematic cross-section through ceramer type A: where the ovals represent porosigens (50-60% volume fraction); the porosigen particles tended to sediment to the bottom of the membrane. Their distribution was also distorted by shrinkage of the polymer. Some particles remained at the top. Looking at ceramer type B: (ovals represent porosigens and circles represent hydroxyapatite particles). Hydroxyapatite particles tended to aggregate but, were generally well distributed (in clumps). The intention was to enclose the porosigen particles in hydroxyapatite and allow for gaps between porosigens for interconnections. In addition, the polymer should support a large fraction of evenly dispersed hydroxyapatite particles. As can be seen at B, there is competition for space between the porosigens and hydroxyapatite particles. Unfortunately, there were no mechanisms to attract porosigen and hydroxyapatite particles together. Referring to type C ceramers; when very high volume fractions of porosigen are added to monomer mixtures sedimentation takes place and shrinkage of the polymer matrix distorts their packing arrangements. Higher volume fractions lead to improved interconnectedness between porosigens, but there often exist isolated clusters of porosigens. In the schematic cross-section through Ceramer D, the etched surfaces provide surface rugosity of varying depths (that cannot be easily controlled) lined by hydroxyapatite ceramic.

A biomimetic technique of mineralisation in a saturated solution (whereby crystals are encouraged to grow on the polymer surface) was more effective at producing substrate consistency. But at the outset the technique was difficult to accurately specify. A suitable habitat modifier (e.g. protein) was not identified and implemented. This would have allowed for the creation of a bone-like porosity within the developing mineral layer. The sol-gel process enabled the formation of a porous ceramer that could become attached to apatite ceramic or polymer. The Sol-gel synthesis is a firmly established technique of making composites with a defined porosity (Xerogels). However, the ceramer structures that were fabricated in this study did not correspond to the required (stated design objectives) set of criteria, particularly with regards to porosity. Porosity was neither large enough nor sufficiently interconnected.

Table 5.15 *Basic Requirements for a Synthetic Structure that Mimics the OOKP Support Frame*

Property	Basic Requirements
Porosity (Tissue integration)	* Highly interconnected in three dimensions * Microporosity: 15-40 micrometers * Macroporosity: 50-150 micrometers * Large pores grading into small pores
Mineral constituency (Biological tolerance, Bioadsorption)	* High degree of crystallinity * Ca/P ratio of 1.5-1.67 * Moderate ionicity * Calcium phosphate+ carbonates
Low rate of resorption in biological fluids (Stability & permanency)	* Non-stoichiometric hydroxyapatite * High fluorine-to-carbonate ratio
Periodontal Ligament/ cementum substitute (Stop membrane downward growth)	* Flexible, crosslinked network * Cell adhesive but inhibits proliferation

** denotes requirements satisfied by structures made as described in this chapter*

Fabrication of porous materials with a highly specific pore structure and mechanical stability was not achieved as it ultimately required very precise control of forming conditions and synthesis during fabrication. The complex challenge of forming intricate pore networks from biological ceramic can be alleviated to a degree (although it does not overcome the problem of combining the pore network with a polymer matrix) by employing (pre-formed) porous natural artifacts.

Table 5.16 *Achievements and Problems Fabricating Hydroxyapatite and Polymer Composites*

Achievements	Problems
Ceramers (PMMA & hydroxyapatite) with pores, to limited extent	Phase separation of ceramic particles and polymer matrix
Etched surfaces generated rugosity to depth of 300 micrometers	Correct viscosity for dispersion of particles
Fabricated Xerogel and bonded it to hydroxyapatite disc	Growing crystals with complex structure
	Creation of a highly specific porosity

CHAPTER 6 RESULTS:
Marine Derived Natural Artifacts as Potential
Structures for an Artificial Cornea Support
Frame

CHAPTER 6 RESULTS:

Marine Derived Natural Artifacts as Potential Structures for an Artificial Cornea Support Frame

“Life in the sea is extravagant almost beyond imagining-in its abundance, its variety, its antiquity, its oddity, its beauty and, balancing it all in nature’s way, its mindless ferocity”

Leonard Engel

6.1 Introduction

The production of a synthetic bone replica analogous to the OOKP support frame, made from tooth and bone (as described in scope and objects) was unsuccessful in this study. An alternative strategy was employed, to make an OOKP analogue by exploiting skeletal frameworks found in nature. This chapter is concerned with a search for a natural artifact with a porous structure that matched dental alveolar bone in the size of pores and their arrangement. These features are important to allow rapid tissue integration and firm attachment, as demonstrated by the osteo-odontokeratoprosthesis (OOKP). A suitable natural artifact must possess the following ‘ideal’ pore attributes if it is to be successful:-

- a uniform pore diameter that induces custom cellular responses in space and time
- diameter of pore interconnections equal to pore diameter- this maximises transport of nutrients and waste and maximises the number of possible cell contacts for a minimum expenditure.
- a solid-to-void ratio of one- which means, (a) it optimises space filling for support and (b) maximises available space for cell distribution
- an exceptionally high permeability, preferably in which, every pore is in contact with all adjacent pores (periodic minimal surface)

In the natural world there are a vast array of structures to choose from, as will be emphasised in the following survey of porous natural frameworks. If a desirable

naturally derived structure was to be found, there was the option of casting it with a ceramer material, for safe implantation into the human body. Alternatively, if the structure was made from an inorganic material, and the organic component could be easily removed, then casting would not be necessary and it could be used directly. Obviously, the latter would be the most advantageous by virtue of its simplicity. The following section previews the various types of natural artifact, whose porosity most closely matched the porosity of alveolar bone (See **Figure 4.1.1**).

6.2 Survey of Porous Structures (Bone-like?) in the Animal and Plant Kingdoms

The animal and plant kingdoms are replete with foam structures and materials for a variety of disparate functions. A comprehensive table was constructed to illustrate and categorise the diversity of spongy structures across the animal and plant kingdoms (**Table 6.1**). Looking at the table, we find that sedentary (non-mobile) invertebrates dominate, because they possess more elaborate porous structures than higher organisms which, do not rely upon them for support and defence.¹⁰¹ In the following paragraphs there is an overview of all available organisms, with structures likely to induce tissue integration and hence, firm attachment.

Table 6.1 A List of Foam Structures In the Plant And Animal Kingdom: Angiosperms and Lower Invertebrates

Name of Organism	Skeletal Structure	Comments
<i>Angiosperm-Higher plants</i>	Honeycombs	Closed cells almost as regular as a perfect honeycomb
Protistans	Globular shells	
<i>Coccoliths</i>	Plated spheres	Marine algae
<i>Diatoms</i>	Filigree patterned porous shapes	
<i>Radiolaria</i>	Meshwork of hexagons	
Bryozoans (shell)	Two dimensional layered plates	
Porifera (Sponges)	Two and three dimensional plates, tubes and globules	Open network of struts with connectivity* of 3,4,5 or 6
<i>Hexactinellid</i>	Box-girder arrangement of spicules	Open network of struts with connectivity* of 3,4,5 or 6
<i>Calcarea</i>	Three dimensional porous solids	Open network of struts with connectivity* of 3,4,5 or 6
<i>Demosponges</i>	Loose network of entangled fibres	Open network of struts with connectivity* of 3,4,5 or 6
Anthozoa-Coral skeleton	Three dimensional porous blocks	Vronoi type foam#: "co-equal cylinders compressed into hexagonal prisms"(2)

Table 6.11 *A List of Foam Structures In the Plant and Animal Kingdom: Higher Invertebrates and Vertebrates*

Name of Organism	Skeletal Structure	Comments
Brachiopod (Shell)	Three Dimensional Stacked Lamellae	
Mollusca Bivalve Shell	Prismatic: Lamellar and Foliated also Cross-Lamellar	
Cephalopoda Cuttlefish Skeleton	Regular Cuboid Network	
Arthropoda Insecta exoskeleton	Plywood effect: Helicoidal Lamellar	Chitin is Orientated in Many Directions to Lower Modulus
Crustacea Barnacle Shell	Parallel Series of Sacs	
Echinodermata Echinoderm Spines	Cylindrical Rods	Periodic Minimal Surface: Most Efficient Space Filling Framework@
Reptilia Eggshell	Planar Sheets	
Aves Eggshell	Planar Sheets	
Mammalian Bone Cow Bone and Human Bone		Highly Interconnected Pores and Channels#

*An explanation of the concept of connectivity is found in chapter 3; section 3.6.3^{103,104}

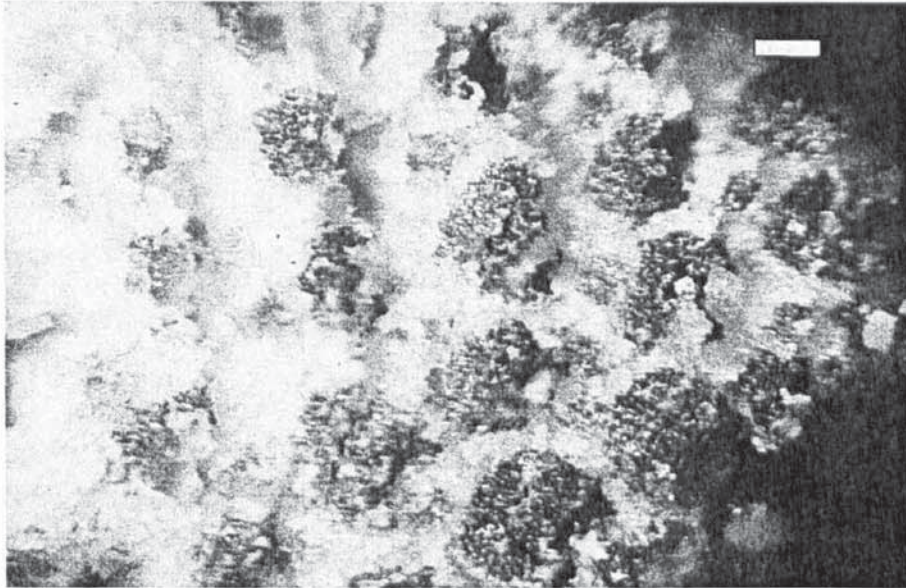
@ See Section 6.3.23

Vronoi Honeycombs are formed by competitive growth of active cells. There are two types of Vronoi Honeycomb: One for a set of random points in which, cells nucleate at random points at the same instant and grow with the same linear growth rate, and another for a set of fixed points in which, cells nucleate closer together than a critical spacing and grow with the same linear growth rate.

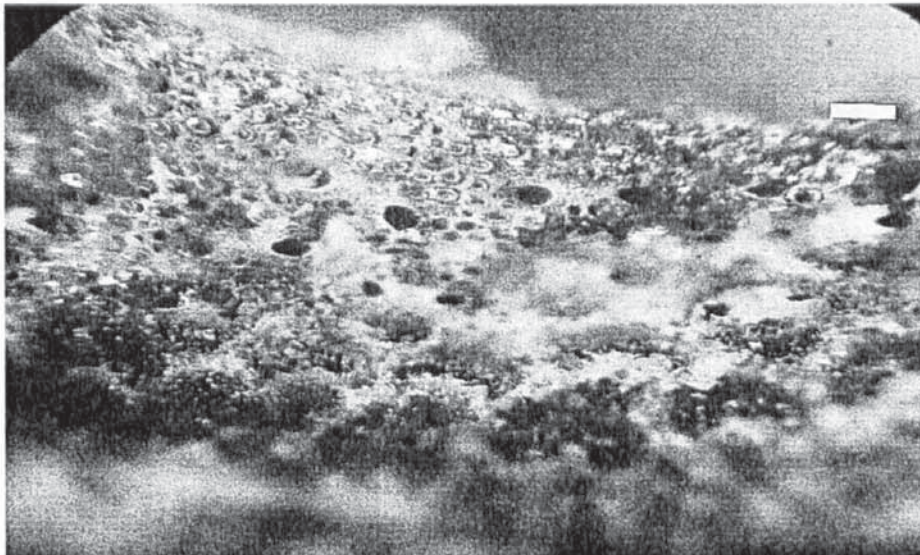
Beginning at the top of table 6.1-higher plants build bodies composed of a parenchyma honeycomb formed by highly uniform, many sided cells tightly packed into a regular array. The best examples available for a keratoprosthesis support frame are Bamboo stems and woody stem tissue (mature secondary tissue), since both are built up from

cells with a shape and size that matches the cylinders of haversian bone (In its open texture form haversian bone is cancellous or spongy).¹⁰²

Photograph 6.1 *Cross-Section through the Stem of Mature Bamboo (Phyllostachys sp.) Scale Bar=200 μ m.*



Photograph 6.11 *Cross-Section through the Stem of Immature Bamboo (Phyllostachys sp.) Scale Bar=200 μ m.*



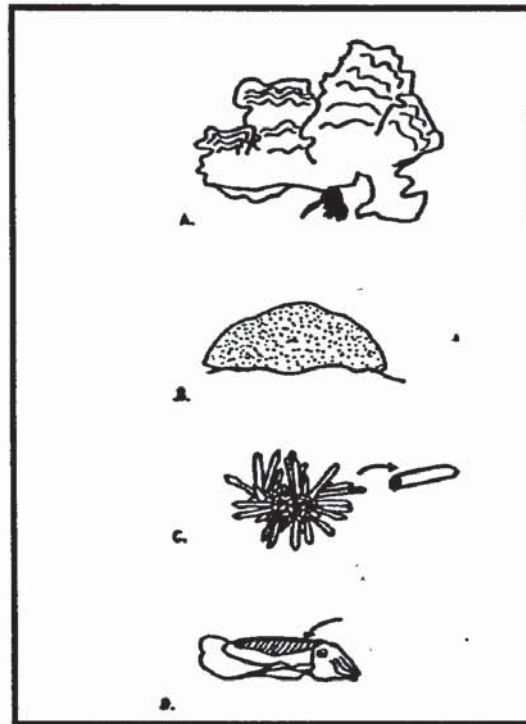
First on the list in the animal kingdom (next step from bacteria in the evolutionary tree of life) there are organisms called Protistans, that secrete exquisitely patterned mineral capsules containing micrometer scale pores and voids. Protistan mineral capsules are exquisitely patterned into micrometer sized pores (10-50 μ m) and voids, but as

frameworks for hosting human cells they are inadequate, since the voids need to be well into the low hundreds of μm .¹⁰³

Porous structures with pore dimensions matching alveolar bone (a type of bone which possesses a cancellous texture), are widespread amongst lower marine invertebrates. As an added bonus, there are many of these creatures with a similar mineral composition to bone-high fractions of calcium salts and phosphate salts. Among invertebrates, with the exception of insects, substantial calcified tissues are found in most species. In outward appearance lower invertebrates and higher plants such as coral,¹⁰¹ sponge¹⁰⁴ and bamboo, respectively possess characters particular to the application developed in this study, with compatible pore sizes and a similar mineral content.¹⁰¹

Coral skeletons, sea urchin spines and bamboo possess a pore geometry (the specific arrangement of cells) very similar to common types of bone, such as primary lamellar and haversian bone with either open and closed cells.¹⁰⁵ A particularly diverse group of sponge possesses a structure of interwoven strands that build to form felts and webs, as employed by previous keratoprosthesis engineers (e.g. Legeais⁷). These four disparate groups of marine organism were studied in more detail to find the best candidate for a keratoprosthesis support frame. In other words, the challenge was to find a species with a skeletal framework with the correct average porosity, mineral composition and which, is amenable to processing, in the likelihood of making a prototype.

Figure 6.1 *A Selection of Invertebrate Skeletal Structures Investigated in Greater Detail (Section 6.3.2). (a) Verongid Sponge; (b) Coral; (c) Sea Urchin; (d) Cuttlebone*



6.3 Examination and Selection of Natural Artifacts as Potential Candidates for a Keratoprosthesis Support Frame

6.3.1 Introduction to Selection Scheme

The skeletons of innumerable marine organisms possess an internal architecture favourable for tissue integration. The geometry of spaces within the solid crystalline matter is uniform, continuous and unrestricted, creating a framework which provides unrestricted access for cell invasion and the passage of blood vessels, capillaries and body fluids, from one point in the solid to every other.¹⁰⁶ It also makes possible impregnation of biologically absorbable gels containing growth factors or biopsies to assist tissue regeneration and minimise complications. Porous, semi-rigid materials are found widely in the marine environment and include spiny starfish, sea urchins and coral.

A number of natural porous artifacts were gathered from various sources (see Table 6.12). Other than the four primary groups of organism (believed to be the most applicable to this study) the anatomy of other useful and interesting candidates, such as

cuttlebone, dogfish eggcase, sea urchin testa were examined, since they were freely available. The results are tabulated below in table 6.12.

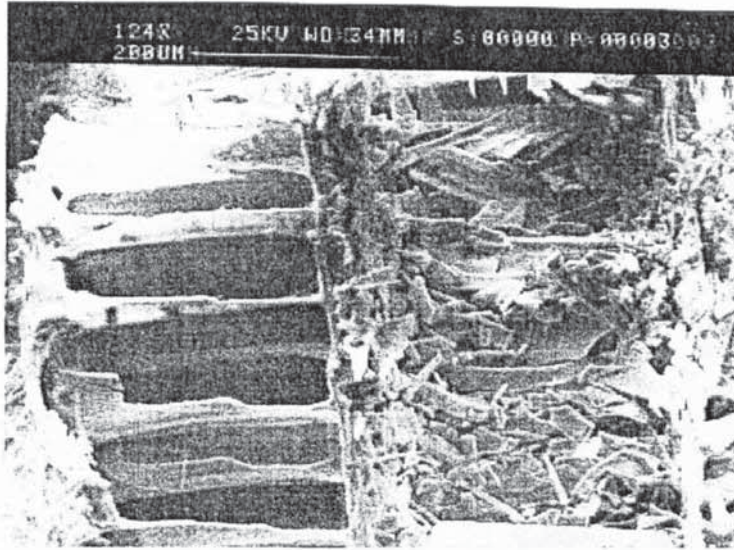
Cuttlebone is a symmetrical stacking of cells framed with calcium carbonate. It is light and relatively flexible with spaces between 200µm to 600µm formed by a series of stacked cuboids, well within the desired range of pore sizes (see **Table 6.12**). Unfortunately cuttlebone is very compact, and so difficult to cast, and very brittle. The eggcase of the dogfish is un-mineralised, but possesses an arrangement of collagen fibrils reminiscent of the patterning in stromal collagen. (see **Table 6.12**)

Table 6.12 *Observed Pore Architecture for Natural Marine Artifacts Selected in this Study*

Natural Artifact	Description of Internal Architecture
Cuttlebone	Stacked Cuboids
Dogfish Eggcase	Orthogonally Woven Collagen
Sea Urchin Testa	Dispersed Parallel Channels and Regular Pore Networks

Sea urchin skeletal plates are punctured by a very regular series of pores. Approximately three quarters of the pores are exits for tube feet (200µm pore diameters at the spine bases to 600µm pore diameters for the tube feet in *Centrostephanus nitidus*) while the remainder are channels connected to the reproductive and alimentary systems and are very much larger to accommodate larger throughputs of fluid (1000µm-2000µm pore diameter).¹⁰⁶ An additional problem is that there is no discernible interconnection between pores. The better candidates, again all derived from the sea, were studied in more detail with examination under SEM and light microscopes.

Photograph 6.12 *An SEM Image of the Cellular Structure of Cuttlebone*



6.3.2 Marine Derived Skeletal Frameworks of Particular Interest

Marine derived skeletal frameworks have been successfully used in bone replacement therapies. Table 6.13 lists the species, from two groups of marine invertebrate with skeletal frameworks that have been used to replace damaged and diseased tissue in the human body.¹⁰⁶ Logically, each one temporarily deputises for bone in non-load bearing areas of the body and provides spaces for the regeneration of newly formed bone and connective tissue. There is a large body of evidence for the use of coral in surgery as hard tissue substitutes.¹⁰⁶ Coral skeletons tend to be more widely available and can be cut into a greater number of possible shapes than tubular sea urchin spines. In contrast to coral skeletons, sea urchin (echinoderm) spines are rarely employed as tissue replacements, perhaps because of the greater effort in finding and collecting suitable material.¹⁰⁷

Table 6.13 Naturally Derived Frameworks Applied for Human Reconstructive Surgery

Type	Structure	Biomedical Applications
<i>Echinoderm spine:</i> <i>Heterocentrotus trigonarius</i>	Periodic minimal surface	Screws and plugs for bone replacement (experimental)
<i>Echinoderm skeletal plates and spines:</i> <i>Acanthaster plancii</i> and <i>Nardoa</i>	Periodic minimal surface	
<i>Madrepore corals</i> <i>Porites porites</i>	Vronoi foam #: Three Dimensional/ highly interconnected	Replacement and augmentation of maxillofacial bones, vertebrae and orbital implant
<i>Goniopora lobata</i>	Vronoi foam #: Three Dimensional/ highly interconnected	Replacement and augmentation of maxillofacial bones

Vronoi Honeycombs are formed by competitive growth of active cells. There are two types of Vronoi Honeycomb: One for a set of random points in which, cells nucleate at random points at the same instant and grow with the same linear growth rate, and another for a set of fixed points in which, cells nucleate closer together than a critical spacing and grow with the same linear growth rate.

Compared with the many hundreds of possible and undiscovered natural artefacts, the selection of examples listed in table 6.13 are limited to just two animal groups-echinodermata and anthozoa. There are no records of say, *Porifera* (natural sponges) or the little known *Bryozoans* as ever being employed as a replacement for human tissue, despite the variety of pore structures. In this study, many species of marine derived skeleton were evaluated for similarity with the list of structural characteristics associated with alveolar bone and, listed in the introduction to this chapter. Unfortunately, many targeted natural artefacts were either poorly classified or difficult to get hold of. Poor classification would hinder collection of new material. A common

problem associated with this classification confusion was that the features used to name and classify an organism rarely corresponded to the features such as internalised corallite pore sizes, required for the purpose of this study, namely tissue integration. This limited the search to species in which, a sample could be collected or obtained.

The following sections describe groups of organisms (identified by Phyla and Classes) with suitably, well structured skeletal frameworks, defined in the main by, pore size, pore geometry and mineral type. Single celled candidates have been ignored for pragmatic reasons, and we have started with a group of primitive marine organisms called *Bryozoans*. *Bryozoans* were selected as possible contenders, because they possessed an outward morphology, comprising flattened lobes with a dense regular array of small pores.¹⁰⁸ *Porifera*, *Anthozoans* and *echinodermata* are examined in turn. For each of the four classes of organism (including *Bryozoans*) selected, their suitability as a support frame to the tooth and bone was assessed on the basis of pore size and pore architecture.¹⁰⁸

Table 6.14 *Final List of Animal Groups (mainly Marine) Investigated as Candidates for an Artificial Cornea Support Frame*

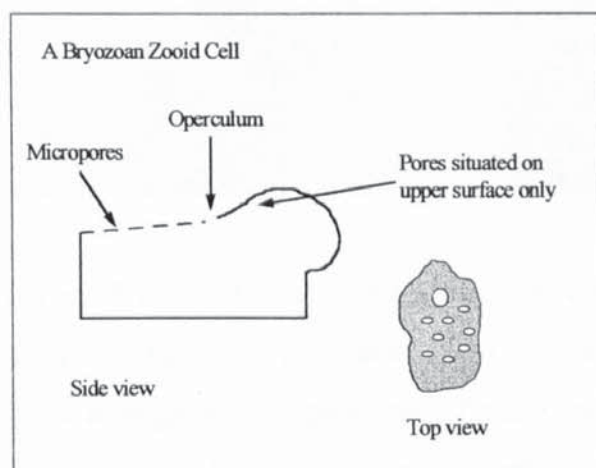
Phylum%	Class
Bryozoa	Ascophoran
Porifera	Hexactinellid, Calcarea and Demospongia
Coelenterata	Anthozoa (Hard corals)
Echinodermata	Echinozoa
Vertebrata	Mammalia

% Rank immediately below kingdom within the zoological hierarchy of classification¹¹⁸

6.3.21 Bryozoans (*Moss animals*)

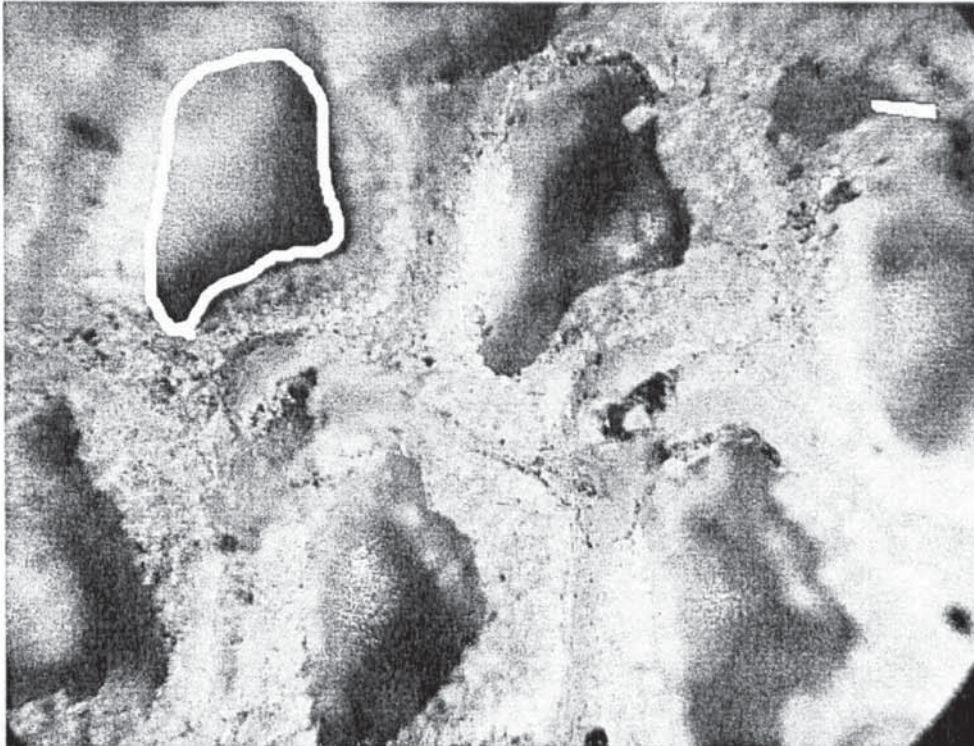
Bryozoans are sessile colonial animals that are very common on rocky shores. Colonies are very small and inconspicuous and approximately 4,000 species have been described. They are found globally from tidal regions to the abyssal depths which makes them suitable for collection and moderate exploitation. The morphology and geometry is most complex in Ascophoran *Bryozoans*.¹⁰⁹ Problems with specific identification has hampered research in all matters of their biology and distribution. In structure they consist of replicated series of zooids equivalent to polyps formed by budding. Zooids are supported by mineralised protein cups moulded into the main body of the organism.

Figure 6.11 Diagrammatic Representation of a Zooid Structure



Bryozoans were considered as a candidate structure because, they possessed an outward morphology that may be suitable as a keratoprosthesis support with a regular array of pores. Microscopical measurements were carried out on a species of a ubiquitous Bryozoan possessing small pores and opercula (at least below 250 μm). A sweeping survey of British Ascophoran *Bryozoans* shows that, the average diameter of pores for an individual zooid cell was between 70 μm -200 μm . This fits in well with the required pore dimensions for an alveolar bone analogue (50-150 μm).¹⁰⁹

Photograph 6.13 *Enlarged Exterior View of Bryozoan Zooids. The white line is drawn around one zooid. (x18) (Scale Bar = 400 μ m)*



However, colonies are small and delicate to the touch, between 2mm and 20mm in length. *Bryozoans* are flattened laterally to a thickness of 0.25mm. They also possess a very restricted series and arrangement of pores with limited interconnections between cells (**Figure 6.11**). The contrast between *Bryozoans* and trabecular alveolar bone is stark as shown in Photograph 6.13, above. An alveolar bone macropore is 1/10 the size of the opening to the zooid chamber, although there is greater variation in zooid sizes across the group.

Photograph 6.14 *Contrast of Porosity Between Bryozoan (Natural History Museum) and Trabecular Bone (Birmingham Dental Hospital) (x18 magnification)*

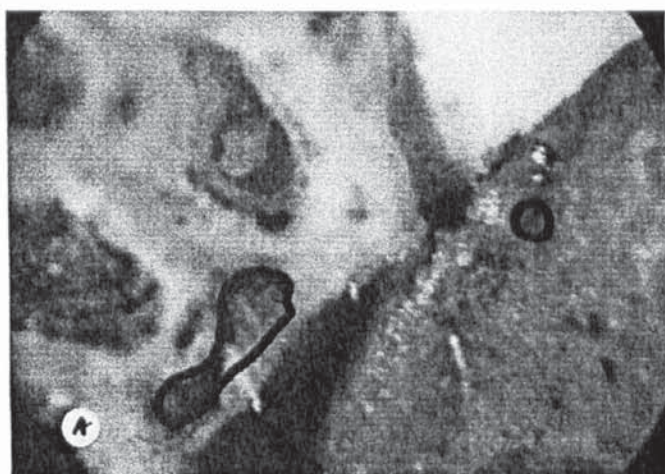


Figure 6.15 *Pore Sizes (μm) of Selected British Marine Bryozoans*

Zoological Name	Pore Sizes
Tessaradoma boreale (Busk)	70-100
Turbicellepora avicularis (Hincks)	200-250
Ragionula rosacea (Busk)	125-150
Schizoporella errata (Waters)	150-175
Phylactellipora collaris (Norman)	125-150
Porelloides laevis (Fleming)	175-200

+ *Bracketed names refer to first person to identify and describe the species*

6.3.22 Sponge Skeletons

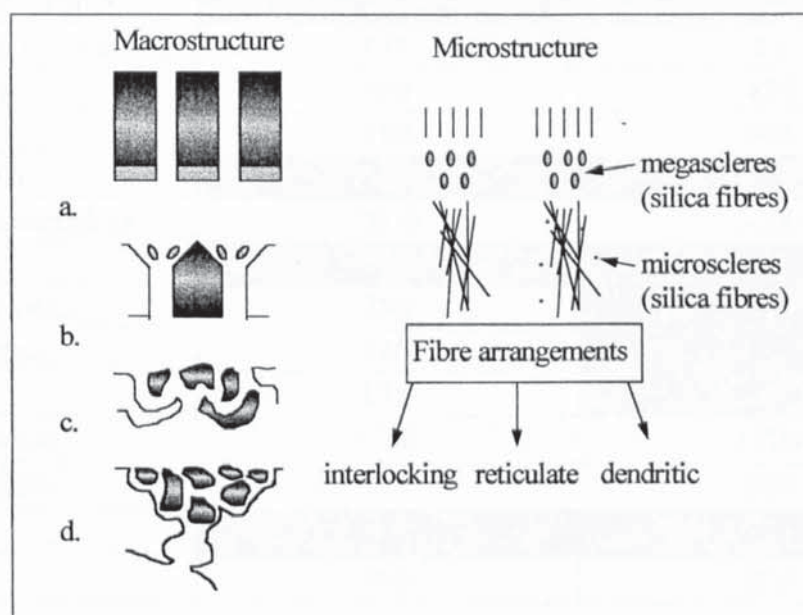
Sponges are a very diverse group of 'simple' sedentary (animals fixed to one spot) and live in all oceans of the world from shallow to deep waters in addition to tropical freshwaters. Sponges fabricate highly intricate skeletal frameworks upon which the cellular mass (the whole animal body) is supported. Nearly every cell is in contact with a structural element. This is a crucial attribute for use as an implant.¹¹⁰

The complex arrangement of pores exhibited by sponges, allows for the maximum amount of living matter to be arranged in the smallest volume of space, while the maximum surface area of space is created. As a result each cell is in sufficient contact with food containing water currents. Features such as these ensure that tissue at the centre of the structure remains alive and is healthy. A tissue scaffold, surrounding the

optical window of an artificial cornea must do the same to provide long-term attachment. Can the geometrical qualities of inorganic sponge skeletons be put to use as tissue frameworks for integration of an artificial cornea in the same mode as alveolar bone?

The arrangement of pore spaces in a sponge can be typed according to the average pore dimension and the degree of branching, as shown in figure 6.12. Most sponges possess interconnected pores and channels that are likely to host human tissue, because of the ideally suited arrangement of channels (meshworks) and matching pore dimensions, (250 μ m to 500 μ m) in some species. In the context of implantation into the cornea, or onto the cornea in association with mucosal augmentation tissue (as in the OOKP) a dendritic microstructure and macrostructure as (d) provide the best available void structure for, adequate nutrition to invading cells and an adequate framework to support ingrowing tissue. Pore dimensions between 50 and 200 μ m would optimise the degree of penetration of tissues involved in wound closure and so, guarantee long term material and host integration. Are there any sponges, freely available with these essential features?

Figure 6.12 Pore Structures of Sponges after Brusca and Brusca¹¹¹ Example c and d is characteristic of *Keratosa*. The *Verongids* are best represented by b.



Sponges boast the greatest genetic and morphological (based on a single body plan)

diversity of any group of extant animal. Three main classes of sponge were selected as broadly fitting the required architectural features as described in Scopes and objects, Chapter two. Featured below is a list of selected sponges, studied at the Natural History Museum in London, and the range of pore dimensions measured under a light microscope. According to the selection criteria set out previously, the optimal features for a tissue scaffold, included an interconnected porosity, regular pore dimensions, low cost and good availability.

Looking at Table 6.16 few sponges possess pore sizes within the desired limits, except for a little known species of *Verongid* and a species of *Calcareous* sponge. Although, many Sponges possess a wide range of excellent pore architectures and associated mechanical properties.

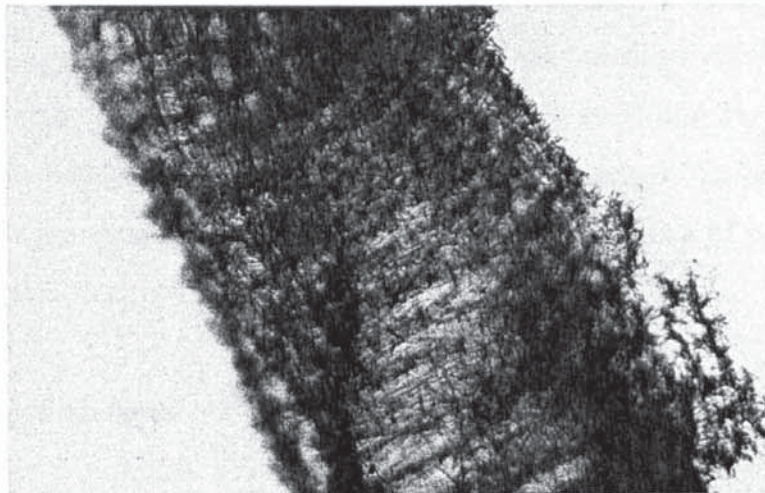
Table 6.16 Pore Sizes (diameter in μm) for Selected Sponges. The upper limit for desired pore sizes can be $500\mu\text{m}$, although a pore size of $250\mu\text{m}$ was a more satisfactory upper limit.

CLASS and Species	Minimum Pore size	Maximum Pore size
VERONGIDA		
Ianthella basta	500	2500
Ianthella	420	700
Verongia tenella	110	250
DICTYOCERATIDA		
Crateromorpha meyeri	175	1270
Aplysina massa	300	420
Aplysina	510	400
AXINELLIDA		
Potamolepis schontedeni	2800	3000
CALCAREA		
Leucosolenia cavata	750	
Clathrina cariaceae	780	
Clathria	175	
Grantia compressa	1750	1720
Grantia labyrinthica	210	300
LITHISTID		
Thoenella sp.	760	820

Photograph 6.15-*Potamolepis schoutedeni*; (x10 magnification) A freshwater sponge from the Congo. One of the candidates selected for casting and cell culture because of the regular hexagonal pattern of voids.



Photograph 6.16-*Grantia compressa*; (x4) A Selected Calcareous Sponge.

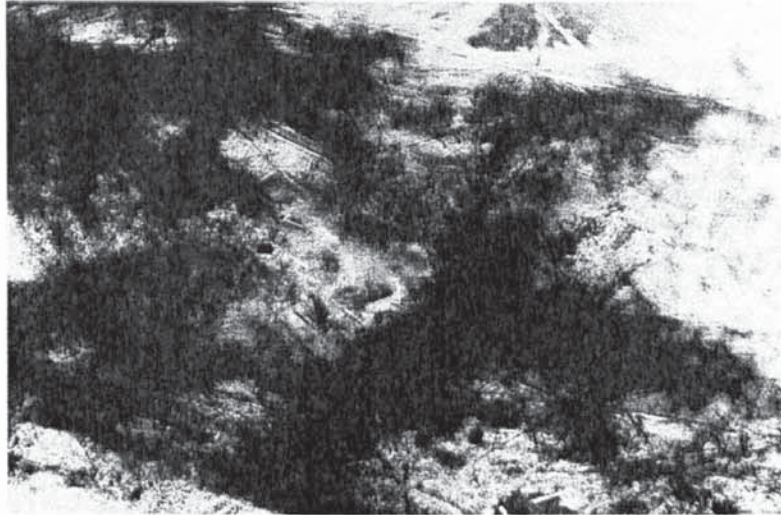


(i) The Dictyoceratida Sponges

Members of the *Dictyoceratida* (Table 6.16) are, in general structurally alike to pumice stone in the shape and arrangement of pores, but unlike pumice they have a fleshy texture. Pore sizes are just beyond the upper limit for a keratoprosthesis support frame, varying between 125 and 400 μm . The larger pore network, however approaches a size well beyond the requirements, at 1270 μm . On the positive side, sponges of this kind come in many different forms: digitate, ramose, lamellate, pedunculate and thin fans. The surface is formed of conulose and stellate patterns and is intricately complex and this is important for ensuring a sound tissue interlock. Individual members of the group *Dictyoceratida* construct a fine network of

intertwined fibres as shown in (d), Figure 6.12.

Photograph 6.17-*Crateromorpha meyeri*; (x10 magnification) belonging to the group of bath sponges was one selected according to the criteria set out in Table 5.15.



A family member of *Dictyoceratida*, *Spongia* (or *Keratosa*), is the archetypal natural sponge familiar to people, as bathsponges. They are very readily available and the most popular and common species are 'cultivated'. From a structural viewpoint the fibre network is both highly elastic and compressible, an advantage during surgery. The matted types of sponges are alike to the structural configurations of polymer felts and webs, already used to construct keratoprosthesis support frames.

(ii) The Verongid Sponges

Members of the *Verongida* (Table 6.16) are very dense, cheeselike, and suitably elastic-matching the flexibility of human skin. The problem, however with *Verongida* is the dense fleshy coating of collagen surrounding the inorganic skeleton which, must be removed before implantation to avoid rejection. *Ianthella basta* (Gray) is a common coastal species with a regular, stiff, grid-like structure and was the one of the most promising candidates for a tissue framework with a void structure as shown at (b) in Figure 6.12. *Ianthella* consists of an anastomosing, reticulated fibre skeleton compressed into two dimensions radiating from a central point, and supported by abundant connecting fibres.¹¹² There is a good spread of space for cell migration, proliferation and angiogenesis.

Photograph 6.18 *Ianthella flabelliformis* (x4) A Selected Verongid Sponge



The complex reticulation of fibres is orientated within a single plane and is arranged into a very regular rectangular meshwork.¹¹² *Ianthella* possesses both a good stiffness, strength and was much less compliant than say, the *Lithistid* sponges. It was, therefore thought to be a better companion to the semi-rigid optic. The size of spaces between the skeletal struts were very large (100-2500 μ m pores making 75% of the total), but it was supposed that after casting, if it were deemed necessary, these spaces would be reduced to half their original size.

(iii) The Lithistid Sponges

Lithistids are characterised as being rock-like although some maybe rubbery and wrinkled. Shapes, as in all other groups, vary enormously. Unlike many other sponges, the microscopic spicules of *Lithistida* are knotted together into a rigid network making them highly suited as a mechanical support, especially in the context of this study for a relatively heavy optical cylinder. Furthermore, the presence of fused spicules reduces the likelihood of debris and chronic inflammation. Pore sizes are well above the desired 250 μ m maximum, at 750-850 μ m and this fact severely limits their potential.

Overall, the sponges are fascinating candidates for a keratoprosthesis support frame, in terms of the variety of suitable pore architectures and useful mechanical properties. Unfortunately, the pore sizes are consistently too large, as compared with the OOKP

alveolar bone. The next group of natural artifacts to be looked at, are the reticulated spines of tropical sea urchins (belonging to the group echinodermata).

6.3.23 Sea Urchin Spines

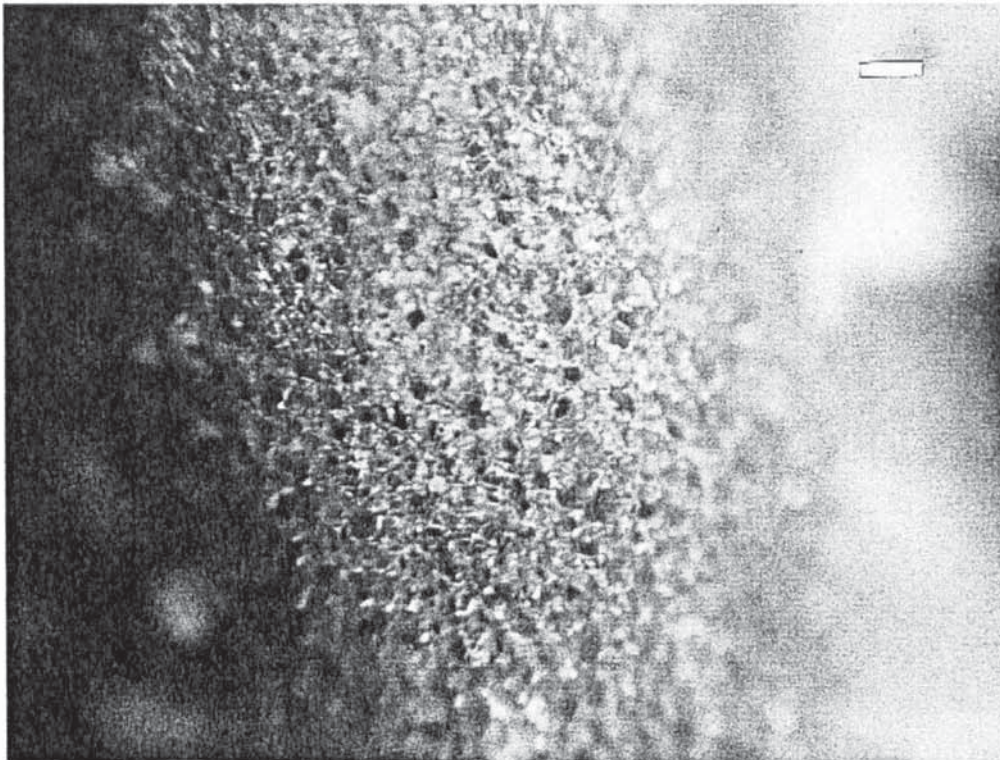
Echinoderms are a group of marine invertebrates that include sea urchins, sea stars, crinoids and brittle stars. All members of the phylum secrete a magnesium calcite exoskeleton rather than the more common aragonite form. The spines, which are extensions of the exoskeleton, are sculptured into a highly intricate three dimensional fenestrate structure. The internal surfaces of echinoderm spines are unique to the animal kingdom in that they partition space in such a way that there is maximum contact for crystal growth and a maximum amount of interconnected spaces, known as a periodic minimal surface. Pore sizes are comparatively small (20 μ m-70 μ m) and very closely match the pores of alveolar bone. (See **Table 6.18**)

Table 6.18 Pore Sizes (diameter in μ m) of Spines for Three Species of Sea Urchin

Zoological Name	Pore sizes
Heterocentrotus trigonarius	20-70
Sphaerechinus granularis	10-15
Acanthaster planci	70

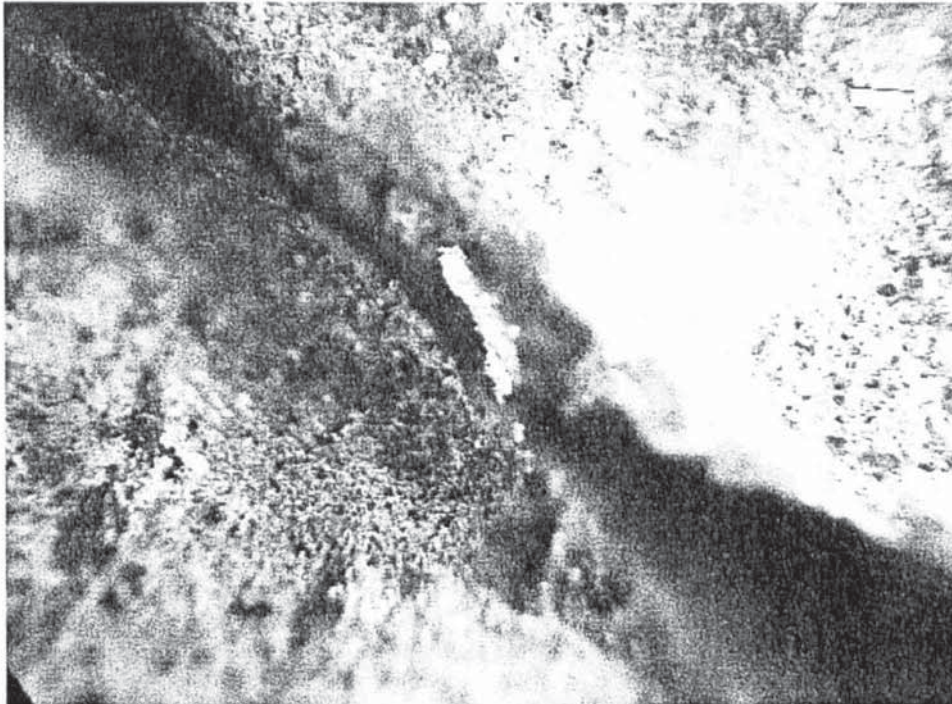
Echinoderm spines possess all four characteristics essential for tissue integration and support, including two that are not universal to coral skeletons:- (1) a solid-to-void ratio of one- which means, (a) it optimises space filling for support and (b) maximises available space for cell distribution; and (2)an exceptionally high permeability, preferably in which, every pore is in contact with all adjacent pores (periodic minimal surface)

Photographs 6.19 *Light Microscope Images of the Internal Structure of an Echinoderm Spine (Heterocentrotus trigonarius) (x18)(Scale bar=200µm)*



Comparing alveolar jawbone and the internal structure of an echinoderm spine, there is a striking similarity. Of particular importance is the closely matched size of pores. Lack of availability hindered further exploitation of this interesting and unique structure.

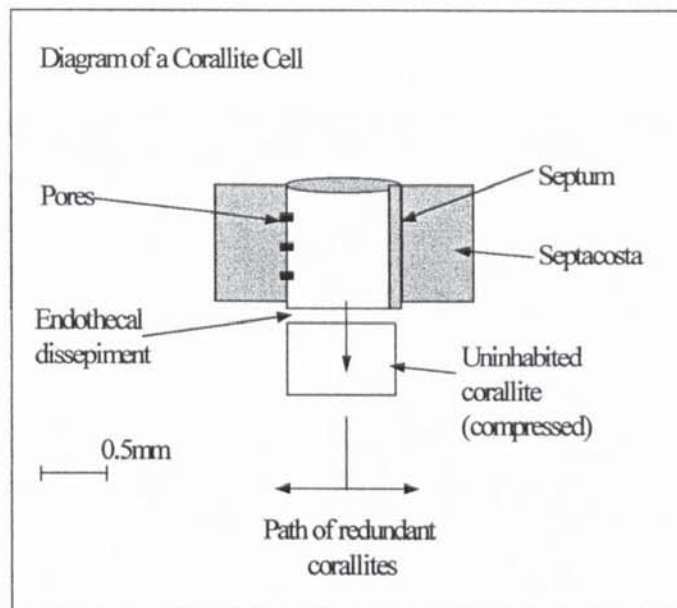
Photograph 6.2 *Contrast Between a Section Through an Echinoderm Spine and Trabecular Jaw Bone (Scale Bar=200 μ m)*



6.3.24 Coral Skeletons

In the aragonite skeletons of reef building corals there are very many different types of intricate structure. In contrast to sponges, corals are more rigid and more highly structured (pore and channel walls on average three times as thick) due to the larger quantities of ceramic deposits. *Porites* deposits calcium carbonate in the form of small corallites either in a radial manner or perpendicular to the axis of growth (**Figure 6.3**). Both types essentially resemble trabecular bone (lamellar and haversian types) but, possess contrasting space geometries.

Figure 6.13 *Basic Anatomy of Coral Skeleton.*



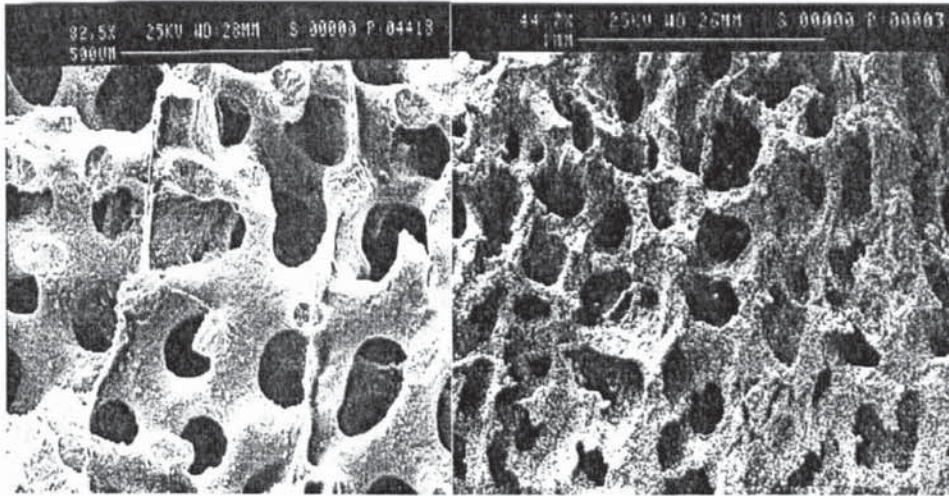
Coral is a name for a variety of marine animals belonging to the phylum Coelenterata. Coelenterates are a primitive group of invertebrates with a very simple body plan consisting of two tissue layers and perfect symmetry.¹¹³

Corallites are voids that give rise to pores and channels when the filter feeding animal disposes of them. Their morphology and how they are arranged during growth and development determine their suitability for a tissue framework. The mineral shell or corallite surrounding a polyp consists of well ordered clusters of acicular aragonite crystals. The corallite walls are normally perforated and interrupted by septa at regular intervals. Septa are also perforated and this is what gives coral the element of microporosity. All the distinctive features of a corallite are somewhat compacted and re-arranged during growth introducing numerous interconnections.

6.3.25 Selection Criteria for Coral Skeletons

The primary feature of a coral skeleton, that makes it highly suited as a tissue scaffold in providing support and space for cell migration and proliferation is an ordered uniform porosity (See **Table 6.19**). In relation to fabrication, coral skeletons are easy to cut and shape into moderately intricate shapes, such as a contact lens. The reason for this is that mechanical properties of coral are unexpectedly good for the given amount of porosity (50%-70% upwards) and mineral constituency.

Photograph 6.21 Thermal SEM Images Comparing two Open Cell Natural Foams of *Goniopora lobata* (left) and *Porites porites*. Both structures consist of relatively thin struts and a highly ordered and interconnected pore system.



All coral skeletons possess open porosity in which, corallites are connected by pores. In general, interconnectivity did not vary greatly enough for it to feature prominently in selection. A significant advantage for selection of an appropriate coral skeleton is that they are relatively simple to identify. Much is now known of the most abundant species of coral, their taxonomy and distribution; although there are limits on exploitation of uncommon coral species because it could irreversibly reduce the population. This will restrict the number of choices for the support frame.

Habitat conditions in which, the coral grows determines the degree of uniformity in structure. In general, corals can only thrive in uniform conditions, but slight changes do occur and affect form and structure to a considerable degree. Corals closer to the equator and distant from land masses are less subjected to alterations in sea temperature and nutrient loading. Corals express great morphological 'plasticity' in response to slight environmental differences. Despite this fact the physical attributes of cellular frameworks are reasonably uniform, as shown in Table 6.19.¹¹³

Table 6.19 Physical Characterisation of *Goniopora* and *Porites*.⁸⁹ It was shown that *Goniopora* and *Porites* are physically similar, despite the clear differences in the open-ness of pore volume. The cellular framework has many features in common.

Property	GONIOPORA	PORITES
Contact	Open	Open
Ze/ Zf	06/02	06/02
Cell shape	Ovoid S.D. below 1	Oblong S.D above 1
Symmetry	Radial	Radial
Fraction of material at edges	0.7	0.5
L1/ L2	3.75	3.3
S.D Ratio	0.7	1.3
Density of mineral	0.5 g/cm +/- 0.2 g/cm	0.9 g/cm +/- 0.35 g/cm

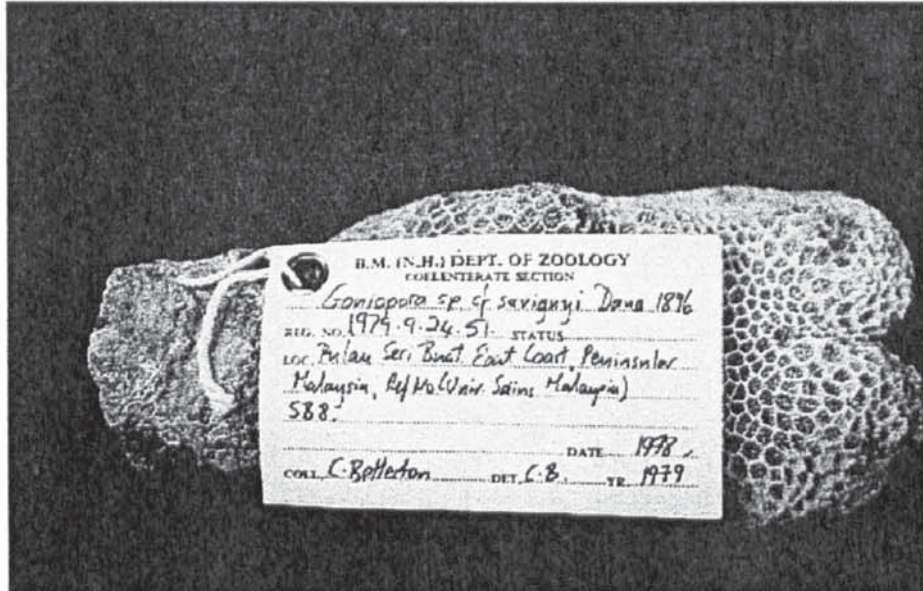
See Section 3.6.3 for explanation of terms

A selection of suitable coral candidates was carried out according to the following; (a) porosity (b) ease of identification and collection (c) naturally abundant and (d) a high degree of structural uniformity. As can be viewed in Table 6.2, there are a large number of corals with an acceptable growth form, abundance and structural uniformity. The majority of coral skeletons possess pores up to 500µm and are easily identifiable with a magnifying glass.

Coral species with a rounded growth form, high abundance and widespread distribution were preferred as potential candidates. Skeletal samples of these species were obtained from the Natural History Museum for closer examination under a light microscope and SEM to measure pore sizes and unravel the specific type of pore geometry. The list of final candidates for closer investigation are listed overleaf:

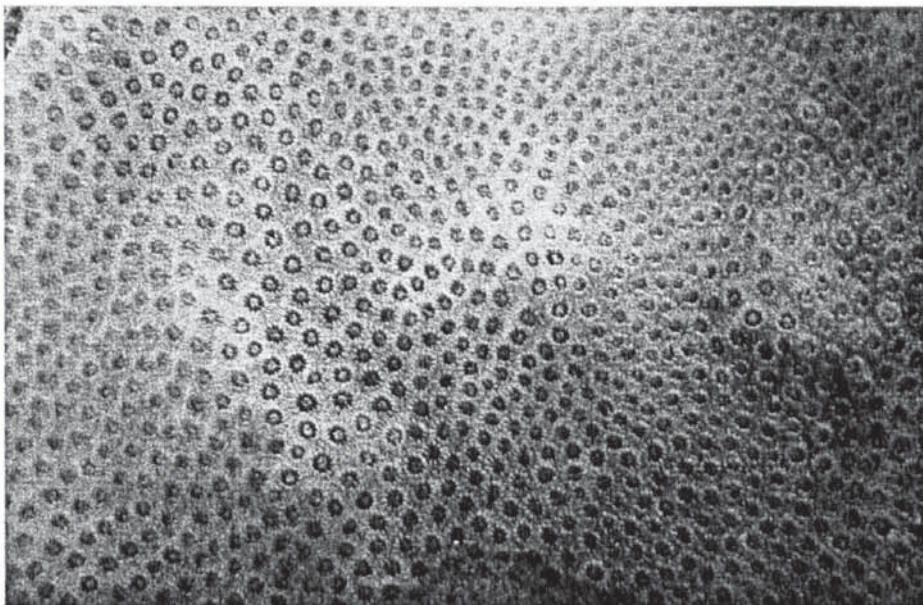
- *Goniopora lobata* (de Blainville, 1830#) (Photograph 6.22)

Photograph 6.22-*Goniopora coral* (with kind permission of Sheila Halsey & the Natural History Museum, London)#



- *Porites astreoides* (Link 1807#)

Photograph 6.23 Surface of *Porites astreoides* Coral showing a unique porosity and surface texture.

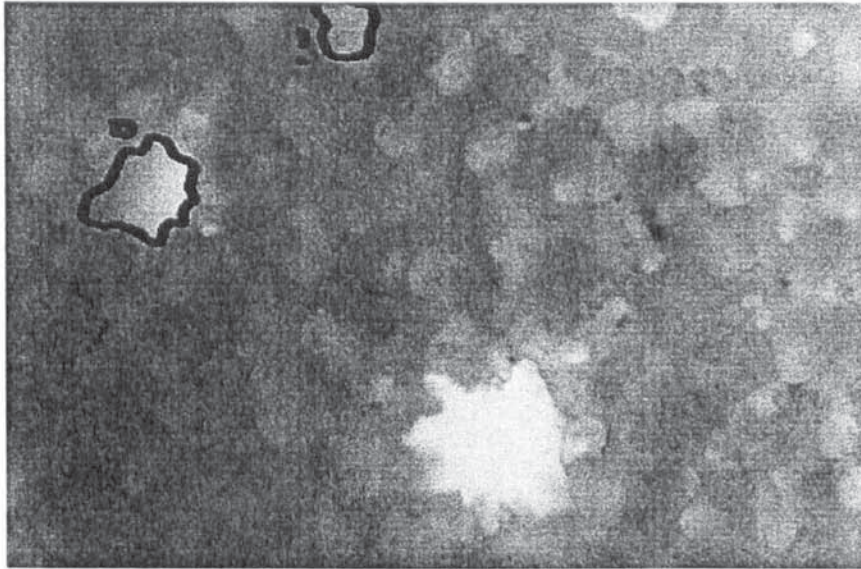


- *Montastrea annularis* (de Blainville, 1830#)
- *Dichocoenia stokesi** (Milne-Edwards and Haime, 1848#)

#Note that corallite diameter at surface is slightly larger than corallites below

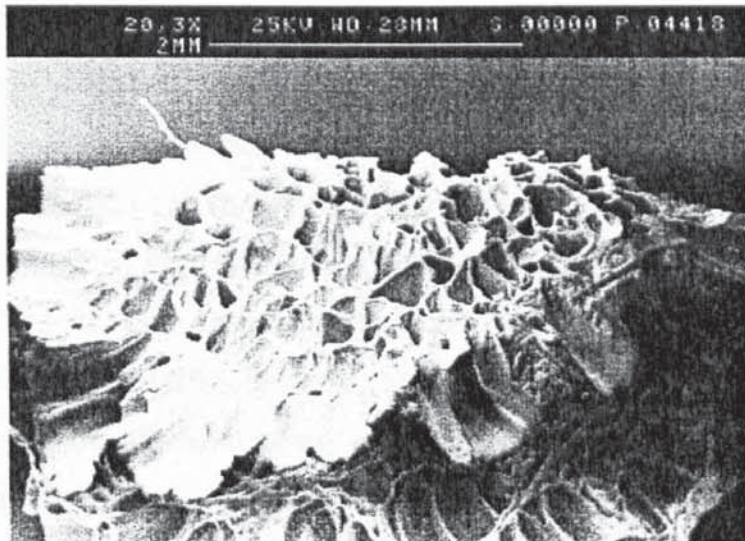
- Stylophora sp.(Pistillata?) (Schweigger, 1819)
- Seriatopora octoptera (Lamarck, 1816)

Photograph 6.24 *Internal Structure of Seriatopora octoptera Featuring Two Grades of Pore size.*



- Seriatopora sp.S.hystrix? (Dana, 1846)

Photograph 6.25 *An SEM Image of Seriatopora sp.Coral (x20)*



Note: many of the species (marked with symbol #) selected are presently used in bone replacement surgery.

After close examination with a hand lens and light microscope a list was compiled of pore dimensions for the final group of corals that were selected (**Table 6.21**). *Seriatopora*, *Porites*, *Goniopora* and *Stylophora* possessed pore dimensions within

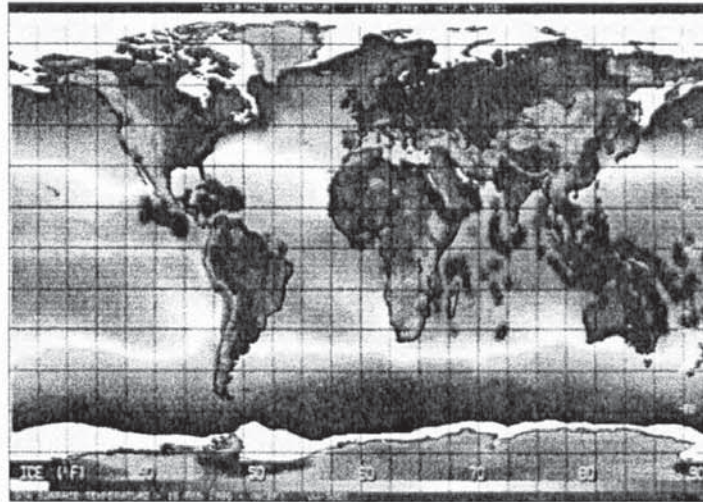
acceptable limits for tissue inward growth and attachment, by mechanical interlock, as outlined in Section 2.8 (See also **Appendix 1** for more details of criteria). *Seriatopora* and *Stylophora* though, did not possess an ‘open’ enough interconnected porosity, as shown in Photograph 6.25, due to a greater degree of pore compaction and mineral aggregation around adjoining struts.

Table 6.2 Pore Sizes (diameter in μm) of Common Trabecular Bone-like Corals

Name of Coral	Macropore Diameter	Micropore Diameter
<i>Seriatopora</i> sp.(Dana 1846)	390-410	86-126
<i>Porites porites</i> (Link 1807)	160-188	29
<i>Goniopora lobata</i> (de Blainville 1830)	134.82	90
<i>Stylophora</i> sp.(Schweigger 1819)	243.2	130-150

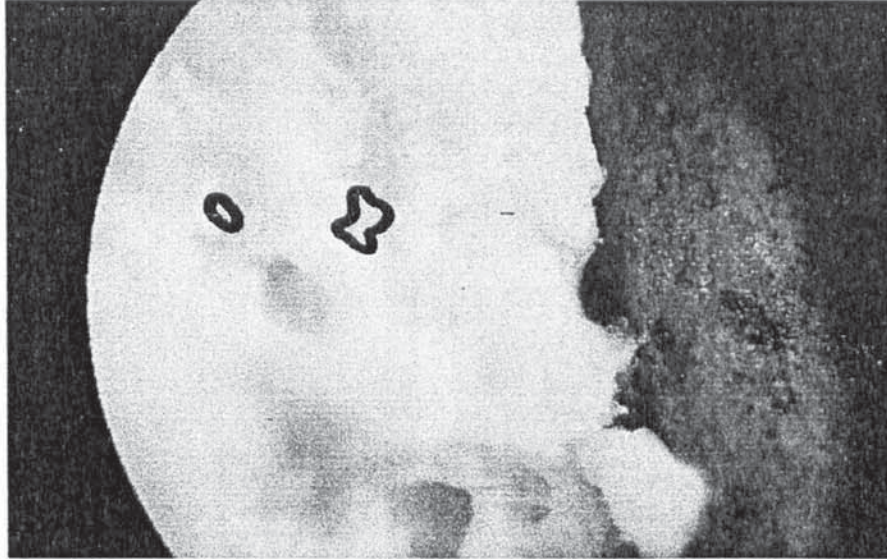
On the basis of information presented in table 6.21, *Porites* and *Goniopora* corals were selected as the candidates with the best potential for a keratoprosthesis support frame, by virtue of their extensive and substantial growth form (massive reef builders), structure (highly porous) and their availability in the required amounts (they are both widespread and abundant). Both *Porites* and *Goniopora* occur over a wide range of habitats across the globe, from the Indo-Pacific to the Caribbean (**Figure 6.14**). As displayed in Table 6.21, pore sizes vary between 90 μm and 390 μm , well within the limits of pore sizes for the alveolar bone, although a direct comparison of the two structures by eye show the contrasting concentration of macropores (**Photograph 6.14**). In *Porites* the difference is less obvious. However, this feature may allow for more vascularisation, as demonstrated by Hatt¹⁹, and so improve chances of survival.

Figure 6.14 *Global Distribution Map of Porites species.: Most Commonly used Coral for Bone Replacement.*



Compared with other investigated natural artefacts, corals are used extensively in bone replacement therapies such as, spinal surgery, maxillofacial repairs and have been for some twenty years. Corals possess a larger variation of highly interconnected open porosity- with each cell having open contact with every other in the vicinity enforcing secure interpenetration and hence, long term attachment.¹¹⁴ From a practical viewpoint, corals are easier to obtain, in large amounts, from a number of commercial manufacturers as listed in Section 6.4.

Photograph 6.26 Contrast Between a Large Open Cell Coral (marked A) and Compact Alveolar Jaw Bone. The large pores in the alveolar bone correspond well with the macropores of coral, but the density of micropores is much greater in alveolar bone (right).

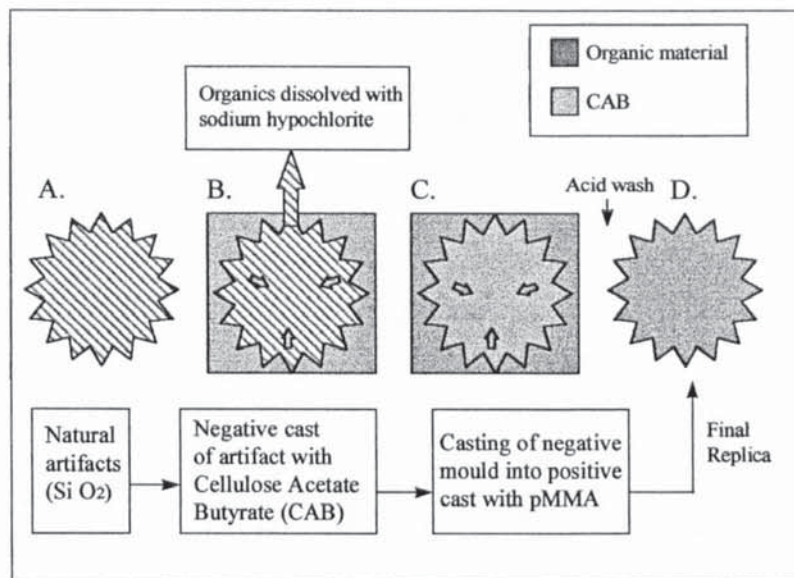


6.3.4 Polymer Casting of Sponge and Coral Skeletons

The major concern of using natural artefacts such as coral is the damage caused by removing them from their natural environment. Coral reefs are under threat from pollution and extraction, in most areas of the tropics. It is also expensive to acquire specific types of coral. A more environmentally tolerable and cost effective way of using these unique porous structures for a keratoprosthesis support frame, would be to duplicate suitable natural frameworks with a synthetic polymer or ceramer. Precision polymer casts of *Stylophora* and *Goniopora* coral skeletons were fabricated by Replamineform processing, as described in Section 3.4.6. In essence, it involved casting the natural artifact with an easily degradable material, dissolving away the natural artifact and re-casting it (the mould) with a synthetic polymer or ceramic slurry into the new structure, before dissolving away the degradable negative cast to produce a synthetic polymer replica of the natural artifact. It is a relatively straightforward technique and does not require expensive apparatus. Skeletal structures were accurately duplicated by this method in fine detail, including the micropore structure. Similar results were also obtained from casts of a number of *Keratosa* Sponges. However, not all the organic matter from the natural sponges could be removed at the first stage of processing because, the organic framework was shielded, in places by

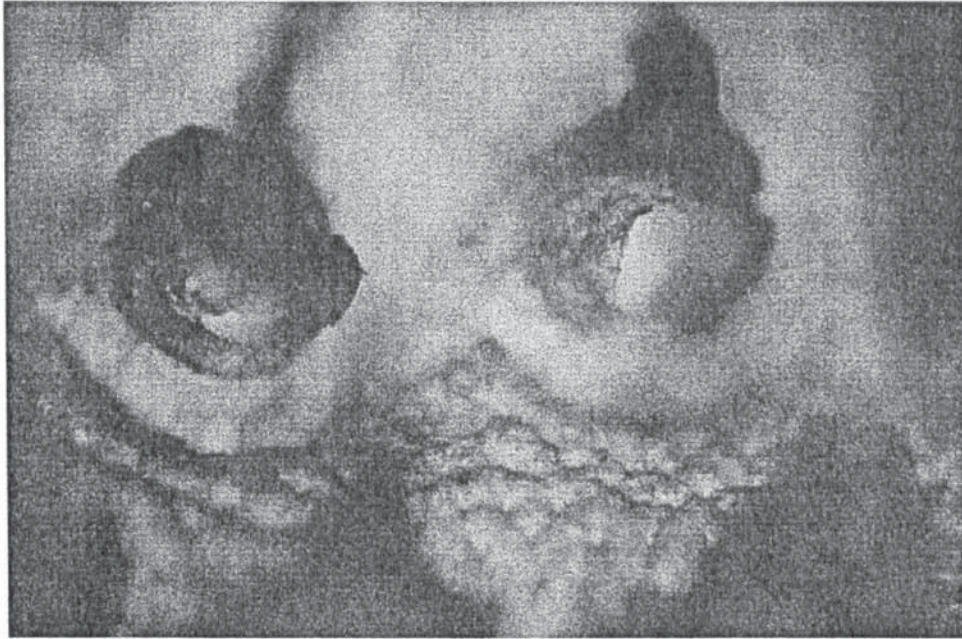
thick layers of CAB. A second problem was that washing with acid, to remove completely the organic matter, tended to dissolve away important structural elements (e.g the struts) of the first synthetic cast structure, as can be seen in Photograph 6.3.

Figure 6.15 *Replamineform Processing of Natural Artifacts*

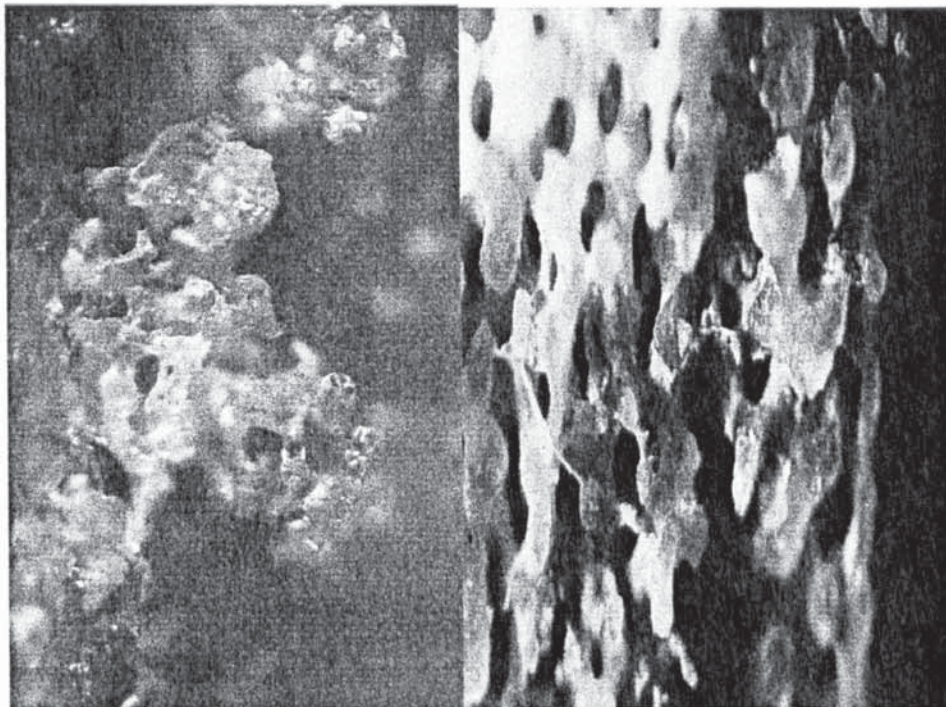


Looking first at *Stylophora* coral we see an accurate copy of fine detail in the negative cast (Stage B from Figure 6.15). Photograph 6.28 compares the bio-polymer cast with the coral mould it was placed into.

Photograph 6.27 A pMMA Negative Cast (U.V polymerisation) of *Stylophora Bifurcated Macropore Channels*. (B. in **Figure 6.15**) (*Stylophora* species.; NHM dry collection)



Photograph 6.28 A pMMA Negative Cast (U.V polymerisation) of a small section of *Goniopora lobata*. The original 'template' is shown on the right for comparison.



In the positive cast (C) there is again precise duplication of both micropores and

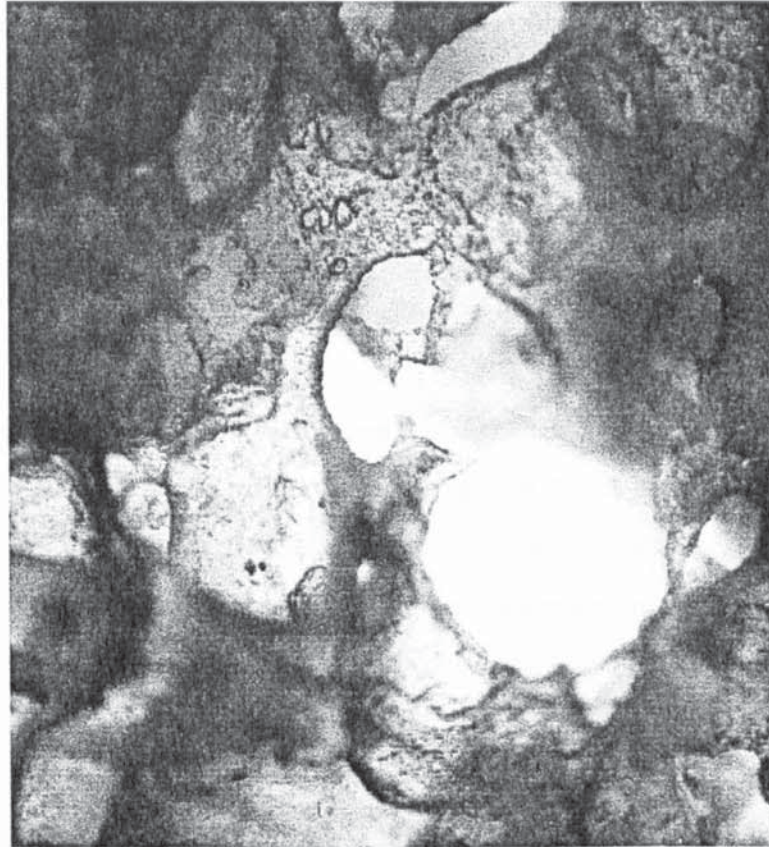
macropores (**Photograph 6.29**).

Photograph 6.29 A pMMA Positive Cast of *Stylophora* Showing the Distinctive Micropores and Macropores. (C. in **Figure 6.15**) (*Stylophora* sp. NHM dry collection)

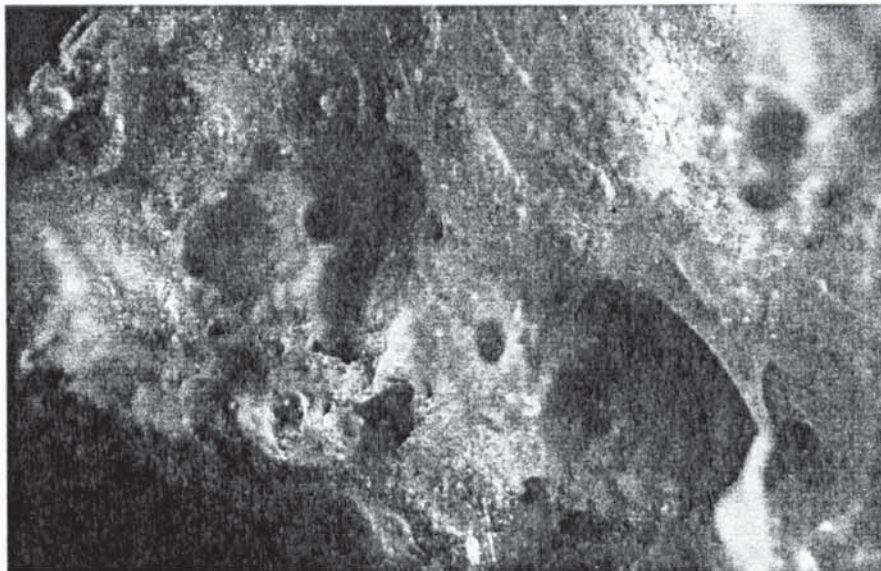


In conclusion, coral skeletal structures were accurately duplicated by this method in fine detail after many attempts. Similar results were also obtained from casts of a number of *Keratosia* sponges. However, not all the organic matter could be satisfactorily removed. Acid dissolution, to remove organic matter, degraded important structural elements of the synthetic cast, as shown in the photographs of the sponge cast and replica, shown below (**Photographs 6.3-6.31**).

Photograph 6.3 *A pMMA Negative Cast (B) (U.V polymerisation) of a Spongia(Keratoso) Sponge with Broken Struts Caused by repeated acid washing.*



Photograph 6.31 *Positive pMMA cast (C) of a Keratosa*



6.3.5 Final Remarks about the Suitability of Marine Skeletons

In general, marine-derived skeletons are very useful tissue bonding elements for the proposed role of securing a non-porous synthetic implant, such as a rigid optical cylinder. A varied assortment of natural skeletons were for their similarities to the

structural and chemical composition to alveolar bone. The features of importance in selecting a viable structure were pore sizes, the specific arrangement of pores, chemical composition and whether the structure was easily obtainable. Calcareous skeletons were favoured over the skeletons made from silica, despite having suitable pore structures and despite being easy to obtain. The primary advantages of using calcareous skeletons (e.g. calcium phosphate) are that:-

- biological ceramics are highly tolerated by the human body; attested to by a long record of uncomplicated success.
- coral skeleton is tolerated in the cornea and does not illicit inflammation.
- coral also possesses a superb porous structure for tissue integration and long term attachment with a high pore volume and trabeculated pore network.
- the high surface energy of coral enables strong adhesion of synthetic polymers. An extensive porosity enables the inter-penetration of pre-polymer and an optimal surface for permanent fusion (**Chapter 7 Section 7.3.3**)
- there is an enormous diversity of coral skeletons from which to choose a structure for a specific application.

Coral skeletons are available commercially, for use as bone void fillers. There are two distinct types: Pro-Osteon[®] and Biocoral[®]. The following section presents the advantages of each type, in relation to the features (pore sizes, interconnectedness etc.) required in this study.

6.4 Processed Coral Skeletons and Trabeculated Cow Bone Ceramics

Compared with *Porifera* skeletons and Echinoderm (sea urchin) spines, coral skeletons, and even bone possess a structure that better matches alveolar bone in the arrangement and dimensions of pores and channels. Coral skeletons are, in addition of the same mineral composition and are more readily obtainable. Before coral can be safely implanted into humans all organic material needs to be removed. A conscious decision was made to employ coral skeletons derived from industry, to reduce the amount of time and effort involved in collection, cutting and processing.

Naturally derived coral skeletons are processed commercially by Inoteb (B.P 26-56920 Saint Gonnery, France), who market their product as Biocoral[®] and Interpore (California, USA) who market their product as Pro-Osten[®]. Both types of coral skeleton, are (a) sterilized with gamma radiation to reduce infection and (b) have organic components removed to prevent rejection. Both coral derivatives possess the desired physical characteristics (macrostructure and a microstructure) with pore sizes between 150 and 250 μ m, and a mineral composition similar to the dental plate analogue (Chapter 3). In the next two sections the coral derivatives, manufactured by Interpore (Pro-Osteon[®]) and Inoteb (Biocoral[®]) are described, to highlight their bone-like features and hence, their suitability as an OOKP analogue. (according to the criteria set out in scope and objectives in chapter 2).

6.4.1 Pro-Osteon[®]

Pro-Osteon[®] is derived from reef dwelling coral skeletons. It is chemically transformed from a calcium carbonate crystalline form into hydroxyapatite by hydrothermal processing (described in Appendix 1). The crystals of hydroxyapatite are more robust and are resorbed at a considerably slower rate than calcium carbonate (e.g. Biocoral[®]). On this basis alone Interpore, is therefore the preferred material for an artificial cornea which must remain intact throughout its lifetime (Over ten years if the OOKP model can be reproduced accurately).¹¹⁵

Pro-Osteon[®] is used for the same purposes as its rival and counterpart, Biocoral[®]. Porosity is given as one of the 'key' merits of a temporary tissue replacement. Growth into the porosity reduces encapsulation. The parameters of porosity directly influence the form that the tissue takes and the rate of inward growth. Pore sizes must range from 15 μ m to allow fibrovascular inward growth and 150 μ m to facilitate osteoid development.¹¹⁶ On average, coral consists of a network of pores ranging in diameter between 10-80 μ m.

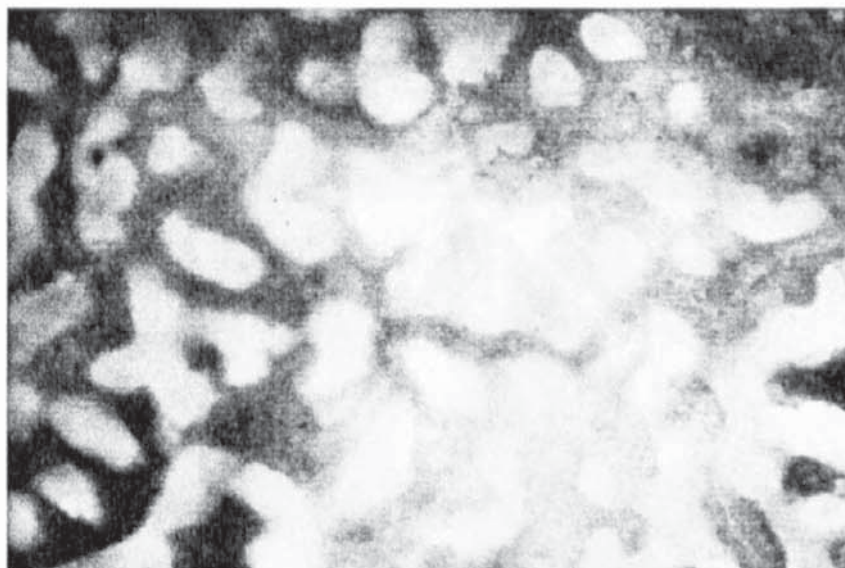
6.4.2 Biocoral[®]

Biocoral[®] is a thermally treated derivative of a species of *Porites* coral skeleton, with the zoological name *Porites porites*, Link 1807. It is a highly biocompatible⁺ biological material and functions as a resorbable bone graft substitute owing to the many chemical, mineral (crystallographic regularity) and morphological similarities with natural bone.¹¹⁷ *In vivo*, Biocoral[®] as any type of thermally treated coral skeleton, initially induces a transient inflammatory reaction, perhaps caused by friction between new developing tissue and the implant. Importantly, there is no acute chronic inflammatory reaction and infectious reaction present, particularly with neutrophils. Neither is there fibrous encapsulation¹¹⁷ As yet, an adequate host tolerance is only guaranteed if the site of implantation is relatively free from:-

- (a) infection,
- (b) necrosis and
- (c) malignant tumours.

These complications can be alleviated by competent, sterile surgical technique.

Photograph 6.32 *Thin Transverse Section through a Piece of Biocoral[®], Showing an Interconnected Void Structure. (x18 magnification)(Scale 1cm=100 μ m)*



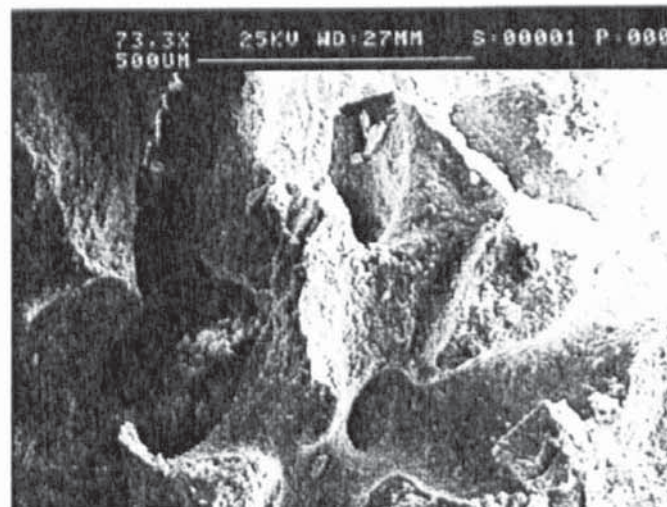
⁺Biocompatibility is "the exploitation by materials of the proteins and cells of the body to meet a specific performance goal"

So, like Interpore's Pro-Osteon[®], Biocoral[®] does not cause adverse biological reactions when implanted. Similarly, Biocoral[®] comprises an interconnected network of pores (**Photograph 6.32**). The pores fall into an optimal range of sizes that allow for the penetration and rapid inward growth of structural proteins such as elastin and collagen matrices (the foundation for the construction of a collagen framework) and a well-formed vasculature, essential to wound healing.

Table 6.21 *Physical Characteristics of Biocoral.[®] Physico-mechanical features of Biocoral are virtually identical to other coral species collected. (see Table 6.19)⁸⁹*

Property	BIOCORAL
Contact	Open
Ze/ Zf	06/04
Cell shape	Oval + circular
Symmetry	Radial
Fraction of material at edges	0.5
L1/ L2	3
S.D Ratio (Span/ depth)	1.3
Density	2.78 g/cm

Photograph 6.33 *SEM Thermal Image of a Fragment of Biocoral[®] Showing the Large Struts between Channels (giving a high fraction of material at the edges)*



Below is a list of the exceptional attributes, Biocoral[®] may offer for a Keratoprosthesis support frame. They are as follows:-

- excellent mechanical properties at 50% porosity
- defect-free
- ease of cutting and shaping
- selection of optimised pore configuration
- transient inflammation
- no fibrous encapsulation
- extensive in vivo experimentation
- small fraction of intracrystalline proteins and amino acids
- very varied pore and mechanical characteristics

While there are very few differences between Pro-osteon[®] and Biocoral[®] in terms of their strong credentials as an alveolar bone substitute, Biocoral[®] was selected for two reasons. Firstly, Biocoral[®] was available in a shape that was suitable for cutting and shaping on a lathe and secondly, the pore sizes were, on average at the lower limit of the desired range. The table below compares the physical features of Pro-Osteon[®] and Biocoral[®] together with a material derived from cow bone. Cow bone is derived from the highly spongy areas of the long bone, where pore sizes are very large (1500 μ m) and so was rejected, as a alveolar bone substitute which, possesses a variation in much smaller pore sizes (below 500 μ m).

Table 6.22 Selected Physical Properties for Commercially Available Bone Replacements

Name	BIOCORAL <i>Inoteb</i>	ENDO BON <i>Merck</i>	PRO_ OSTEON <i>Interpore</i>
Description	Derived from natural corals consisting of metastable crystalline calcium carbonate	Hydroxyapatite ceramic derived from animal bone	Hydroxyapatite porous ceramic derived from corals that have been hydrothermally processed
Pore Diameters	100–200 μ	100–1500 μ	190–600 μ
Porosity	20-50%	30-80%	50-75%
Density	2.78- 1.35g/cm	0.4-1.3g/cm	0.75-1.1g/cm
Youngs Modulus	8 GPa	7GPa	10 GPa

Where A.Source; B.Pore sizes; C.Density; D.Youngs modulus (E)

The above table compares the three porous biological ceramics commercially developed for bone replacement surgery. Biocoral[®] and Pro-Osteon[®] are both derived from scleractinian corals. Endobon[®] is the exception since it is derived from the spongy bone of cows and possesses a wholly dis-similar pore architecture to Pro-Osteon[®] and Biocoral[®]. There are some differences between the two coral derivatives. The primary difference is density. To reduce the load exerted on the cornea the density should be as low as possible. So Pro-Osteon[®] maybe a slightly better candidate. Pro-Osteon[®] possesses a wider variation in pore sizes than Biocoral[®] (Interpore produces two variants, one with an average pore size of 200 μ m and a second with average pore size of 500 μ m). Biocoral[®] is produced in a 150 μ m (average pore size) and 200 μ m form. Consequently, Porosities differ. In all three the stiffness is virtually identical with Endobon[®], possessing a slightly smaller value owing to the larger values of porosity. *Biocoral[®]*¹¹⁷; *Pro-Osteon[®]*¹¹⁵; *Endobon[®]*¹¹⁸

6.5 Summary and Conclusion

The focus of the research was to make use of biomimetics, all be it at a superficial level. Biomimetics is an infant discipline devoted to transferring properties of natural materials and structures into modified synthetic variants. It first involved scrutinising biological artefacts with properties required for an implant with very specific demands and then finding simple methods for mimicking them.¹⁰⁵ These properties and biological demands have been clearly identified (Section 2.8, Chapter 2). Methods for copying natural artefacts involve a small number of novel techniques; sol-gel derived structures,⁸⁵ template induced mineralisation, in-solution mineralisation⁸¹ and replamineform processing.⁸⁶

A major difficulty arose in identifying biological objects with the right set of properties, such as stiffness, toughness, porosity and density (Appendix A1.1). Another major difficulty was determining the exact biological nature of the potential implant site and whether it is compatible with the various biological structures. Fortunately, as we discovered in this chapter, there are many objects found in nature with a porous architecture suited to tissue (cells, blood vessels and extracellular matrix) infiltration and support, i.e implantation ranging from protective and ambulatory spines of echinoids (sea urchins; *Heterocentrotus trigonarius*, *Nardoa sp.* or *Acanthaster sp.*¹⁰⁷) to the hard skeletons of Scleractinian corals (*Goniopora*, *Porites sp.*etc.¹¹³) and Lithistid sponge skeletons (*Verongia sp.*¹¹⁰). Additionally, within each group of organism, there are many different variations in construction associated with the individual organisms own peculiar lifestyle, which means there is a large number of designs to choose from.

Natural porous solids were selected according to the following: pore sizes (between 90-150µm), pore interconnectedness (Vronoi foam, but graded abruptly), material type (preferably carbonate inorganic), availability (easily obtained and widely distributed). Sponges and Corals are Vronoi foams with a large spread of pore sizes and degrees of interconnectedness, but all essentially three dimensional.¹¹³ Natural sponges are very abundant and some species are farmed. Sponges are generally flexible and tough. They

also possess anti-inflammatory and anti-bacterial properties that may tame infection events if they were implanted into the body.¹¹³ Removal of organic components from the inorganic silica framework, is difficult and time consuming, and may make them unsuitable for human implantation.

Corals are much closer to the structure and mineral composition of most types of bone.¹⁰⁵ Coral is highly biologically tolerant and possesses a structure with two pore size ranges-one compatible with supporting blood vessels and another compatible with tissue infiltration and reconstruction.¹¹⁵ Bone-like corals are easily obtained because they are abundant. The replamineform process would enable a specific coral pore structure to be replicated into a negative metal (vitallium) cast. This established technique would avoid the removal of coral from its natural habitat.

Pre-processed coral is produced by two companies, Interpore and Inoteb.^{114,115} Pro-Osteon[®] and Biocoral[®], respectively are derived from the *Porites* group of hard corals, but are different species. They differ slightly in the amount of mineral, crystallinity, composition and mechanical properties. Pro-Osteon[®] is harder and less resorbable. Biocoral[®] was used in this study, owing to the lower cost and the suitable shape and size of pieces commercially available.

Natural sponges (*Porifera*) and corals possess a suitable structure for cell growth, supported and have been safely implanted into humans. Natural sponges however, were difficult to obtain in the required quantities and with the correct qualities. Attention thus focused upon the highly credited use of coral skeletons.

Table 6.23 *Achievements and Problems with the Selection of Suitable Natural Porous Solids and the Replamineform Process*

Achievements	Problems
Identified large numbers of likely candidate skeletal structures	Finding readily obtainable skeleton
Selected three highly suitable types of natural skeletal structure: Hard Coral, Sponges and Echinoderm spines	
Made reasonably good polymer (pMMA) replicates	Polymer replicates were not of a good enough quality using simple methods
Selected commercially available coral used for bone replacement surgery	

CHAPTER 7 RESULTS:
Fabrication of a Prototype Artificial Cornea
from Coral and pMMA

CHAPTER 7 RESULTS:

Fabrication of a Prototype Artificial Cornea from Coral and pMMA

“Full fadom five thy father lies;

Of his bones are coral made;

Those are pearls that were his eyes:

Nothing of him that doth fade,

Both doth suffer a sea-change into something rich and strange.”

The Tempest (Act I, Sc.II)

7.1 Introduction

In previous chapters (4-6) were results detailing the selection and fabrication of materials for the support frame of an artificial cornea, enabling fixation of the optical window. Hydroxyapatite was selected over and above polymer, bioglasses and oxide ceramics because of its extraordinary biological properties. Assorted methods were analysed, for creating complex pore architectures with hydroxyapatite particles and with ceramers-composites of ceramic and polymer. Those methods that were carried out in full (although not extensively) delivered promising results, but were unworkable in the time allowed and with the resources available (Table 7.1). An intractable problem was constructing a sufficiently well built pore structure. Techniques in deposition of mineral onto polymer surfaces are worthy of further investigation, because of their potential to build a complex biological ceramic structure with precise control onto a synthetic polymer. In the end a ‘bone-like’ structure, suitable for this study, was exploited; coral.

Table 7.1 *Fabrication Methods Carried out in this Study*

Methods carried out
Powder compaction and sintering Chapter 4
Mixing and blending Chapter 5
Solution-Gelation synthesis Chapter 5
Langmuir template induced mineralisation Chapter 5
In-Solution mineralisation Chapter 5

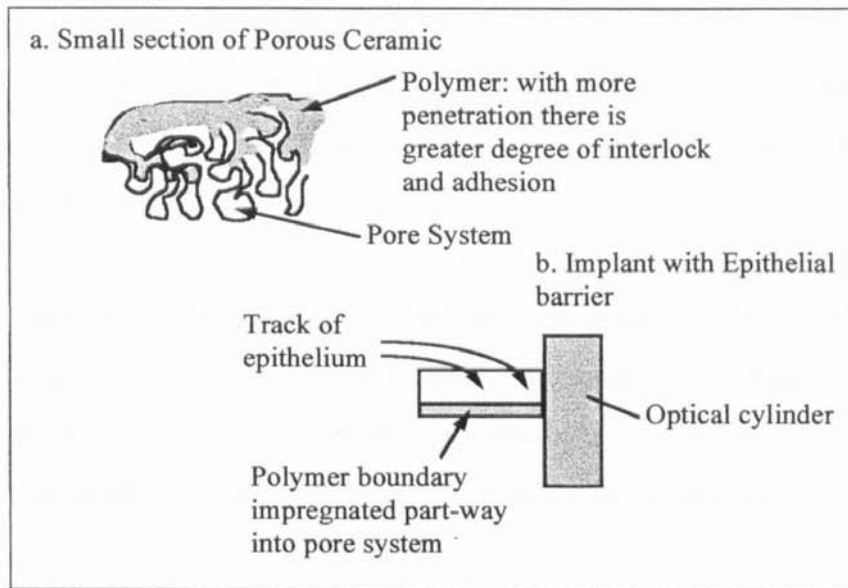
This Chapter begins with surface characterisation of a selection of fabricated materials to assess the degree of structuring (surface topography and roughness) for tissue interlock. The remainder of the chapter describes the development of two coral and perspex prototype keratoprostheses and how they will function when implanted.

7.2 Surface Characterisation:

7.2.1 Fractal Analysis

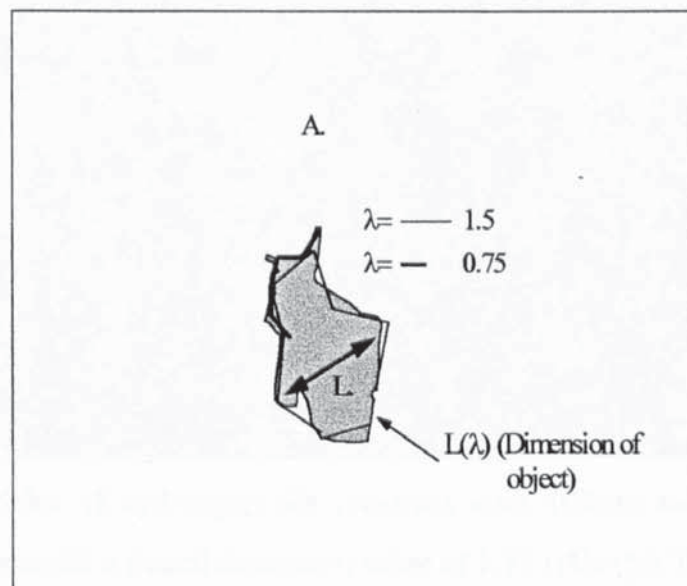
Most porous solids possess structural self-similarity at many different scales, particularly solids built up from crystals. Now, by creating a yardstick with fractional values greater than the topological dimension of the object being measured fractal dimensions can be calculated at length scales to the size of individual molecules. For the purposes of this study the fractal magnitude may increase the degree of bonding between a biological ceramic and polymer. More specifically there was a desire to maximise the coverage of polymer over the internal surfaces of a porous ceramic to create the best possible attachment, and also to provide a solid barrier to stop epithelial downward growth.

Figure 7.1 Diagrams Illustrating the Reasons for Maximising Polymer Coverage into Pore System



There is a definite scaling relationship between cross sectional distance across the object and the length of the measuring rule. This is best illustrated by plotting the two values as logarithms (Richardson's Law). Such a graph may give an empirical measure for the perimeter of an object (as in b; **Figure 7.1**) with fractal qualities.⁹⁰ (**Graph 7.1**)

Figure 7.11 Fractal Concepts Discussed in this Section

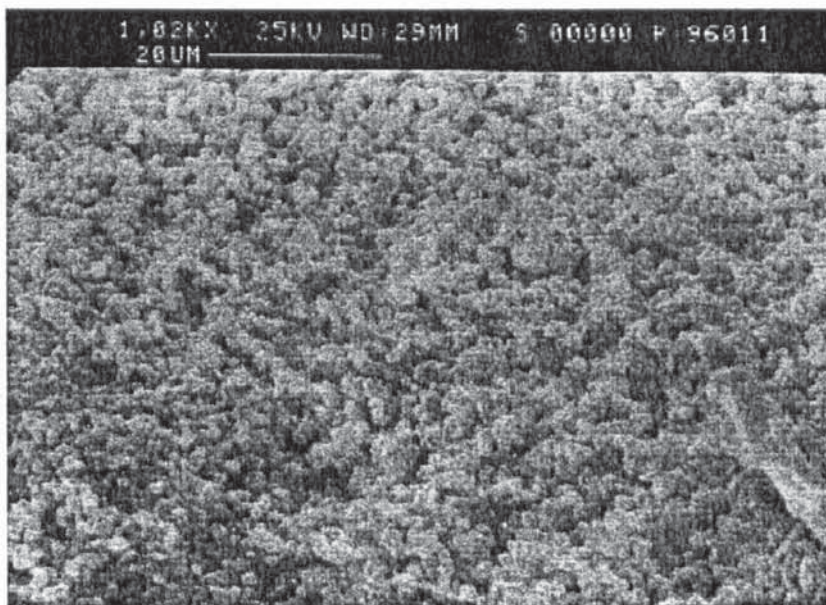


Referring to Figure 7.11, a quantity can be assigned to roughness of a surface by measuring the perimeter with dividers (λ) a number of times at serially decreasing

length scales ($L\lambda$) and relating this to the maximum width (L^1) of the object. As the size of the measuring stick approaches zero the length or area approaches infinity. Fractal dimensions occur when the yardstick is raised to a certain power (α) for the measure of the object to be finite. This yields the fractal dimension. Fractals were used as a measure for the degree of surface roughness of ceramics made in this study or obtained elsewhere. Fractal dimensions have a bearing on two activities in implant design-(a) the degree of monomer adsorption and polymer contact; (b) the likely degree of protein adsorption. Fractal surfaces increase the available surface area for interpenetration of mobile substrates such as monomer solutions. Cell adhesion mediated by the pattern of protein deposition is also influenced by fractal micro-morphologies. Fractal dimensions of three materials were calculated, plotted and then compared:-

- sintered particles of hydroxyapatite (Large mixed with whiskers) possessed a fractal dimension value of 2.36. (**Graph 7.1(c)**)

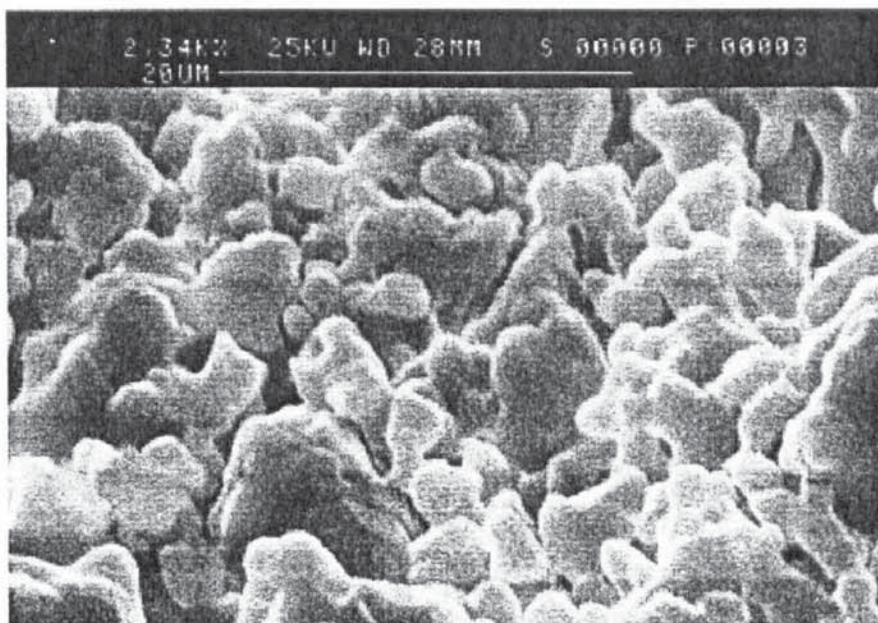
Photograph 7.1 *Sintered Particles of Hydroxyapatite (Large particles mixed with whiskers)*



- sintered particles of hydroxyapatite (medium size: 100 μ m and 36 μ m (order is unimportant)) possessed a fractal dimension value of 1.75 ((**Graph 7.1(b)**))

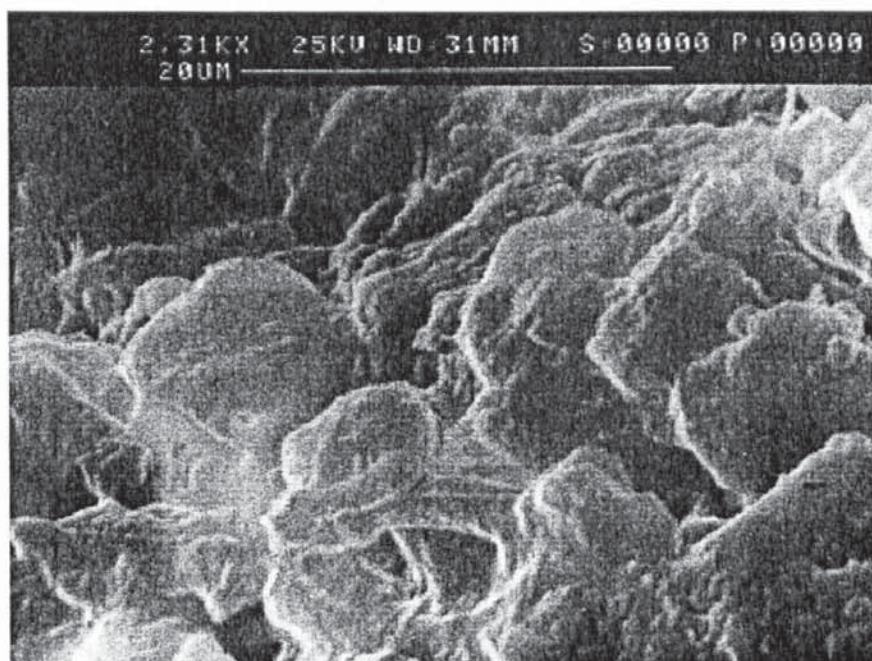
Photograph 7.11 *Thermal SEM Image of Sintered Particles of Hydroxyapatite (a*

mixture of 100 μ m and 36 μ m particles)

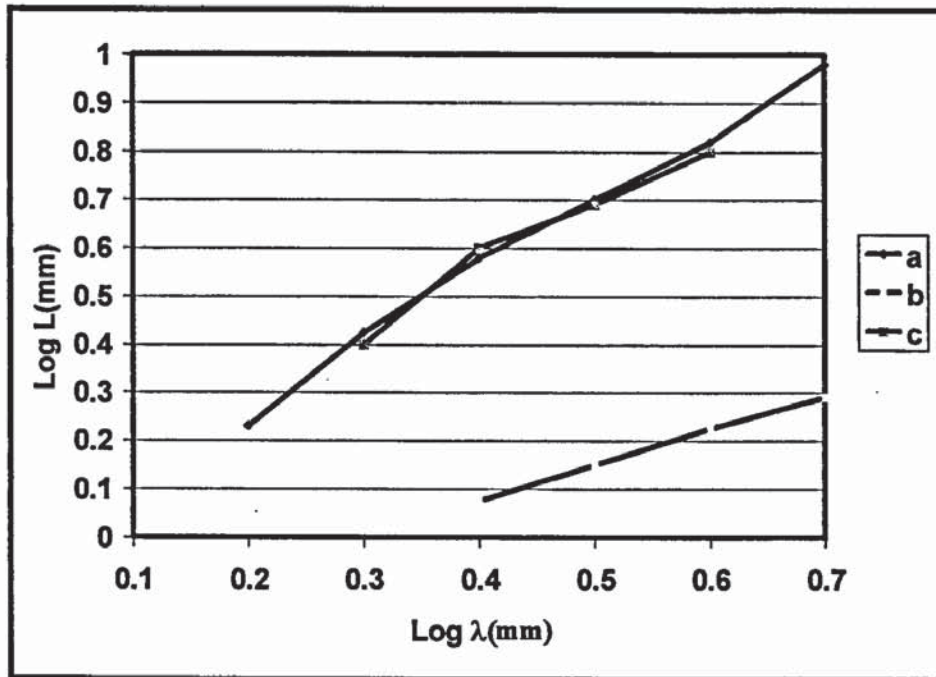


- Biocoral[®] crystals (value of fractal dimension = 1.1)(Graph 7.1(c))

Photograph 7.12 *Thermal SEM Image of Biocoral[®] Crystals*



Graph 7.1 A Richardson Plot Comparing Three Kinds of Biological Ceramic Considered as a Tissue Bonding Support Frame



Key: λ =length of dividers; L=Ferrets diameter

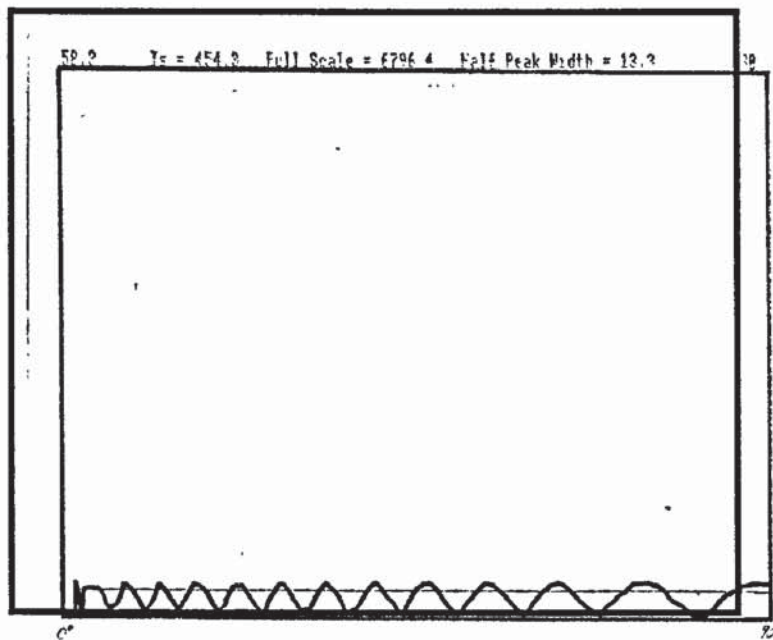
Biocoral[®] and sintered particles (a 50:50 mix, by mass of 500 μ m hydroxyapatite spheres and hydroxyapatite whiskers) were calculated as having exactly the same fractal dimension of 2.36. This was unexpected because coral is constructed from well formed crystals, whereas the powder particles are welded together by melting. This may be attributed to the presence of whiskers, since the material made from medium sized particles gave a much lower value of 1.75. Other sintered products possessed coalesced grains with relatively smooth surfaces and the fractal dimensions would therefore, approach a value of one, i.e non-fractal.

Under SEM both materials (Biocoral[®] and large ceramic grains melded with whiskers) displayed platy segments. In the compressed and sintered discs there was a significantly large proportion of tube-like and rounded particles at this level of magnification (approx 2,000x) In comparison, a fibroblast with a 'spiky' outline has a value for fractal dimensions of 1.06.

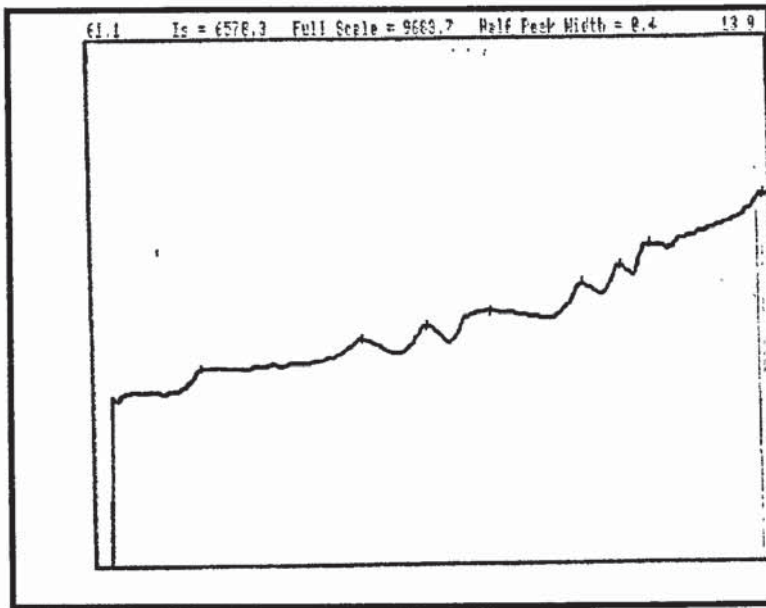
7.2.2 Goniophotometer Measurements of Surface Roughness

Goniophotometry was originally developed to measure albedo or the *glossiness* of biodegradable polymeric materials. Increasing degrees of degradation directly lead to increased surface roughness and this can be measured with a goniophotometer. Such a technique was a useful aid to see how the surface porosity or topography of fabricated ceramics compared with that of bone-like biological ceramics. The surface traces for corals were virtually identical, consisting of repeated mountain-like undulations with little variance in spread or shape. The graph below show the changes in light intensity as the photocell is moved in an arc around the sample.

Graph 7.2 *Goniophotometry: Trace of light Intensity for Porites Coral (x-axis=Reflectance intensity; y-axis=Angle of Reflectance, over a range from 0-180 degrees to the specimen)*

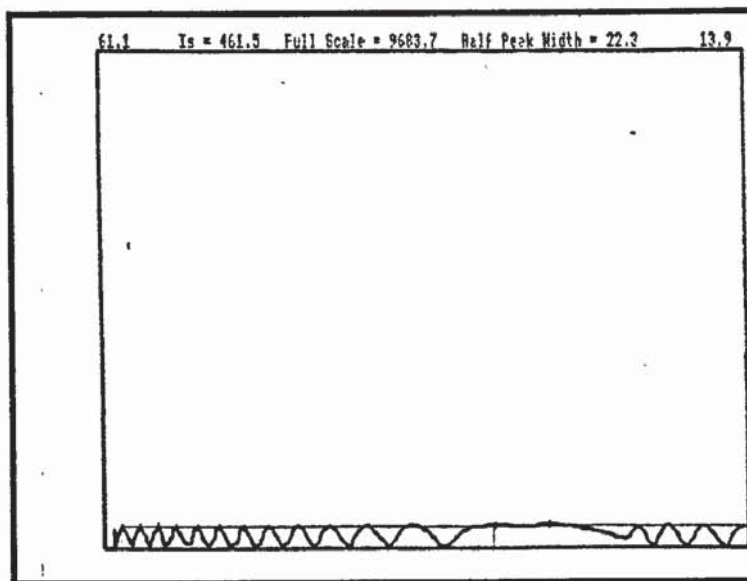


Graph 7.3 *Goniophotometry: Trace of Light Intensity for a Collagen Gel (x-axis=Reflectance intensity; y-axis=Angle of reflectance , over a range from 0-180 degrees to the specimen)*



Similar traces occurred across the surfaces of hydroxyapatite beads and ceramers loaded with sample A, for example.

Graph 7.4 *Goniophotometry: Trace of Light Intensity for Hydroxyapatite Beads (x-axis=Reflectance intensity; y-axis=Angle of reflectance, over a range from 0-180 degrees to the specimen)*



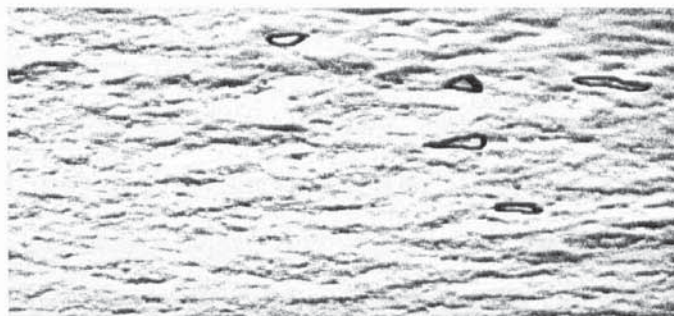
Strangely the surface of sample F induced an identical pattern of reflected (diffuse) light. Sample F was a sintered product from Jesse Shirley ceramics that possessed very few pores and a low level of observable roughness under SEM.

Table 7.1 *Surface Roughness Measurements of Ceramers, Corals and Compacted Ceramic Grain Mixtures Using a Goniophotometer*

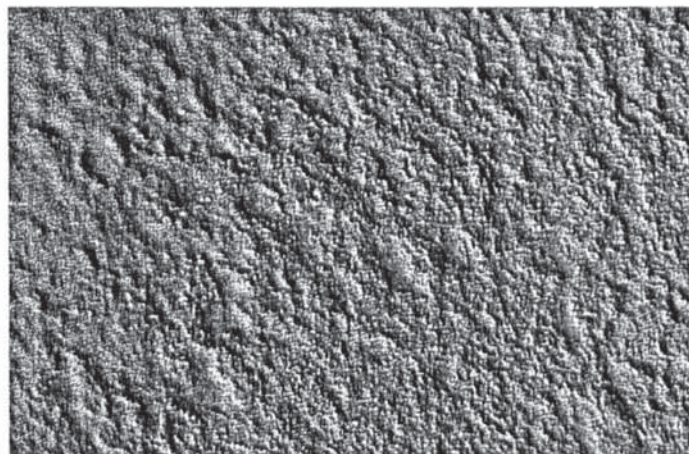
Biological Ceramic/ Ceramer	Polymer	Description of Trace
HA 36	pMMA	Small number of well dispersed peaks separated by an undulating plain
HA 100	pMMA	Small number of well dispersed peaks separated by an undulating plain
HA beads	pMMA	Very regular series of peaks and deep troughs
HA C	pMMA	Repeated series of jagged peaks
HA A	pMMA	Regular series of jagged peaks and troughs
Sample F		Very regular series of peaks and deep troughs
Corals		
Seriatopora		Very regular series of peaks and deep troughs, some flattening of peaks toward 90 degrees
Porites		Very regular series of peaks and deep troughs
Biocoral		Very regular series of peaks and deep troughs

All materials possessing a surface roughness would give rise to low light intensities at low angles of reflectance, between say $0-40^{\circ}$ compared with much higher values as the beam is at right angles to the surface, where light scattering should be at its minimum. Furthermore, the intensity will peak and trough in correspondence with significant depth changes to the surface. In future, this may be traced in finer detail using a thinner, more intense beam of light. It must be pointed out that such measurements are limited to a certain depth of indentation or cratering by the constraints imposed by the angle of the beam

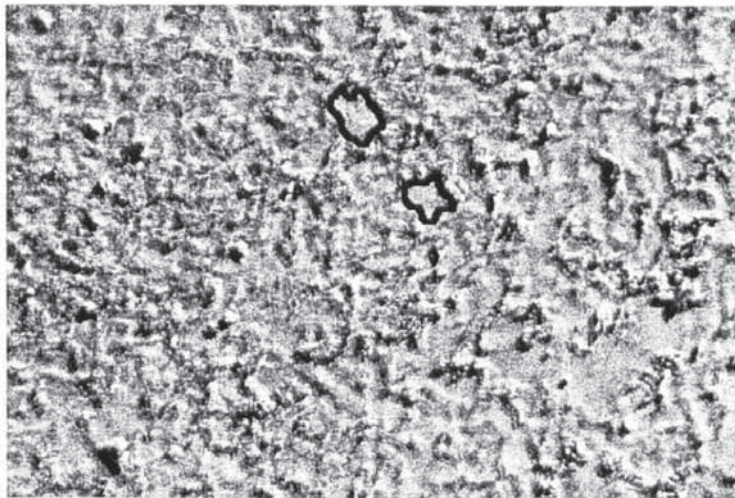
Photograph 7.13 *Computer Embossed (to depth of $15\mu\text{m}$ using Image-in-Color) Surface View of Ceramic Disc Made from Spherical Particles ($500\mu\text{m}$) Surface indentations in the ceramer are highlighted.*



Photograph 7.14 *Computer Embossed (to depth of $5\mu\text{m}$ using Image-in-Color software) Surface View of Ceramic Disc Made from Hydroxyapatite Particles ($100\mu\text{m}$ and a)*



Photograph 7.15 *Computer Embossed (to depth of 5 μ m, using Image-in-Color software) Surface View of Ceramic Disc Made from Hydroxyapatite Whiskers. Two indentations in the ceramer are highlighted.*



7.3 Fabrication of Keratoprotheses

7.3.1 Design Solutions For Common Causes of Implant Failure

The main causes of implant failure and rejection have been collated and tabulated by Barber et al. with suggestions for overcoming them successfully¹¹⁹. Causes can be either biological or mechanical. Additionally, a sterile surgical technique was an equally important factor in preventing failure. Up to this point, the imperative was to eliminate biological causes of prosthesis failure by using biologically tolerant structures favourable to wound healing and tissue support. Sources of biological failure include:-

- infections (e.g), enzymatic degradation
- poor vascularisation
- fibrous membrane deposition
- epithelial downward growth and prosthesis dislodgement.

Whereas, in this chapter the focus is upon minimising causes arising from the mechanical behaviour of the implant.

In theory, a coral and polymer hybrid would be able to minimise or prevent many biological causes of failure with varying levels of success (see **Table 8.14 & 8.15**). However, a firm guarantee can only result from implantation trials. A series of

experiments were undertaken to infiltrate coral with pMMA (polymer) so that it might be very firmly welded to a pMMA optical cylinder.

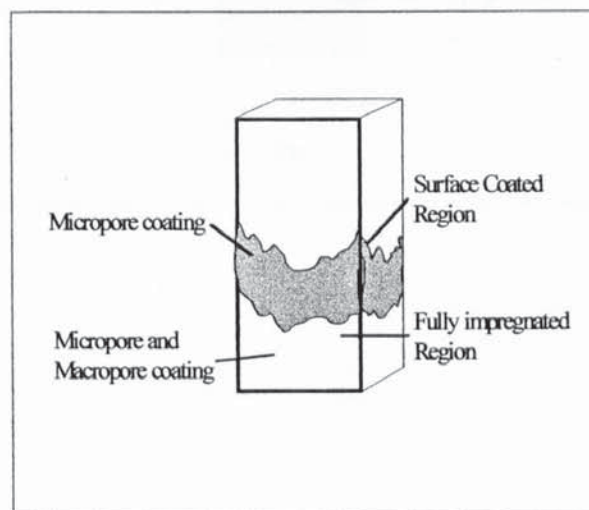
7.3.2 Stage 1:-Polymer Bonding to Coral

Overall polymer welding to coral was very satisfactory since coral possesses a significantly larger surface energy than methylmethacrylate (MMA). Inter-penetration of polymer into the coral was enhanced by combining the two substituents in a vacuum. Photographs 7.17 and 7.18 illustrate the superb effectiveness of polymer infiltration into corals with restricted and unrestricted porosities.

7.3.2.1 Incorporation of Polymer into Biological Ceramics

Polymer was incorporated into the network of voids by favourable capillary forces. Adhesion was thought to result from inter-diffusion into surface vacuities and between crystal plates and bonding to surfaces by physisorption, in which the fluid covers all the surface that is physically accessible (Van der Waals forces). Polymer was finally solidified at these locations either by heating or treatment with short wave irradiation in the ultraviolet region.

Figure 7.12 Typical Distribution of Polymer In a Small Block of Coral



Note:-Distribution pattern of monomer as it rises by capillarity into the block of coral. Characteristically there is a thin (1/3 of total height of the block) irregular layer of thickly coated coral below a large layer of thinly coated coral as the monomer is only able to rise by capillarity through micropores.

7.3.22 Thermal Cast polymerisation

A whole implant was constructed in a single stage using a novel mould assembly. It consisted of a hollowed out polytetrafluoroethylene (PTFE) cylinder. The apparatus was sealed with silastic and inserted into a polymer tube and left in a water bath for three days (See **Figure 7.13 and 7.14**). A ring of *Porites* coral was shaped to fit the upper surface of the hollow and glued to the upper surface of the mould prior to the addition of the monomer solution. Unfortunately due to shrinkage of the polymer during its formation and the large hydrostatic pressure caused by pressing down the plunger, the fracture prone coral 'ring' disintegrated. This result made it necessary to fabricate prototypes in two stages not one.

Figure 7.13 A PTFE Mould Assembly for Cast Polymerisation

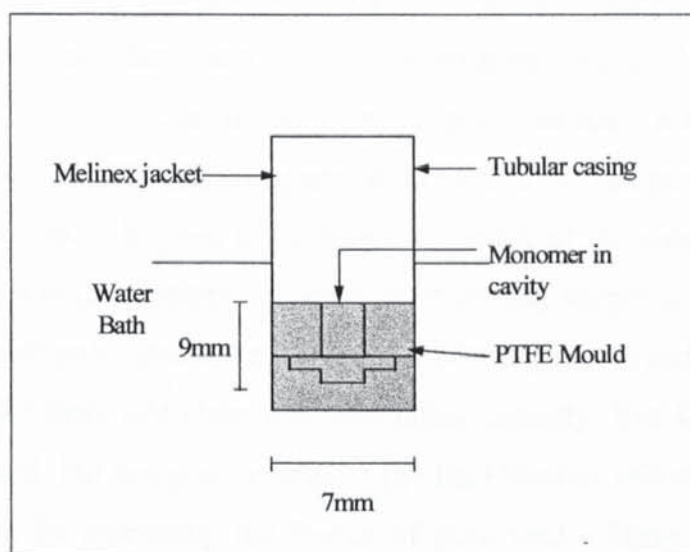
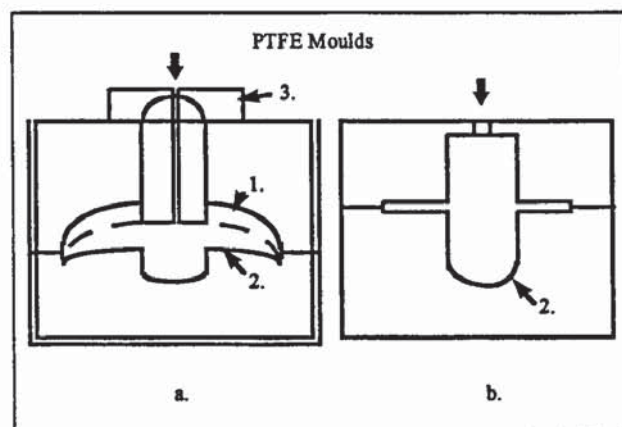


Figure 7.14 *Two Mould Assemblies Fabricated in this Study (a) with coral periphery (b) without coral*



7.3.23 Ultraviolet Radiation Assisted Polymerisation

Tests for polymerising MMA monomer in coral proved that ultraviolet radiation was very rapid, averaging thirty five minutes, for polymerisation (cast polymerisation takes up to three days), and that there was polymerisation within the void structure (**Photograph 7.17**) which coated the internal pore surfaces evenly, but only a maximum of 35% (+/- 6.7%) of pore space could be filled in this manner, perhaps due to polymer contraction or trapped pockets of air. Much of the polymer is taken into the micropores. It is in the macropores where poor infilling happens. It was also found that a more restricted pore system, i.e a less dense porosity (pores and channels per unit volume) and smaller pore size improved pore filling capacity (See **Graph 7.2**). This was inversely related, but not proportional to the final level of infiltration (See **Graph 7.19**). The reason for examining the degree of pore void infilling is that it roughly indicates overall adhesive strength between the two components, polymer and coral.

Table 7.11 Assessment Criteria for Strength of Bonding Between *Porites* and pMMA

Assessment Criteria	Section A	Section B	Section C
Area of Contact of Polymer as a % of Available Surface Area	61% (+/-4)	72% (+/-9)	65% (+/-16)
Contact Area per Pore Space	100%	100%	100%

The measurements in Table 7.11 are taken from the central region of the base (0-680 μ m) above which (ii) decreases considerably as (i) remains the same.

Several requirements for fabricating a polymer and coral hybrid were tested to identify the one that optimised polymer impregnation into the pore system. Two protocols were implemented: immersion into monomer followed by polymerisation and immersion with either wax impregnation or no wax impregnation, vacuum assistance or no vacuum assistance, followed by thermal polymerisation or, ultraviolet polymerisation. Wax impregnation into macropores effectively stopped infilling of macropores with monomer but did not completely stop the upward movement of monomer into the system of micropores. Vacuum assistance improved the uniformity of wax deposition. Partial polymerisation of the immersion fluid prevented capillarity

7.3.3 Measurement and Manipulation of Polymer Uptake into Coral

A means of precisely controlling the rate of polymer uptake and pore infilling is important to optimise bond strength and manipulate the distribution of strain energy in the final prototype by optimising the span to depth ratio of each component (which can be thought of as two juxtaposed beams) and minimising second moment of area. Coral possesses a high surface energy and an extensive directional pore structure, so that when coral is immersed in monomer it is rapidly imbibed and sucked along the interconnected channels.

Table 7.12 Distances from Base, that MMA Monomer is Carried to by Capillary Action in a Fully Open Cell Coral, *Goniopora* (Refer to Figure 7.15) After 5 Minutes of Immersion.

5 minutes (45x11.5)	Fully Impregnated Region#	Surface Coated Region+
	6mm	20mm
	6mm	21mm
	11mm	13mm
	7mm	15mm

Table 7.13 Distances from Base, that MMA Monomer is Carried to by Capillary Action in a Fully Open Cell Coral, *Goniopora* (Refer to Figure 7.15) After 90 Minutes Immersion

90 minutes (33x9)	Fully Impregnated Region #	Surface Coated Region+
	6mm	20mm
	6mm	21mm
	11mm	13mm
	7mm	15mm

#, + Refer to Figure 7.15

There were further complications. Monomer solution rose more rapidly within the system of micropores rather than spreading and filling macropores (See Tables 7.13 and 7.14). Open ended tubes with a comparatively smaller diameter cause a larger rise in fluid than larger capillary tubes. In contrast, polymerisation was more straightforward. Ultraviolet light induced cross-linking was found to be very effective especially deep inside the coral block. However, heat generated by the ultraviolet lamp could have assisted polymerisation. Coral has a high albedo (reflects more light radiation than it does absorb it) to visible light but may, in addition have a high albedo to ultraviolet light and this could explain why cross-linking occurred inside a thick block of coral.

The mode of uptake was described by capillary action and surface tension. In *Goniopora* corals capillarity is swift impregnating a third of the pore system in the first

five minutes from immersion into a solution of monomer. This rate can be slowed significantly by increasing viscosity so that the monomer solution becomes more alike to a syrup. Viscosity is crudely manipulated by illuminating the MMA monomer solution for different periods of time. A longer illumination with ultraviolet light increases viscosity.

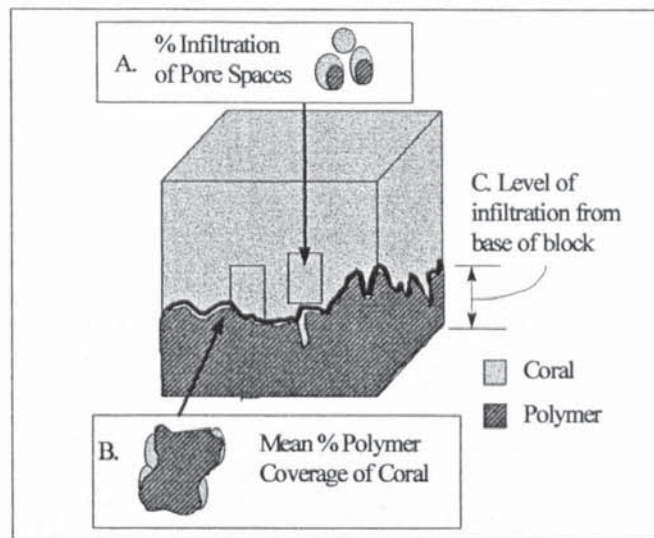
When this is done the level of impregnation is determined by the height of the syrup into which the porous body is immersed, but a high viscosity increases the work required for pore infilling and so requires vacuum assistance or ultrasonic agitation. The required skill was to optimise a number of conflicting (and somewhat independent) demands simultaneously:

- viscosity
- pore infilling
- capillary action
- uniform and complete polymerisation.

A mixture of partial polymerisation, vacuum assistance and ultraviolet radiation assisted free radical polymerisation were combined in a novel way. The effectiveness of polymer integration was measured by the extent of pore infilling using two calculations:

- percentage infiltration of individual pores, taken as a mean.
- percentage of polymer coverage, at the base, taken as a mean.

Figure 7.15 *Criteria to Measure the Degree of Polymer Integration and Adhesion to Coral*



There was a moderate variation in these values between samples of coral (standard errors of 10-8%). Three quarters of the pore space were infilled, but the overall polymer coverage (including pores and struts) was patchy with 46% of available surface area of coral covered with polymer.

Table 7.14 *Percentage Coverage and Infiltration of Polymer into Open Cell Coral Skeletons*

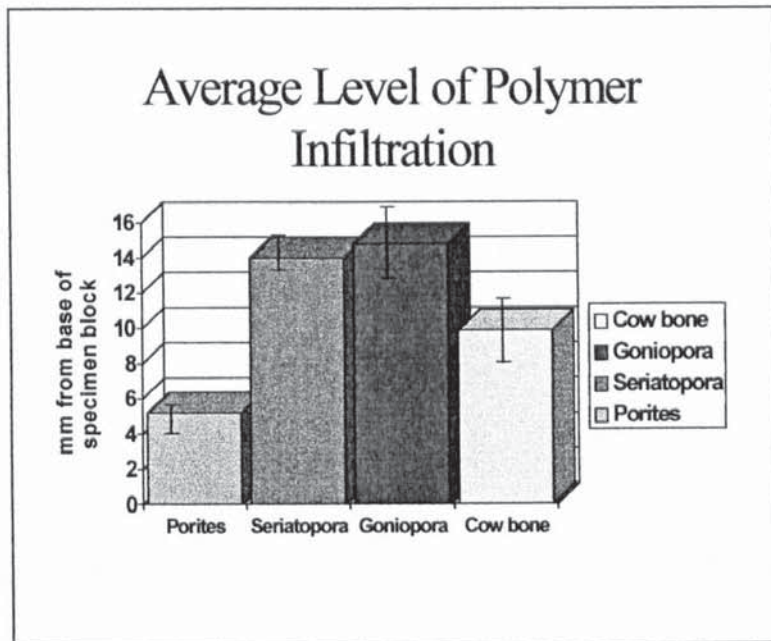
% Infiltration of Pore Space	% Polymer Coverage per Unit Area of Coral
65-85%	38-54%

Referring to Graph 7.19-There was found to be a negative correspondence between polymer infiltration and open-ness of porosity. The level of polymer infiltration after immersion was larger in the more open celled varieties of coral (pyrolysed and non-pyrolysed) and cow bone (Endobon®). The results demonstrate:-

- the ease at which fluids can enter the pore spaces and

- the variability in fluid mobility between coral species.

Graph 7.5 *Extent of Polymer Infiltration into Open Celled Corals and Cow bone (with standard error bars) (Refer to Figure 7.15 (C) for explanation of the level of infiltration)*

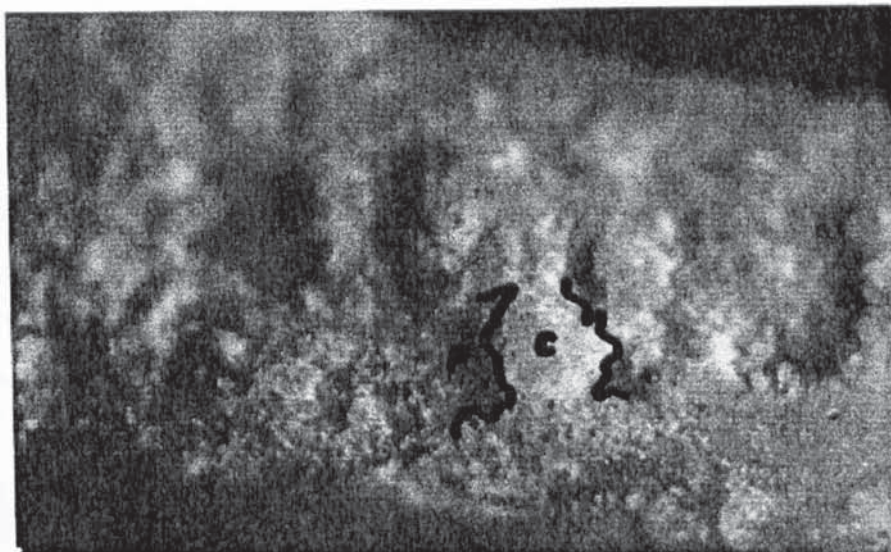


Referring to Graph 7.2 While infiltration is more rapid in *Seriatopora* and *Goniopora* the actual quantity of polymer that fills each pore completely, is significantly smaller than in *Porites* because the pore system is more restrictive.

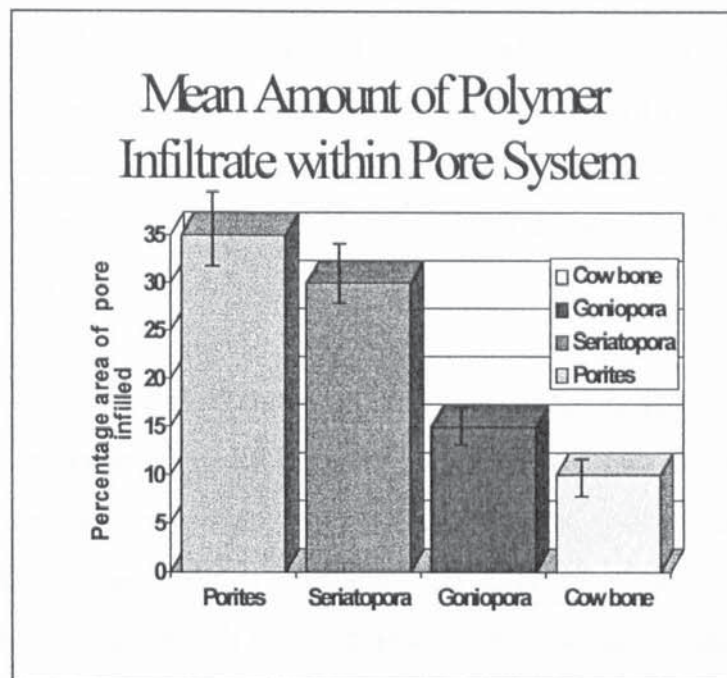
Photograph 7.16 *Porites* Coral Coated with pMMA in a Vacuum. Coral is dyed with Alcian blue and polymer is dyed with congo red) The impregnated layer is very thin due to massive shrinkage during polymerisation.



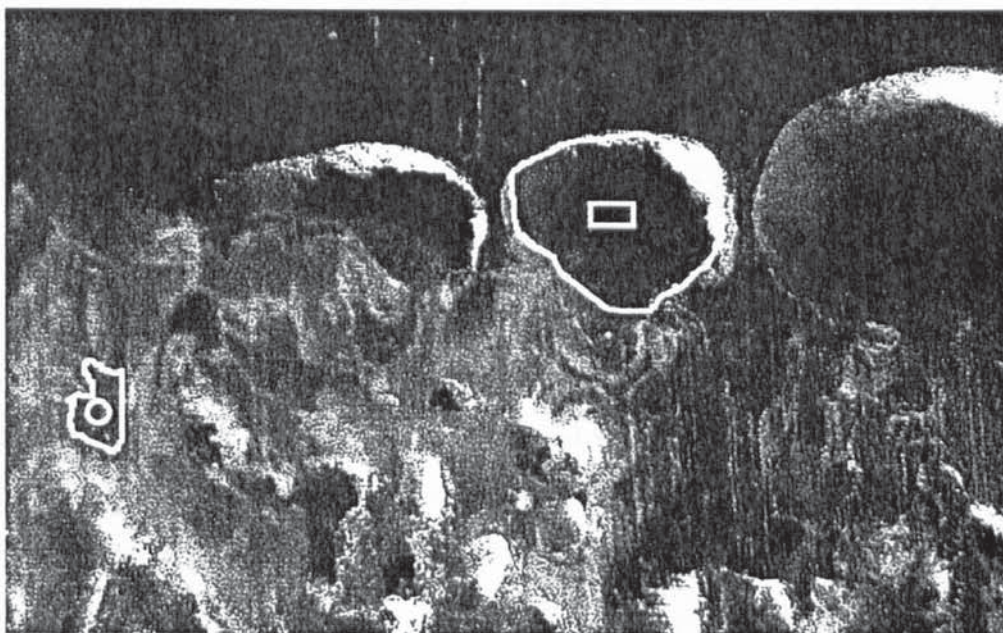
Photograph 7.18 Fully Impregnated Region of *Porites* Coral in a Vacuum (c=region of coral; p=pore space)



Graph 7.6 Graphical Representation of the Amount of Polymer Infiltrated into Pores (with error bars) (Measured as in **Figure 7.15 (B)**)



Photograph 7.18 Cross-section Through the Interface Between pMMA Polymer and Base of *Goniopora* Coral. The Photograph shows contrasting areas of pore in-filling (white circle) and air spaces (white rectangle). The latter is caused by release of trapped air from the monomer mixture.



6.3.4 Measurement of Viscosity

The optimum time required for ultraviolet irradiation was determined exactly when monomer would (a) rise gradually throughout the coral block and (b) cover a maximum area of the internal surfaces of the pore system. It was found that the viscosity slowly increased with each five minute increment of irradiation time and reached a peak at twenty minutes. . At this point, monomer would barely rise by capillary action and would collect in the larger pores. This arose because of an increased internal cohesion and a reduction in the contact angle of monomer with the vessel walls which, reduced the upward force on the liquid.

The flow of monomer was restricted over the pore surfaces, yet it was sufficient to infiltrate the whole system of pores if a block was dropped into it. Even so, vacuum assistance was needed to ensure extensive infiltration. Observations under the microscope confirmed the extent of infiltration and surface coverage. A polymer syrup restricted capillary action through the micropores and so increased the polymer loaded into the macropores. Better control of loading characteristics could be sought by simultaneous irradiation and vacuum assisted impregnation of a monomer syrup.

Table 7.15 *Relation between Irradiation Time and Viscosity Caused by Increased Cross-Linking Density*

Irradiation time minutes	Time to travel through capillary tube	Viscosity
5 minutes	1.17	0.02N/cm
15 minutes	7.1	0.11N/cm
20 minutes	16.32	0.27N/cm
25 minutes	***	too viscous!

In which, the the relative viscosity of MMA monomer is $\rho_1 t_1 / \rho_2 t_2 = 0.015N/cm^2$

In summary, coral and polymer integration and adhesion are consistently strong as determined by the degree of integration and low stress fracturing, assessed mainly by microscope examination for *Porites* and scanning electron microscope observations of *Goniopora* coral. *Porites* was found to possess the best polymer loading characteristics because the depth of infiltration was shallower, but more complete in its

coverage than other porous biological ceramics tested e.g. cow bone, *Goniopora* and *Seriatopora*. Biocoral® is derived from a yet unspecified *Porites* coral with, on average a higher ceramic volume fraction (density=1.1gcm³) and a smaller density of pores and channels.(strut thickness of biocoral = 45µm; Strut thickness of Porites = 55µm)

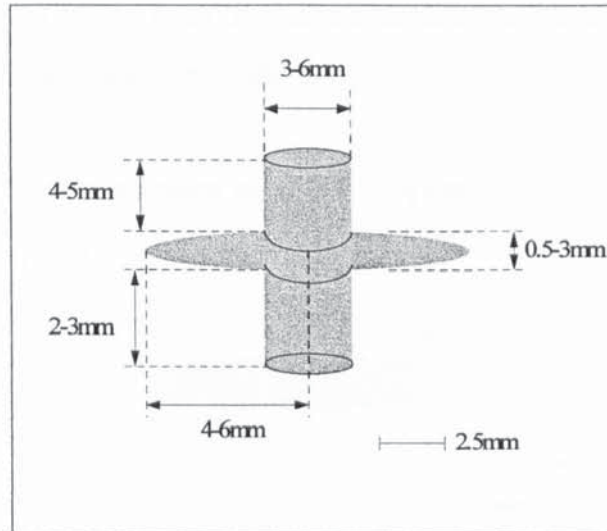
7.4 Stage 2:-Construction of Keratoprotheses Prototypes

In the next and final stage of development attention focused upon combining the dental plate analogue with the optical cylinder.

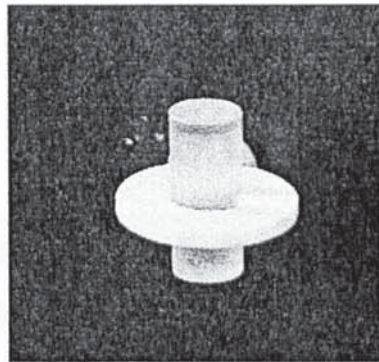
7.4.1 Introduction

The first prototype was made according to the design specifications as shown in Figure 7.16. These are the standard dimensions for a typical core and skirt artificial cornea.¹⁴ The first prototype consisted of an optical rod, 6.5mm long, 4mm in diameter with a coral washer, 0.5mm thick and 10mm in diameter bonded to the optical rod with acrylate glue. The second prototype included a basal disc, representing the dentine plate in the OOKP. The optical cylinder was 10mm long. The diameter of the base measured 10 mm, and the coral ring was 3mm thick, while the acrylate glue bonding the coral and base together was 1mm thick. When it came to the third prototype the base measured 11mm across, with a layer of acrylate glue, 1.5mm thick and a coral ring, 4mm in thickness. For this prototype a 4mm hole was hand drilled through the centre of the coral ring, using a tungsten drill. Very careful drilling ensured that there was no chipping around the edge of the hole, which was a problem in the initial stages of cutting and shaping. It was important that all interfaces were tightly apposed to each other.

Figure 7.16 *Variation in Dimensions of a Typical Keratoprosthesis¹⁴*



Photograph 7.19 *First Prototype Constructed from a Simple Optical Rod of pMMA and a Hydroxyapatite 'Washer' made by, Jesse Shirley Advanced Ceramics*

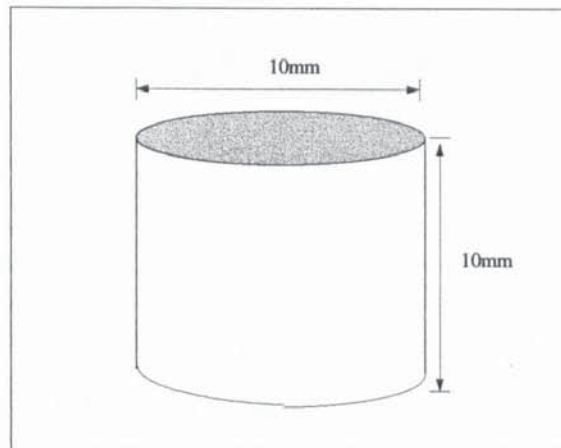


7.4.2 Assembly of Component Polymer and Coral Skeleton

A design blueprint was drawn-up for the construction of a prototype coral and perspex keratoprosthesis. Optical grade tinted pMMA was obtained from Vista Optics and cut using a contact lens lathe designed for convex curves using 'standard' design diamond tools. Later, these tools were found to be unsuitable for producing a right angle cut necessary to produce the shape required in the optical cylinder. Consequently, specific tooling was then fitted to the machine to cut the required diameters and leaving the flange at the correct position on the device. Problems were availability of tooling for cutting and obtaining jigs for holding the piece accurately in the lathe to set it against the cutting tool.

The order assembly can be broken down into four discrete stages, designated A,B,C, and D. Fabrication is summarised graphically as follows:-

Figure 7.17 STAGE A: Fabrication of pMMA Cylinder



A cylindrical 'starting' block of pMMA measuring 10mm by 10mm was cut for fine shaping into an optic.

Photograph 7.2 Close-up View of pMMA Rod with Repetitive Machining Grooves

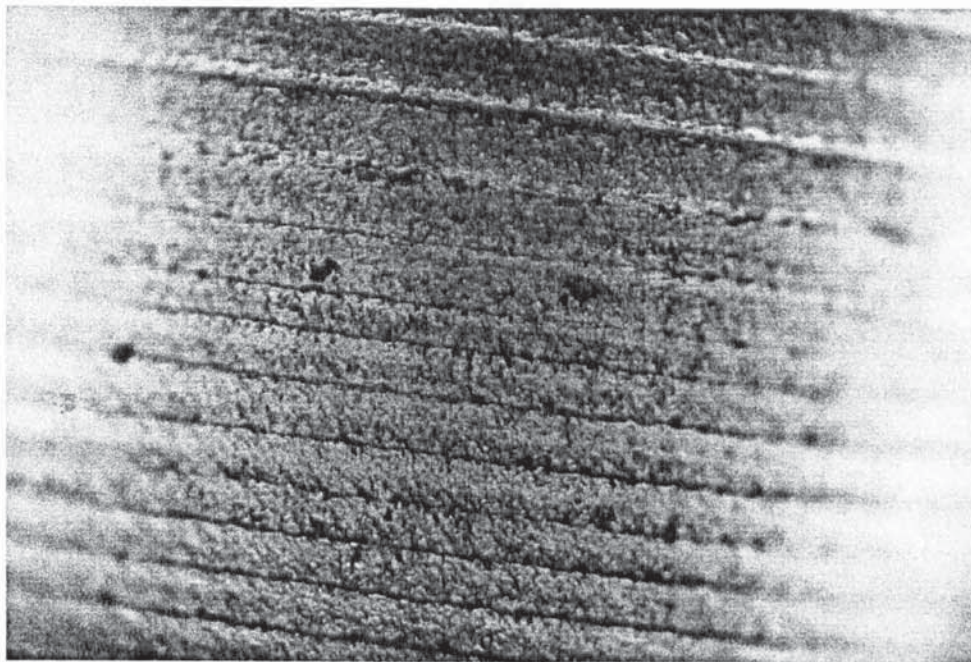
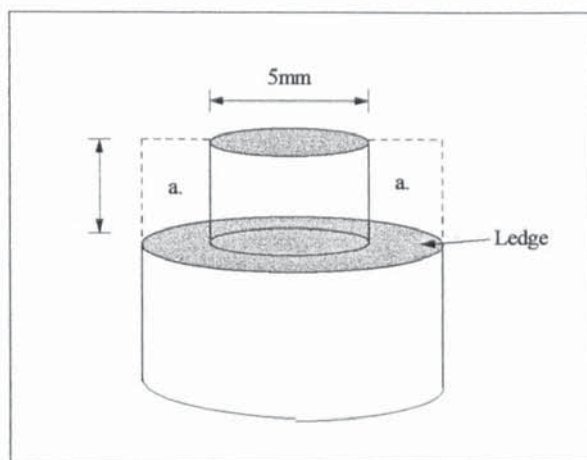
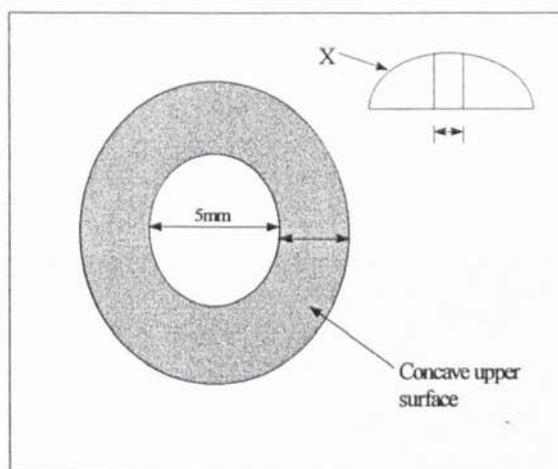


Figure 7.18 STAGE B: *Cutting of pMMA Cylinder to Accommodate the Ring of Biocoral[®]*



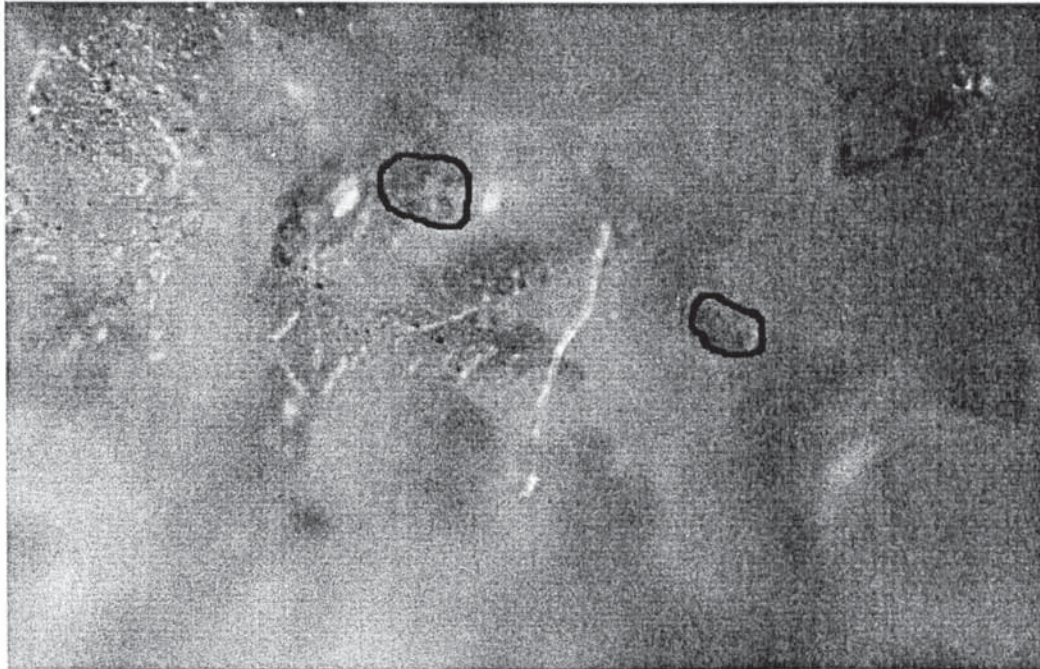
At Stage B, a 2.5mm (width) x 4.5mm (length) ring of pMMA is removed from the top part of the main block at (a) to form a ledge.

Figure 7.19 STAGE C: *Cutting and Shaping of Biocoral[®] Trepine Plug*

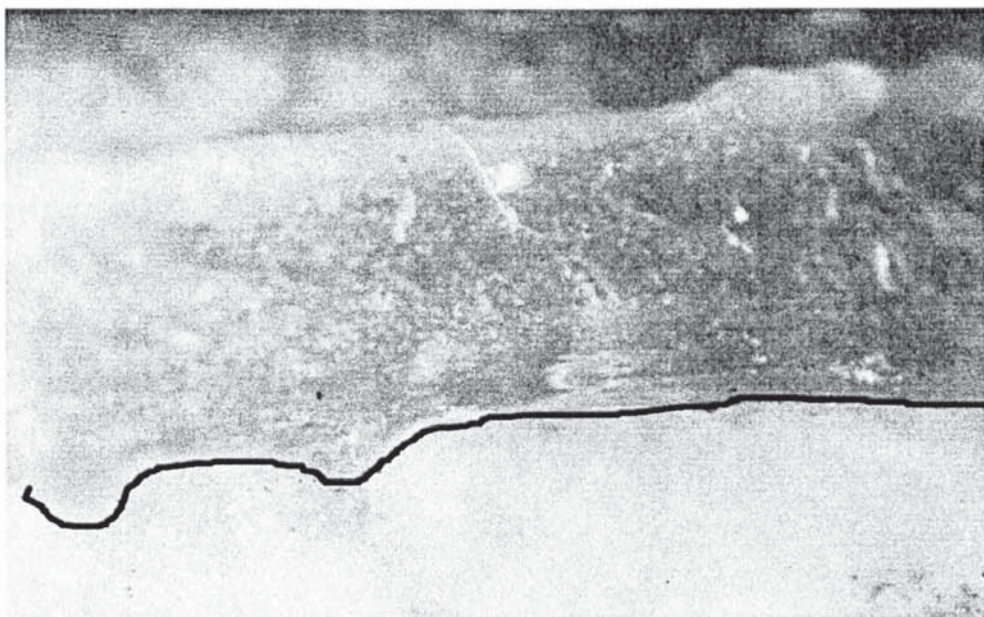


In Stage C, a plug of Biocoral was machined into a dome with a central hole. It was then glued onto the ledge, around the optical cylinder. A 5mm hole was drilled through the plug before either (a) putting it through the optic and gluing and machining the top surface into a concave shape, at (x); or (b) machining the top surface into a dome and then gluing it onto the ledge.

Photograph 7.21 *Region of Biocoral[®] Completely Infilled with Acrylic Glue. (From prototype III) Two pores are highlighted.*



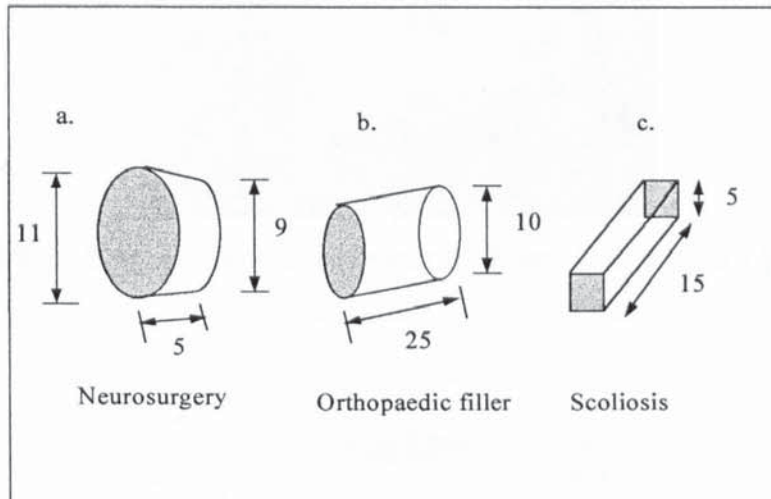
Photograph 7.22 *Layer of Acrylic Glue Bonding Biocoral[®] to the Optical Cylinder. (Biocoral[®] is below the black line line)*



7.4.21 Biocoral® Shaping

Biocoral® was available in a large number of different shapes and sizes as orthopaedic fillers, scoliosis and cranial fillers. Trepine plugs were found to be an ideal starting structure in shape and size for a support frame.

Figure 7.2 Available Biocoral® Shapes



a. Trepine plug; Long bone void filler; Vertebral arthrodesis

Shaping was painstakingly slow because of the frequency of sudden breakage. Embrittlement was thus, prevented with a series of incremental shallow tangential cuts. Trepine plugs were machined into two shapes using a contact lens lathe (Peter Carr, c/o Vista Optics, Stockport):

- Dome (infilled)
- Lens (unfilled dome)

A 5mm hole was excavated through the dome piece with a hand held tapered dental burr, to insert the optical cylinder . This was achieved very accurately by eye (Chris Parker, Matthew Boulton College, Birmingham).

Photograph 7.23 A Biocoral[®] Trepine Plug with a 5mm Hole for the Insertion of an Optical Cylinder (with kind thanks to Chris Parker of Matthew Boulton College, Birmingham).

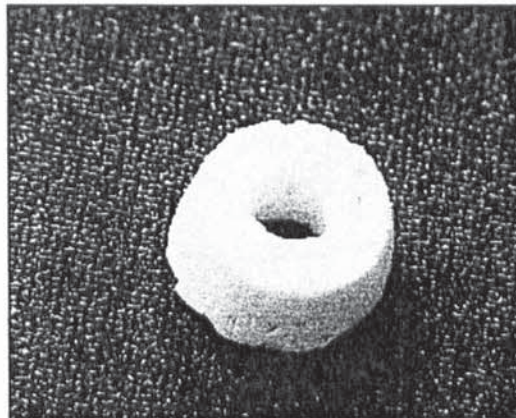
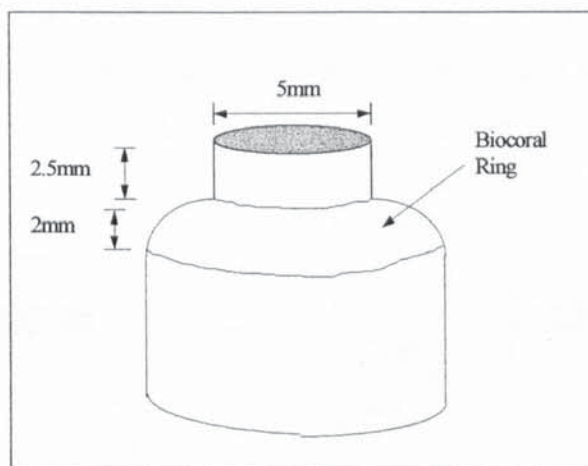
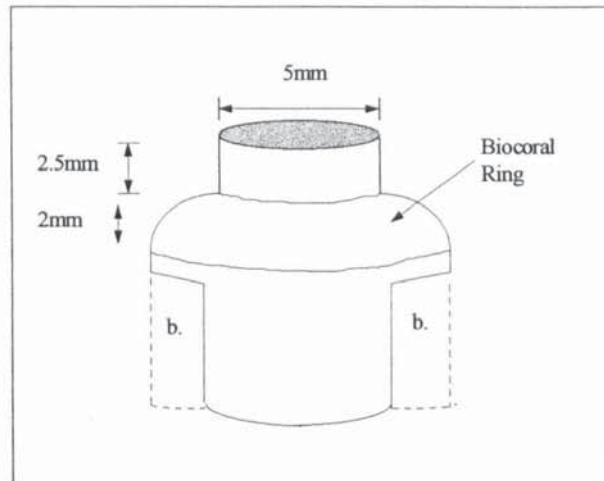


Figure 7.21 STAGE D: Attachment of Biocoral[®] Ring to the pMMA Optical Cylinder



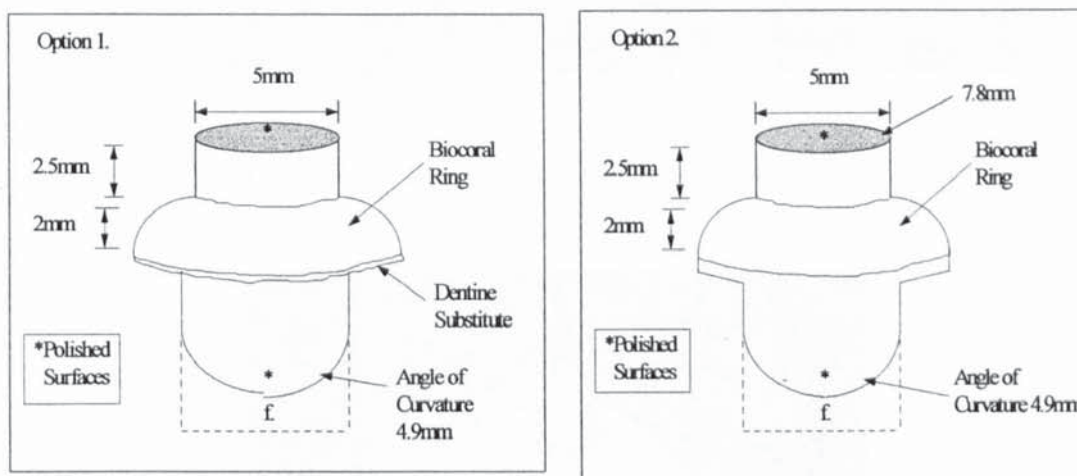
Biocoral ring glued onto ledge (d) and machined into PMMA block. Posterior surface is made convex and smoothed.

Figure 7.22 STAGE E: Fabrication of Optical Base and pMMA Support Frame



At Stage E two segments 2mm in width by 3.5mm in length were cut from either side of the optical cylinder base, (b).

Figure 7.23 and 7.24 STAGE F: Fine Machining and Polishing of Surfaces. A 3mm deep by 7mm wide segment is cut away from the bottom part of the optical cylinder, shown as f. Option 2 was the design that was fabricated.

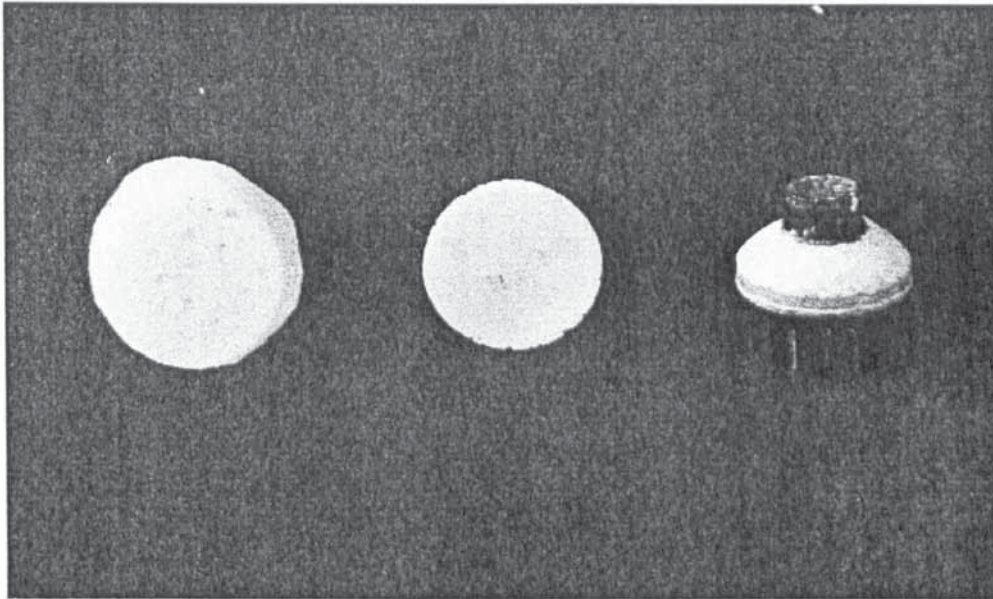


The first possibility for making a base for the Biocoral[®] ring could involve bonding a layer of dentine substitute such as, leucite porcelain to the base of the Biocoral[®]. The second possibility could involve cutting and shaping of the pMMA basal region to cover the entire base of the Biocoral[®].

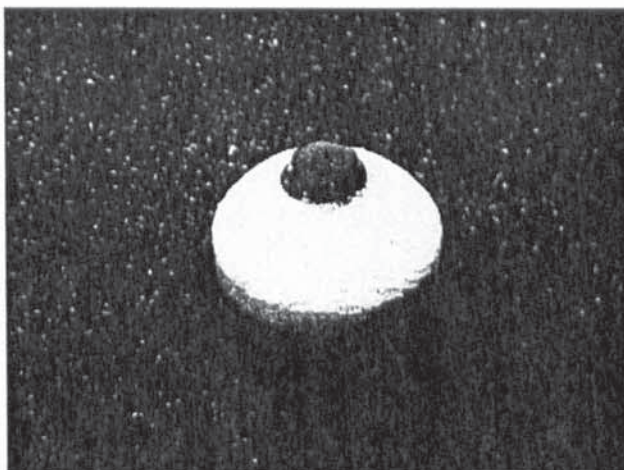
Further modifications to this final design were implemented after consultation with an ophthalmic surgeon, Mr. Christopher Liu at the Sussex Hospital in Brighton. First opinions were positive, but concerns were expressed about the stability of the bond

between coral and pMMA polymer. The third prototype possesses a wider Biocoral[®] ring for increased strength of attachment and a flatter posterior surface on the base plate ensuring better fit into the cornea.

Photograph 7.24 *Biocoral[®] Shapes and the Second Prototype Coral and pMMA Artificial Cornea.: Left:Trephine plug; Middle: Contact lens shape;*



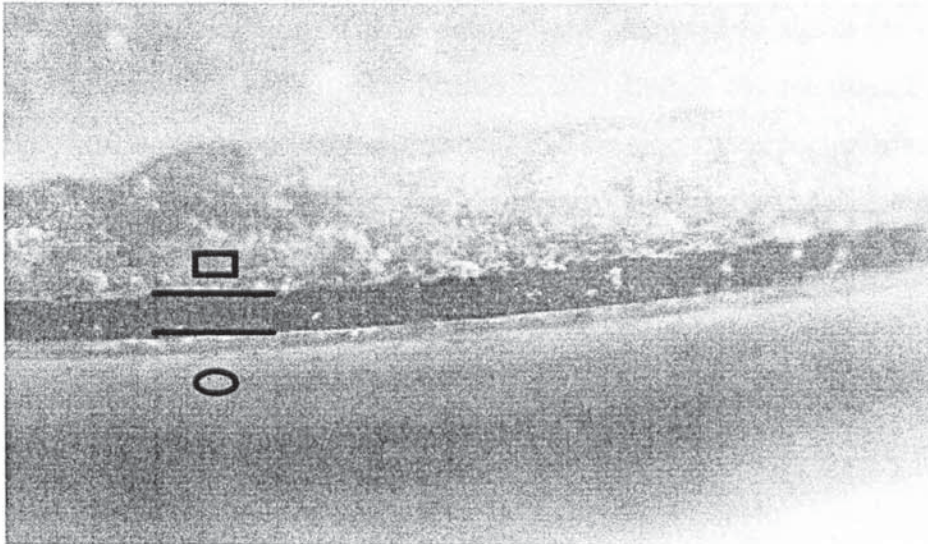
Photograph 7.25 *A Third Prototype with a Larger Support Frame Diameter and Smaller Base*



The coral keratoprosthesis consisted of an OOKP styled optical cylinder but slightly modified in form and outline. There was, for example a base plate extension to the optical cylinder. Its thickness is at least one third of the thickness of the overlying Biocoral[®] to shift the neutral axis and enable more strain energy to be stored therein. A

ring of Biocoral[®], with dimensions analogous to a dental plate is machined into an infilled dome. As opposed to gluing the two components were fused with a layer of viscous methyl methacrylate (MMA) impregnated into the base of Biocoral[®].

Photograph 7.26 *Layer of Acrylic Glue Bonding Biocoral[®] to the Optical Cylinder. From top to bottom: Impregnated Biocoral[®] (region below rectangle), layer of glue and the pMMA cylinder (region below oval).*



Surface modification of polymer and inclusion of factors involved in tissue reconstitution are additional features that may be included to improve implant retention, especially if it is to be inserted into corneal stroma. Biocoral[®] is not without its problems. Biocoral[®] was embrittled and chipped, during construction which, involved regular handling and machining. Unlike the dental lamina (ODAL) there was no structurally accurate substitute for the dental ligament or cementum instead a layer of non cell adhesive polymer was designed to function as a barrier to epithelial downgrowth and its inhibition.

The predicted functions of the keratoprosthesis made in this study are summarised as follows:-

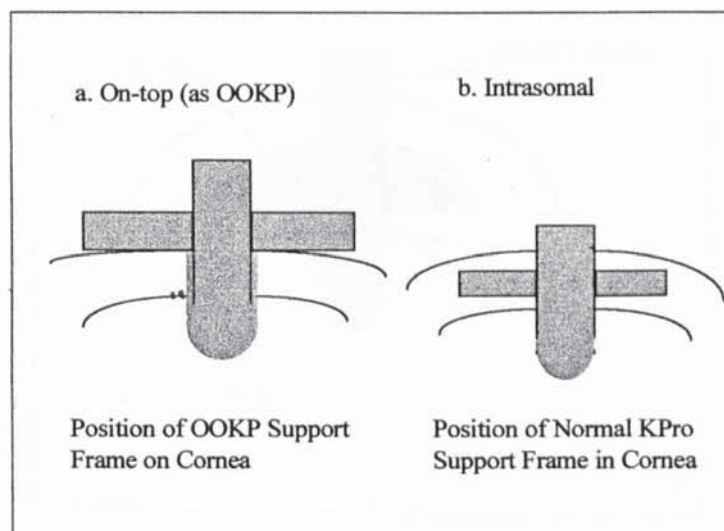
- to encourage healing at surface of biological ceramic
- to inhibit or reduce excessive proliferation of mucosal epithelium
- to encourage vascularisation

- to optimise mechanical stabilisation
- to minimise stress patterns within surrounding tissue
- to separate traumatised tissue from healthy covering tissue

The ideal implant would possess a shape emulating the natural healthy cornea. With such a corneal-like morphology the implant would be best suited to insertion into the remaining cornea, and thus minimise ocular reconstructive surgery. Two prototype corneal keratoprotheses developed in this study were designed to sit on the cornea, in the same manner as the OOKP (See **Figure 7.39**). Indeed the modifications for an intrasomal version would be slight, necessitating re-shaping of the posterior surface and a reduction in the length of the base plate. However, there were no satisfactory design solutions to:-

- provide sufficient reinforcement to the cornea and
- impede epithelial migration from the cornea or conjunctiva.

Figure 7.25 *Illustrating the Two Alternate Positions for the Support Frame and the Cornea*

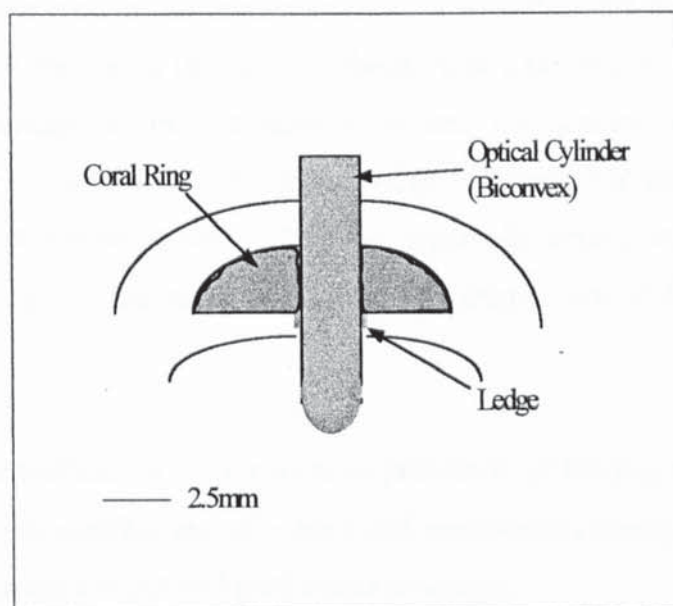


Ideally, the method of construction should be enacted in one solitary stage, and again would involve vacuum assisted polymer impregnation. Infiltration of polymer between crystal plates and between the walls of pore channels could significantly improve the

strength of attachment. Clearly the crystallography of Biocoral[®] should be transformed into a stronger and more durable calcium phosphate form. INOTEB, the manufactures of Biocoral[®], while chiefly providers of resorbable coral implants, are able to supply pieces in this form to order, in a range of shapes and sizes.

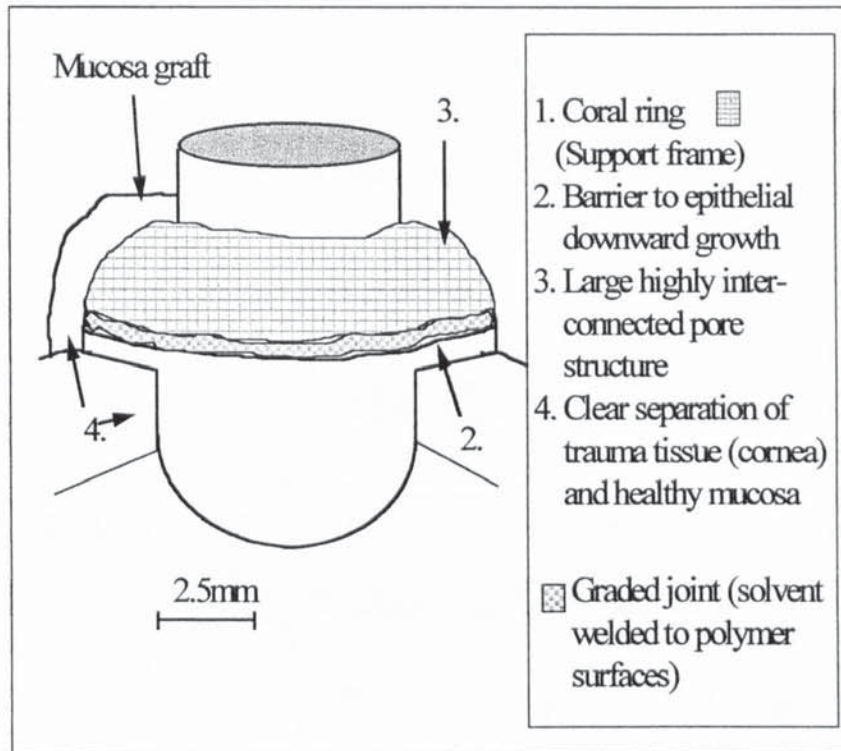
Prototypes developed in this study have converged with the prosthesis by Leon et al., who has also employed coral for the support frame. Leon has very recently patented a design consisting of a pMMA optical 'window' ringed by a coral 'washer'.¹²⁰ The design by Leon glues the coral ring (the coral is a different species by the way) to the optical cylinder, whereas in this study there has been an attempt to integrate the two more fully and use a slightly different shaped optical cylinder. Furthermore, the design of Leon does not use the OOKP as a blueprint for principle features of design, such as placing the support frame on the exterior side of the cornea, preferring to embed the coral in the corneal stroma.¹²⁰

Figure 7.26 *The Coralline Hydroxyapatite Artificial Cornea Devised by Leon et al.*¹²²



As mentioned in the introduction other prosthesis exist with specific features emulating the OOKP. All attributes remain starkly uniform because of the limits imposed by the shape and size of the outer section of the eye. Disc thickness, diameter and optic length are all comparable and differ only slightly.

Figure 7.27 *A Marine Inspired Coral and pMMA Keratoprosthesis.*



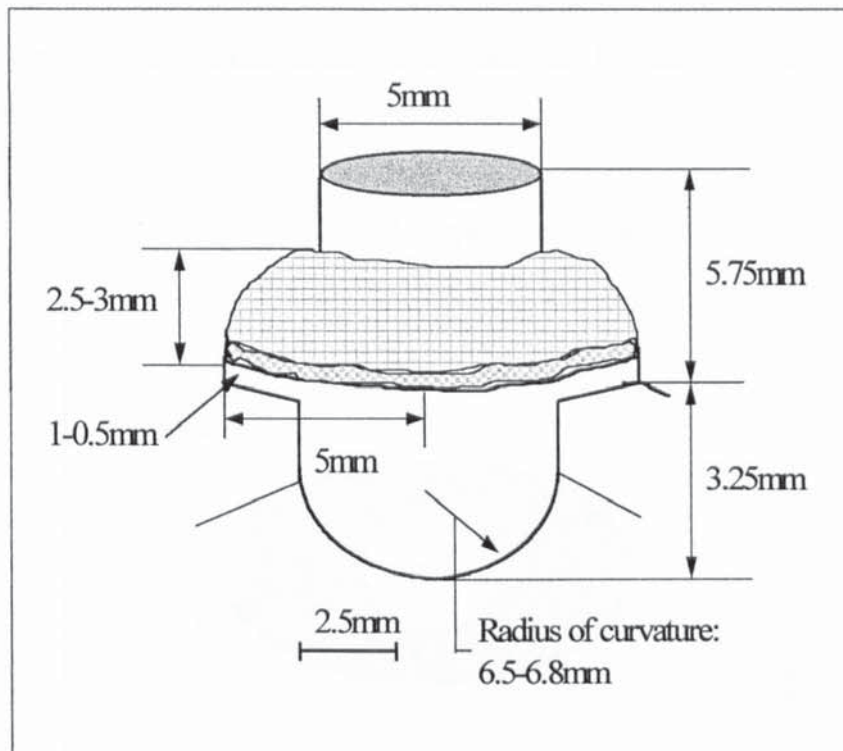
The optical cylinder used in this fabrication project is as the OOKP optical cylinder of Falcinelli et al.²⁶ A section of Biocoral[®] is shaped with a convex profile on the anterior surface. This minimises stress concentration and the amount of required tissue covering of inner cheek mucosa. A polymer ledge rests onto the cornea and acts as a barrier to further downward growth. Polymer is partially impregnated into the porous base of the coral piece. The mode of surgical implantation would follow Strampelli⁶⁴, such as:-

- re-enforcement of cornea with mucosa to prepare it for loading with the implant
- three month pre-conditioning of implant and periosteum coverage
- mode of insertion and sutured graft tissue coverage.

The unique pore structure of Biocoral[®] or Pro-Osteon[®] would ensure a tight sealant of living non-pathogenic mucosa reducing the probability of infection, necrosis and ulceration. A strongly hydrophobic polymer base separates the cornea from mucosa and hinders epithelial migration. (Refer to **Figure 7.26** listing the functions of the

keratoprosthesis) What are the absolute changes required by a surgeon and what changes should take priority? The next section explores design modifications sought by the ophthalmic surgeon and states whether they can be included.

Figure 7.28 *Specific Dimensions of Marine-Inspired Artificial Cornea (Prototype III)(Photograph 7.25)*



7.4.3 Discussion: Likely Surgical Performance of Prototypes

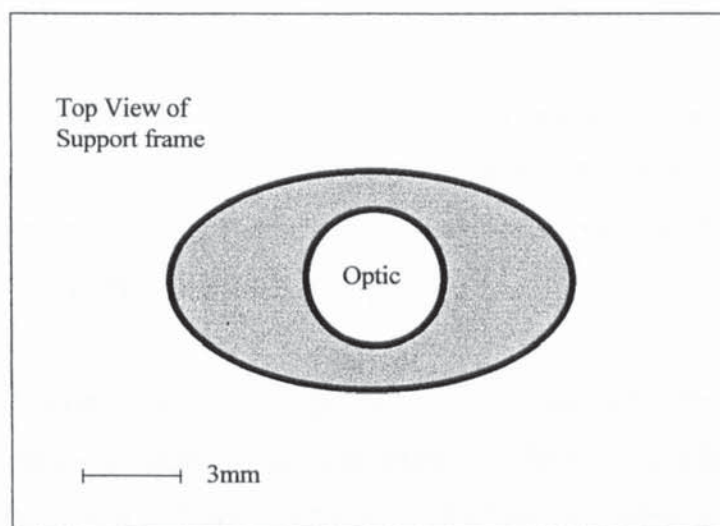
Much effort was expended, tackling the causes of biological complications arising from enzyme degradation, membrane proliferation and infection. Above all the primary aim was to stop implant expulsion. Obviously, there are other, surgical constraints that must be catered for. Features developed for enhancing biological attachment such as a thinner, larger cornea shaped porous disc, must not, for example impede insertion or handling during surgery. Naturally, some features that aid biological integration also match the design features that reduce the degree of surgical intervention. A well designed implant should take the shortest possible time to prepare, and insert. This requires a high degree of fine tuning and hence numerous design modifications.

After the first prototype was constructed this assessment began through a process of

subjective analysis. Firstly, a number of questions were posed to determine the likely effectiveness of the design, during and after surgery. An important question was, what design features could improve the ease of insertion? (ease in this case refers to lack of impediments to manipulation by hand and during insertion into the host and arrangement in the tissues).

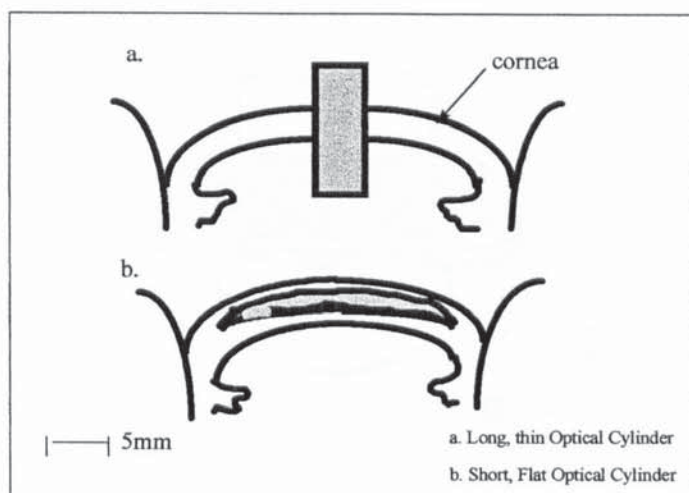
Surgical concerns raised by the design included the following four minor points. In shape the support frame should be an oval contact lens because it is easy to insert and secure. Scleral fixation provides a stronger attachment.

Figure 7.29 *Ideal Support Frame Shape*



Particularly from the viewpoint of patient and surgeon it is best to produce a keratoprosthesis, support frame and optical system combined that is as close as possible to the natural shape of the cornea. However, a shape such as this increases the probability of tissue overgrowth over the top of the optical cylinder. Keratoprostheses comprising an optical cylinder that fully penetrates the host cornea significantly reduces the danger of exclusion and expulsion. Hence, the compromise has been to fabricate a contact lens support fused with a long optical cylinder as used by Falcinelli and other OOKP pioneers.

Figure 7.3 *Two Shapes of Artificial Cornea; Long thin optical cylinders stop epithelial overgrowth, short thin optical cylinders reduce invasive surgery but, may allow tissue overgrowth over the optic.*

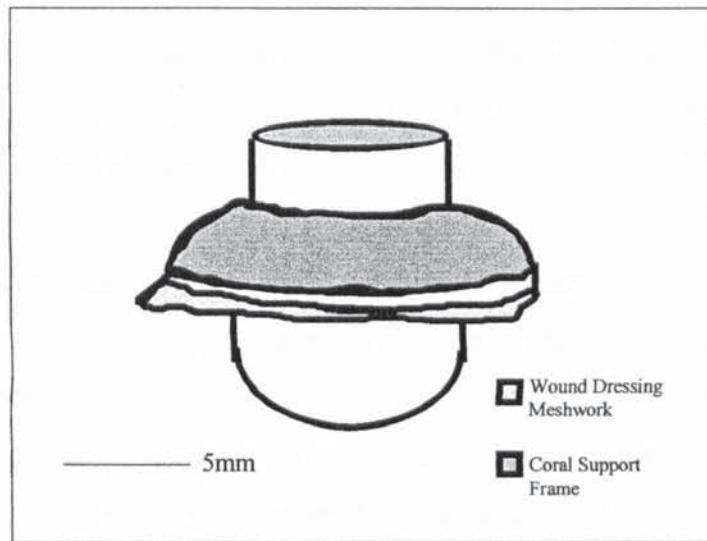


The maximum diameters for the prototypes were set between 10 and 13 mm, so that the implant edge extends into the sclera, and no further, otherwise it could irritate and inflame the conjunctiva. All prototypes were made with a diameter of 10mm corresponding to the anterior-posterior length.

The weight and density of all prototypes were within reasonable limits, as adjudged by an ophthalmic surgeon. Both weight and density of the implant affects how well it is supported by the cornea and adjacent tissue. If it places excessive amounts of strain on tissue it could also damage supporting and reinforcing tissue. Consequently the surgeon has to spend more time preparing the wound site.

Finally, for ease of suturing it may be necessary to include 'pre-inserted' sutures or a layer of nylon mesh inserted in the layer of polymer between coral and base plate, however if tissue penetrates and interlocks with the porous support frame sufficiently well suturing is not necessary.

Figure 7.31 *Attached Nylon Mesh for Insertion of Sutures*



A second question relevant to implantation of the prototype was, What features would be useful for regular examination of the anterior segment?-to record observation of possible trauma by inflammation or infection. A reduction in the diameter of annulus and length of the optical cylinder provides for easier access to regions surrounding the anterior segment and a regular assessment of pathology. However, such issues do not apply in the OOKP where all ocular elements are obscured by covering graft tissue. Unlike the tooth and bone element the support frame of our synthetic cornea can be made to have any desired shape and size which means we are able to modify the shape and size of the OOKP optic to improve the size of the visual field and reduce the depth of penetration into the eyeball.

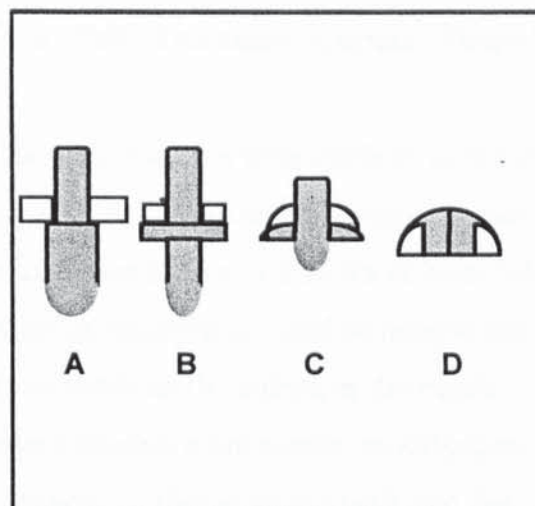
Ideally there would be a desire to approach the ideal shape of a full thickness artificial cornea. By which the optic is flattened in the anterior-posterior plane and widened. However the anterior should project above the epithelium of 0.75mm and posteriorly by 3.4mm to dis-encourage formation of encapsulating membranes. It is not entirely clear how these proposed modifications would affect focal power and light quality and how they are compensated for, but the field of view would be increased (further discussion in the next section).

It is not terribly important to have the sutures directly attached to the implant; what is required is a well attached layer at the top surface of the coral to enable suture attachments. A contact lens annulus would be advantageous for two reasons, one structural, the other biological. First a dome is less likely to be fragmented by oblique loads. Secondly, it is minimally invasive when placed in the corneal stroma. For this is the ultimate goal of any research into the design and fabrication of an artificial cornea.

7.4.4 Future Directions: Changes to the Optical Cylinder

While not a major focus for improvement in this study, changes to the optical cylinder were deliberated upon to increase the size of the visual field and shape the optic to be more like the cornea. The stepwise modifications starting from the OOKP optic toward a cornea shape optical cylinder are drawn in figure 7.31.

Figure 7.32 *Likely Evolution of a Keratoprosthesis Optic by Artificial Selection (with Biocoral ring incorporated). The tendency in keratoprosthesis optics design is toward a cornea shaped artificial cornea at D. A is the shape of the OOKP optic, B is the shape of optic made in this study, with an extended ledge for support of coral, while C. is a possible intermediary: a shorter and thicker optical cylinder. The unshaded blocks are Biocoral.[®]*



The optic replaces all layers of the central cornea and projects a clearly defined image on the retina. This inevitably results in a high visual acuity and good contrast sensitivity. pMMA is the material most often used because it has excellent clarity and

refractive properties. Sapphire is also used due to an enormous refractive power, enabling a corresponding reduction in the length of the optic. Other more flexible materials are being developed to replace pMMA, e.g. Collagen, Polytrifluoropropylmethyl siloxane and Polydimethylsiloxane.¹²¹

As the refractive index increases light rays are more concentrated and image size is reduced. As with all optics the field of vision is limited analogous to looking through a toilet tube. By decreasing the periphery below the length of the optic and increasing the optic diameter, the field of view is enhanced. There needs to be a compensatory change in the surface curvatures at the back and front of the cylinder so that one clear image is formed on the retina. However, by making the periphery smaller than the optic length there are problems of centration and stability and by reducing length, to increase field of view, retro-corneal formation is more likely¹²⁰.

An optical cylinder should possess a large diameter to overcome decentration and instability, but the length must not be reduced too greatly otherwise tissue overgrowth could lead to loss of vision. Surface manipulation using ion bombardment techniques could be a solution to the problem of tissue overgrowth and could assist the acceptance of cornea shaped synthetic corneas.

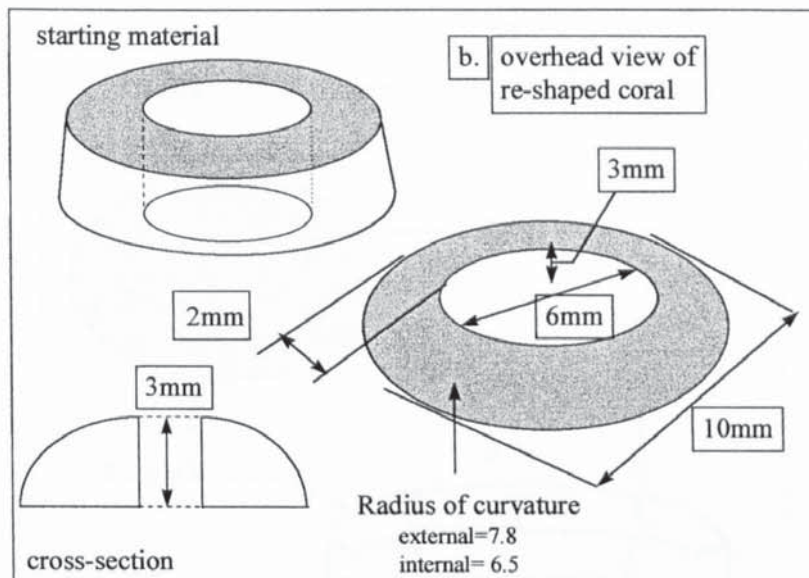
7.4.5 Production of a Full Thickness Cornea Shaped Coral and Perspex Keratoprosthesis

In the final stages of this study attempts were made to construct a prototype, emulating the shape and structure of an ideal artificial cornea (see Section 1.5.45). The advantages of a design as shown in figures 7.33 are reduction in glare, considerably less surgical intervention, with for example, no need to remove the lens or vitreous humour, and a very low loading of strain on the cornea at the edges. Unlike former prototypes, there would be a greater imperative for surface modification over the anterior of the “optical window” to prevent epithelial overgrowth and bacterial adhesion, since the intention of this design is for insertion into existing corneal stroma. In addition, the diameter of the optical window should also be increased to extend the visual field beyond 35 degrees (tunnel vision).

In the first stage of production a hole was drilled through a trephine plug of Biocoral and machined using a contact lens lathe, designed for convex curves, into a shape as close to the one shown in the figures below: 7.48 and 7.49 (angle of curvature anterior = 7.8mm; posterior = 6.5-6.8mm).

Figures 7.33 to 7.35 *Diagrams Illustrating the Stages of Assembly for an Artificial Cornea with Natural Cornea Shape and Ring of Coral.*

Figure 7.33 *Stage 1: Shaping of the Coral Support Frame*



In a more elaborate design blueprint a staggered joint was devised to fashion an interlocking joint together with a posterior polymer flange on which, the coral rests. The aim was to then glue the two pieces together either with dental acrylic or preferably by solvent welding. The latter involves impregnation of a monomer syrup (i.e. it is pre-polymerised) into the Biocoral[®], part way-about 1-2 mm into the porous solid- before it is pressed firmly against the optical window, which is surface etched with the same solvent (dichloromethane).

Figure 7.34 (a)-Stage 2: Method of Attachment Between Coral and Optical Cylinder

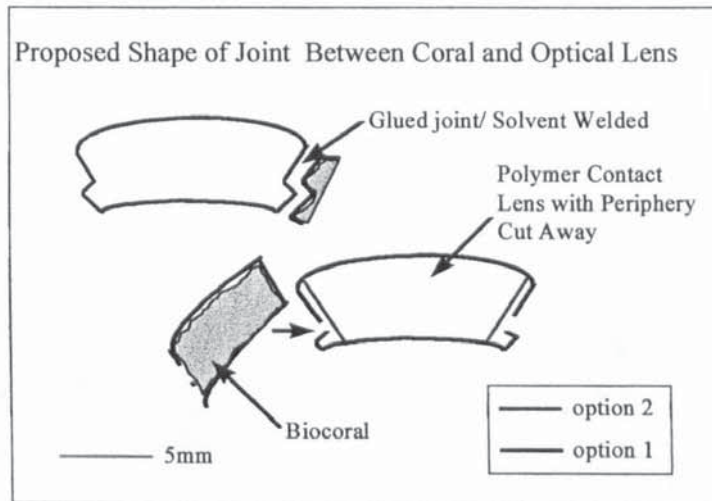
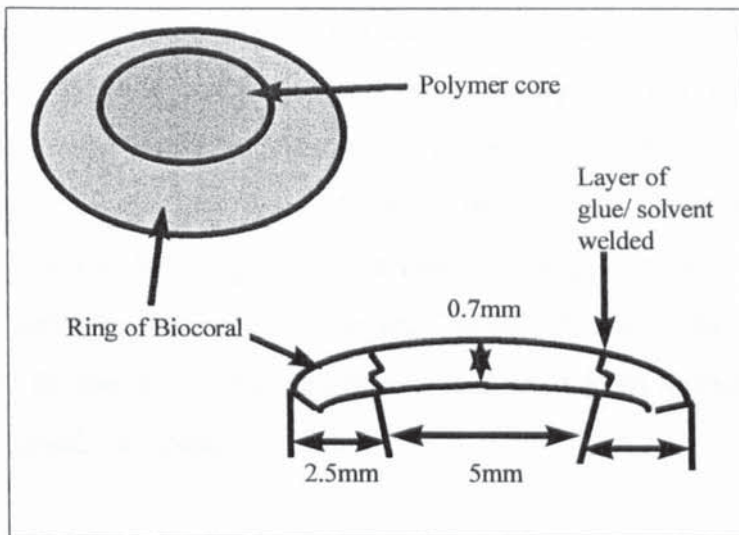
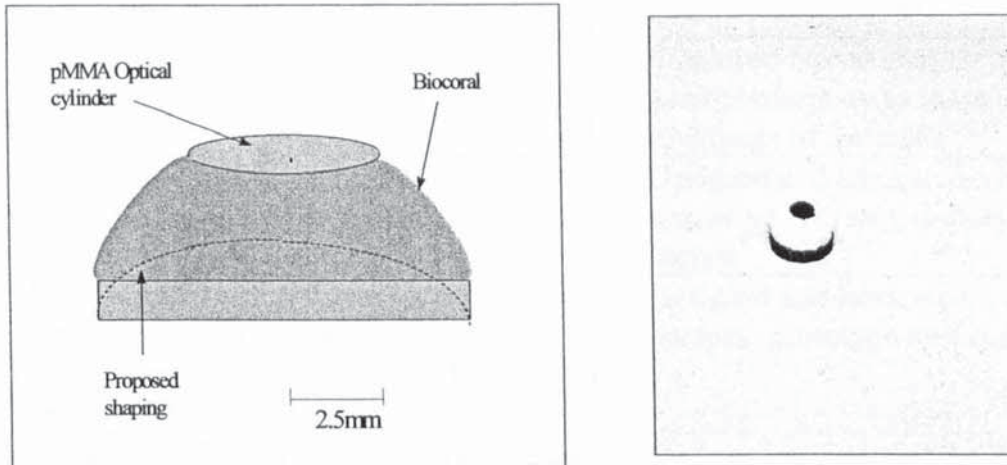


Figure 7.35 (b) Final Shape and Dimensions



The method of manufacture is extremely difficult due to the difficulty in holding the device in the lathes and machining properties of the Biocoral[®]. The first attempt resulted in the Biocoral[®] shattering when trying to machine it to the required diameter before putting a radius onto it. A further problem was that the Biocoral[®] could not be held in the lathe with a chuck while the back-curve was machined, for fear of shattering the coral. The best attempt at a cornea shaped coral and perspex piece is shown diagrammatically in figure 7.36 overleaf.

Figure 7.36 *The Best Attempt to Fabricate a Natural Cornea Shaped Coral and Perspex Artificial Cornea*



7.5 Conclusions

Overall it is best to produce an artificial cornea that is as close as possible to the natural cornea in shape, size and mechanical properties, since for the patient it is more comfortable and for the ophthalmic surgeon it is easier to insert. The latter minimises the degree of intervention. In terms of optical design an artificial cornea shaped as natural cornea, would reduce glare and widen the field of vision. Such a 'push' towards true biological mimicry (copying design features of the cornea) is counterbalanced by the 'pull' of complications that arise from fabrication of a device that is cornea shaped, particularly rejection.

Optical cylinders that pass through the cornea tend to alleviate serious pathological problems that lead to expulsion such as, the formation of retroprosthetic membranes.²⁵ Consequently, the immediate focus of research was the tooth and bone artificial cornea and its method of attachment to the eye. In this thesis, three prototypes were designed and fabricated with the approximate size and dimensions of the OOKP, but with minor modifications to facilitate surgery and improve the stability of the artificial cornea. The achievements associated with the design and fabrication of a coral and perspex artificial cornea are listed in the table below (**Table 7.16**).

Table 7.16 *Achievements and Problems Associated with the Design and Fabrication of Prototype Coral and Perspex Artificial Corneas*

Problems	Challenges
Goniophotometry results were confusing	Employed fractal analysis and goniophotometry to measure surface roughness of materials
Insufficient porosity in hydroxyapatite support plate and no base plate present	Designed and fabricated a hydroxyapatite and perspex prototype artificial cornea
Angle of curvature for anterior and posterior ends of optical cylinder flatter than should be. Adhesive layer was too thick	Designed and fabricated 2 coral and perspex prototype artificial corneas
Cutting and shaping coral into contact lens shape was practically difficult	Designed and partly fabricated a natural cornea shaped prototype artificial cornea

Coral was used as a support frame for the construction of later prototypes. It most suited the criteria for an analogue of alveolar bone. Perspex was used for the optical region and as a base plate to support the coral. Perspex is widely used by artificial cornea engineers, because it possesses excellent optical clarity and is extremely well tolerated by the body.

Coral consists of a highly biocompatible material, hydroxyapatite and it possesses a bone-like structure that is highly suited to supporting and guiding the growth of living tissue. However, there are three minor concerns associated with Biocoral[®], as a support frame which, must be pointed out. The first concern is the degree of brittleness. The second concern is the mismatch in stiffness with pMMA and with host tissues. Finally, resorption of the coral may occur over long periods of time. Thus, Biocoral[®] must be transmuted into a stoichiometric calcium phosphate form, rather than be left in its natural occurring mineral form of calcium carbonate.

Satisfactory tissue reconstruction within and around the implant may not always occur with certainty, especially in severely damaged wounds. This may be a reason to employ tissue engineering therapies. A tissue engineered approach would combine living tissue

with a synthetic structure. Applying this strategy to the design of an artificial cornea; there should be a scaffold made from a suitable type of coral that provides a specific framework for artificially cultured tissues (stroma or covering tissue e.g. buccal mucosa), previously removed from the afflicted patient.

Despite the expressed concerns, coral derivatives are superb scaffolds for human tissues, due to their considerable biological tolerance and orchestrator of cellular activities characteristic of healthy tissue.¹¹⁵ Since it is not ethical to implant any of the prototypes into a human patient, the next step would be to implant the best prototype into either, organ culture (various research groups are devising multi-layered tissue constructs) or much more likely, at an appropriate animal body site. If so, it should be implanted in a region that bears close resemblance to the mucosa habitat, i.e at an intermuscular site.

CHAPTER 8:
RECAPITULATION, DISCUSSION and
CONCLUSION

CHAPTER 8

RECAPITULATION, DISCUSSION and CONCLUSION

"The surgery of the ancient Indian physicians was bold and skilful. A special branch of surgery was devoted to rhinoplasty or operations for improving deformed ears, noses and forming new ones, which European surgeons have now borrowed."

Sir W.Hunter.

8.1 Recapitulation of Materials Synthesis

Over the past 200 years there have been at least 300 designs of artificial cornea. Since its speculative inception in 1789 by Guillaume Pellier de Quengsy the artificial cornea has had a very chequered history of development.¹ It has been estimated that between 8%-53% of inserted artificial corneas fail completely within 3 months to 5 years, respectively.¹⁴ Contrast that, with a 95% success rate for donor corneas in the first 5 years after implantation.¹⁷ Better surgical techniques and better performing materials have improved the success of recent keratoprotheses, such as those developed by Legeais⁷, Chirila⁶ and Pintucci.^{28,48} This demonstrates the level of interest and considerable level of difficulty in creating a universal replacement for severely damaged corneas. There are still many long-standing complications to be fully overcome after the artificial cornea is implanted. They are:-

- bacterial infection
- enzyme degradation of surrounding tissue
- proliferation of membranes
- raised intraocular pressure
- poor stabilisation

Most of these biological complications are satisfactorily controlled by the tooth and bone keratoprosthesis (OOKP), although raised IOP is a consistent problem. Owing to this fact, the Osteo-odonto-keratoprosthesis (OOKP) is claimed to be the most clinically successful of artificial corneas up to now.^{63,64,65,69} The particular features of the OOKP that might explain such success are structural, they are: a bone-like porosity

(graded in the size of pores); a semi-rigid block anchored to the optical cylinder and a suspensory periodontal ligament linking them together. This whole structure of tooth and bone is called the dental lamina. The inter-connected pore spaces of the bone, to the exterior, provides fixation of supporting tissue, while the periodontal ligament and cementum prevent encapsulation by exclusion membranes (**Figure 8.1 (1)**). During an operation to implant an OOKP there is insufficient dental tissues (particularly dentine and bone), free of disease to ensure long-term stabilisation and improve significantly, the field of view. A synthetic analogue of this structure would make the OOKP easier to use and more widespread. It is only presently employed in a few centres in Spain and Italy. So, there are clear surgical, economic and therapeutic advantages in employing a synthetic analogue of this structure. The structural specification of an OOKP is tabulated below, as a blueprint for the fabrication of a successful OOKP analogue.

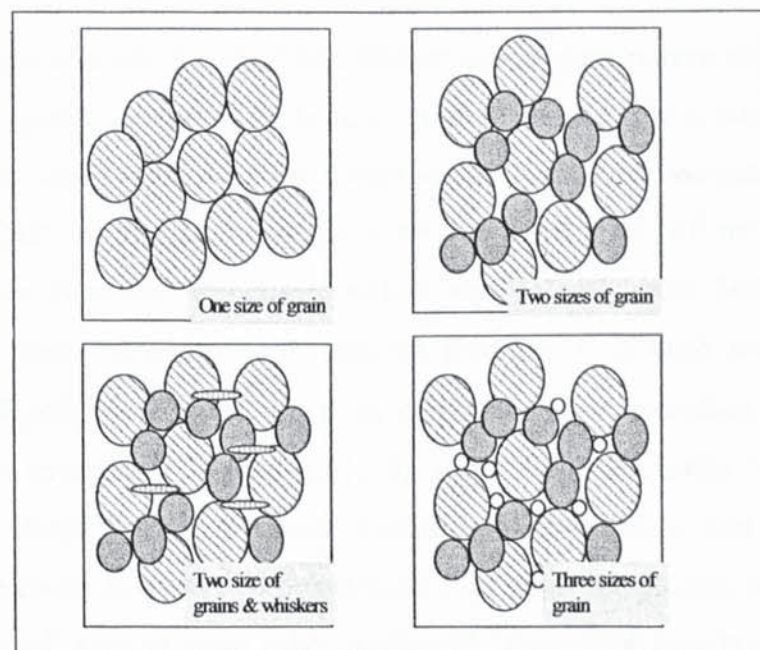
Table 8.1 *Basic Requirements for a Synthetic Structure that Mimic the OOKP Support Frame*

Property	Basic Requirements
Porosity (Tissue integration)	<ul style="list-style-type: none"> *Highly interconnected in three dimensions *Microporosity: 15-40 micrometers *Macroporosity: 50-150 micrometers *Large pores grading into small pores
Mineral constituency (Biological tolerance, Bioadsorption)	<ul style="list-style-type: none"> *High degree of crystallinity *Ca/P ratio of 1.5-1.67 *Moderate ionicity *Calcium phosphate+ carbonates
Low rate of resorption in biological fluids (Stability & permanency)	<ul style="list-style-type: none"> *Non-stoichiometric hydroxyapatite *High fluorine-to-carbonate ratio
Periodontal Ligament/ cementum substitute (Stop membrane downward growth)	<ul style="list-style-type: none"> *Flexible, crosslinked network *Cell adhesive but inhibits proliferation

The obvious choice for a synthetic analogue of the bone surrounding dental tissue would be one of the many bone replacements. However, many of them did not have matching pore sizes (15-150 μ m). Thus, a structure was specified to copy the physical characteristics of the alveolar bone; and was fabricated in the laboratory with the simplest method possible. Specific methods were also needed to fabricate a synthetic analogue of the dentine, periodontal ligament and cementum. Then it would be necessary to combine these 3 structural elements with the bone analogue and optical cylinder. In the course of this study, structural approximations to the three layered OOKP dental lamina were made using conventional (compacting and sintering) and various un-conventional (in-situ mineralisation) techniques for synthesising materials (Figure 8.11).

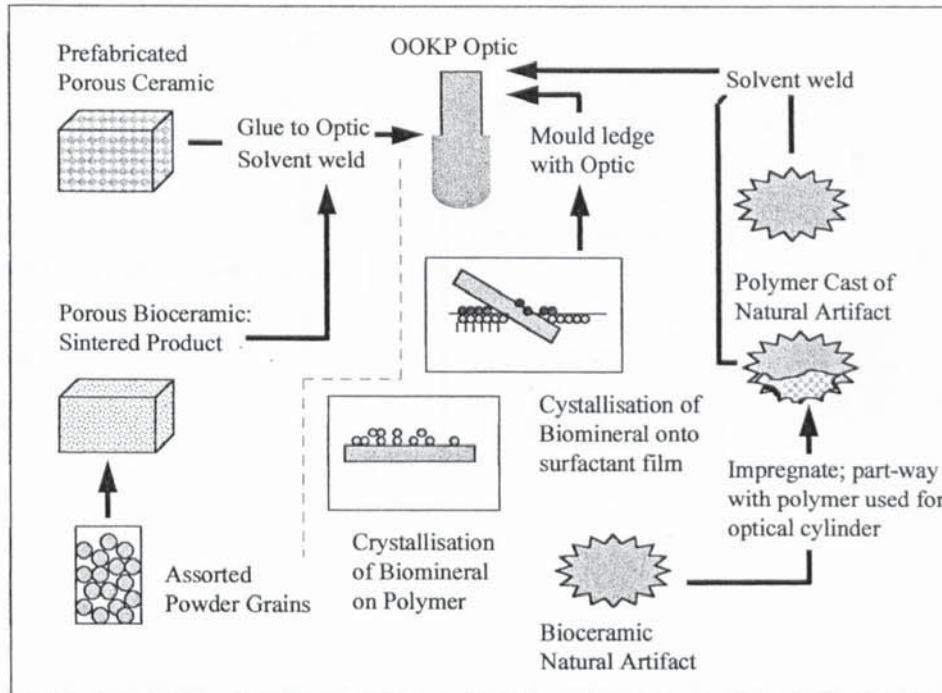
Structural analogues of the porous bone were fabricated by compacting and sintering hydroxyapatite powder formulations and this was, later followed by the employment of pre-fabricated porous biological ceramics. Assorted powder mixtures were formulated to produce a bone-like pore structure, after compacting and sintering (Figure 8.1)

Figure 8.1 *Cartoons of Assorted Powder Mixtures Before Compacting that Were Employed in this Thesis*



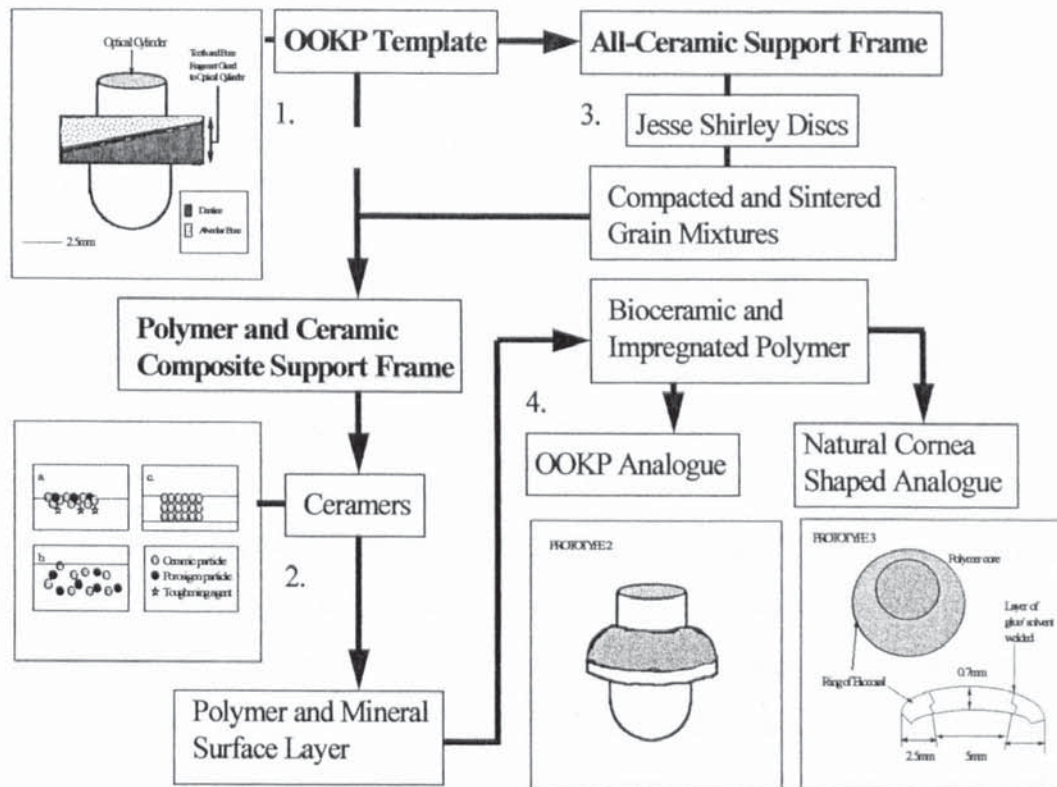
A substitute, (only in the sense it was solid and dense) of the dentine was made from pMMA while an analogue of the periodontal ligament was made with a collagen (type 1) gel. The periodontal analogue was not incorporated into the final design.

Figure 8.11 Schematic Representation of Methods used for Making a Ceramic Support Frame for a Synthetic OOKP



The first subject of study was the fabrication of an inorganic porous structure with very small internal pores, increasing in diameter gradually into larger external pores, and so mimicking the distribution of pore spaces in the bone layer surrounding the dental lamina. Work in this study began with the fabrication of moderately porous hydroxyapatite discs and structures with a surface roughness, both of which are constructed from compacted and sintered powders ($<250\mu\text{m}$) and fine granules ($>250\mu\text{m}-500\mu\text{m}$). As a result, a number of calcium phosphate discs were made with varying pore structures, (**Figure 8.12; 2**) These were fabricated by a commercial collaborator, Jesse Shirley Advanced Ceramics. However, it was not possible to accurately re-create a suitable porous structure for tissue integration; one that emulated the structure of bone or even other moderately successful keratoprosthesis support frames.

Figure 8.12 A Flow Chart Summarising the Types of Experimental Work Carried Out in this Thesis (in order of precedence: 1 to 4).



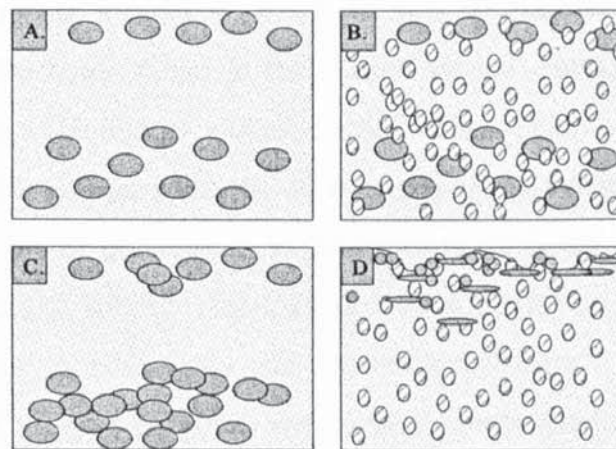
A porous support frame composed of biological ceramic (calcium phosphate) could not be made with the required structural attributes (**Table 8.1**), for two reasons. Firstly, pores and channels with the desired dimensions could not be fabricated by compacting and sintering biological ceramic powders or granules. Secondly, there was a strong propensity for catastrophic fracture in the biological ceramic discs. If such a support frame were welded to an optical cylinder, fracture would also occur at the interface between the ceramic plate and the optical cylinder, so that the two could come apart. So there are two likely regions of mechanical failure and these must be toughened to reduce the formation and propagation of fractures.

Table 8.11 *Achievements and Challenges of Making Hydroxyapatite Discs from Assorted Powders*

Achievements	Challenges
Fabricated porous hydroxyapatite discs from varying assortments of starting powders to generate ordered and connected porosity	Pore sizes too small and not enough connections between them
	Poor fracture toughness and strength

Longer heating times or heating rates can increase the degree of particle welding leading to increased stiffness, but in doing so it removes up to 3/4 of the total porosity otherwise present. Improvements in mechanical performance without the concomitant reduction in porosity, was achieved by amalgamating hydroxyapatite with the same polymer as used for the optical cylinder, into ceramer composite materials. Porosity was imprinted into the polymer during its formation by adding soluble porosigens. Difficulty arose, though in ensuring pores were surrounded by ceramic only and not polymer, because ceramic particles would agglomerate into dense patches. All surfaces in contact with open space should be coated with biological ceramic to create a maximum area for tissue attachment with the ceramic. Ceramers were made to varying degrees of quality with rough surfaces, and with pores (**Figure 1 (3)**).

Figure 8.13 *Cross-sectional Cartoon through Ceramers Fabricated in this Thesis*



Key: Ovals represent porosigens; circles represent hydroxyapatite particles; Sticks represent whiskers.

All of the ceramers fabricated were inconsistent in quality, despite the inclusion of various additives to overcome phase separation and improve blending of the substituents. Insurmountable technical difficulties were encountered in creating the correct sizes of pores and a consistent arrangement of pores. When mineral was seeded and grown onto membranes of methacrylate polymer, the crystals could not be induced to coat the polymer completely and so it was not possible to form interconnecting pores using protein modifiers of crystal shape and size. Yet with some hard effort and refinement these methods could have given rise to some useful 'tailored' pore structures. Due to a lack of time and money it was not possible to exploit these fascinating and valid techniques further.

Table 8.12 *Achievements and Challenges of Making Hydroxyapatite and Polymer Composites*

Achievements	Challenges
Ceramers (pMMA & hydroxyapatite) with pores, to limited extent	Phase separation of ceramic particles and polymer matrix
Etched surfaces generated rugosity to depth of 300 micrometers	Correct viscosity for dispersion of particles
Fabricated Xerogel and bonded it to hydroxyapatite disc	Growing crystals with complex structure
	Creation of a highly specific porosity

Interest in the immense structural variety of natural skeletal frameworks and the similarity to alveolar bone, found in the 'dental lamina' support frame, lead to the mixing and blending of biological ceramic slurries. These slurry mixtures were intended for casting of suitable natural artefacts. Fine details of microstructure can be cast with either a ceramic slurry or polymer. In initial experiments polymer was casted into and around suitable natural sponge skeletons and coral skeletons. The suitability was measured according to pore sizes and inter-connectedness. The casts possessed accurate details of all existing pores and surface topography, but there were nearly always regions of degradation caused by repeated acid washing which, dissolved away some of the casting material. For example, struts linking the pore boundaries were often broken. Owing to the difficulty in making ceramic slurries for the purpose of

casting natural frameworks, this synthetic process of replication was put to one side. In order to make a prototype it was easier to use natural biological ceramic skeletons than synthesize them from their substituents-hydroxyapatite and polymer matrix. In particular, coral skeletons were employed (and possibly certain species of sea urchin spines), because they were easy to obtain and were of a consistently high quality. Coral skeletons and sea urchin spines (*Heterocentrotus trigonarius* and *Acanthaster planci*) were found to be very close matches to compact regions of the alveolar bone-the region adjoining the periodontal ligament (Table 8.13). And are, therefore suitable structures for securing an optical cylinder, assuming it is dealt with in the same manner as the tooth and bone support frame.

Table 8.13 *Achievements and Challenges of Selecting Suitable Natural Porous Solids and Employing the Replamineform Process*

Achievements	Challenges
Identified large numbers of likely candidate skeletal structures	Finding readily obtainable skeleton
Selected three highly suitable types of natural skeletal structure: Hard Coral, Sponges and Echinoderm spines	
Made reasonably good polymer (pMMA) replicates	Polymer replicates were not of a good enough quality using simple methods
Selected commercially available coral used for bone replacement surgery	

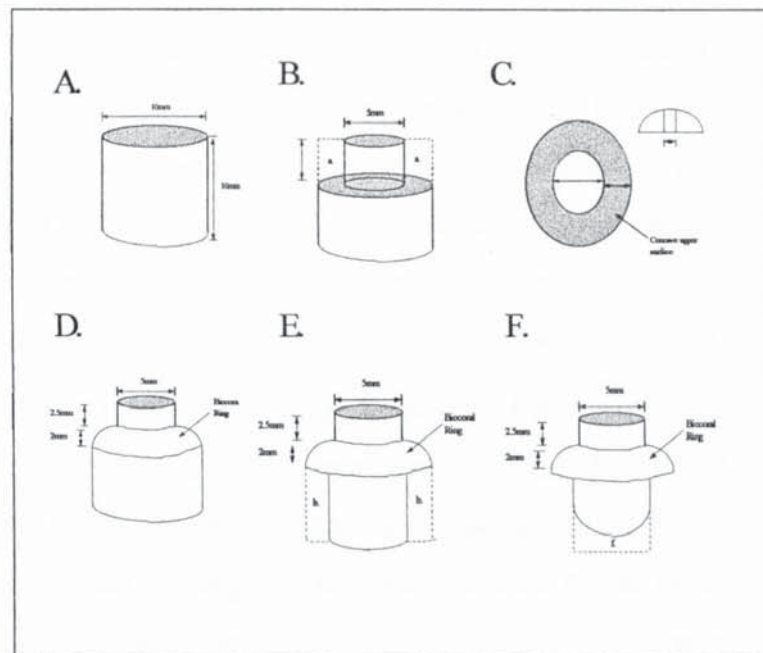
In the final stage of investigation-involving direct observations and measurements-coral skeletons were selected in preference to the equally suited varieties of sea urchin spines, because corals are used extensively to replace damaged bone and have been used successfully for approximately twenty years. Whereas, there is very little information of human tissue reactions (*both in vitro and in vivo*) to the implantation of sea urchin spines. This fact should not preclude them for consideration at a later date.

Corals as a distinct taxonomic group, possess a greater variation of highly interconnected open porosities; with each cell having open contact with every other in the immediate vicinity. Tissue that grows into such a pore system is firmly integrated with the solid structure, giving rise to long term attachment. The eventual species of

coral was *Porites porites*, since it possessed the recommended combination of: desired pore sizes, abundance and good availability (Table 8.1). Furthermore, corals were easier to get hold of, in large amounts from a number of commercial manufacturers to a medical grade of quality. Coral skeletons are not absolutely ideal, but are presently the strongest candidate available. Prototypes were designed and constructed with coral and pMMA-a material with excellent optical qualities.

In this study a synthetic analogue was constructed from porous biological ceramic Biocoral[®] (without a polymer matrix) bonded to a polymer base that part-way infiltrates the porous solid. Fabrication is in 4 distinct stages of cutting, shaping and polishing. The pMMA optical cylinder and Biocoral[®] are cut and machined separately before they are integrated by solvent welding which, is preferable to gluing. This relatively unique artificial cornea is shown schematically below in its various stages of fabrication (Figure 8.14). An optical pMMA cylinder is cut, to support a coral ring-convex on one side (A-C). Further cuts are made below the attached coral ring, before the coral and pMMA are shaped and polished (D-F).

Figure 8.14 Stages of Fabrication of a Coral and pMMA Artificial Cornea (A-F)



The structural features of the support frame for the prototypes included elements reasoned to be essential for the success of the Osteo-odonto-keratoprosthesis, including: a polymer ledge as a barrier to membrane proliferation and encapsulation (a function served by the impermeable cementum) and a porous structure for tissue integration and attachment (a function served by the uniformly complex graded porosity of alveolar bone).

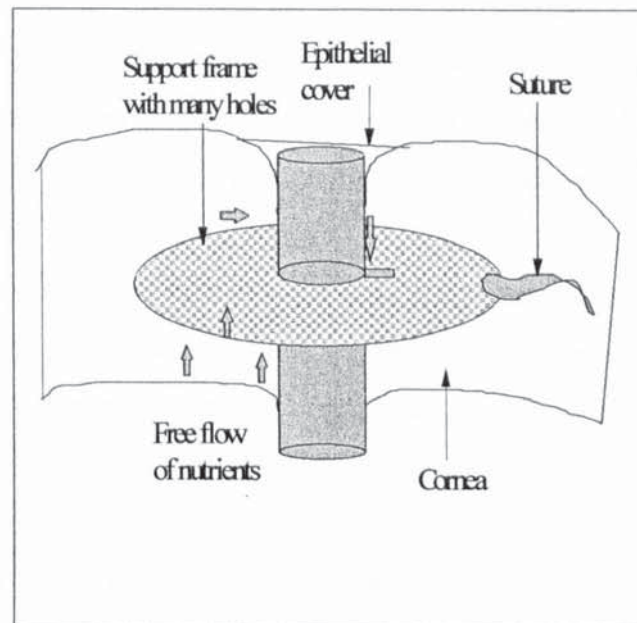
8.2 General Discussion

The aim of this study was to understand more about the mechanisms of biological attachment for the highly successful, tooth and bone (OOKP) support frame, and then incorporate them into a synthetic analogue. The process of fabricating a successful copy of the OOKP from the outset was not intended to slavishly replicate every physical and chemical feature of the tooth and bone. Rather the approach was to establish what were the key features that gave rise to the stable retention of the OOKP in situ. It was established that the properties of hydroxyapatite were vital to successful biological integration. Thus, the use of synthetic polymers for the support frame of the optical window was reduced to a minimum-only to provide a suitable interface for bonding with the optical cylinder. Polymers are a feature of the OOKP only to work in

increasing fracture toughness and strength without compromising stiffness.

Polymers of many types are widely employed in the construction of artificial corneas, however none have achieved the level of success of the OOKP. Although that could change judging by the potential of some recent designs. The outstanding clinical success of the OOKP strongly suggested that a biological ceramic could be used to stop common causes of rejection such as, tissue melting at the implant interface, ulceration and encapsulation by a shielding membrane. Engineers of artificial corneas have nearly always used polymers for the support frame.¹⁴ From the start of the most active period of research into keratoprosthesis, around the 1950's, the support frame was constructed with large holes to enable the secure attachment of sutures. Many of these devices induced melting of the cornea, and so it was thought that the support frame should possess many thousands of pores, to allow for transfer of nutrients around the implant and so nourish tissue more extensively than was possible with large pores in the support frame. Design features employed by keratoprosthesis engineers to reduce the major unwanted biological reactions are shown in Figure 8.16. Despite this, stable and healthy tissue reconstruction happens rather intermittently and is often linked to the mechanical properties of the material.

Figure 8.15 *A Schematic Drawing of a Standard Core and Skirt Artificial Cornea with Important Functions that Must be Allowed by Design*



Extensive investigations into the design of a support frame have demonstrated the importance of specific pore sizes, their distribution and the degree of interconnections between them. In recent times two important keratoprosthesis engineers: Chirila⁴⁹ and Legeais⁴⁷ focused on obtaining an optimal pore size, to maximise tissue integration and minimise the number of likely complications. Chirila found that pore size has a direct bearing upon the speed and amount of tissue inter-penetration. This may explain the moderate clinical successes of porous DacronTM and polytetrafluoroethylene (PTFE) felts.^{47,48} Legeais found that pore size influenced the amount of collagen synthesised and the number of cells per unit volume. Pore structure has been an important structural element in the design of a successful support frame and this finding is supported by studies demonstrating a direct causal link between local environment and tissue responses.

An implant will function for longer if these properties are maximised, i.e there is rapid and extensive integration and strong attachment. Both porous solids and fibrous meshes are structures that provide coherent frameworks for strong and stable tissue attachment and residence. This is because the structure of the immediate surroundings has a direct influence on tissue function. Both the arrangement of spaces in a structure

and surface texture convey information that directly influence cell phenotype¹²² as a result of stresses placed on the cell membrane and the connecting intracellular framework. Structure therefore, has the capacity to re-organise damaged tissue that has lost many of the cues for growth orientation and direction necessary for repair. This concept could be used to perfect the features of a porous framework for stable, long term attachment of the optical cylinder to the bulbar surface of the eye.

Material type also has strong influence on how surrounding tissue behaves. Stromal tissue behaves in a regular manner in and around fluoropolymers, although the rates of extracellular matrix deposition are not rapid enough to ensure complete enclosure before the attachment of bacteria or fibrous encapsulating membranes. However, success or failure of an artificial cornea is governed by many other factors of design and the mode of implantation, as described by Barber et al.

Barber et al. compiled a comprehensive list of causes of failures arising from implantation of an artificial cornea.¹¹⁹ (Table 8.1 and 8.11). He described two generic causes of failure arising from biological responses and mechanical effects. Many of the biological causes of failure can be ameliorated or eliminated through the application of specific design features. Mechanical causes of failure can be removed almost entirely with intelligent use of composites and use of optimised implant dimensions. Certain causes of failure can only be sorted out by rigorous and precise surgery and vigorous application of antihistamines and drugs to combat infection. So, the importance of design should not be over-emphasised.

In Table 8.3 (a & b) the OOKP reduces infection by the very rapid inward growth of buccal mucosa into the bone and the excellent sealing qualities that result. A well formed vasculature enables infectious agents to be attacked rapidly and prevents enzyme degradation. Membrane encapsulation is the prelude to expulsion, but is prevented in the OOKP by the periodontal ligament and cementum. The vitality of the graft tissues enables remodelling and adaptation to unforeseeable challenges. This property cannot be mimicked.

Table 8.14 *The Major Causes of Keratoprosthesis Failure:(a) Infections and Enzyme Degradation.*¹¹⁹

CAUSES OF PROSTHESIS FAILURE	SUGGESTED SOLUTIONS	SURGICAL METHODS	SOLUTIONS TACKLED BY OOKP	SOLUTIONS TACKLED BY CORAL KPRO*
Infections	Continuously intact epithelial barrier	Control infection; Use meticulous sterile technique & antibiotics	Buccal mucosal covering	Buccal mucosal covering
	Vascularisation of supporting tissue	Vascularisation of junction material	Combination of macro- and micropores to promote vasculature	Combination of macro- and micropores to promote vasculature
Enzyme Degradation	Continuously intact epithelial barrier	Meticulous surgery to uncover core		
	Vascularisation of supporting tissue	Use of anti-proteases		
	Control of leucocytes		Biotolerant materials	Biotolerant materials
	Inhibit collagenases		Excellent vascular network	Excellent vascular network

Table 8.15 *The Major Causes of Keratoprosthesis Failure (b) Membranes, Epithelial Downward Growth, IOP and Prosthesis Movement.*

CAUSES OF PROSTHESIS FAILURE	SUGGESTED SOLUTIONS	SURGICAL METHODS	SOLUTIONS TACKLED BY OOKP	SOLUTIONS TACKLED BY CORAL KPRO*
Membranes	Anterior barrier to conjunctiva	Adequate anterior core length	Periodontal ligament and cementum	Polymer barrier to inhibit proliferation
	Decrease inflammation	Minimise surgical trauma	Ability to repair and redesign to fit new circumstances	Biotolerant materials to ameliorate immunity; HAP: excellent bioadsorption properties
	Prevent fibrous tissue	Heparin coatings	Completely matched	
			Sound buccal mucosa attachment	Sound buccal mucosa attachment
Epithelial downward growth	Continuously intact epithelial barrier		Graded pore sizes; pores at two scales	Graded pore sizes; pores at two scales
	Rapid & continuous seal	Pre-vascularisation of implant site		
	Buccal mucosa covering	Buccal mucosa covering		
Intra-ocular pressure	Control & treat glaucoma	Aggressive control by Ahmed shunts		
Prosthesis Movement	Enhance tissue invasion of skirt		Optimised tissue scaffold	Polymer reinforced porous ceramic
	Minimise contact: lid & core			Adaptable plate size to allow optimal optic shape & size

Even the best qualified polymers for the support frame do not consistently last as long *in vivo*, as a large proportion $\frac{3}{4}$ of OOKP's, where retroprosthetic membrane formation and epithelial downward growth is uncommon.⁶⁴ The wound heals with the keratoprosthesis in place. These complications are more prevalent when materials are

implanted directly into the corneal stroma rather than placement on top of the cornea. Polymers used to construct previous artificial corneas support frames structures are not predisposed with a surface chemistry that prevents tissue melting or alternatively encourages a co-ordinated reconstruction of extracellular matrix. The OOKP is interesting in that it provides a pore system that allows inward growth of tissue (cells and matrix), rapidly and extensively and a surface biological compatibility.

The OOKP was a significant innovation because of its unusual method of implantation and employment of novel graft tissues. The OOKP is restricted to a small number of patients due to the complexity of surgery and costs. The aim of research in this study was to fabricate a synthetic version of the OOKP would overcome the lack of availability, reduce complex surgery and costs as shown in Table 8 a synthetic analogue could conceivably cut the total cost by half, mainly because it removes the major stage of operation to remove a piece of tooth and bone and cut it to shape.

A synthetic analogue is a clear improvement on the limited amount of available graft tissue in a number of ways: it can be tailored to suit the individual, it costs less to obtain, it is free from infection and it reduces surgical interference at least by half (Table 8.16). But it lacks the vitality and self-repair inherent in living graft tissue. The greatest improvement on the OOKP of a synthetic analogue would be that the optical properties can be enhanced, adapted and specified to increase the field of view and can allow for a decrease in the length of the optic which, should reduce the need for anterior segment reconstruction. However, such a synthetic analogue would require a similar mode of biological preparation, as the OOKP which, involves implantation in a pouch of flabby tissue under the lower eyelid for 3 months. This enables the support frame to acquire a level of self-immunity. The belief is that the healthy state of the buccal mucosa supporting tissue together with the polymer barrier, impregnated part-way into the pore structure, should be capable of inhibiting epithelial downward growth, the major cause of rejection. Assimilation of healthy buccal mucosa covering tissue, into the porous ceramic does not lead to tissue melting, chronic infection etc.

Table 8.16 A Cost Comparison Between the OOKP and a Future OOKP Analogue (At 1999 Prices)

OOKP	Approximate cost	OOKP analogue	Approximate cost
Operation (2 stages) 2x5hours		Operation (1 stage) 1x 5hours	
Anaesthetist (i)	£300	Anaesthetist (i)	£150
Surgeons x2 + Dental surgeon (ii)	£750	Surgeons x2 (ii)	£375
Nurses x3 (iii)	£300	Nurses x3 (iii)	£150
Facilities (iv)	£8,000	Facilities (iv)	£4,000
Cost of surgery	£9,350	Cost of surgery	£4,675
Cost of optic	£180	Cost of implant	£120
Cost of drugs	£2,000	Cost of drugs	£2,000
Total (Approximate)	£11,350		£6,675

There are three major functional components to the OOKP support frame which, overcome many significant complications. They are: (i) a porous framework, (ii) a meshwork structure and (iii) solid base. The important structural characteristics of these components that operate to reduce complications, have been identified and should all ideally be incorporated into a workable synthetic analogue.

(i) Porous Solid Framework

A large, disproportionate effort was expended on designing and fabricating a porous solid framework. There were at least three fabrication options available: fabrication of a polymer sponge, fabrication of a porous solid made from biological ceramic and fabrication of a composite structure. The second strategy is an obvious and pragmatic approach. There are a variety of methodologies for making porous ceramic solids but, more importantly biological ceramics are extremely well tolerated by the body. This excellent tolerance is explained by the list of attributes in Table 8.2. However, such materials are not strictly identical to bone, since there is an absence of polymer matrix.

Table 8.17 *Positive Attributes of Hydroxyapatite as a Biological Material for Human Implantation*

Hydroxyapatite: Physical Attributes	Hydroxyapatite: Biological Attributes
Forms stable micro- and macroporosities	Ready adsorption of Serum proteins (selective?)
Very stable in biological fluids	Stimulation of growth factors (TGF)
Non-toxic/ no synthetic organic or inorganic components present	Jumpstarts progenitors of tissue reconstruction
Amenable to surface manipulation	Constructive effect on matrix formation and maturation
Undergoes weak chemical surface reactions	

Naturally occurring hydroxyapatite was used to make a synthetic analogue of the alveolar bone surrounding the OOKP support frame. Skeletal frameworks, particularly from the marine environment possess structures similar to bone, since in one respect they perform similar roles for supporting living tissue under similar shear and compressive forces. For this reason coral skeletons are used extensively in bone replacement therapies.

The clinical literature describing the results of coral skeletons implanted into the human body is very positive.^{114,115,116,117} Both hard tissues and soft connective tissue penetrate the pores and channels rapidly and remain healthy, therein. Inflammation is uncommon because of the healthy state of tissue and neither this also inhibits bacterial contamination. Many natural artefacts were observed and characterised for their suitability as a bone analogue. On the basis of the large body of good quality clinical data, coral skeletons were selected in this study, as the porous structure for the support frame.

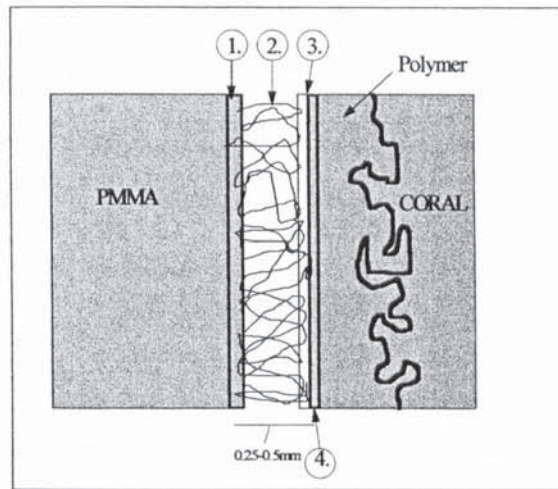
The pore structure of different coral skeletons matches up with different varieties of bone (haversian, lamellar). *In Porites*, for example the thickness of interconnecting

struts and pore sizes closely matches the open foam of long bone and jawbone. Species of *Seriatopora* closely match the porous structure of 'finer' bone types (thin struts and many interconnections) such as alveolar bone. In the past, support frames were punctured with holes. The number of holes or the number of interconnections between them, where they existed, were small so that surrounding tissue could not interweave itself into the material and be fully supported. Polymer meshes are employed in recent artificial corneas. While the pore spaces present are more connected and extensive, the structure is looser and provides less support. A three dimensional interconnection of pores and channels, as exemplified by OOKP bone, enables rapid and extensive inward tissue growth.

(ii) Meshwork Structure

A meshwork structural component could conceivably be copied with fibrous synthetic polymers (Dacron™) or biological polymers (collagen type I). A polymer barrier should impede encapsulation by epithelium, that functions to plug the wound and exclude the artificial cornea embedded at the wound site. In this study a meshwork was not incorporated into the prototypes, because it was too complicated to do so. An artificial cornea should be simple in design and therefore, simple to fabricate. In Figure 8.13 below, is a suggested scheme to fabricate a synthetic periodontal ligament, if the solid pMMA polymer barrier does not function as an anti-encapsulation device.

Figure 8.16 Hypothesised Synthetic Periodontal Ligament Analogue Between pMMA and Porous Coral



1. Dichloromethane and pMMA layer; 2. Ligament analogue (ePTFE, Collagen, DacronTM, chemically altered Fibrin mesh); 3. Phosphodiester layer; 4. PEG Spacers, Silanol linkages (Dimethyl chlorosilane)

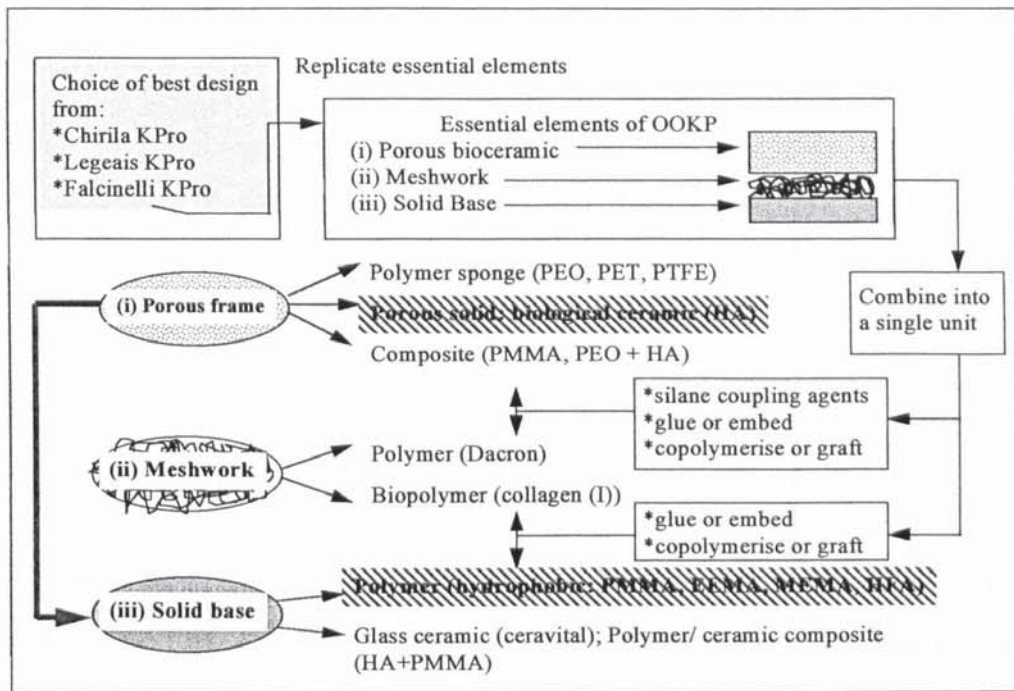
The inclusion of a periodontal ligament into a prototype was very difficult to achieve in practice. Substitutes of the periodontal ligament, though have been devised as tooth replacements to establish a strong attachment to the jaw bone. They have been integrated successfully.^{123,124} In both implants, synthetic fibres were physically embedded into them and functioned as substrates for bone re-generation. Incorporation of a periodontal ligament thus, replicating the features of the tooth and bone construction is not a feasible option, since it would have to be combined with the block of biological ceramic at its formation to get the fibres embedded. In any case the polymer ledge should be sufficient as a barrier to retroprosthetic membrane formation and epithelial downward growth. This can only be proved by implantation trials.


(iii) Solid Base

The solid base of an OOKP analogue can be made from methacrylate polymer-compatible with an optical cylinder-glass ceramic or a composite of polymer and ceramic. The greatest challenge was to formulate a method for combining the three elements into one integral, functional unit. This is illustrated in the figure below

(Figure 8.14). What was actually fabricated is highlighted in the same figure.

Figure 8.17 Fabrication Strategies for a Biomimetic Osteo-odonto-keratoprosthesis

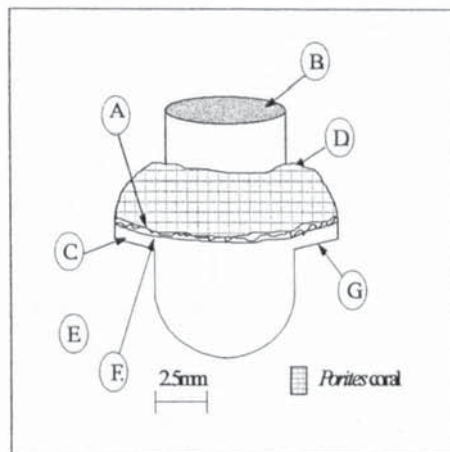


Key	
PEO	Polyethyleneoxide
PET	Polyethyleneterephthalate
PTFE	Polytetrafluoroethylene
PMMA	Polymethylmethacrylate
HA	Hydroxyapatite
Dacron	Polyethyleneterephthalate mesh
EEMA	Ethoxymethacrylate
MEMA	Methoxymethacrylate
HFA	Hydrofluoroacetate
Ceravital	silicon dioxide/ Magnesium oxide/ Calcium oxide/ Disodium oxide/ Dipotassium oxide/ Calcium phosphate
	What was actually carried out

The design of artificial cornea fabricated in this study provides similar solutions to overcome causes of keratoprosthesis failure.¹¹⁹ It also possesses a small selection of improvements such as, no gluing of components and a convex Biocoral^(R) surface to reduce the amount of covering tissue needed. The dimensions of the optical cylinder match those of the OOKP. A polymer flange is integrated with a the porous coral piece

and provides a barrier between functioning and non-functioning tissue. All the features of a coral and pMMA analogue of the OOKP are represented below in Figure 8.18.

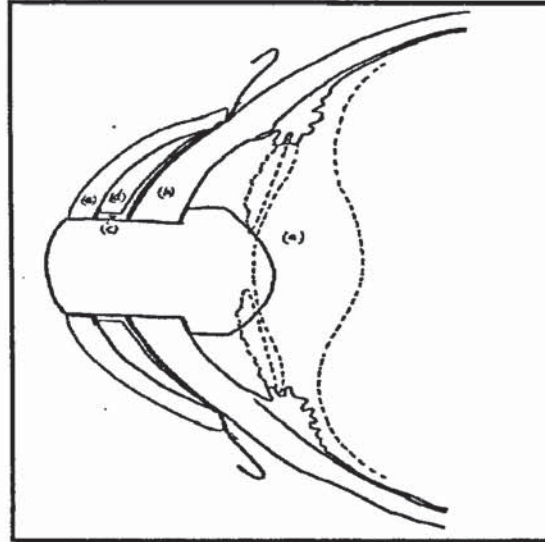
Figure 8.18 *Essential Features of the Coral and pMMA Keratoprosthesis*



(A). Regions of impregnation into Biocoral[®] pore spaces; (B). Optical cylinder as used in Falcinelli KPro; (C). Tailor Polymer mechanical properties at contact area to coral (i.e stiffness and strength); (D). Curvature to anterior surface of Biocoral: minimise stress concentrations and amount of buccal mucosa; (E). Optimum ratio of coral and polymer for best stiffness in bending; (F). Gluing of components is avoided; (G). Polymer ledge to rest on cornea and separate healthy graft from potentially pathogenic tissue

On the basis of information given before, it seems certain that the healthy and organised state of graft mucosal tissue within the porous coral, will ensure tight sealing qualities, so stopping egress of fluids and ingress of pathogens, a reduced incidence of scarring and improved mechanical performance (i.e relieving build up of strain energy). Crucially there was not a totally analogous replacement to the periodontal ligament, because of the difficulty of attaching fibres to the pre-formed biological ceramic. Implantation trials will determine whether a polymer ledge is a sufficiently good replacement.

Figure 8.19 *Cross-sectional View through the Anterior Eye to Show an Implanted Coral Keratoprosthesis (dotted lines represent removed iris and lens)*



The prototype was designed to be inserted just as the OOKP would be, and using the same surgical techniques. Attachment will be facilitated by buccal mucosal bandaging. Using this mode of insertion and means of attachment to the eye, in itself prevents some of the difficulties that have arisen in other keratoprosthesis that are inserted into the cornea. Intracorneal insertion is an equally valid option as 'on-top' placement, but may require surface modification of the polymer. On balance this design is likely to provide firm uncomplicated attachment to buccal mucosa on the strong basis of clinical data for coral bone replacement materials. While the polymer base should stop any possible epithelial downward growth and likely extrusion.

8.3 Conclusion

A successful keratoprosthesis support frame should be able to carry out two primary functions. They are to dissipate the mechanical loads uniformly aiding stabilisation and to provide a suitable framework for tissue reconstruction. Together they are effective at reducing opportunities for infection, preventing: fistulation, necrosis and ulceration.

Experiments were devised to fabricate a biological ceramic with suitable porosity and combine it with an optical cylinder in an attempt to make a synthetic approximation of

the Osteo-odonto-keratoprosthesis (OOKP). There was particular use of novel biomimetic strategies such as, sol-gel derived ceramic gels,⁸⁵ template induced mineralisation,⁸² in-solution calcification⁸¹ and replamineform processing.¹¹⁵ The latter required use of natural artifacts as casting templates. Natural artifacts could also be used without replacing the initial biological material with a synthetic material. However, major difficulties arose in identifying biological objects with the right set of properties, such as compliancy, porosity (75% of total volume and interconnected) and density. Fortunately, as we discovered there are many objects found in nature with a porous architecture appropriate for cellular infiltration and support, ranging from protective spines of echinoids to the hard skeletons of Scleractinian 'reef building' corals.

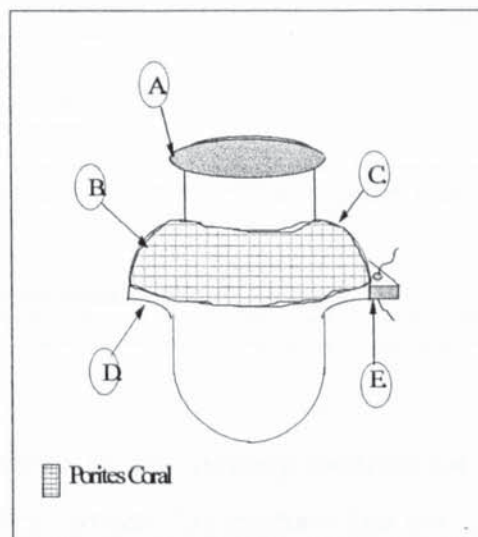
Coral derivatives such as, Biocoral[®] and Pro-Osteon[®] were chosen for tissue integration and as a structural analogue of the dental lamina alveolar bone, as used to support an artificial cornea. They are some of the most clinically acceptable and proven structures available.^{120,117} Biocoral[®] and Pro-Osteon[®] are derived from massive coral skeletons and in addition to their much examined biological tolerance possess a unique architecture and high compressive stiffness. There are certain problems with Biocoral[®] because, of its brittleness and the mismatch in modulus of stiffness with pMMA and at the host-implant interface. Coral resorption may reduce long term support. Thus, it must be transformed into a stoichiometric calcium phosphate form to enable a more permanent attachment.

Coral derivatives are superb frameworks for structuring and supporting living tissue. This is attested to, by their considerable biological tolerance and serves as a passive matrix for the formation of fully functioning healthy tissue and a well developed vasculature.¹²⁵ But, for a more insightful evaluation of how the implant will perform, the next step should be implant prototypes into an animal body site (e.g. intermuscular site), that bears close resemblance to the habitat of mucosa.

8.4 Suggestions for Further Work

The best design of prototype should be implanted into an animal model preferably in the eye or alternatively in subcutaneous tissue (i.e cheek). Once this has been completed the development and condition of tissue in and around the implant should be checked at regular intervals from 1 week up to 6 months. During this time measurements should be carried out of the depth of tissue penetration and rate of penetration to establish the strength of attachment, together with histological observations to establish the quality of tissue (maturity, health). A desirable implant would induce rapid and extensive tissue inward growth, vascularisation and the ability to inhibit epithelial development and encapsulating membranes.

Figure 8.2 *Suggested Additional Features of Design for a Coral and pMMA Artificial Cornea.*

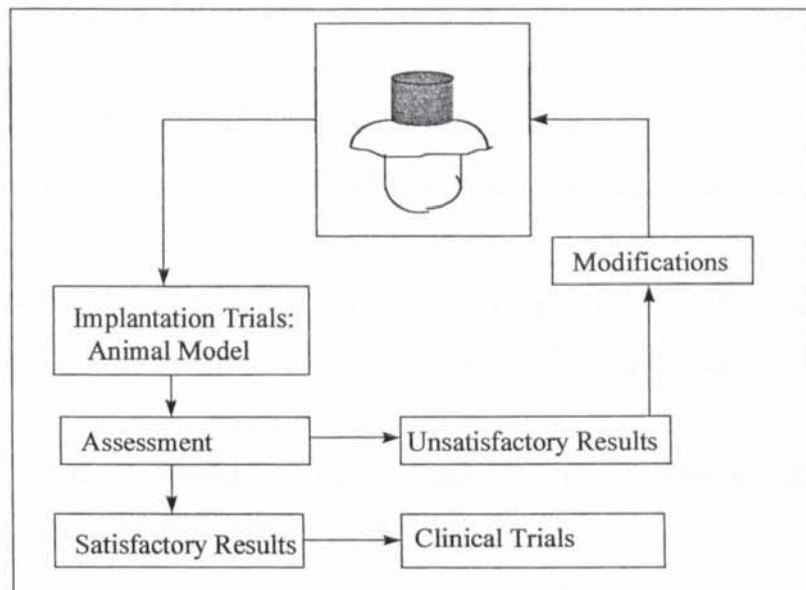


Key: A Circular flange; B Oval shaped disc; C Increased diameter; D. Curved lower side to polymer ledge; E Suture hole in extended polymer ledge

While sol-gel synthesis and in-situ mineralisation did not as predicted, produce a bone-like biological ceramic, it would be nevertheless fruitful to spend more time developing these biomimetic techniques further. By using such techniques, biological ceramics can be chemically attached to polymer in precisely controlled ways. For example the thickness of the ceramic layer and pore size distribution within that layer could be precisely determined. Further experimental work should seek to prevent the direct use

of natural artefacts that cause damage to natural habitats. More attention should be placed on using the replamineform process to produce casts of natural artifacts. At the same time it would reduce production costs and damage to the natural environment. Alternatively, there is scope for looking to use ceramer composites. Better methods would have to be developed, though to manufacture ceramers with a graded pore structure, so that porous hydroxyapatite is exposed on one side and solid polymer on the other side.

Figure 8.21 *Summary of Suggested Further Work*



It may also be worthwhile to try and develop methods for producing a full thickness contact lens shaped artificial cornea, for insertion into the corneal stroma. As a result of intrasomal implantation, the invasiveness of surgery and need for re-inforcement tissue is further reduced. Attempts at fabrication of a cornea shaped device in this study, hinted to its feasibility. What is required is highly specified diamond edged tooling to perfect the machining of coral skeleton. A better alternative to inclusion of coral skeletons are sea urchin spines. In the past these spines have been cut into small screw shapes and are less liable to fracture during production since they are composed of a single crystal rather than many crystals packed together, as one finds with coral skeletons.⁸⁶

LIST OF REFERENCES:

- 1 Barber, J.C., (1988): Keratoprotheses: Past and Present. *International Ophthalmology Clinics*; Vol 28, No. 2; Summer: pages 103-110.
- 2 Allcock, H., (1992): Rational Design and Synthesis of New Polymeric Materials. *Science*; Vol. 255: pages 1106-1112.
- 3 Cardona, H., (1964): Keratoprosthesis: Acrylic Optical Cylinder with Supporting Intralamellar Plate. *Am. J. Ophthal*; 64: pages 228-233.
- 4 Barber, J.C., (1993): Modifications of Keratoprosthesis to Improve Retention. *Refractive and Corneal Surgery*; Vol. 9, May/June 1993: pages 200-201.
- 5 Dohlman, C.H., Nehaud, P.A., W.-C. Fung, (1995): Experience with a Keratoprosthesis. *An. Inst. Barraquer (Barcelona)*; 28 (Suppl): pages 105-109.
- 6 Chirila, T.V., Constable, I.J., Crawford, G.J., Russo, A.V., (1994): Keratoprosthesis. *US Patent 5,300,116*, 5 April.
- 7 Legeais, J.M., Rossi, C., Renard, G., Savoldelli, M., D'Hermies, F., Pouliquen, Y., (1992): A New Fluorocarbon for Keratoprosthesis. *Cornea*; 11: pages 538-545.
- 8 Gipson, I.K., and Sugrue, S.P., (1992): Corneal Surfaces: Cell Biology of the Corneal Epithelium. In: *Principles and Practice of Ophthalmology*, Albert, D.M., et al. (eds). W.B. Saunders Co, Philadelphia.
- 9 Tighe, B.J., (1990): Blood, Sweat and Tears-Some Problems in the Design of Biomaterials, Nissel Memorial Lecture, Royal Society of Medicine; Reprinted in *Journal of B.C.L.A*, 13; (1): pages 13-19.
- 10 Berman, E.R., and Blakemore, C., (1991): *Biochemistry of the Eye*; Perspectives in Vision Research Series, Plenum Press, New York.

- 11 Benedek, G.B., (1971): Theory of Transparency of the Eye. *Applic Optics*; 10: page 459.
- 12 Trinkaus-Randall, V., (1993): Cornea. Chapter 26: pages 383-401 In *Principles of Tissue Engineering*; eds. Lanza, R.P., Langer, R., and Chick, W.L. Landes Bioscience.
- 13 Foster, A., (1993): Worldwide Blindness, Increasing but Avoidable!. *Sem Ophthal*; Vol.80, April: pages 167-170.
- 14 Mohan, M., and Panda A., (1988): Artificial Cornea. Chapter 69: pages 383-385. In *The Cornea: Transactions of the World Congress on the Cornea III*, ed. Cavanagh, H.D., Raven Press, Ltd., New York.
- 14 Singh, D., (1984): Keratoprosthesis. *Indian J. Ophthalmol*; 932, (5): pages 405-407.
- 16 Van-Andel, M.V., and Singh, I., (1999): Artificial Corneas for the Third World? The Best Efforts for the Worst Cases: *An. Inst. Barraquer*, (Barcelona); 28 (Suppl): pages 177-179
- 17 Fehervari, Z.T.F., (1997): Immunomodulation of Rat Corneas by a Gene Therapy Approach. *MSc. Thesis*. Royal Postgraduate Medical School, London.
- 18 Thoft, R.A., Friend, J., and Dohlman, S.N., (1975): Corneal Glucosae Flux. Its Response to Anterior Chamber Blockade and Endothelial Damage. *Arch Ophthalmol*, (Fr); 86: pages 685-691.
- 19 Hatt, M., (1979) Experimental Osteokeratoprosthesis. *Ophthalmic Res*; 11: pages 40-51.

- 20 Mazhdrakova, L., and Vybov, S., (1978): Experimental keratoprosthetics with the use of Claw Particles Implanted in the Cornea, In: *Papers of the International Conference on Keratoplasty and Keratoprosthetics*. pages 135-136. Ministry of Health of the USSR, Moscow.
- 21 Krasnov, M.M., and Udintsov, B.E., (1975): Autoallokeratoplasty Reconstructive Autotransplantation of the Cartilage, the periosteum and the Sclera as the Basis of Keratoprosthetics. *Vestnik Oftal'mologii*; 1: pages 35-39.
- 22 Barber, J.C., (1993): Modifications of Keratoprosthesis to Improve Retention. *Refractive and Corneal Surgery*; Vol.9, May/ June: pages 200-201.
- 23 Kruse, F.E., (1994): Stem Cells and Corneal Epithelial Regeneration. *Eye*; 8: pages 170-183.
- 24 Van Andel, J., (1993): Results of Champagne Cork Keratoprosthesis in 127 Corneal Blind Eyes. Kpro Abstracts, *Refractive and Corneal Surgery*; May/ June Vol 9: pages 189-190.
- 25 Fyodorov, S.N.; Moroz, Z.I., Zuev, V.K., (1982): Keratoprostheses. Churchill Livingstone. Edingburgh.
- 26 Falcinelli, G., (1993) Osteo-odonto-keratoprosthesis: Present Experience and Future Prospects. *Refractive and Corneal Surgery*; 9: pages 193-194.
- 27 Wintermantel, E., Mayer, J., Blum, J., K.-L., Eckert, Luscher, P., and Mathey, M., (1996): Tissue Engineering scaffolds using Superstructures. *Biomaterials*; Vol 17, No.2: pages 83-91.
- 28 Langer, R., Vacanti, J., Vacanti, C.A., and Vunjak-Novakovic, G., (1995): Tissue Engineering: Biomedical Applications. *Tissue Engineering*; Vol 1, Number 2: pages 151-161.

- 29 Parel, J-M., (1999): 200 Years of KPro: Pellier de.Quengsy and the Artificial Cornea. *An. Inst. Barraquer, (Barcelona)*; 28 (Suppl): pages 33-41.
- 30 Nussbaum, I., (1856): Die Behandlung der Nornhauttrubungen mit besonderer Berucksichtigung der kunstlicher Hornhaut (cornea artificialis), Munchen.
- 31 von Hippel, A., (1877): Uber das operative Behandlung totaler stationarer Hornhauttrubungen. *Graeffes Archiv fur Klinisch und Experimentall Ophthalmologie* 23, 2: pages 79-160.
- 32 Dimmer, F., (1891): Notiz uber Cornea artificialis. *Klinische Monatsblätter fur Augenheilkunde*; 29: pages 104-105.
- 33 Salzer, F., (1895): Uber Kunstlichen Hornhautsatz. *Deutsch Ophthalmologie Gesell schaft*, Berlin; 23: pages 230-235.
- 34 MacPherson, D.G., and Anderson M.J., (1953): Keratoplasty with Acrylic Implant. *British Medical Journal*; pages 330-353.
- 35 Stone, W, and Herbert, E., (1953): Experimental Study of Plastic Material as Replacement for Cornea. Prelim Report. *Am. J. Ophthalmol*; 36, 6: pages 68-73
- 36 Knowles, W., (1961): Effect of Intralamellar Plastic Membranes of Corneal Physiology. *Am. J. Ophthalmol*; 51: pages 274-284.
- 37 Bock, R. and Maunemee, A., (1953): Corneal Fluid Metabolism. Experiments and Observation. *Archives d'Ophthalmologie*; 50: pages 282-285.
- 38 Bagrov, S.N., (1973): Corneal Damages in the Case of Non-Penetrating Keratoprosthetics (Pressing problems of Ophthalmology) Medical Institute, Kuibyshev: page 185.

- 39 Stone, W., (1958): Alloplasty in Surgery of the Eye. *New England Journal of Medicine*; 258: pages 486-490, 596-602.
- 40 Krasnov, M.M., Udintsov, B., and Malaeva, L., (1978): Results of Penetrating Autochondrokeratoprosthetics and the Post-operative Care of Patients, In: Papers of the International Conference on Keratoplasty and Keratoprosthetics. Filatov Res. Inst. Odessa: pages 132-135.
- 41 Puchkovskaya, N.A., Udintsov, B.E., Labush, M., (1970): Corneal Alloplasty. *Oftal'mologicheskii Zhurnal*; 4: pages 247-252.
- 42 Krasnov, M. M., Udintsev, B.E., Labash, M., (1984): A New Technique of a Through Keratoprsothesis. (The Simultaneous Implantation of a Keratoprosthesis with Retrocorneal autochondrokeratoplasty). *Vestr Oftalmol*; 5: pages 31-34.
- 43 White, E., (1988): Corneal Implant. *United States Patent*. 4,772,283, September 20^h.
- 44 Cremona, C.M., (1995): Keratoprosthesis from the Methyl Methacrylate Periosteum: In *Abstracts of the 2nd KPro Study Group Meeting*; 20-23 June 1995, Pontifica Universitas Urbana, Rome, Italy.
- 45 Blencke, A. Hagen, P., Bromer, H., Deutscher, K., (1978): Untersuchungen uber die Verwendbarkeit von Glaskeramiken zur Osteo-Odonto-Keratoplastik. *Ophthalmologica, Basel*; 176: pages 105-112
- 46 Hoffman, F., Harnisch, J.P., Strunz, V., Bunte, M., Gross, U.M., Manner, K., Bromer, R., Deutscher, K.,(1978): Osteo-keramo-keratoprosthese. Eine Modification der Osteo-odonto-keratoprosthesis nach Strampelli. *Klinische Monatsblätter fur Augenheilkunde*; 173: pages 747-755.
- 47 Legeais, J-M., (1993): A Novel Colonizable Keratoprosthesis. KPro Abstracts, *Refractive and Corneal Surgery*; Vol.9., May/June: pages 205-206

- 48 Pintucci, S., Pintucci, F., Caiazza, S., (1993): The Dacron Felt Colonisable Keratoprosthesis. *Refractive Corneal Surgery*; 9:pages 196-197.
- 49 Chirila, T.V., (1994): Interpenetrating Polymer Network (IPN) as a Permanent Joint between the Elements of a New Type of Artificial Cornea. *Journal of Biomedical Materials Research*; Vol.28: pages 745-753.
- 50 Choyce, D.P., (1968): The Present status of Intra-Cameral and Intra-corneal Implants. *Canadian Journal of Ophthalmology*; 3: pages 647-652.
- 51 Abel, R., (1988): Development of an Artificial Cornea: I. History and Materials. Chapter 39. The Cornea: Transactions of the World Congress on the Cornea III, eds., H. Dwight Cavanagh. Raven Press, New York: pages 225-229.
- 52 Villain, F., Hostyn, P., Kuhne, F., Parel, J-M., (1992): Polyethylene Oxide Hydrogel and Siloxane Polymers for Cornea Refractive Surgery. *10th Congress of European Society of Cataract and Refractive Surgery*; 10: pages 137.
- 53 Kain, H.L., (1990): A New Concept for Keratoprosthesis. *Klin Monatsbl Augenheikld*; 197, (5): pages 386-92.
- 54 Capecchi, J.T., Heilmann, M., Krepski, L.R., Kwon, O-S., Olson, D. B., (1992): Corneal Implants and Manufacture and use Thereof, *U.S. Patent 5, 108,428*, April 28th.
- 55 Wu, X.Y., Tsuk, A., Leibowitz, H.M., and Trinkaus Randall, V., (1998): In vivo Comparison of Three Different Porous Materials Intended for Use in a Keratoprosthesis. *British Journal of Ophthalmology*: 82: 5: pages 569-576.
- 56 Chirila, T.V., (1997): Artificial Cornea with a Porous Polymeric Skirt. *Trends in Polymer Science*; Vol. 5, No. 11, November: pages 346-348.

57 Hicks, C.R., Chirila, T.V., Clayton, A.B., Fitton, J.H., Dalton, P.D., Vijaysekaran, S., Lou, X., Hatten, S., Ziegelaar, B., Hong, Y., Crawford, G.J., Constable, L.J., (1998): Clinical Results of Implantation of the Chirila Keratoprosthesis in Rabbits.

British Journal of Ophthalmology; 82: pages 18-25.

58 Kornmehl, E.W., Bredvik, B.K., Kelman, C.D., Raizman, M.B., DeVore, D.P., (1995): In vivo Evaluation of a Collagen Corneal Allograft Derived from Rabbit Dermis. *Journal of Refractive Surgery*, Volume 11; November/December: pages 502-507.

59 White, J., and Gona, O., (1988): Proplast for Keratoprosthesis. *Ophthalmic Surgery*; 19: pages 331-333.

60 Caldwell, D.R., and Jacob-LaBarre, J.T., (1989): Intraocular Prostheses, *US Patent*. 4,865,601, Sept. 12th.

61 Liu, C. and Tighe, B.J., (1995): The Properties of the Ideal Keratoprosthesis. *Poster at 2nd KPro Study Group Meeting*; 20-23 June 1995, Pontifica Universitas Urbana, Rome, Italy.

62 Ratner, B. (1993): New Ideas in Biomaterials Science-A Path to Engineered Biomaterials. *Journal of Biomedical Materials Research*; Vol 27: pages 837-850.

63 Ianetti, F., (1988): 20 Years Follow-up of OOKP. In *Blodi, F. Acta XXVth. Congress Ophthalmol*, Roma, Berkley Milano, Ghedini; Vol 1: pages 1165-1168.

64 Strampelli, B., and Marchi, V., (1970): Osteodontokeratoprosthesis. *Annali di Ottalmologia e clinica oculistica*; Vol. XCVI, No. 1: pages 1-29.

65 Casey, T.A., (1965): Osteo-odonto-keratoprosthesis and Chondrokeratoprosthesis; *Proc Royal Soc.Med.* 63: pages 313-314.

66 Temprano, A.J., (1993): Keratoprosthesis with Tibial Autograft. *Refractive and Corneal Surgery*; Vol. 9, May/June: pages 192-193.

- 67 Liu, C., and Pagliarini, S., (1999): Independent Survey of Long Term Results of the Falcinelli OOKP. *Ann. Inst. Barraquer, (Barcelona)*; 28: (Suppl): pages 91-93.
- 68 Caiazza, S., Pintucci, S., and Falcinelli, G., (1990): Exceptional Case of Bone Resorption in an Osteo-odonto-Keratoprosthesis: A Scanning Electron Microscopy and X-Ray Microanalysis Study. *Cornea*; 9, (1): pages 23-27.
- 69 Marchi, V., Ricci, R., Pecorella, A., Ciardi, A., and Di Tondo, U., (1994): Osteo-Odonto-Keratoprosthesis: *Description of Surgical Technique with Results in 85 Patients*. *Cornea*; 13, (2): pages 125-130.
- 70 Caiazza, S., Pintucci, S., and Donelli, G., (1993): Biointegrable Keratoprosthesis: Performances and Recent Improvements. *Italian Journal of Ophthalmology*; VII/ I: pages 13-20.
- 71 Berkowitz, B.K.B., (1992): A Colour Atlas and Text of Oral Anatomy: Histology and Embryology. 2nd Edition. Mosby-Wolfe, London.
- 72 Williams, D., (1990): Concise Encyclopedia of Medical and Dental Materials. Eds, Williams, D., Cahn, R.W., and Bever, M.B. Pergamon Press. Oxford.
- 73 Ricci, R., Pecorella, I., Ciardi, A., Della Rocca, C., Di Tondo, U., Marchi, V., (1992): Strampelli's Osteo-odonto-keratoprosthesis. Clinical and Histological Long-Term Features of Three Prostheses. *British Journal Ophthalmol*; 76, (4): pages 233-234.
- 74 Structure of Metals. S247 Inorganic Chemistry, Open University Publications, Milton Keynes, U.K.: pages 6-10.
- 75 Hulbert, S.F., Young, F.A., and Mathews, R.S., (1970): Potential of Ceramic Materials as Permanently Implantable Skeletal Prostheses. *Journal of Biomedical Materials Research*; 4: pages 433-456.

- 76 J.D., Bobyn, Wilson, G.J., MacGregor, D.C., Pilliar, R.M., Weatherly, G.C., (1982): Effect of pore size on the Peel Strength of Attachment of Fibrous Tissue to Porous Surfaced Implants. *Journal of Biomedical Materials Research*; Vol. 16: pages 571-584.
- 77 Liu, D.M., (1996): Porous Hydroxyapatite Bioceramics. *Bioengineering Materials*; 1996, Vol.115: pages 209-232.
- 78 Piddock, V., (1991): Production of Bioceramic Surfaces with Controlled Porosity, *The International Journal of Prosthodontics*; Vol. 4, No.1: pages 58-61.
- 79 Lydon, F., (1994): *Novel Hydrogel Co-Polymers and Semi-Interpenetrant Polymer Networks*. Ph.D. Thesis, University of Aston in Birmingham, U.K.
- 80 Singh-Gill, U., (1994): The Use of Novel Plasma Etching and Monitoring Systems (PEEMS) in Contact Lens Spoilation Studies. Poster Presentation at *British Contact Lens Association Meeting, Torquay*.
- 81 Kokubo, T., Hata, K., Nakamura, T., and Yamamuro, T., (1991): Apatite Formation on Ceramics, Metals and Polymers Induced by a CaO-SiO₂-Based Glass in a Simulated Body Fluid. In *Bioceramics*; Vol. 4. Edited by W.Bonfield, Hastings, G.W., Tunner, K.E., Butterworth Heinemann, Guildford, UK: pages 113-120.
- 82 Mann, S., Heywood, B.R., Rajam, S., and Birchall, J.D., (1988): Controlled Crystallisation of CaCO₃ under Stearic Acid Monolayers. *Nature*; Vol. 334, 25th August: pages 692-695.
- 83 Wong, K.W., Brisdon, B.J., Heywood, B.K., Hodson, A.G.W., Mann, S., (1994): Polymer Mediated Crystallisation of Inorganic Solids: Calcite Nucleation on the Surfaces of Inorganic Polymers. *J. Mater. Chem*; 4: pages 1387-1392.

- 84 McAteer, J.A., and Davis, J., (1994): Basic Cell Culture Technique and the Maintenance of Cell Lines: In Davis, J.M., (ed.); *Basic Cell Culture: A Practical Approach*. IRL Press, Oxford University Press, Oxford.
- 85 Yanagida, H., Koumoto, K., Miyayama, M., (1996): *The Chemistry of Ceramics*. Wiley and Maruzen. Chichester, U.K.
- 86 Weber, J.N, and White, E.W. (1972): Replamineform: A New Process for Preparing Porous Ceramic Metal, and Polymer Prosthetic Materials. *Science*; 26 May: pages 922-924.
- 87 Yasin, M., (1988): *Melt Processable Biomaterials for Degradable Surgical Fixation Devices*. Ph.D. Thesis, Aston University in Birmingham, U.K.
- 88 Harrison, A., (1995): *Fractals in Chemistry*. Oxford Primer Series, Oxford Science Publications. Oxford.
- 89 Gibson, L.J., and Ashby, M.F., (1988): *Cellular Solids: Structure and Properties*. Pergamon Press.
- 90 Graham, C., (1997): *Cellular Interaction with Novel Biomaterials*. Ph.D. Thesis, University of Aston in Birmingham, U.K.
- 91 Mann, S., (1996): *Biomaterialisation and Biomimetic Materials Chemistry*: pages 1-37. In: *Biomimetic Materials Chemistry*; Mann, S., (ed.). VCH. New York.
- 92 Atkins, P.W., (1995): *The Periodic Elements*. Wiedenfield and Nicolson, London.
- 93 Hulbert, S.F., Bokros, J.C., Hench, L.L., Wilson, J., and Heinke, G., (1987): *Ceramics In Clinical Applications Past, Present and Future*. In: *High Tech Ceramics*. Vincezine, P., Elsevier, Amsterdam, Netherlands: pages 189-213.

- 94 Hench, L., and Wilson, J., (1984): Surface-Active Biomaterials. *Science*; Vol 236, 9 November: pages 630-635.
- 95 Young, R.A., (1975): Biological Apatite vs. Hydroxyapatite at the Atomic Level. *Clinical Orthopaedics and Related Research*; Number 113, November-December: pages 249-262.
- 96 Bonfield, W., (1998): Composite Biomaterials. In: *Bioceramics*, eds. Kokubo, T., Nakamura, T., and Miyaji, F., Vol. 9: pages 11-13.
- 97 Verheyen, C.C.P.M., de Wijn, J.R., van Blitterswijk, C.A., and de Groot, K., (1993): Evaluation of Hydroxylapatite/ poly(L-lactide) Composites: Physico-Chemical Properties. *Journal of Materials Science: Materials in Medicine*; 4: pages 58-65.
- 98 Rodriguez-Lorenzo, L.M., Salinas, A.J., Vallet-Regi, M, and San Roman, J., (1996): Composite Biomaterials Based on Ceramic Polymers I. Re-inforced Systems Based on Al_2O_3 / PMMA/ PLLA. *Journal of Biomedical Materials Research*; Vol.30: pages 515-522.
- 99 Yokogawa, Y., Reyes, J.P., Mucalo, M.R., Toriyama, M., Kawamoto, Suzuki, T., Nishizawa, K., Nagata, F., and Kamayama, T., (1996): Preparation of Calcium Phosphate Compound-Chitin Fiber Composite Material, In: *Bioceramics; Otsu, Japan. Vol.9* : pages 427-430.
- 100 Aksay, I.A., Staley, J.T., Prud'homme, R.K., (1996): Ceramics Processing with Biogenic Additives; Chapter 13: pages 361-378: Mann, S., (ed): In *Biomimetic Materials Chemistry*. VCH. New York.
- 101 Clarkson, E.N.K., (1984): Invertebrate Palaeontology, 2nd Edition. Harper Collins. London.

- 102 Bold, H.C., (1987): *Morphology of Plants and Fungi*. Fifth Edition. Harper and Row, New York.
- 103 Barnes, R.D., (1987): *Invertebrate Zoology*. Fifth Edition. Saunders College Publishing, International Edition.
- 104 Berquist, P.R., (1978): *Sponges*. Hutchison. London.
- 105 Vincent, J.F.V., (1993): *Structural Biomaterials*. Princeton University Press.
- 106 Weber, J.N., and White, E.W., (1973): Carbonate Minerals as Precursors of New Ceramic, Metal, and Polymer Materials for Biomedical Applications. *Min Sci. Engng*; Vol 5, No.2, April: pages 312-323
- 107 Donnay and Pawson, D.L., (1969): *Science*; 166: pages 1147-1152.
- 108 Lincoln, R.J., and Boxshall, G.A., (1987): *The Cambridge Illustrated Dictionary of Natural History*. Cambridge University Press.
- 109 Hayward, P.J., and Ryland, J.S., (1984): *British Ascophoran Bryozoans. Synopses of the British Fauna (New Series)*; Kermack, D.M., and Barnes, S.K, (eds). The Linnean Society of London. Academic Press.
- 110 Kelly-Borges, M., Vacelet, J., and Pomponi, S.A., (1994): *A Simple Fool's Guide to Sponge Taxonomy*. Version 2; Saturday, July 9th. Zoology Department, The Natural History Museum, London.
- 111 Brusca, R.C., and Brusca, G.J., (1990): *Invertebrates*. Sinauer Assoc., Inc.: page 922.
- 112 Berquist, P.R., and Kelly-Borges, M., (1995): *Systematics and Biogeography of the Genus *Ianthella* (Demospongiae:Verongida:Ianthellidae) in the South West Pacific. *The Beagle, Records of the Museums and Art Galleries of the Northern Territory*, Vol.12: pages 151-176.*

- 113 Vernon, J.E.N., (1986): Corals of Australia and the Indo-Pacific. Angus and Robertson Publishers. London
- 114 Bouchon, C., and Rouvillain, J-L., (1986): Use of Coral in Bone Surgery. *Osseuse compte rendu du XX Congres des Medecins de Langue Francaise de l'Hemisphere Amercain*; Hopital de la Meynard, Fort de France, April: pages 38-41.
- 115 White, E., and Shors, E.C., (1986): Biomaterial Aspects of Interpore-200 Porous Hydroxyapatite. Reconstructive Implant Surgery and Implant Prosthodontics I. *Dental Clinics of North American*, January; Vol. 30, No.1: pages 49-67
- 116 Ouhayoun, Shabana, J.P., Isshahakian, A.H.M., Patat, L., Guillemin, G., Sawaf, M.H., and Forest, N., (1992): Histological Evaluation of a Natural Coral Skeleton as a Grafting Material in Miniature Swine Mandible. *Journal of Materials Science: Materials in Medicine*; 3: pages 222-228.
- 117 Mugat, M.P., (1989): From Coral to Biocoral. Inoteb. Saint Gonnelly, France.
- 118 Troster, S.D., (1993): Die Hydroxylapatitkeramik Endobon-Eine Alternative Therapiemoglichkeit fur Knochendefekte. In: *Yearbook of Orthopaedics (Jahrbuch der Orthopadie)*. Zulpich: Biermann: pages 231-246.
- 119 Barber, J.C., (1993): Modifications of Keratoprosthesis to Improve Retention. *Refractive and Corneal Surgery*; Vol. 9, May/ June 1993: pages 200-201.
- 120 Leon, C.R., (1997): Hydroxyapatite Keratoprosthesis Made from Coral. *Oculoplastic and Reconstructive Surgery*; March 15th: pages 61-65.
- 121 Rol, P., Parel, J-M., Lacombe, E., Legeais, J-M., Villain, F., (1993): Optics of Keratoprostheses. *Refractive and Corneal Surgery*; Vol 9, May/ June: pages 212-213.
- 122 Bissell, M.J., and Barcellos-Hoff, M.N., (1987): The Influence of Extracellular Matrix on Gene Expression: Is Structure the Message?. *J. Cell Sci., Suppl.*; 8: pages

123 Caiazza, S., Taruscio, D., Crateri, P., Chistolini, P., Bedini, R., Colangelo, P., Pintucci, S. (1991): Evaluation of an Experimental Periodontal Ligament for Dental Implants; *Biomaterials*, Vol. 12, July: pages 474-478.

124 Pitaru, S., and Noff, M., (1993): The Development of a Novel Implant: Induction of a Non-Rigid and Self-Renewing Anchorage of Artificial Implants to Bone. *Clinical Materials*; 13: pages 29-34.

125 Grenga, T.E., Zins, J.E., and Bauer, T.W., (1989): The Rate of Vascularisation of Coralline Hydroxyapatite. *Plastic and Reconstructive Surgery*; Vol 84, No.2: pages 245-249.

126 Vincent, J.F.V., (1994): The Mute Dogs of Nature (Feature). *Science and Public Affairs*, British Association for the Advancement of Science; Autumn Issue: pages 41-43.

127 El-Shahed, F.S., Sherif, M.M., and Ali, A.T., (1995): Management of Tissue Breakdown and Exposure Associated with Orbital Hydroxyapatite Implants. *Ophthalm. Plastic and Recon. Surgery*; Vol 11, No.2: pages 91-94.

128 Jammet, P., Souyris, F., Bonnel, F., Huguet, M., (1994): The Effect of Different Porosities in Coral Implants: An Experimental Study. *J.Cranio-Maxillo-Facial Surgery*; 22: pages 103-108.

129 Remes, A., and Williams, D.F., (1991): Relationship Between Chemotaxis and Complement Activation by Ceramic Biomaterials. *Biomaterials*; Vol.12; No.7, September: pages 661-667.

130 Nimni, M.E., Cheung, D., Startes, B., Kodama, M., Sheikh, K., (1987): Chemically Modified Collagen: A Natural Biomaterial for Tissue Replacement. *J.Biomed. Mats. Res*; Vol.21:pages 742-767.

APPENDICES

Appendix 1

A1.1 Detailed Description of Attributes for an OOKP Analogue

A bone-like porosity and a tough and flexible ligament have been identified as crucial to the retention of the support frame, *in vivo*. Other desirable properties for an OOKP analogue were extracted from related biological ceramic implants, also involving tissue integration.

Aspects such as, mineral type and resorption characteristics have been highlighted as factors controlling the degree of biological tolerance. Following below are brief descriptions of the properties considered as imperative for a synthetic OOKP support frame, based upon current literature and a study of the OOKP. The order of attributes denotes a preferred order of importance. Porosity is the most important of these because, it has a profound effect on tissue responses. This is followed by mineral properties and resorption rate which, govern the lifespan of the biological ceramic. While a periodontal ligament analogue prevents epithelial downward growth that leads to rejection.

- *porosity*
- *mineral properties*
- *rate of Resorption*
- *periodontal ligament substitute*

Biomimetics is the science of abstracting good design from nature and the development of synthetic systems using knowledge obtained from biological systems.¹⁰⁵ Essentially there are two possible biomimetic approaches. The first approach is to fabricate exact copies of biological materials and structures. And the second approach is to fabricate materials and structures by copying biochemical processes that form biological materials. Preference was given to the former.

A1.11. Porosity

Porosity is a generic property to denote the volume of pore space and the pore dimensions. An optimised porosity enables effective ingrowth of live tissue. In

general, porous natural artifacts such as bone and even coral are deemed as optimal frameworks for tissue integration.

An effective porous structure is governed by the capacity to control both the quantity and the rate at which matrix proteins are laid down and the amount and rate of tissue integration together with the degree of vascularisation. Matrix proteins are a particularly important element of the integration process, since they determine the competency of tissue reconstruction. This fact also explains the significance of pore architecture for integration because, the architecture of a porous structure acts as a template for matrix protein assembly. If all these factors are present to a sufficient degree there can arise strong attachment and long-term stability.

A high rate of biological inward tissue growth ensures coverage over the total surface of the scaffolding and this excludes bacterial contamination. Infections give rise to inflammation and detachment of the implant from its surroundings. In order to create a stable union there must be sufficient living material to fill all the available spaces.

The overall completeness of vascularisation is directly improved by larger pore sizes (150-400 μ m) and also by a scleral cloak guarding against infection. Scleral and conjunctival coverings have contributed to the success of orbital implants¹²⁷ A healthy and well constructed vasculature is necessary for minimising complications because it supplies all the building blocks of repair.

By far the most important attribute for healthy prolonged cell attachment is surface texture. On the other hand, porosity is the most influential factor for tissue organisation and healthy, orderly reconstruction. There are reports that the geometry of the solid enclosures can strongly influence phenotypic differentiation.¹²²

It was found that pore sizes of <10 μ m prevented cell inward growth, while pores between 15-50 μ m allowed for the formation of osteoids and so, in theory this could apply to cells with similar dimensions, such as fibroblasts. Pore diameters above 150 μ m mineralised tissue can take hold and be supported. The rate of resorption is also

correlated with porosity. A large porosity presents a proportionately larger surface area of contact with host tissues and as a result this increases the rate of degradation.

128

As alluded to earlier, the degree of confinement in which a cell is subjected to, has a powerful effect on cell behaviour. Both cell-substrate and cell-to-cell contacts are strongly influenced by mechanical loading transferred through the surrounding substrate. Such forces function as organisational and spatial cues for tissue repair that are otherwise degraded. Tissue repair is chaotic and dis-organised in damaged and diseased tissue due to lack of such cues for re-development. It has long been a desire of tissue engineers to understand the nature of operation of these signals to modulate cell responses through material design.

TABLE 1.1 *Pore Size and Tissue Response*

Pore sizes	Tissue Response
280–600 μ	Rapid Infiltration in 2 weeks moderately cellular, moderately vascular mature collagen
600+ μ	After 4 weeks infiltration of substantial amount of collagen is absent
100 μ	Highly vascularised connective tissue

A1.12. Mineral properties

The type (hydroxyapatite, calcium carbonate), crystal habit and ionicity (valency) of a mineral lattice may strongly affect cell behaviour. Small differences in these properties can lead to large differences in cell activity, because such activities are directed by very specific signals and extracellular contacts. The latter would include micro-rugosity. The degree of micro-rugosity depends upon crystallisation. Identifying the precise

influences upon cellular activity is not straightforward. There are, however certain well defined limits which, guide a favourable host response. The first of these is a calcium phosphate ratio of between 1.5-1.67.⁹⁵

The calcium and phosphate ratio, the quantity of fluorine (F-) and carbonate (CO₃-) ions present in the latticework determine the stability of the biological precipitate surrounding a ceramic implant.⁹⁵ Evidence is strong that a combination of tetracalcium phosphate (TCP)/ hydroxyapatite (HA) elicits the most beneficial tissue response although TCP by itself gives a less favourable tissue response than hydroxyapatite.¹³⁰

A1.13. Rate of Resorption

While biological ceramics are well tolerated by the human body such tolerance also allows for resorption. Resorption is a process of degradation by the hosts defences. Biological degradation is the process whereby the body challenges and incorporates or rejects a material inserted into tissue and body fluids. The mechanism of resorption is carried out by macrophages and immunoglobulin molecules that are selectively adsorbed onto calcium phosphate ceramics. This along with alpha-glycoproteins and complement factors.¹²⁶ Resorption of highly inert materials by cells of the immune system does not occur. As such a 'walling-off' response takes place in which fibrous tissue encapsulates all surfaces and removes any possibility of interaction. Usually under these circumstances an implant cannot function.

Microscopic porosity is considered to be highly influential on the rate of decomposition due to correlation between increasing porosity and surface area,¹²⁷ with a larger surface area exposed to phagocytes. Another affect on resorption rate is the presence of certain ions that can alter the rate of degradation. For example, fluorine ions act to reduce solubility, whereas high concentrations of carbonate ions lead to a higher metabolic activity.

A1.14 A Periodontal Ligament Substitute

There is some confusion as to the biological significance of the periodontal structure and for that matter the cementum which, has also been implicated in stabilising encapsulating membranes. Unfortunately, there are few case studies to rely upon for evidence. Marchi et al.⁶⁹ were able to carry out a detailed histological examination of dental lamina extracted from OOKP patients after five, ten and twenty years in the body. What this study in particular reveals is intriguing, but fails to answer one important matter for those trying to imitate the basic form and structure of the ODAL.

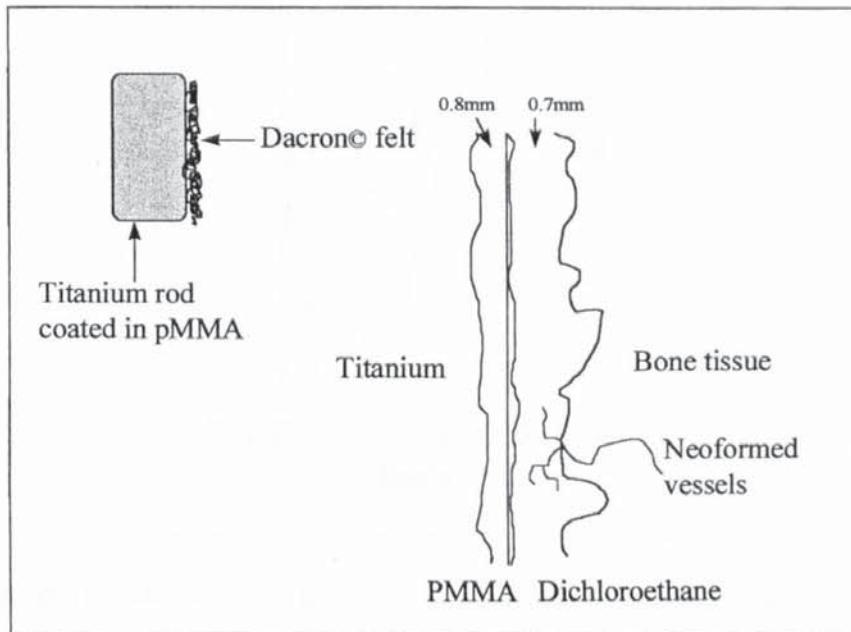
Is the structure of the ligament key to the success of the OOKP, or is biochemistry at the surface the key? The role of the ligament in its natural situation is to cushion, (tissue hydrostatic pressure is high to give the ligament a large degree of incompressibility) the tooth against the jawbone and be an attachment for gum tissue at the tooth surface. This cushioning or yielding effect absorbs forces generated and transmitted by soft tissue that would otherwise dislodge a stiff mineralised tooth. An identical system is recreated in the OOKP operation. There are a surprising array of functions for the periodontal ligament. The key biological attributes for mechanical functioning are summarised below:-

- a soft fibrous connective tissue made from collagen (Type II & III). The periodontal ligament is pre-stressed or made taught and able to flex to remove shear strain under large compressive loads.
- a uni-modal size frequency of collagen fibrils. This maintains a uniformity of space between the dentine and bone. Such uniformity may be important in evenly spreading compressive loads.
- a high degree of collagen cross-linking. A major property of an archetypal structure expressing tensegrity.
- a rapid mechanism for repair and re-alignment under changes of load or when damaged. This is one property which as yet cannot be crafted into a synthetic material.

The primary adaptive function of a self-renewable and flexible fibrous ligament is to accommodate the differential responses of attached materials with different moduli to external forces and keep the whole system intact and stable. The tooth and bone system is a perfect example of the principle. Biomaterial scientists have focused on the form and function of ligamentous anchorage owing to the frequent problem of implant loosening. This often arises as a consequence of the way in which many implants are fixed to the body- mechanically (clipping and gluing). However, a periodontal ligament anchorage is difficult to fabricate synthetically because of difficulties embedding a fibrous material into solid materials with contrasting chemistry. There are two novel synthetic analogues to a periodontal ligament; Caiazza employed Dacron™ felt and Pitaru et al. employed collagen.^{123,124}

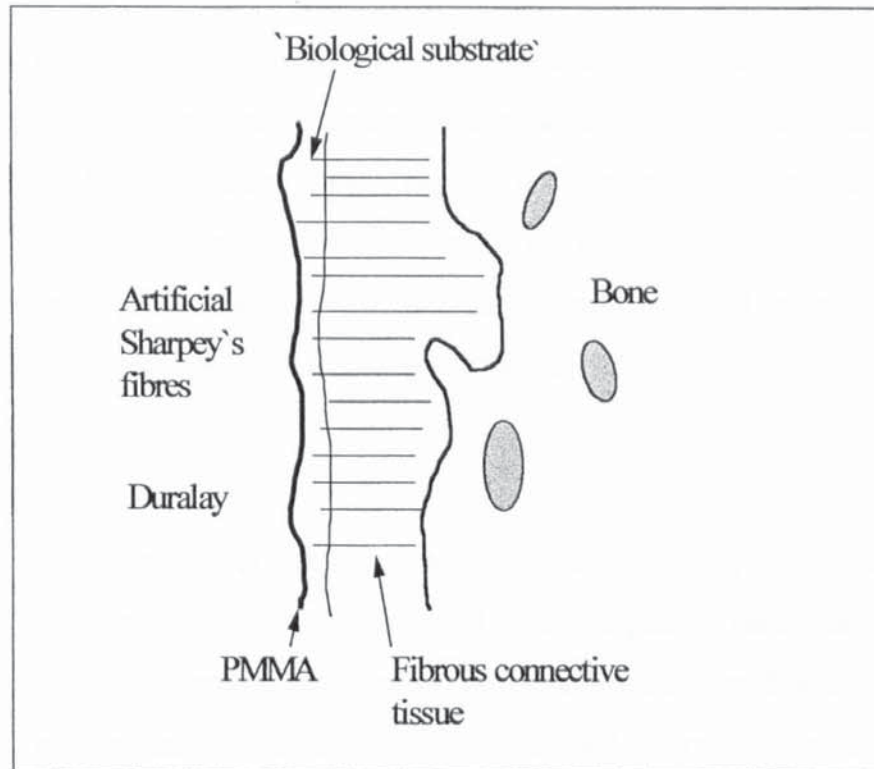
In the experimental periodontal ligament of Caiazza a titanium rod is coated in polymethylmethacrylate (pMMA). Dacron™ tissue is fixed part-way into the layer of using dichloroethane as a solvent. It was inferred by Caiazza the above implant would provide the following, a reliable mechanical anchorage and act as a barrier against epithelial proliferation and microbial contamination.

Figure A1.1 *Caiazza et al.:-Experimental Periodontal Ligament.*¹²³



Dacron™ apparently deputises for the periodontal ligament which is nature's embedded linkage with bone and soft tissue. Dacron™ tissue has been evaluated as a material for a keratoprosthesis retention plate and fulfils most of the criteria, set out in chapter one, for tissue incorporation in pathological eyes. Dacron™ induces a relatively short period of inflammation and a minimum accumulation of granulation tissue. In summary, it would provide a sound gingival seal by establishing a platform for connective tissue attachment and a gingival derived overlay.

Figure A1.11 *Pitaru and Noff's Non-rigid Ligamentous Anchorage.*¹²⁴



The diagram in Figure A1.11 consists of surface meshwork of lyophilised and dehydrated collagen fibres part way embedded into a thin paste of pMMA at one edge. The pMMA is directly polymerised at room temperature on contact with a core of Duralay covered metal. The collagen fibres provided both a ligament-like anchorage and induced a mirror image of healthy collagen, a sort of template for reconstruction.¹²⁴

Appendix 2

A2.1 Methods for Making Ceramic Blocks

Ceramics are made from non-metallic inorganic minerals which have been pressed and heated to very high temperatures. Their manufacture is relatively straightforward. First the mineral is ground down into a fine powder. This powder is then suspended in solution before it is compacted into shape. Very high heating temperatures are then needed to preserve this compacted solid.

Porosity is introduced into the solid by adding polymeric fillers with the ceramic

powder prior to compaction. When heated the polymer dissolves away to leave pores and channels. Heating to high temperatures is not always necessary when making a ceramic. At high enough pressures the powder particles will melt and weld together to form a solid mass. Uniaxial pressing uses a hard metal punch to compact a dry powder usually with few percentage water, to produce a brittle solid. With hot uniaxial pressing heat and pressure are combined at the same time to fabricate a solid with a higher density and smaller grain sizes. Isostatic (or dynamic) pressing also produces a high and uniform density but, without the need for sintering. Powder compaction at room temperature preserves the structure and composition of sintered pieces and enables organic substances, that would otherwise be dissolved during sintering, to be included.⁷⁶

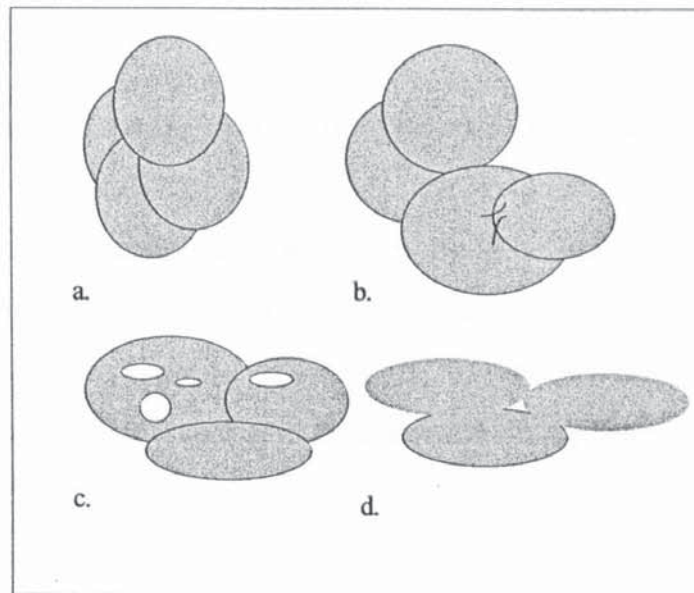
Slip casting is a very common manufacturing process in which a ceramic suspension is drained of its liquid suspension to leave a solid mass. Injection moulding is commonly used to shape plastic materials but a ceramic filler can be added with a liquefied organic polymer and poured into a mould to produce a stable composite material. *In-situ* precipitation is a method of reinforcing a polymer matrix with ceramic particles. The particles grow by crystallisation within the matrix to a limited extent to form a network in two dimensions.⁸⁵

A2.11 Fabrication of Biological Ceramics with Uniform Porosity

The first series of experiments were designed to use pure ceramic powders and manufacture a highly porous and coherent ceramic disc. The support frame should possess macropores and micropores to allow for the interpenetration of cells, blood vessels and connective tissue (as explained in 3.1.1). The arrangement of pores and channels needs to be uniform and well structured to provide a proper fixation for the implant when inserted into the eye. Porosity may be introduced into a ceramic solid during its synthesis by the following methods. Only the latter was used in this study:-

- foaming by casting and subsequent gasification
- compaction of particle mixtures followed by sintering

Figure A2.1 *The Sintering Phenomenon and its Effects on Closely Packed Ceramic Particles.*



The formation of pores and changes in their size and shape during sintering are shown in figure A2.1. At a). Randomly distributed particles that produce neck growths with neighbouring particles on heating at b). This process is driven by minimisation of surface free energy. At c). channel shaped voids are produced causing particle size to increase dramatically. At d). there is a decrease in the numbers of channel shaped voids, but voids remain at triple points at grain boundaries.⁸⁵

A2.12 Dynamic Changes to the Porosity of Ceramics

One of the most accurate and reliable way of fabricating a void structure is by adding deformable polymer particles to the starting powders, before compacting and followed by high temperature heating. In general, the size distribution of pores is controlled by the following:-

- initiation of a temperature gradient of during sintering, so that the rates at which, particles weld together are not constant and uniform along the gradient of temperature. This creates regions with differing pore sizes. In practice there needs to be a sophisticated control unit integrated into the kiln.
- rheological or flow properties of additives (fillers and binders) during compacting and heating.

Pore geometry, i.e shape and size may be controlled by:-

- Defining the forming pressure and specifying particle size(s) and shape(s)

Appendix 3

A3.1 A More Detailed Assessment of the Potential Usefulness of a Prosthesis by Tissue Culture

The next and most important stage is to test the reaction of cultured tissue to an assortment of ceramic structures. It will be necessary to quantify the rate of cell growth into the pores, the eventual depth of penetration, cell densities within the body of the material, cell-to-cell/cell-substrate adhesion and finally the respiratory activities of the cultured cells.⁸⁴

Determination of cell growth is a useful tool for characterising age-related changes and changes induced by the culture environment. Such data is a reliable, accurate index of the physiological and physical state of tissues in culture which is very helpful when assessing the short term responses of cells to a synthetic material. A comparison of cell growth kinetics between cells exposed to ceramic and cells unexposed to ceramic is a simple and effective experiment to carry out. Cell density can be approximated by eye or by the intensity of a histological stain.

Different plane sections through the material would give a three dimensional image of the interpenetrating tissue. A useful implant material should encourage a uniform and orderly arrangement of cells. The level of Respiratory activity is a more accurate measure of cell viability in a given culture environment. Respiratory activity is determined by measuring the concentration of certain key enzymes, such as lactate dehydrogenase, acid phosphatase and cytoplasmic oxidoreductase. Enzyme concentration assays will be used to measure cell respiration and the secretory activity of immune cells (e.g. Macrophages). Immune cells are of course a major constituent of the framework of response to prosthetic implants.